THE UNIVERSITY *of* EDINBURGH

Vascular lesion development: influence of endogenous and exogenous glucocorticoids

Lucinda Low

Doctor of Philosophy
University of Edinburgh
2011

Abstract

Atherosclerotic and restenotic lesions develop as a result of an excess inflammatory response to vascular injury. Glucocorticoid hormones have widely-recognised anti-inflammatory and anti-proliferative properties which appear to make them ideal candidates for inhibition of vascular lesion development. Indeed, administration of glucocorticoids to experimental animals does inhibit the growth of vascular lesions in some models. In addition, glucocorticoids are currently being trialled clinically as anti-restenotic agents. However, glucocorticoid excess in patients, either as a result of Cushing's syndrome or chronic steroid therapy, is associated with enhanced CVD risk. Therefore, the effects of glucocorticoids on vascular lesion development remain imperfectly understood.

The overall objective of these studies was to explore the influence of endogenous and exogenous glucocorticoids on vascular lesion development using murine models of atherosclerosis ($ApoE^{-/-}$ mice fed a "western" diet) and neointimal hyperplasia (wire-induced femoral artery injury). The work described in this thesis addresses the hypothesis that glucocorticoids are pro-atherogenic, yet anti-restenotic.

Mice were bilaterally adrenalectomised to investigate the role of endogenous glucocorticoids on vascular lesion development. Removal of the adrenal glands had no influence on atherogenesis or neointima development. The influence of exogenous glucocorticoids on lesion development was assessed by orally administering dexamethasone (0.1 or 0.8mg/kg/day). Atherosclerotic lesion burden was augmented by dexamethasone administration. Conversely, fibro-proliferative neointimal proliferation was inhibited by dexamethasone. However, this effect was obscured by thrombotic lesion development. It was proposed that this thrombotic effect is attributable to increased plasminogen activator inhibitor-1 (PAI-1), which was tested using PAI-1 deficient mice. Although PAI-1 was found to mediate the systemic pro-thrombotic effect of dexamethasone, it is not required for the enhanced development of thrombotic lesions at the site of intra-luminal injury.

These results suggest that physiological levels of endogenous glucocorticoids play a limited role in vascular lesion development. Conversely, although exogenous glucocorticoids inhibit fibro-proliferative intimal hyperplasia, they appear to have significant detrimental influences on lesion development, augmenting atherosclerosis and inducing thrombotic neointimal lesion formation following vascular injury. Further research is therefore required to improve the cardiovascular outcome of patients requiring glucocorticoid therapy and for the use of glucocorticoids as anti-restenotic agents.

Declaration

I declare that this thesis and the work described within are solely my own work with the following exceptions:

Dr Patrick Hadoke performed some adrenalectomy and wire-injury surgeries and carried out independent semi-quantitative scoring of atherosclerotic lesions; Mrs Susan Harvey performed picrosirius red staining of brachiocephalic arteries; Miss Jessica Blom performed the PAI-1 and tPA ELISA assays in the PAI-1 study (Chapter 6).

I confirm that this thesis has not been previously submitted for any other degree.

Lucinda Low

Acknowledgements

Firstly, I would like to thank my supervisor Dr Patrick Hadoke for his continual support, unfaltering optimism and, perhaps most importantly, for teaching me the correct use of a semicolon. In addition, I would like to express my gratitude to Professors Brian Walker and Jonathan Seckl for their expertise and guidance throughout my PhD.

An important acknowledgement must go to The Royal Society of Edinburgh and Carnegie Trust for awarding me their Henry Dryerre Scholarship which funded this work.

It has been a great pleasure and honour to be a part of Team Paddy and I would like to thank all of my team mates, past and present, for the scientific discussions and not-so-scientific laughs we have shared. In particular, a very special thank you must go to Dr Nicholas Kirkby for all of his help and advice. I do not know what I would have done without him.

I would also like to extend my appreciation to everyone else who has helped me in the CVS, CIR and BRF over the past three and a half years. In particular, I wish to thank Dr Paul Harley for sharing his extensive expertise in platelet biology and his enlightening perspectives. I must also thank my office mates who have contributed to the success and enjoyment of my time in the CVS, through their advice, gossip and baking.

And finally, I would like to thank Rachel and Yvonne who have kept me motivated and smiling through the highs and the lows of my PhD.

Presentations and prizes

Oral Presentations

Increased plasminogen activator inhibitor-1 mediates dexamethasone-induced pro-thrombosis but not the response to intra-luminal wire injury. Arteriosclerosis, Thrombosis and Vascular Biology Scientific Sessions, Chicago, IL, USA, April 2011.

Vascular lesion development: influence of endogenous and exogenous glucocorticoids. BHF-sponsored Vascular Biology Summer School, Bristol, UK, July 2010.

Dexamethasone augments atherosclerosis in mice. Scottish Society for Experimental Medicine, Dundee, UK, June 2010.

Exogenous, but not endogenous, glucocorticoids augment atherosclerosis in mice. Scottish Cardiovascular Forum, Glasgow, UK, February 2010.

Glucocorticoid administration reduces neointimal proliferation but exacerbates atherogenesis in mice. British Pharmacological Society Summer Meeting, Edinburgh, UK, July 2009.

Poster Presentations

Increased plasminogen activator inhibitor-1 may explain dexamethasone-induced thrombosis as site of intra-luminal wire injury. British Atherosclerosis Society/British Society for Cardiovascular Research Spring Meeting, Manchester, UK, June 2010.

Exogenous glucocorticoids inhibit neointimal proliferation but increase local thrombosis in mice. Arteriosclerosis, Thrombosis and Vascular Biology Scientific Sessions, San Francisco, CA, USA, April 2010.

Exogenous, but not endogenous, glucocorticoids augment atherosclerosis in mice. Arteriosclerosis, Thrombosis and Vascular Biology Scientific Sessions, San Francisco, CA, USA, April 2010.

3-dimensional ex vivo analysis by optical projection tomography demonstrates that exogenous glucocorticoids augment atherogenesis in ApoE$^{-/-}$ mice. British Atherosclerosis Society Spring Meeting, Cambridge, UK, April 2009.

Influence of endogenous and exogenous glucocorticoids on neointimal proliferation. Scottish Cardiovascular Forum, Inverness, UK, January 2009.

Presentation prizes

BHF-sponsored Vascular Biology Summer School Free Communications Presenter, July 2010.

BHF-sponsored Vascular Biology Summer School Poster Award, July 2010.

University of Edinburgh's CVS Symposium Day Student Poster Award: second prize, June 2010.

Scottish Cardiovascular Forum's Young Investigator Award: oral presentation, Feb 2010.

Travel awards

University of Edinburgh Page Bursary to attend ATVB Scientific Sessions, April 2011.

Scottish Society for Experimental Medicine Travel Award to attend SSEM Spring Meeting, June 2010.

British Society for Cardiovascular Research Travel Award to attend BAS/BSCR Joint Meeting, June 2010

British Pharmacological Society Travel Bursary to attend ATVB Scientific Sessions, April 2010.

Publications

Papers

Quantitative 3-dimensional imaging of vascular lesions by optical projection tomography. NS Kirkby, L Low, RA Riemersma, JR Seckl, BR Walker, DJ Webb and PWF Hadoke. *PLoS ONE* 2011; 6(2): e16906.

Abstracts

Increased plasminogen activator inhibitor-1 may explain dexamethasone-induced thrombosis as site of intraluminal wire injury. L Low, JR Seckl, BR Walker and PWF Hadoke. *Heart* 2010; **96**; e16.

Exogenous glucocorticoids inhibit neointimal proliferation but increase local thrombosis in mice. L Low, JR Seckl, BR Walker and PWF Hadoke. *ATVB* 2010; 30(11): e183, P411.

Exogenous, but not endogenous, glucocorticoids augment atherosclerosis in mice. L Low, NS Kirkby, JR Seckl, BR Walker and PWF Hadoke. *ATVB* 2010; 30(11): e183, P579.

Glucocorticoid administration reduces neointimal proliferation but exacerbates atherogenesis in mice.
L Low, NS Kirkby, JR Seckl, BR Walker and PWF Hadoke *pA_2 Online* 2009; **7**(2).

3-dimensional ex vivo analysis by optical projection tomography demonstrates that exogenous glucocorticoids augment atherogenesis in ApoE$^{-/-}$ mice. L Low, NS Kirkby, JR Seckl, BR Walker and PWF Hadoke. *Heart* 2009; **95**; e2: 6-7.

Contents

List of figures

List of tables

List of non-standard abbreviations

11βHSD	11β-hydroxysteroid dehydrogenase
AAo	ascending aorta
ACE	angiotensin-converting enzyme
ACTH	adrenocorticotropic hormone
ADP	adenosine diphosphate
adx	adrenalectomy
AMV	avian myeloblastosis virus
ANOVA	analysis of variance
ANP	atrial natriuretic peptide
AP-1	activator protein-1
APC	activated protein C
ApoE	apolipoprotein E
AVP	arginine vasopressin
BABB	benzyl alcohol, benzyl benzoate
BCA	brachiocephalic artery
bFGF	basic fibroblast growth factor
BMS	bare metal stents
BSA	bovine serum albumin
CABG	coronary artery bypass graft
CBG	corticosteroid-binding globulin
CCR2	chemokine (C-C motif) receptor 2
Cp	crossing point
CRH	corticotropin-releasing hormone
CT	computed tomography
CVD	cardiovascular disease
DAB	diaminobenzidine
Dao	descending aorta
DES	drug-eluting stents
dex	dexamethasone
DEXA	dual energy X-ray absorptiometry
DexES	dexamethasone-elutin stents

DHEA	dehydroepiandrosterone
DKO	double knock out
ECM	extracellular matrix
EDHF	endothelial-derived hyperpolarising factor
EEL	external elastic lamina
EES	everolimus-eluting stents
ELISA	enzyme-linked immunosorbent assay
F	clotting factor
FITC	fluorescein isothiocyanate.
FPLC	fast protein liquid chromatography
FSC	forward scatter
GMFI	geometric mean fluorescence intensity
GP	glycoprotein
GR	glucocorticoid receptors
GRE	glucocorticoid response elements
HDL	high-density lipoprotein
HMWK	high-molecular-weight kininogen
HPA	hypothalamic-pituitary-adrenal
HRP	horseradish peroxidase
ICAM-1	intercellular adhesion molecule-1
IEL	internal elastic lamina
IFN-γ	interferon-γ
IGF	insulin-like growth factor
IHC	immunohistochemistry
IL	Interleukin
IL-1	interleukin-1
iNOS	inducible nitric oxide synthase
Lac-Z	β-galactosidase
LASMA	late acquired incomplete stent malapposition
LCA	left carotid artery
LDL	low density lipoprotein
LDLR	low density lipoprotein receptor
LFA	left femoral artery

LRA	left renal artery
LSA	left subclavian artery
MACCE	major adverse cardiovascular events
MCP-1	monocyte chemotactic protein-1
M-CSF	macrophage colony-stimulating factor
MI	myocardial infarction
MIP-1α	macrophage inflammatory protein-1α
MMP	matrix metalloproteinase
MR	mineralocorticoid receptor
MRI	magnetic resonance imaging
mRNA	messenger ribonucleic acid
MTI-MMP	membrane type 1 matrix metalloproteinase
mTOR	mammalian target of rapamycin
NFκB	nuclear factor κB
NO	nitric oxide
NOS	nitric oxide synthase
OCT	optical coherence tomography
OPT	optical projection tomography
PAF	platelet activating factor
PAI-1	plasminogen activator inhibitor-1
PAR	protease-activated receptor
PBS	phosphate-buffered saline
PCI	percutaneous coronary intervention
PCR	polymerase chain reaction
PDGF	platelet-derived growth factor
PE	R-phycoerythrin
PES	paclitaxel-eluting stents
PGE_2	prostaglandin E_2
PGI_2	prostacyclin
PPP	platelet-poor plasma
PRP	platelet-rich plasma
PSGL-1	P-selectin glycoprotein ligand-1
qPCR	quantitative real time polymerase chain reaction

RANTES	regulated upon activation, normal T cell expressed and secreted
RCA	right carotid artery
RFA	right femoral artery
ROS	reactive oxygen species
RRA	right renal artery
rRNA	ribosomal ribonucleic acid
RSA	right subclavian artery
RT-PCR	reverse transcription polymerase chain reaction
SAME	syndrome of apparent mineralocorticoid excess
SMα-actin	smooth muscle α-actin
SOD	superoxide dismutase
SpA	scintillation proximity assay
SSC	side scatter
STEMI	ST-segment elevation myocardial infarction
TAFI	thrombin-activated fibrinolysis inhibitor
TF	tissue factor
TFPI	tissue factor pathway inhibitor
TGF	transforming growth factor
TIMP-1	tissue inhibitor of matrix metalloproteinase-1
TMB	tetramethyl benzidine
TNF-α	tumour necrosis factor-α
tPA	tissue plasminogen activator
TVR	target vessel revascularisation
TXA_2	thromboxane A_2
uPA	urokinase plasminogen activator
uPAR	urokinase plasminogen activator receptor
UST	United States trichrome
VCAM-1	vascular cell adhesion molecule-1
VN	vitronectin
VSMC	vascular smooth muscle cells
vWF	von Willebrand factor
ZES	zotarolimus-eluting stents

Chapter 1

Introduction

Cardiovascular disease (CVD) and its complications, such as stroke, myocardial infarction (MI) and peripheral vascular disease, are the single biggest cause of death in the developed world, accounting for almost 191,000 deaths (33.3% of all mortality) per annum in the UK alone. Almost half of these deaths are from coronary heart disease, with around one in seven women and one in five men dying from this condition (www.heartstats.org; accessed January 2011). The mortality rates for CVD have declined by ~40% in the last decade, which has been attributed mostly to the reduction in major risk factors, primarily smoking, and also to advances in treatment and secondary prevention. In contrast, morbidity rates have been increasing, in parallel with the current pandemic of cardiovascular risk factors such as obesity and diabetes (www.heartstats.org; accessed January 2011). It is, therefore, imperative to improve our current understanding of the factors involved in the pathogenesis of CVD and advance research into new therapies for this condition.

Central to the pathogenesis of CVD is vascular lesion development, which can manifest itself in a number of clinical conditions, including atherosclerosis and restenosis following percutaneous coronary interventions (PCI). Both atherosclerosis and restenosis are reactions to vascular injury, involving inflammation and cellular proliferation (Kibos *et al.*, 2007; Ross *et al.*, 1977). Glucocorticoid hormones have widely-recognised anti-inflammatory and anti-proliferative properties (Barnes, 1998) which appear to make them ideal candidates for inhibition of vascular lesion development. Indeed, administration of glucocorticoids to experimental animals does inhibit the growth of vascular lesions in some models (Asai *et al.*, 1993; Makheja *et al.*, 1989; Naito *et al.*, 1992). In addition, glucocorticoids are currently being trialled clinically as anti-restenotic agents (Ferrero *et al.*, 2009; Ribichini *et al.*, 2005). However, chronic glucocorticoid excess in patients, either as a result of Cushing's syndrome (Colao *et al.*, 1999; Etxabe *et al.*, 1994) or of chronic administration (Solomon *et al.*, 2006; Souverein *et al.*, 2004), is associated with enhanced CVD risk (e.g. central obesity, insulin resistance, dyslipidemia and hypertension). Therefore, the net effects of glucocorticoids on vascular lesion development remain imperfectly understood. Elucidating these effects will improve our understanding of the role of glucocorticoid activity in regulating atherogenesis and restenosis and the therapeutic

potential of glucocorticoids as a treatment for, or as a target in, CVD. This introduction will consider the mechanisms that contribute to atherosclerotic and restenotic vascular remodelling, the physiological role of glucocorticoids and their influence on the cardiovascular system.

1.1 Vascular remodelling

In order to appreciate the processes that occur during vascular remodelling it is necessary to understand the structure of the healthy arterial wall and the functional role of the three component layers – the tunica intima, tunica media and tunica adventita (Figure 1.1).

1.1.1. The structure of the normal artery wall

1.1.1.1 Tunica intima

The innermost layer of the artery wall consists of a confluent monolayer of endothelial cells, lying on a basement membrane of collagen, laminin and proteoglycans. In some arteries the intima can be more extensive containing focal accumulations of vascular smooth muscle cells (VSMCs) and additional layers of extracellular matrix (Stary, 1990). Underneath this lies the internal elastic lamina (IEL) which separates the intima from the media (Newby, 2000). The endothelium is crucial to the regulation of vascular tone as it produces a number of vasodilators: nitric oxide (NO) (Furchgott et al., 1980; Ignarro et al., 1987; Palmer et al., 1987), endothelial-derived hyperpolarising factor (EDHF) (Busse *et al.*, 2002; Chen *et al.*, 1988) and prostacyclin (PGI_2) (Weksler *et al.*, 1977), as well as vasoconstrictors: endothelin-1 (Yanagisawa *et al.*, 1988) and thromboxane A_2 (TXA_2) (Ingerman-Wojenski *et al.*, 1981; Moncada *et al.*, 1976). Importantly, the endothelium also acts as an anti-thrombotic barrier between the circulation and the basement membrane (section 1.1.4.1). In addition, it is an important modulator of vascular inflammation and angiogenesis (Levick, 2003).

1.1.1.2 Tunica media

The tunica media is the middle layer of the vascular wall, which lies between the IEL and the external elastic lamina (EEL). It is made up exclusively of VSMCs surrounded by an extracellular matrix (ECM) and interlaced within a network of

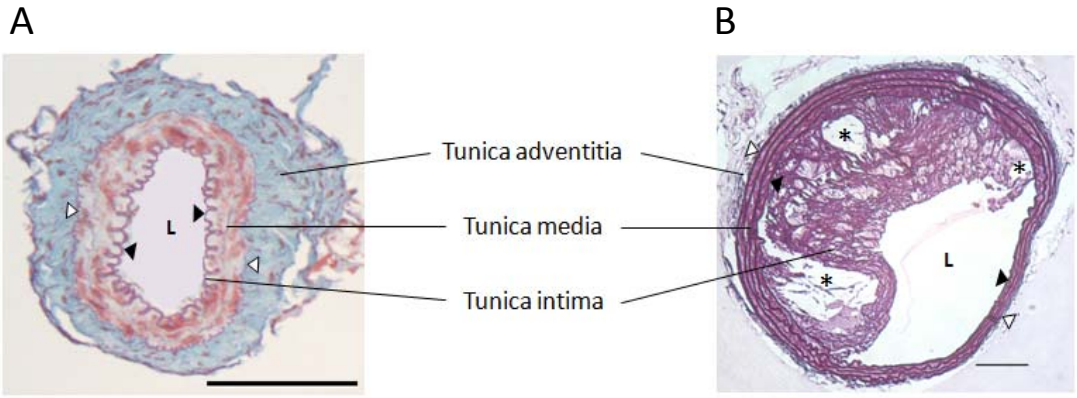

Figure 1.1: Structure of the artery in health and disease.
A: Transverse section of a normal mouse femoral artery stained with United States trichrome (UST) histological stain (collagen: green, smooth muscle: red, elastin: purple). The tunica adventitia lies outside the external elastic lamina (EEL, white arrowheads) and stains strongly for collagen. The tunica media lies between the EEL and the internal elastic lamina (IEL, black arrowheads) and stains strongly for smooth muscle. The tunica intima consists of a monolayer of endothelial cells on the luminal side of the IEL. L: lumen. B: Transverse section of a brachiocephalic artery from an apolipoprotein $E^{-/-}$ mouse, which is susceptible to atherosclerosis, stained with UST. A large atherosclerotic lesion has developed, incorporating lipid (*) and fibrous material in the intima of the vessel wall. Medial remodelling is also evident in this artery. Scale bar = 100μm.

elastic and collagenous fibrils and layers of elastic laminae (Newby, 2000). The principal function of the media is to control vessel diameter through regulation of smooth muscle tone by circulating factors, endothelium-derived factors and neurotransmitters. In large elastic arteries, such as the aorta and brachiocephalic artery, the media is rich in elastic laminae and fibres and relatively poor in VSMCs, allowing the vessel to accommodate pulsatile cardiac output. In addition, the media in these arteries is rich in collagen, to maintain vessel shape and integrity and to prevent over-expansion of the vessel wall. In contrast, muscular arteries, such as the brachial and femoral arteries, are rich in VSMCs providing greater regulation of blood flow and pressure (Levick, 2003).

1.1.1.3 Tunica adventitia

The outermost layer of the vessel wall is separated from the tunica media by the EEL. It consists of a collagen-rich ECM containing VSMCs, fibroblasts, macrophages and adipocytes (Newby, 2000). In larger vessels, the adventitia contains nerves and capillaries (*vasa vasorum*) to supply the vessel wall with nutrients (Bohr *et al.*, 1980). The main function of the adventitia is to provide mechanical strength and stability to the vessel and to anchor it to the surrounding tissue. However, the adventitia can also regulate vascular function through the release of NO (Muller *et al.*, 2000; Pluta, 2006) and vasoactive adipokines (Yudkin *et al.*, 2005). The adventitia may also influence vascular remodelling as it has been suggested that proliferation and migration of adventitial fibroblasts may contribute to atherosclerotic lesion development (Xu *et al.*, 2007).

1.1.2. **Atherosclerosis**

Atherosclerosis is the most clinically relevant manifestation of vascular lesion development. It is defined as a slowly progressing inflammatory disease, which involves medium- and large-sized arteries, such as the coronary and carotid arteries (Leys, 2001; Ross, 1999). Atherosclerosis is characterised by the accumulation of lipid and fibrous material within the artery wall. The development of these fatty lesions usually occurs slowly over several decades, starting in childhood, and often does not manifest itself until middle-age or later (Stary, 1990). Atherosclerotic lesions are largely asymptomatic prior to a cardiovascular event giving

atherosclerosis the reputation of a ‘silent killer’. When symptoms do occur, their nature is determined by the location of the lesion and the vulnerability of the organ supplied by the affected artery. For example, stenosis in the coronary artery results in myocardial ischaemia, which can produce angina or MI (Tortora *et al.*, 2003).

There are three main mechanisms by which atherosclerosis leads to symptoms. Firstly, the lesion can expand sufficiently to occlude the lumen and tissue ischaemia will occur, as in angina pectoris. However, atherosclerotic arteries can outwardly remodel to accommodate expanding lesions, maintaining a near normal lumen diameter (Glagov *et al.*, 1987). Secondly, spasm of the atherosclerotic artery can interrupt blood flow and potentially lead to the acute coronary syndromes of angina and MI (Zhang *et al.*, 2005b). However, the most clinically-significant mechanism of symptom emergence is the rupture of an unstable plaque, leading to intravascular thrombosis, unstable angina and MI (Davies *et al.*, 1984).

Atherosclerotic plaques are categorised by pathologists into 8 grades of lesion (Stary et al., 1995; Stary et al., 1994). These are more generally described in three categories of lesion: the fatty streak, the fibrous plaque and the complicated lesion (Ross *et al.*, 1976a; Ross *et al.*, 1976b). The separate lesion types are distinguished by their characteristic morphological features. Atherosclerotic lesions are predominantly intimal in nature but more advanced lesions can modify the underlying media and adventitia (Stary et al., 1994).

1.1.2.1 The fatty streak

The earliest recognisable lesion of atherosclerosis is the ‘fatty streak’. It is common in infants and young children (Napoli *et al.*, 1997) but can also be found in adults, (Stary *et al.*, 1994). Fatty streaks may be visible as yellow-coloured streaks or patches on the intimal surface of arteries, and often occur at branch points and areas of low shear stress. They consist primarily of lipid-filled macrophages, also known as foam cells, and VSMCs (Aqel *et al.*, 1985; Vedeler *et al.*, 1984), but T-lymphocytes have also been identified in these lesions (Munro *et al.*, 1987). Fatty streaks characteristically have little extracellular lipid (Munro *et al.*, 1988). These lesions cause little or no obstruction in the artery and are symptomatically silent.

1.1.2.2 The fibrous plaque

The fibrous plaque, the fundamental lesion of atherosclerosis, often projects into the arterial lumen and may impede the flow of blood. These plaques consist of: a fibrous cap composed of smooth muscle cells, collagen fibrils and proteoglycans (Murata *et al.*, 1986; Yla-Herttuala *et al.*, 1986); a cellular area beneath the cap consisting of foam cells, VSMCs and T-lymphocytes, many of which are activated (Jonasson *et al.*, 1986); and a deep core of lipid and necrotic tissue. There is morphological and chemical evidence for the presence of an 'intermediate' lesion, bridging the fatty streak and the fibrous plaque (Katz *et al.*, 1976; Small, 1988; Stary, 1992). This evidence, along with the verification of the development of fibrous plaques in the same anatomical location as fatty streaks, supports the hypothesis that fatty streaks are the precursor of fibrous plaques during the pathogenesis of atherosclerosis (Stary *et al.*, 1994). However, it has been suggested that fatty streaks are reversible (Birch, 1965) and therefore may not all develop into fibrous plaques.

1.1.2.3 The complicated lesion

Complicated lesions are characterised by having undergone necrosis, rupture and repair. Consequently, they often contain thrombi or remnants of thrombi on their surface. Repeated rupture or ulceration of lesions can result in the development of multilayered fibrous atheromas, which can include new blood vessels and calcification (Weissberg, 2000). Lesions defined as complicated may or may not occlude the lumen and may or may not produce clinical manifestations. As described above, lesion rupture and thrombosis, are more clinically significant than stenosis (Davies *et al.*, 1984). The vulnerability of a lesion to rupture or fissure is primarily determined by its composition. Plaques with a large lipid core and a thin fibrous cap are more prone to rupture than those with a thick cap. Importantly, the composition of the fibrous cap is a crucial determinant of plaque stability, with a prevalence of inflammatory cells and a relative paucity of smooth muscle cells promoting plaque rupture (Weissberg, 2000). As there is a plethora of differences in size, lipid content and cap thickness, there is a wide variation in the susceptibility of lesions to rupture.

1.1.2.4 Pathogenesis of atherosclerosis

1.1.2.4.1 *Initiation of atherosclerosis*

In 1856, Rudolph Virchow proposed that the lesions of atherosclerosis result from an excessive wound-healing response to injury of the artery wall (Virchow, 1856). This hypothesis has subsequently been updated and revised a number of times (Ross, 1999; Ross, 1993; Ross *et al.*, 1977; Ross *et al.*, 1976a; Ross *et al.*, 1976b), evolving into the proposal that atherosclerosis is a response to endothelial dysfunction. Importantly, atherosclerotic plaque development results not only from the progressive inflammatory response to endothelial dysfunction, but also from the ongoing repair and remodelling of the vessel.

Endothelial dysfunction can be caused by a number of risk factors, including elevated and modified low density lipoprotein (LDL) cholesterol, hypertension, diabetes mellitus, elevated homocysteine concentrations, some infectious organisms and free radicals. Endothelial damage results in a compensatory response that alters the normal homeostatic properties of the endothelium, increasing its adhesiveness and permeability (Figure 1.2A). Increased adhesiveness is mediated by an up-regulation of leukocyte and endothelial adhesion molecules such as intercellular adhesion molecule-1 (ICAM-1) (Collins *et al.*, 2000), vascular cell adhesion molecule-1 (VCAM-1) (Preiss *et al.*, 2007), and the P- and E-selectins (Dong *et al.*, 1998). Monocytes and T-lymphocytes adhere to the endothelium and migrate into the sub-endothelial space under the influence of chemoattractant molecules such as monocyte chemotactic protein-1 (MCP-1) (Gu *et al.*, 1998) and osteopontin (Giachelli *et al.*, 1998). In addition, there is increased lipid transport across the endothelium resulting in an accumulation in the sub-endothelial space (Mora *et al.*, 1987). Within the intima of the vessel, monocytes mature into macrophages and proliferate under the influence of macrophage colony-stimulating factor (M-CSF). These tissue macrophages act as scavenger cells, taking up oxidised-LDL cholesterol, via the CD36 receptors present on their surface (Nicholson *et al.*, 1995), and forming the characteristic foam cells of the early fatty streaks of atherosclerosis (Figure 1.2B). Activation of macrophages and T-lymphocytes results in expression of a variety of pro-inflammatory cytokines and growth factors, including tumour

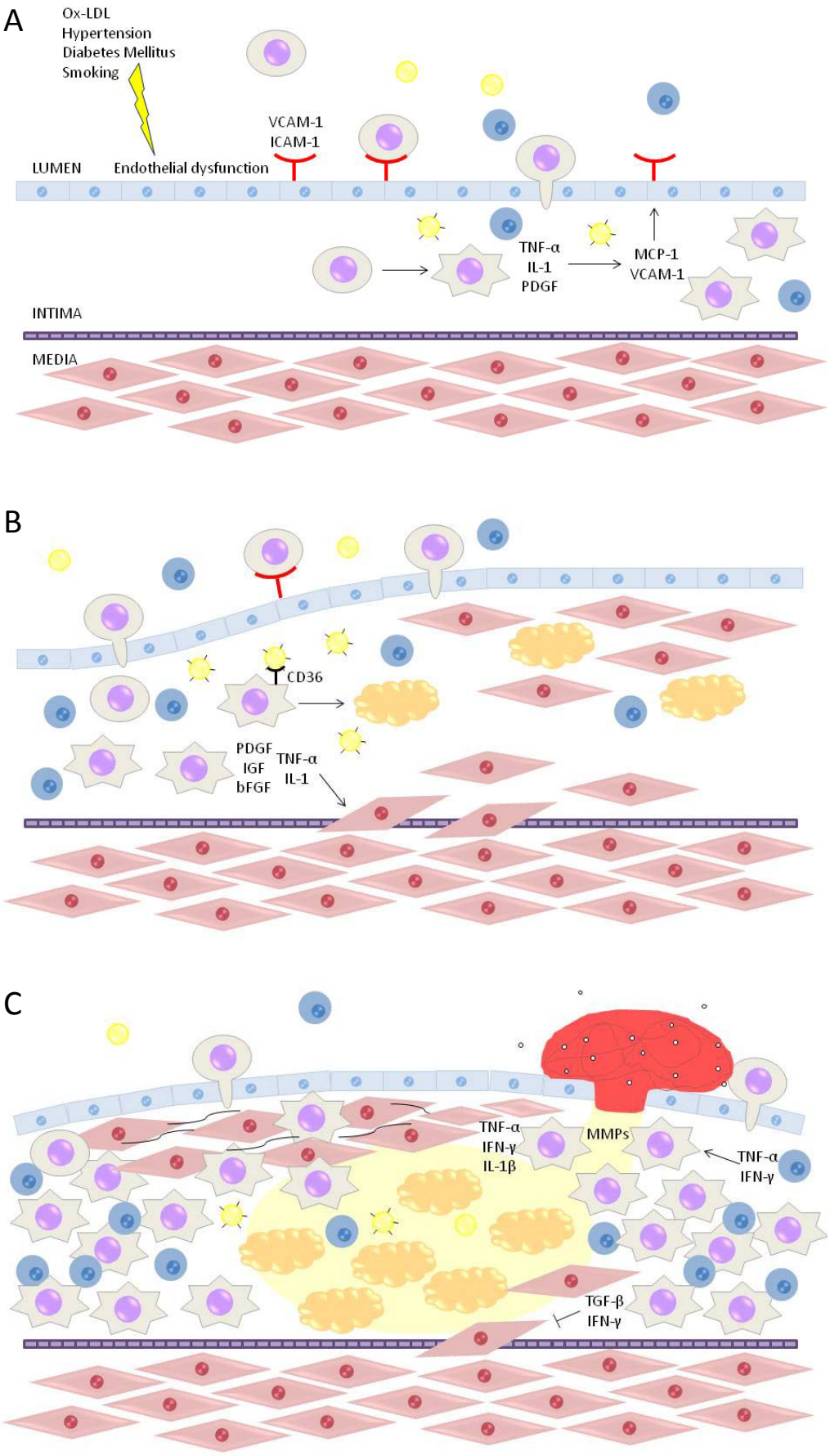
A
Ox-LDL
Hypertension
Diabetes Mellitus
Smoking
VCAM-1
ICAM-1
LUMEN
Endothelial dysfunction
TNF-α
IL-1
PDGF
MCP-1
VCAM-1
INTIMA
MEDIA
B
CD36
PDGF
IGF
bFGF
TNF-α
IL-1
C
TNF-α
IFN-γ
IL-1β
MMPs
TNF-α
IFN-γ
TGF-β
IFN-γ

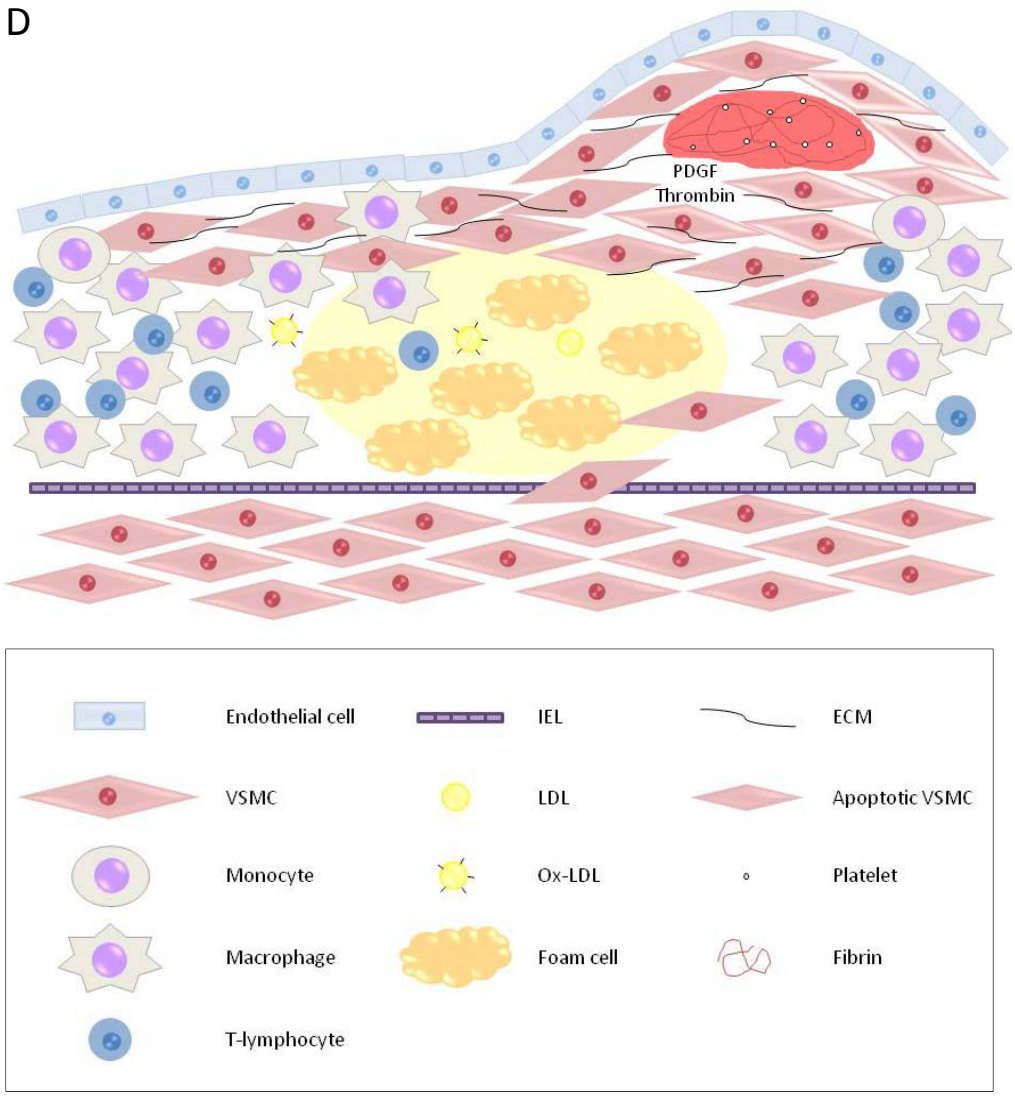

Figure 1.2: Pathogenesis of atherosclerosis.
A: Endothelial dysfunction results in an increased permeability to monocytes, T-lymphocytes and low density lipoprotein (LDL) cholesterol, allowing accumulation in the intima of the vessel wall. Monocyte-derived macrophages and T-lymphocytes propagate the inflammatory response by proliferating and promoting further leukocyte infiltration, through release of cytokines and chemokines. B: Macrophages mobilise vascular smooth muscle cells (VSMC) from the media and stimulate their proliferation, and scavenge oxidised (ox)-LDL to form foam cells. C: Continuation of the inflammatory response, lipid accumulation and VSMC recruitment, results in the development of a fibrous plaque; with a lipid-rich necrotic core and fibrous 'cap'. However, T-lymphocytes and macrophages can promote plaque rupture by inducing VSMC apoptosis and extracellular matrix (ECM) degradation, and inhibiting further VSMC recruitment and proliferation. Exposure of the lipid-rich core of the plaque to the circulation will trigger platelet activation and coagulation, resulting in the formation of a thrombus of activated platelets and fibrin. D: Activated platelets can stimulate VSMC migration, proliferation and ECM deposition to form a new fibrous plaque. IEL: internal elastic lamina, VCAM-1: vascular cell adhesion molecule-1, ICAM-1: intercellular adhesion molecule-1, TNF-α: tumour necrosis factor-α, IL-1: interleukin-1, PDGF: platelet-derived growth factor, MCP-1: monocyte chemotactic protein-1, IGF: insulin-like growth factor, bFGF: basic fibroblast growth factor, IFN-γ: interferon-γ, TGF-β: transforming growth factor-β, MMPs: matrix metalloproteinases.

necrosis factor alpha (TNF-α), platelet-derived growth factor (PDGF) and interleukin (IL)-1, which recruit and activate additional inflammatory cells, and stimulate VSMCs and endothelial cells to produce further inflammatory mediators (Libby, 2000). This leads to the formation of the first stage of atherosclerotic lesions, the fatty streak, comprising lipid-filled macrophages and T-lymphocytes. At this stage lesion development is reversible but with continued exposure to atherosclerosis risk factors, the inflammatory response cannot overcome the chronic vessel wall injury and so continues indefinitely.

1.1.2.4.2 *Progression of atherosclerosis*

As injury and the inflammatory response continue, macrophages and lymphocytes continue to migrate from the blood into the lesion and release a cascade of chemotactic and proliferative growth factors and cytokines (including PDGF (Ferns *et al.*, 1991), insulin-like growth factor (IGF) (Bornfeldt *et al.*, 1992), basic fibroblast growth factor (bFGF) (Lindner *et al.*, 1991), TNF-α and IL-1 (Fukumoto *et al.*, 1997)) that stimulate VSMCs to migrate to, and proliferate in, the intima (Figure 1.2B). This leads to the development of a fibrous plaque with a VSMC-rich cap, which plays a pivotal role in maintaining plaque stability and protecting against plaque rupture. VSMCs in the intima change from a 'contractile' to a 'synthetic' phenotype and secrete ECM, including elastin and collagen (Newby *et al.*, 2000). Therefore, although VSMCs play a large role in the development of the lesion by producing pro-inflammatory mediators, they also play a major role in the creation of the fibrous cap through synthesising matrix molecules. It is not clear whether these VSMCs originate from the media or are derived from circulating smooth muscle progenitor cells (Dzau *et al.*, 2002). In addition, continuation of the inflammatory response, increasing numbers of macrophages and T-lymphocytes and release of pro-inflammatory cytokines, eventually leads to further damage and focal necrosis (Ross, 1999). Necrosis of foam cells releases their internalised lipids along with the pro-inflammatory contents of the foam cell, contributing to the cholesterol-rich lipid core (Witztum, 1994). The exact mechanism behind macrophage apoptosis, preceding secondary necrosis, remains incompletely understood but has been suggested to be a reaction to oxidised-LDL overload (Colles *et al.*, 2001; Salvayre *et al.*, 2002).

Therefore, as the pro-inflammatory environment is maintained by the activated macrophages, T-lymphocytes and VSMCs, the lesion develops into a characteristic fibrous plaque, with a fibrous cap overlying a lipid-rich necrotic core (Figure 1.2C). This can be compensated somewhat by dilation of the artery, maintaining the lumen (Glagov *et al.*, 1987). These fibrous lesions can, however, develop to the point where the artery can no longer compensate by dilatation and the plaque encroaches into the lumen, altering blood flow.

1.1.2.4.3 *Plaque rupture*

As mentioned previously, the vulnerability of a plaque to rupture is largely determined by its composition, rather than size. Indeed, the majority of acute myocardial infarctions result from atheroma that cause < 50% stenosis, as assessed by angiography (Libby, 2000). Compositional factors which influence the susceptibility of a plaque to rupture include: size of the lipid core, thickness and collagen content of the fibrous cap and extent of inflammation (Falk *et al.*, 1995). Aortic plaques containing a core occupying >40% of the plaque are considered particularly vulnerable and at a high risk of rupture and thrombosis (Davies *et al.*, 1993). Fibrous caps are well-recognised to be most vulnerable at the thin, "shoulder" regions, highlighting the importance of cap thickness in plaque stability (Richardson *et al.*, 1989). In addition, the VSMC content and collagen content of fibrous caps are important markers of plaque vulnerability as they provide biomechanical strength to the cap and resistance to local mechanical stresses created by blood flow and pressure (Libby, 2000). Indeed, disrupted aortic caps having been shown to contain less VSMCs and collagen than intact caps (Burleigh *et al.*, 1992; Davies *et al.*, 1993). Inflammatory cells can reduce plaque stability in a number of ways (Figure 1.2C). Activated T-cells may stimulate metalloproteinase (MMP) production by macrophages in lesions leading to enzymatic degradation of ECM proteins in the fibrous cap (Libby, 1995). Pro-inflammatory cytokines, in particular interferon-γ (IFN-γ) and transforming growth factor (TGF)-β, released from macrophages inhibit VSMC proliferation, while inhibiting or promoting collagen synthesis, respectively (Amento *et al.*, 1991; Newby, 2000). Activated macrophages can induce VSMC apoptosis by direct cell-cell contact (Boyle *et al.*, 2001) and by releasing the

cytokines IFN-γ, IL-1β and TNF-α (Geng *et al.*, 1996). This is further compounded by the fact that VSMCs in the fibrous cap of a mature plaque have an enhanced susceptibility to apoptosis and a reduced ability to proliferate (Bennett *et al.*, 1998).

Most deaths from atherosclerosis transpire as a result of occlusive thrombus formation following plaque rupture (Weissberg, 2000). Exposure of the lipid core to the circulation immediately causes platelet activation and aggregation and activation of the coagulation pathway, resulting in thrombosis (Figure 1.2D). The ensuing complications include MI, stroke and acute peripheral vascular occlusion. However, it is now clear that clinically silent non-occlusive plaque rupture plays a role in plaque growth (Burke *et al.*, 2002; Mann *et al.*, 1999). PDGF and thrombin can act to induce further VSMC recruitment, proliferation and ECM synthesis (Ferns *et al.*, 1991; Fingerle *et al.*, 1989; Kanthou *et al.*, 1995), thus stimulating the formation of a new fibrous cap (Figure 1.2D). The atherosclerotic plaque can, therefore, expand due to repeated episodes of rupture and repair, leading to the development of a complicated lesion.

1.1.2.5 Current treatments of atherosclerosis

Primary prevention (i.e. preventing or delaying the clinical disease among asymptomatic patients) of atherosclerosis is largely focussed on promoting lifestyle changes including weight loss, increased exercise, smoking cessation and dietary modification. Secondary prevention of atherosclerosis, in patients with established CVD or a high risk of developing CVD (e.g. patients with diabetes mellitus), can also incorporate pharmacological intervention to manage hypertension (e.g. ACE inhibitors, β-blockers), to reduce heart work load (nitrates), to lower circulating lipids (statins) and to reduce thrombotic risk (anti-platelet/anti-coagulant therapy; aspirin, warfarin). Anti-platelet and fibrinolytic therapy is also administered following MI in an attempt to re-open the blocked coronary artery.

Surgical intervention is often used in patients with severe angina or after an acute MI. Coronary artery bypass graft (CABG) surgery uses saphenous vein or mammary artery grafts from the patient to bypass the blocked coronary artery. This procedure is often used in patients with multiple vessel disease. A less invasive approach is PCI,

based on the technique of percutaneous transluminal balloon angioplasty introduced by Andreas Gruntzig (Gruntzig *et al.*, 1979). The procedure entails the dilation of a stenosed artery by inflation of an intra-luminal balloon catheter, introduced from a femoral arteriotomy via a guidewire. PCI has become the most commonly used intervention for coronary artery disease, with over 80,000 performed in the UK in 2008 (www.heartstats.org). Although PCI has revolutionised the treatment of atherosclerosis, it has been limited by a high incidence (30-50%) of re-occlusion (restenosis) of the vessel, thereby requiring further re-vascularisation intervention. The introduction of vascular stents has successfully reduced the need for re-vascularisation (from 21% to 10% at 1 year in the BENESTENT trial (Macaya *et al.*, 1996)). However, restenosis remains a significant problem, affecting 10-30% patients who receive stents (Bhargava *et al.*, 2003).

1.1.3. **Restenosis**

Restenosis is the re-occlusion of an artery following PCI for the treatment of atherosclerosis. It is understood to occur via several mechanisms including elastic recoil, negative remodelling, early thrombosis and neointimal hyperplasia (Kibos *et al.*, 2007). To address these problems, bare metal stents (BMS) were introduced to provide a rigid luminal scaffold for the vessel. While BMS successfully reduce elastic recoil and negative remodelling in nearly all patients (Fischman *et al.*, 1994; Hoffmann *et al.*, 1996), thrombosis and neointimal hyperplasia remain a significant burden on the success of using stents. In fact, stent implantation augments the fibro-proliferative response by inducing a more intense and prolonged inflammatory state (Welt *et al.*, 2002) due to the severity of injury and the persistence of a foreign body in the vessel wall (Schwartz *et al.*, 1992b). Understanding the pathogenesis of the neointimal proliferation that defines in-stent restenosis is critical for the development of anti-restenotic therapies to improve the clinical outcome following PCI.

1.1.3.1 Pathogenesis of neointimal proliferation

The pathophysiology of neointimal proliferation is complex and incompletely understood but is thought to involve thrombosis, inflammation, cellular proliferation and extracellular matrix production, all of which contribute to lumen loss. In 1992, Schwartz *et al* postulated a hypothesis for the mechanism of neointimal proliferation

following vascular injury (Schwartz *et al.*, 1992a). In his hypothesis there are three stages in neointimal lesion formation; thrombotic (stage I), cellular recruitment (stage II) and proliferative (stage III). It is suggested that the thrombotic stage occurs immediately after, and as a direct consequence of, endothelial damage. This leads to formation of a thrombus composed of aggregated platelets, fibrin and trapped erythrocytes. The second stage of healing comprises cellular recruitment into the thrombus itself. Firstly, re-endothelialisation occurs at the thrombus/blood boundary, followed by recruitment of monocytes (later macrophages) and lymphocytes. The macrophages are responsible for thrombolysis and phagocytosis of thrombus components. The cellular infiltrates, as well as the thrombus, are likely to secrete growth factors and chemo-attractants which facilitate further recruitment of cells (including smooth muscle cells). The final stage involves cellular proliferation, as the thin fibrous cap of smooth muscle cells thickens, and elaboration of extracellular matrix, eventually resulting in a mature, smooth muscle-rich neointima.

1.1.3.1.1 *Thrombosis*

Vascular injury exposes sub-endothelial collagen and tissue factor to the circulation, triggering the coagulation cascade and platelet adhesion and activation. This results in the formation of a thrombus composed of activated platelets, fibrin and trapped erythrocytes. More details on the pathways involved in thrombus formation are described below (section 1.1.4). In addition, endothelial denudation will result in the loss of anti-thrombotic factors (e.g. NO, PGI_2 and tissue plasminogen activator (tPA)), further contributing to thrombus formation (Weintraub, 2007). Activated platelets release a variety of mitogens/chemoattractants which promote monocyte and smooth muscle cell migration and proliferation: PDGF is a potent VSMC chemoattractant and its expression in VSMCs has been shown to peak in accordance with peak neointimal cellular proliferation (Uchida *et al.*, 1996); TGF, TXA_2, thrombin and serotonin have been described to promote VSMC proliferation (Chandrasekar *et al.*, 2000); P-selectin is implicated in platelet-leukocyte interactions and its deficiency has been shown to reduce neointimal proliferation (Kumar *et al.*, 1997a); and platelet-derived IL-1 plays a key role in mediating the inflammatory response at the site of vascular injury (Loppnow *et al.*, 1998). Therefore, the initial

thrombus that develops as a result of endothelial damage clearly has the potential to contribute to neointimal development. In addition, Schwartz *et al* postulate that the thrombus plays a further role by acting as a "scaffold" into which VSMCs and leukocytes can migrate and proliferate to form the neointima (Schwartz *et al.*, 1992a). Certainly, several anti-coagulant/anti-platelet treatments reduce neointimal proliferation in animal models, including low molecular weight heparin and hirudin (Buchwald *et al.*, 1996), acetylsalicylic acid (Clopath, 1980), aurintricarboxylic acid (Matsuno *et al.*, 1998) and anti-platelet serum (Moore *et al.*, 1976). However, several anti-coagulant/anti-platelet regimens have been investigated in clinical trials and shown to have no effect on restenosis (Kastrati *et al.*, 1997; Schwartz *et al.*, 1988). Only one, the platelet aggregation inhibitor cilostazol, has shown an anti-restenotic effect, but this has been attributed to its direct anti-proliferative influence on VSMCs (Take et al., 1997; Tsuchikane et al., 1999). Therefore, whether thrombus formation is obligatory for neointima development is open to debate.

1.1.3.1.2 *Inflammation*

The recruitment and activation of leukocytes induced by vascular injury has been shown to play a critical role in the pathogenesis of neointimal proliferation (Wainwright *et al.*, 2001; Welt *et al.*, 2002). Indeed, in a rmodel of stent-induced injury, monocyte presence in the vessel wall has been shown to parallel proliferation and intimal thickening (Rogers *et al.*, 1998). In clinical studies, circulating monocyte counts after stenting show a positive correlation with neointima area 6 months after PCI (Fukuda *et al.*, 2009). Studies using animal models show leukocytes infiltrate rapidly following vascular injury, with neutrophils observed within 6-24 hours (Cole *et al.*, 1987; Welt *et al.*, 2000) and T-lymphocytes (Tanaka *et al.*, 1993) and monocytes (Miller *et al.*, 1996) after 2-14 and 3-8 days, respectively. In the clinic, leukocytes are activated in patients 24-48 hours after angioplasty (De Servi *et al.*, 1990; Steg *et al.*, 1993). Inflammatory cell recruitment and infiltration are mediated by a number of mechanisms (Welt *et al.*, 2002): interaction with platelet p-selectin via Mac-1 adhesion molecule; release of MCP-1 and IL-8 from VSMCs, endothelial cells and leukocytes; and up-regulation of the endothelial adhesion molecules ICAM-1, VCAM-1 (Tanaka *et al.*, 1993) and E-selectin (Wainwright *et al.*, 2001).

Once recruited and activated, leukocytes produce a wide range of vasoactive substances, including oxygen-derived free radicals, proteolytic enzymes, growth factors, cytokines and chemokines, which may contribute to neointima development. In pathological studies, markers of inflammation in arterial tissue correlate strongly with restenosis after angioplasty or stenting (Farb *et al.*, 2002; Moreno *et al.*, 1996). Indeed, plasma concentrations of inflammatory markers MCP-1, IL-6, IL-1β, M-CSF and C-reactive protein are elevated following PCI and predict the incidence of restenosis (Hojo *et al.*, 2001; Kochiadakis *et al.*, 2007; Pietersma *et al.*, 1995; Suzuki *et al.*, 2000). Also, expression levels of TNF-α, IL-1β and IL-6 are up-regulated following angioplasty in humans and animal models (Wainwright *et al.*, 2001; Wang *et al.*, 2007a). A number of these cytokines, including M-CSF, TNF-α and IL-1β induce smooth muscle cell proliferation (Ikeda *et al.*, 1990; Selzman *et al.*, 1999; Shiba *et al.*, 2007) and administration of these factors augments neointima development in animal models (Fukumoto *et al.*, 1997; Shiba *et al.*, 2007). In addition, IL-6 stimulates VSMC migration (Ikeda *et al.*, 1991; Wang *et al.*, 2003). Furthermore, a number of these inflammatory markers can stimulating further leukocyte recruitment: MCP-1 is a potent monocyte chemoattractant and activator (Gu *et al.*, 1998); TNF-α and IL-1β increase adhesiveness of leukocytes to the endothelium through elevated ICAM-1 and VCAM-1 expression (Wainwright *et al.*, 2001); and IL-1 can promote T-lymphocyte intimal recruitment (Rao *et al.*, 2008).

The importance of inflammation in neointimal proliferation can be demonstrated in animal models, with dramatic reductions in lesion development following depletion of leukocytes (Miller *et al.*, 2001; Wolff *et al.*, 2004). Moreover, reduced neointimal lesion size has been reported after targeted disruption/inhibition of inflammatory mediators including p-selectin (Hayashi *et al.*, 2000; Wang *et al.*, 2005b), Mac-1 (Golino *et al.*, 1997; Rogers *et al.*, 1998), VCAM-1 (Oguchi *et al.*, 2000), ICAM-1 (Yasukawa *et al.*, 1997; Zou *et al.*, 2000), MCP-1 (Egashira *et al.*, 2007; Grassia *et al.*, 2009) or its receptor chemokine (C-C motif) receptor 2 (CCR2) (Liehn *et al.*, 2010; Schepers *et al.*, 2006), IL-1 receptor (Chamberlain *et al.*, 2006; Morton *et al.*, 2005), TNF-α (Lambert *et al.*, 2010) and M-CSF (Shiba *et al.*, 2007). Indeed, inflammation is a key target in current anti-restenotic approaches in the clinic.

1.1.3.1.3 *VSMCs and matrix deposition*

VSMCs are undoubtedly involved in neointimal proliferation as they are the main cell type present in mature neointimal lesions in animal models (Carmeliet *et al.*, 1997c; Lindner *et al.*, 1993; Sata *et al.*, 2000) and in restenotic lesions induced by PCI in the clinic (Gravanis *et al.*, 1989; Ueda *et al.*, 1991). As previously mentioned, leukocytes recruited to the site of injury, as well as activated platelets of the thrombus, secrete growth factors and chemoattractants which facilitate the recruitment of VSMCs. Schwartz *et al* postulate that the VSMCs initially form a "cap" on the luminal edge of the thrombus, before migrating and proliferating inwards, towards the media (Schwartz *et al.*, 2002). In addition, VSMCs actively contribute to neointimal development by propagating the inflammatory and proliferative response, through secretion of adhesion factors, cytokines and mitogens. These include the aforementioned IL-1β, IL-6, TNF-α, MCP-1 and M-CSF as well as bFGF (Libby *et al.*, 1992; Lindner, 1995). The importance of VSMC proliferation can be demonstrated by the reduction in neointimal lesion size with the anti-proliferative drugs paclitaxel (Axel *et al.*, 1997) and rapamycin (Burke *et al.*, 1999), in animal models of neointimal proliferation. Indeed these two drugs are used clinically in drug-eluting stents (DES) to prevent in-stent restenosis (section 1.1.3.2). Paclitaxel binds to and stabilises microtubules of the mitotic spindle thereby inhibiting cell division (Choritz *et al.*, 2010). Rapamycin inhibits mammalian target of rapamycin (mTOR), thereby interfering with the transcription of genes involved in VSMC proliferation. By this mechanism, rapamycin also inhibits the proliferation of T-lymphocytes, contributing to its anti-restenotic effect (Martinet *et al.*, 2007).

As well as providing neointimal mass, VSMCs also contribute to the development of neointima through their deposition of ECM; collagen, elastin and proteoglycans (Bentzon *et al.*, 2010b). A key chemokine mediating ECM production from VSMCs is TGF-β (Bobik, 2006). Its contribution to restenosis is suggested by up-regulation of TGF-β isoforms and their receptors following balloon injury in rats (Ward *et al.*, 1997). In addition, over-expression of TGF-β increases neointima development (Nabel *et al.*, 1993), while TGF-β mRNA degradation (Yamamoto *et al.*, 2000) and suppression of TGF-β expression (Backes *et al.*, 2010) attenuate lesion development.

Somewhat paradoxically, enzymatic degradation of the ECM in the basement membrane and media is likely an important process in migration of VSMCs and subsequent intimal hyperplasia. There is evidence that several MMPs are involved in this process: MMP-9, MMP-2 and membrane type 1 (MT1)-MMP expression increase following arterial injury in rats (Shofuda *et al.*, 1998; Zempo *et al.*, 1994); inhibition or deficiency of MMP-9 or MMP-2 inhibits neointima development in animal models (Cho *et al.*, 2002; Galis *et al.*, 2002; Johnson *et al.*, 2004; Mason *et al.*, 1999); MT1-MMP$^{+/-}$ mice have reduced neointima development (Filippov *et al.*, 2005); tissue inhibitor of matrix metalloproteinase-1 (TIMP-1) administration attenuates neointimal proliferation (Furman *et al.*, 2002). In addition to MMPs, serine proteases have been implicated in VSMC migration and neointima formation. The urokinase plasminogen activator (uPA) receptor (uPAR) is required for VSMC migration and proliferation (Kenagy *et al.*, 2002; Okada *et al.*, 1995) and expression of uPA and uPAR is increased at the site of arterial injury (Plekhanova *et al.*, 2001). Indeed, uPA$^{-/-}$ and plasminogen$^{-/-}$ mice have reduced intimal hyperplasia following injury (Lijnen *et al.*, 1998). In addition, uPA and plasmin can mediate VSMC migration by directly activating a number of MMPs (Lijnen *et al.*, 1998).

Intimal VSMCs found in neointimal lesions are generally accepted to be of a "synthetic" phenotype, rather then the "contractile" phenotype of medial VSMCs (Shanahan *et al.*, 1998; Weintraub, 2007). Characteristically, these VSMCs resemble immature, dedifferentiated VSMCs and have lower levels of contractile proteins, contain fewer myofilaments, and produce 4 to 5 times more ECM than their contractile counterparts (Schwartz *et al.*, 1986), but are defined as "smooth muscle" due to their immunoreactivity for α-smooth muscle actin. The source of VSMCs in neointimal lesions is under debate. There have been recent suggestions that they differentiate from the circulating bone marrow-derived inflammatory cells which infiltrate the vasculature during the initial response to injury (Sahara *et al.*, 2007; Sata *et al.*, 2002; Tanaka *et al.*, 2003). However, there are critics of this proposal who claim to have refuted the existence of bone marrow-derived smooth muscle cells in vascular lesion, suggesting methodological discrepancies account for the confusion (reviewed in (Bentzon *et al.*, 2010b)). Instead, many still believe intimal

VSMCs are derived from mature, medial smooth muscle cells, which have undergone phenotypic modulation, based on seminal papers from the '70s and '80s (Clowes *et al.*, 1989; Clowes *et al.*, 1986; Clowes *et al.*, 1983; Schwartz *et al.*, 1975). Support for this hypothesis comes from observations that cultured adult VSMCs spontaneously undergo a phenotypic change, assuming a number of the characteristics of intimal VSMCs *in vivo* (Chamley-Campbell *et al.*, 1979). This change is thought to be a response to several stimuli, including endothelial denudation (Thyberg, 1998), arterial stretching (Birukov *et al.*, 1995), exposure to mitogens, such as PDGF and bFGF, and remodelling of the ECM (Thyberg, 1998).

1.1.3.2 Current anti-restenotic approaches

As mentioned previously, although BMS virtually eliminate the elastic recoil and negative remodelling aspects of restenosis following PCI, neointimal hyperplasia, or in-stent restenosis, is exacerbated by stent implantation. Subsequently, drug-eluting stents (DES) were developed to target the proliferative response to stent implantation. Briefly, DES are metal stents coated with a polymer containing a pharmacological agent, which is slowly released into the vessel wall. The most widely used DES are coated with the immunosuppressive agent, rapamycin (also known as sirolimus) or the anti-mitotic agent, paclitaxel (Llau *et al.*, 2010). Indeed, angiographic coronary restenosis rates have fallen below 10% with the used of DES in several randomised trials (Newsome *et al.*, 2008; Roy *et al.*, 2007; Stone *et al.*, 2007) and a meta-analysis revealed a 70% reduction in the requirement for target vessel revascularisation (TVR) with DES when compared with BMS (Indolfi *et al.*, 2005).

However, angiographic improvement in restenosis by DES has not been translated into a reduction in clinical cardiac events, such as MI and death. In addition, several concerns have been raised with regard to DES, including, inflammation, delayed healing and endothelialisation, endothelial dysfunction and late acquired incomplete stent malapposition (LASMA) (Carlsson *et al.*, 2007; Rodriguez, 2009). Moreover, observational and randomised studies have demonstrated higher rates of late (>1 month post PCI) and very late (>1 year post PCI) stent thrombosis with the use of DES (Thuesen *et al.*, 2010), which can be translated into a high incidence of death

and MI (Rodriguez, 2009). With that, dual anti-platelet therapy (aspirin and thienipyridines) is required for a minimum of 6 months to 1 year after DES implantation. In addition, ~30-35% of PCI candidates have either restrictions or contraindications for DES implantation, for example diabetics and patients with long (>20mm) lesions or with existing in-stent restenosis (Rodriguez, 2009).

To address these limitations, a new generation of DES has been developed, characterised by improvement in the stent platform, polymer (biodegradable) and drug. Examples include everolimus-eluting stents (EES) and zotarolimus-eluting stents (ZES) (Dangas *et al.*, 2010). Everolimus and zoterolimus are derivatives of sirolimus, thus function as anti-proliferative and immunosuppressant mTOR inhibitors (Chen *et al.*, 2007; Martinet *et al.*, 2007). Indeed, recent large randomised studies have shown that the new generation EES is superior to the first generation paclitaxel-eluting stents (PES) in terms of TVR, MI and stent thrombosis (Kedhi *et al.*, 2010). Importantly, it has been suggested that a moderate suppression, rather than a strong reduction in neointimal growth, will achieve the right balance of attenuating luminal loss while reducing the thrombotic risk (Rodriguez *et al.*, 2009).

Additionally, systemic anti-inflammatory and immunosuppressive therapies, which were originally trialled in the BMS era, are still being considered as alternatives to DES. The main candidates are: the aforementioned immunosuppressant, sirolimus; the glucocorticoid, prednisolone, and the selective phosphodiesterase 3 inhibitor, cilostazol. The influence of systemic sirolimus therapy on restenosis following BMS implantation and on recurrent in-stent restenosis has been assessed in a number of clinical trials, all demonstrating a significant reduction of restenosis, TLR and major adverse cardiac and cerebrovascular events (MACCE) (Hausleiter *et al.*, 2004; Rodriguez *et al.*, 2006; Waksman *et al.*, 2004). Systemic prednisone therapy has been investigated in the two IMPRESS studies, concluding that oral prednisone therapy in patients undergoing coronary BMS implantation significantly reduced the risk of MACCE, TVR and restenosis, over those in the placebo group (Ferrero *et al.*, 2009; Ribichini *et al.*, 2005; Versaci *et al.*, 2002). In the CREST study, cilostazol-treated patients with stent implantation experienced a 52% reduction in the risk of

restenosis, compared to placebo-treated patients (Douglas *et al.*, 2005). As cilostazol acts by inhibiting platelet aggregation, it has also shown potential as an alternative to dual anti-platelet treatment in preventing thrombotic events (Jeong *et al.*, 2009), for example in patients with clopidogrel resistance.

1.1.4. **Thrombosis**

Thrombus formation is the key contributor to haemostasis following vascular damage, alongside vasoconstriction. As has been described previously, thrombosis also plays a significant role in the pathogenesis of both atherosclerosis and restenosis. In addition, most clinical manifestations of atherosclerosis arise as a direct result of thrombosis following plaque rupture: for example, MI and stroke. Also, in-stent thrombosis is a major concern associated with DES. Indeed, anti-thrombotic therapies such as aspirin and clopidogrel are currently used clinically for the management of atherosclerosis and the prevention of in-stent thrombosis.

Thrombosis involves the formation of a 'platelet plug' at the site of injury, which is then stabilised by cross-linked fibrin. The pathways involved in thrombosis are relatively well understood and involve a complex interaction between the endothelium, platelets, inflammatory cells and the coagulation cascade. Resolution of a thrombus is mediated by the fibrinolytic pathway and inflammatory cells.

1.1.4.1 Endothelium

Under normal conditions the endothelium sustains a vasodilatory and local fibrinolytic state in which platelet activation, coagulation and inflammation are suppressed. A non-thrombogenic endothelial surface is maintained though a number of mechanisms: (1) vasodilatation by production of NO, PGI_2, PDHF; (2) prevention of platelet adhesion and activation by adenosine, NO, PGI_2; (3) prevention of leukocyte adhesion and transmigration by NO, IL-10; (4) attenuation of thrombin formation through production of tissue factor pathway inhibitor (TFPI), activation of protein C (to activated protein C (APC)) via thrombomodulin, activation of antithrombin III; (5) inhibition of fibrin deposition though local production of tPA and uPA; and (6) efficient scavenging of oxygen radicals by NO, urate and superoxide dismutase (SOD) (Becker *et al.*, 2000).

In contrast, endothelial dysfunction/damage induces a pro-thrombotic state, characterised by: (1) vasoconstriction due to release of platelet activating factor (PAF) and endothelin-1; (2) platelet and leukocyte adhesion and activation by up-regulation of PAF, von Willebrand factor (vWF), P-selectin, E-selectin, ICAM-1, IL-8, MCP-1, TNF-α; (3) promotion of thrombin formation and fibrin deposition by increased expression of tissue factor (TF), plasminogen activator inhibitor-1 (PAI-1), vWF and Factor (F)V (Wakefield *et al.*, 2008). In addition, endothelial damage exposes the pro-adhesive platelet-activating subendothelial matrix of TF, vWF, and collagens (Becker et al., 2000).

1.1.4.2 Platelets

Platelets (thrombocytes) play a critical role in thrombosis by becoming activated and aggregating to form a 'platelet plug' in response to endothelial damage. This process is referred to as *primary haemostasis*. Circulating platelets initially adhere to vWF of the exposed basement membrane via their glycoprotein (GP) Ib/XI/V receptors. This interaction promotes platelet expression of the GP IIb/IIIa receptor, which binds vWF and collagen, stabilising adhesion of platelets to the vessel wall (Jennings, 2009). These adhesions activate the platelet, stimulating a conformational change from smooth discs into irregular spheroids that protrude filopodia rich in GP IIb/IIIa receptors. These enhance adhesion and mediate platelet-platelet interactions, or platelet 'aggregation' (Brisson *et al.*, 1997).

Activated platelets also release a plethora of factors which influence thrombosis (reviewed in (Anitua *et al.*, 2004)), including an array of agonists (adenosine diphosphate (ADP), TXA_2, PAF) and their receptors, which propagate a platelet activation chain reaction. An important additional platelet agonist is thrombin, which is generated by the prothrombinase complex on the surface of platelets as part of the coagulation cascade. Thrombin activates platelets by cleaving the protease-activated receptors (PAR), PAR1 and PAR4. Platelet activation also induces the expression of adhesive molecules (GPs, P-selectin, fibrinogen, thrombospondin, vWF), which enables platelets to aggregate and interact with other cell types and, importantly, allows fibrin to stabilise the aggregated 'platelet plug'. In fact, thrombin and fibrin generation is localised to the surface of platelets by their release of clotting factors

FV and FXI. Platelets also regulate coagulation through inhibitors of the coagulation cascade (antithrombin III and TFPI) and mediators and inhibitors of the fibrinolysis pathway (uPA, PAI-1, α_2-antiplasmin) (section 1.1.4.5).

1.1.4.3 Coagulation cascade

The coagulation cascade of *secondary haemostasis* is a series of sequential reactions in which zymogens of serine proteases are activated, ultimately resulting in the formation of cross-linked fibrin, which acts to stabilise the aforementioned 'platelet plug'. It was originally proposed that coagulation occurs secondary to platelet activation, however it has now been suggested that these two events happen simultaneously (Furie *et al.*, 2005). The coagulation cascade is classically divided into three pathways, the 'contact activation (intrinsic) pathway' and the 'tissue factor (extrinsic) pathway', both of which activate the 'final common pathway' of FX, thrombin and fibrin (Figure 1.3).

The contact activation pathway is initiated when blood comes into contact with sub-endothelial collagen. A complex of prekallikrein and high-molecular-weight kininogen (HMWK) also interacts with the exposed ECM, activating FXII. FXIIa goes on to sequentially activate FXI and FIX. FIXa, with its glycoprotein FVIII cofactor (activated by thrombin), then activates FX (Ahmad *et al.*, 2003). The importance of the contact activation pathway in thrombosis is demonstrate by the bleeding disorders haemophilia A and B, which result from a deficiency in FVIII and FIX, respectively (Gailani *et al.*, 2007).

The tissue factor pathway is activated when plasma is exposed to extra-vascular TF, constitutively expressed by medial VSMC, pericytes and adventitial fibroblasts (Mackman *et al.*, 2007). Plasma FVII is subsequently activated and forms a TF/FVIIa complex. This complex instantaneously goes on to catalytically activate FX. The main function of the tissue factor pathway is to augment the contact activation pathway. Under physiological conditions vascular cells which are in contact with the blood do not express TF. In contrast, under pathological conditions a number of vascular cells are induced to express TF, including leukocytes, endothelial cells and platelets (Mackman *et al.*, 2007), which may influence the thrombotic state

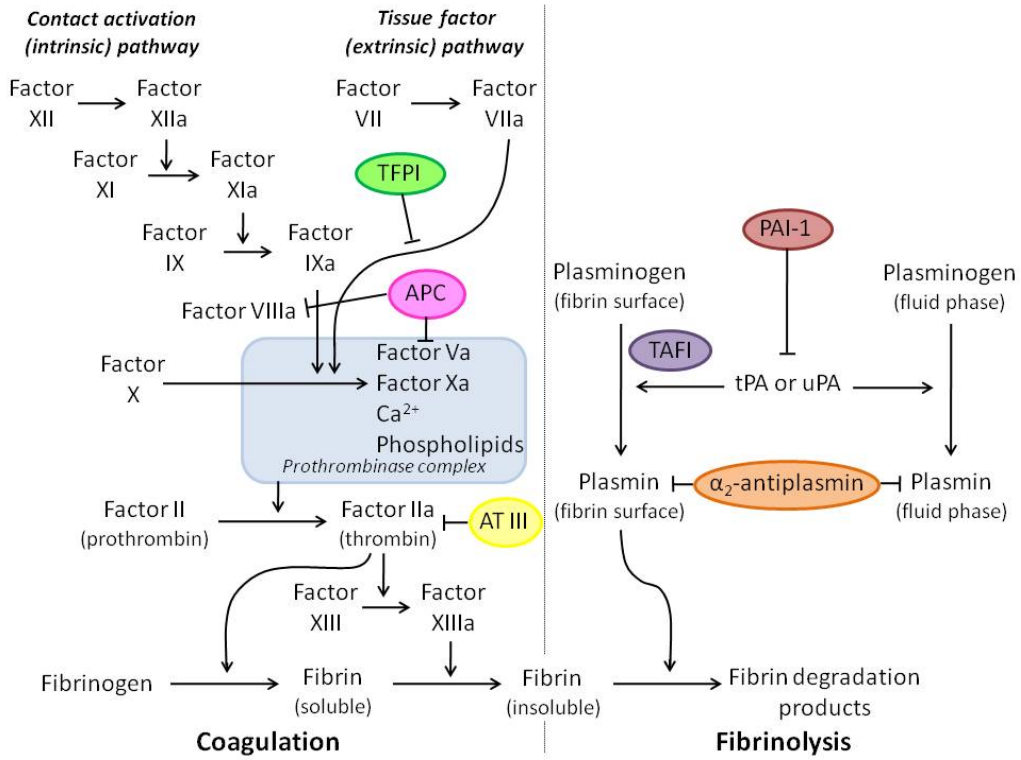

Figure 1.3: Coagulation cascade and fibrinolysis pathway.
The coagulation cascade mediates the formation of cross-linked fibrin through sequential activation of serine proteases. Coagulation is activated when plasma contacts the sub-endothelial surface (contact activation pathway) or extra-vascular tissue factor (tissue factor pathway). Both lead to the activation of factor X, which interacts with activated factor V and phospholipids to form the 'prothrombinase complex'. This complex activates thrombin from its zymogen in a Ca^{2+}-dependent reaction. Thrombin goes on to catalyse the conversion of fibrinogen to fibrin and the activation of factor XIII (factor XIIIa), which cross-links the fibrin strands. Coagulation is regulated by the inhibitors: tissue factor pathway inhibitor (TFPI), activated protein C (APC) and antithrombin III (AT III). Fibrinolysis is the process by which fibrin is degraded by the serine protease plasmin. Plasmin is generated from inactive plasminogen by tissue plasminogen activator (tPA) or urokinase plasminogen activator (uPA). Fibrinolysis is regulated by the inhibitors: plasminogen activator inhibitor-1 (PAI-1), thrombin-activated fibrinolysis inhibitor (TAFI) and α_2-antiplasmin.

of patients with atherosclerosis. The importance of the tissue factor pathway in thrombus formation is demonstrated by patients with FVII deficiency experiencing abnormal bleeding analogous to patients with haemophilia A and B. TF deficiency has never been described in the clinic, but $TF^{-/-}$ mice die during embryonic development due to vascular and haemostatic defects (Carmeliet *et al.*, 1996; Toomey *et al.*, 1996).

Once activated by either FIXa or TF/FVIIa, FXa forms a 'prothrombinase complex' with its cofactor Va (activated by thrombin) on the phospholipid surface of activated platelets, endothelial cells or monocytes (Mann *et al.*, 1988), thus localising thrombus formation to the site of injury (Green, 2006). The prothrombinase complex then cleaves the zymogen prothrombin to generate the serine protease thrombin in a Ca^{2+}-dependent reaction. Thrombin then goes on to catalyse the conversion of fibrinogen to fibrin. Thrombin can act to propagate the coagulation cascade by activating platelets (via PAR1 and PAR4), FV and FIX, as well as FXII, which stabilises the clot through catalysing the cross linking of fibrin (Fenton *et al.*, 1991). Due to its central role in coagulation, thrombin is the main target of anti-thrombotic therapies (Fenton *et al.*, 1998).

Coagulation is modulated by a number of circulating protease inhibitors, including antithrombin III, which rapidly inactivates FXIIa, FXIa, FIXa, FXa and thrombin (Tortora *et al.*, 2003), and TFPI, which inhibits the catalytic activity of TF/FVIIa (Baugh *et al.*, 1998; Lu *et al.*, 2004). In addition, the serine protease APC, activated by thrombin, degrades FVa and FVIIIa (Tortora *et al.*, 2003) (Figure 1.3). As well as by inhibition of the coagulation cascade, thrombosis is modulated by enzymatic degradation of the fibrin strands in a process termed 'fibrinolysis'.

1.1.4.4 Inflammation

Inflammation is a potent pro-thrombotic stimulus, which can promote coagulation, inhibit fibrinolytic activity and increase platelet reactivity. Inflammatory cytokines, TNF-α and IL-1α, induce tissue factor expression in monocytes/macrophages. Indeed, inflammatory cells in atherosclerotic plaques produce abundant tissue factor,

which becomes exposed to the blood following plaque rupture (Libby *et al.*, 2002). Mononuclear leukocytes also appear to release blood-borne tissue factor in microparticles (Giesen *et al.*, 1999). These microparticles also contain P-selectin glycoprotein ligand-1 (PSGL-1), which binds platelet P-selectin and mediates the accumulation of tissue factor into developing thrombi (Falati *et al.*, 2003). In addition, C-reactive protein can lead to complement activation (Wolbink *et al.*, 1998), which is thought to play a role in the formation of the platelet prothrombinase complex (Sims *et al.*, 1989). Activated monocytes are also capable of binding and activating FX and FV (Shantsila *et al.*, 2009), thereby directly augmenting the coagulation cascade and fibrin production. Inflammatory mediators can also promote coagulation through down-regulation of the anti-coagulants antithrombin III, APC and TFPI (Esmon, 2004; Levi *et al.*, 2008). The inflammatory cytokines TNF-α and IL-1β also influence fibrinolysis at the level of plasminogen activation (Biemond *et al.*, 1995). They can induce tPA and uPA release from the endothelium, but also a sustained increase in PAI-1 (Scarpati *et al.*, 1989; van der Poll *et al.*, 1991). The overall effect on fibrinolysis is complete inhibition and, as a consequence, inadequate fibrin dissolution (Levi *et al.*, 2010). Inflammatory cytokines can also directly influence platelets, for example: IL-6 can increase platelet production and reactivity to thrombin (Esmon, 2004) and PAF can directly activate platelets (Levi *et al.*, 2010).

Importantly, communication between inflammation and coagulation is bidirectional, such that coagulation can also mediate inflammatory activity. Indeed, platelets store a host of inflammatory mediators, including growth factors (PDGF, TGF-β, bFGF, IGF-1), cytokines and chemokines (IL-8, IL-1), which are released upon activation (Anitua *et al.*, 2004). In addition, platelet-monocyte binding, mediated by platelet P-selectin and monocyte PSGL-1, markedly enhances the production of IL-1, IL-8, MCP-1 and TNF-α (van Deventer *et al.*, 1990). Thrombin can promote leukocyte adhesion and activation, through elaboration of endothelial adhesion molecules (Esmon, 2000). Furthermore, Factor Xa, Factor VIIa and thrombin can activate mononuclear cells and endothelial cells, eliciting the production of IL-6 and/or IL-8 (Sower *et al.*, 1995; van der Poll *et al.*, 2001). Additionally, fibrinogen and fibrin

directly influence the production of TNF-α, IL-1β and MCP-1 from mononuclear cells and endothelial cells (Szaba *et al.*, 2002). Thrombin can release the potent neutrophil agonist PAF from the endothelium (Bar-Shavit *et al.*, 1986). Thrombin-mediated platelet activation can also induce CD40 ligand release which can in turn induce TF synthesis and increases the cytokines IL-6 and IL-8 (Esmon, 2003). Fibrinolytic factors may also have inflammatory influences: uPAR mediates leukocyte adhesion to the vascular wall (Levi *et al.*, 2010), and cytokine and growth factor production though trans-membrane signal transduction (Blasi *et al.*, 2002).

Furthermore, endogenous anti-coagulants (antithrombin III, TFPI and APC) possess potent anti-inflammatory properties. Many of these properties are a direct result of inhibiting coagulation, and subsequent induction of inflammatory mediators. However, there is increasing evidence that these anti-coagulants possess anti-inflammatory effects that are independent of their influence on the coagulation cascade. Firstly, antithrombin III induces PGI_2 release from the endothelium, which inhibits platelet activation and aggregation, blocks neutrophils tethering to the vessel wall, and decreases endothelial production of inflammatory cytokines and chemokines (Esmon, 2003; Uchiba *et al.*, 1998). Antithrombin III can also bind to receptors on the surface of neutrophils, monocytes and lymphocytes, thereby blocking their interaction with endothelial cells (Harada *et al.*, 1999; Horie *et al.*, 1990), and inhibiting their expression of cytokines and adhesion molecules (Esmon, 2003). Secondly, TFPI has been shown to reduce leukocyte activation and decrease TNF-α (Enkhbaatar *et al.*, 2000). These effects appear to be independent of blood coagulation but the mechanisms responsible remain unknown. Thirdly, APC reduces endothelial expression of adhesion molecules and cytokine formation (Joyce *et al.*, 2001). In addition, binding of APC to monocytes inhibits (nuclear factor κB (NFκB) activation and TNF-α production (White *et al.*, 2000).

While inflammatory cells possess many pro-thrombotic properties, they also play an important role in resolution of the thrombus. Thrombus resolution involves several processes: (1) covering of the thrombus surface with monocytes and endothelial cells; (2) penetration of monocytes inside the thrombus; and (3) thrombolysis and

phagocytosis of thrombus components (Shantsila *et al.*, 2009). MCP-1 is an important mediator of monocyte recruitment to the site of thrombosis and is known to contribute to the organisation and resolution of thrombi (Humphries *et al.*, 1999). Once recruited, monocytes infiltrate the thrombus and promote its dissolution through secretion of the plasminogen activators tPA and uPA (Kung *et al.*, 1993; Soo *et al.*, 1996). It has been shown by electron microscopy that platelets and fibrin are then phagocytosed by the monocytes (Poole, 1966; Shirasawa *et al.*, 1971).

1.1.4.5 Fibrinolysis pathway

Fibrinolysis is the process by which thrombus is dissolved once the damage has been repaired. Plasminogen, a circulating zymogen, is converted by the plasminogen activators (tPA or uPA) to the serine protease plasmin. Once formed, plasmin cleaves fibrin, generating soluble degradation products (Figure 1.3).

tPA is synthesised and secreted primarily by endothelial cells, regulated by a variety of stimuli including thrombin, acetylcholine, histamine, adrenaline, exercise and shear stress (Cesarman-Maus *et al.*, 2005). However, monocytes are the principle source of tPA during thrombus resolution (Soo *et al.*, 1996). tPA-mediated activation of plasminogen occurs on the surface of fibrin and appears to be the major intra-vascular mediator of fibrin dissolution (Cesarman-Maus *et al.*, 2005). Conversely, uPA-mediated plasminogen activation is mainly involved in ECM remodelling and cell migration (Lijnen *et al.*, 1998).

Endothelial cells, monocytes, macrophages and neutrophils all express cell-surface receptors which bind plasminogen and tPA and/or uPA, localising fibrinolysis to the thrombus and protecting it from circulating inhibitors (Cesarman-Maus *et al.*, 2005). The main inhibitors of fibrinolysis include: thrombin-activated fibrinolysis inhibitor (TAFI), which inhibits tPA and plasminogen binding to fibrin, thereby attenuating plasmin production (Dempfle, 2007); plasminogen activator inhibitor-1 (PAI-1), which directly inhibits both tPA and uPA (Gils *et al.*, 2004); and α_2-antiplasmin, which directly inhibits plasmin (Lee *et al.*, 2004) (Figure 1.3). Fibrinolysis is also modulated positively by the ability of plasmin to cleave tPA and uPA, subsequently increasing their activity and generating more plasmin (Cesarman-Maus *et al.*, 2005).

The fibrinolysis pathway is an important target for pharmacologic thrombolysis therapy, which involves administration of analogs of tPA to lyse clots and restore perfusion, following acute thrombotic event such as pulmonary embolism, stroke, deep vein thrombosis and ST-segment elevation myocardial infarction (STEMI). While PCI produces superior outcomes for the treatment of STEMI (Keeley *et al.*, 2003), thrombolysis remains an important first-line treatment for at least one-third of STEMI patients (Carver *et al.*, 2009). In fact, thrombolysis can be as effective as PCI if administered within 3 hours of symptom onset (Hanna *et al.*, 2010).

1.2 Glucocorticoids

Glucocorticoids are steroid hormones synthesised from cholesterol in the adrenal cortex and secreted into the circulation when needed. These steroids play important roles in metabolism and development, and mediate physiological and pathophysiological responses to stress. In addition, glucocorticoids have potent anti-inflammatory and immunosuppressive properties, which are utilised therapeutically for the treatment of inflammatory conditions. Indeed, glucocorticoids have been shown to inhibit both atherosclerotic and neointimal lesion in animal models. However, glucocorticoid excess is also associated with an increase risk of CVD, throught to be attributable to the systemic metabolic influences of glucocorticoids (section 1.2.3). This demonstrates the complexity of glucocorticoid physiology and pharmacology, and the context-dependency of glucocorticoid effects. The primary endogenous glucocorticoid in man is cortisol, whereas in rodents, which lack the enzyme 17α-hydroxylase in the adrenal, corticosterone predominates.

1.2.1. Regulation of glucocorticoid action

Due to their wide range of physiological functions (section 1.2.2), glucocorticoid action is tightly regulated by a number of mechanisms influencing their synthesis, transport, metabolism and receptor activation.

1.2.1.1 HPA axis

Glucocorticoid synthesises and secretion from the adrenal cortex is under the influence of the hypothalamic-pituitary-adrenal (HPA) axis (Figure 1.4). Corticotropin-releasing hormone (CRH) is secreted from the hypothalamus and acts

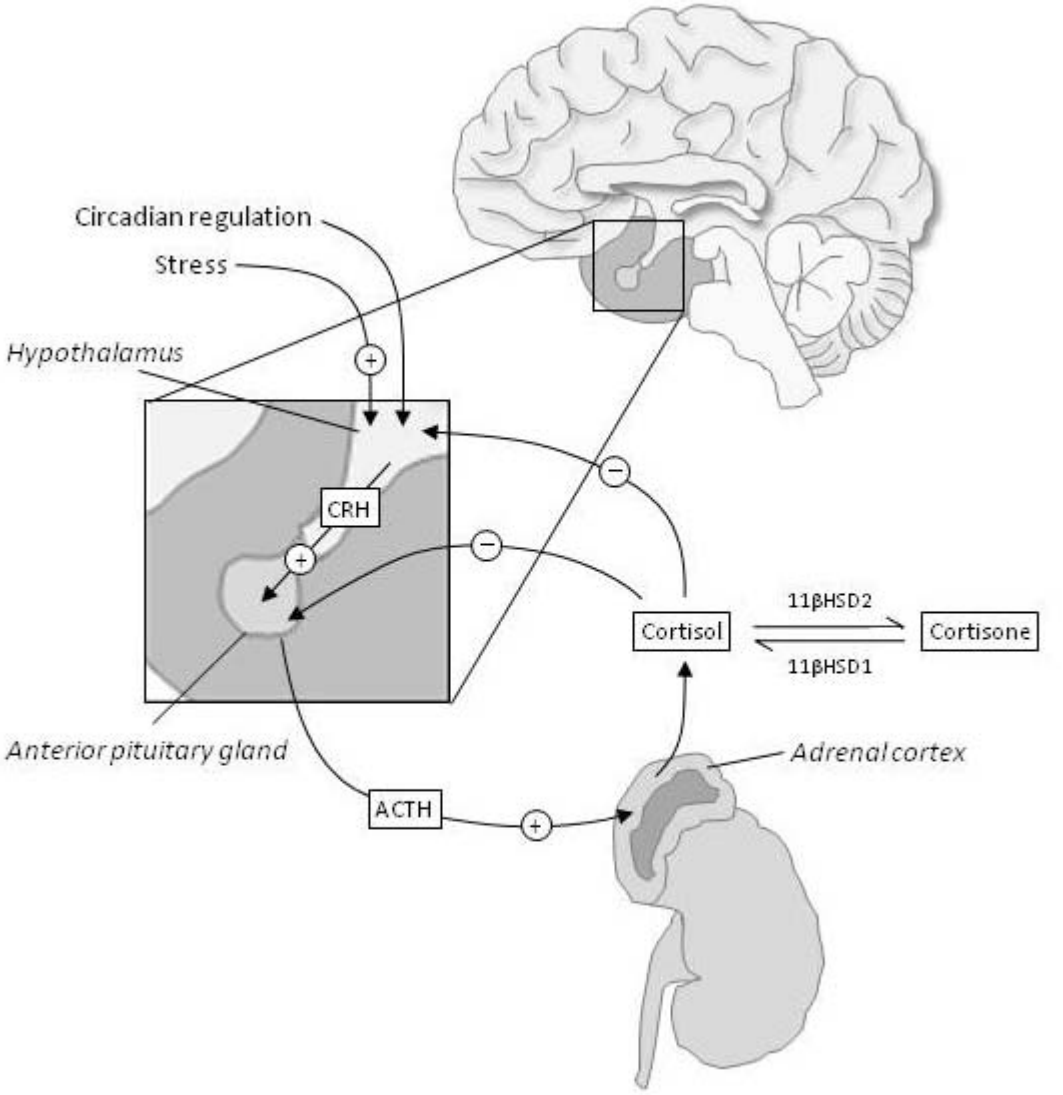

Figure 1.4: Regulation of glucocorticoid production within the hypothalamic-pituitary-adrenal (HPA) axis.
Regulation of the HPA axis occurs under the influence of circadian rhythm, stress responses and negative feedback from circulating glucocorticoid levels. Stimulation of the hypothalamus prompts secretion of corticotrophin-releasing hormone (CRH). This stimulates adrenocorticotropic hormone (ACTH) release from the anterior pituitary, which in turn triggers glucocorticoid synthesis and secretion from the adrenal cortex. The 11β-hydroxysteroid dehydrogenase (11βHSD) isoenzymes interconvert active glucocorticoids, such as cortisol in man and corticosterone in rodents, and their inactive counterparts, cortisone and 11-dehydrocorticosterone, respectively. These enzymes are considered to be important regulators of tissue-specific glucocorticoid action.

to release adrenocorticotropic hormone (ACTH) from the anterior pituitary gland into the circulation. Arginine vasopressin (AVP) can also stimulate ACTH release and acts in synergy with CRF (Antoni, 1993). ACTH then acts on the adrenal glands, stimulating the biosynthesis of glucocorticoids from cholesterol, catalysed by members of the cytochrome P450 oxidase enzyme family and 3β-hydroxysteroid dehydrogenase, resulting in glucocorticoid secretion into the blood. ACTH influences the steroidogenic pathway by a number of mechanisms: (1) stimulating lipoprotein uptake into cortical cells, thus increasing cholesterol bioavailability; (2) increasing transport of cholesterol to, and across, the mitochondrial membrane; and (3) increasing cholesterol binding to side-chain cleavage enzyme ($P450_{scc}$), which catalyses the conversion of cholesterol to pregnenolone (Nussey *et al.*, 2001). In addition to glucocorticoids, ACTH stimulates mineralocorticoid (mainly aldosterone) and androgen precursor (mainly dehydroepiandrosterone (DHEA)) synthesis and secretion from the adrenal cortex. CRH secretion is under the influence of the circadian clock, and therefore produces diurnal variations in ACTH, and subsequently glucocorticoid, secretion, with peak concentrations in the early morning and a nadir in the evening (Nussey *et al.*, 2001). Stimulation of CRH secretion can also be regulated by stressors, including emotional stress, excessive heat or cold, injury, and infection. In addition, glucocorticoids regulate their own release to maintain physiological plasma levels by negative feedback suppression (de Kloet, 1991), at both the hypothalamic and pituitary level. As this negative feedback is mediated through activation of glucocorticoid receptors (GR) (de Kloet *et al.*, 1998) and mineralocorticoid receptors (MR) (Berardelli *et al.*, 2010), synthetic glucocorticoids such as dexamethasone and prednisolone also suppress the HPA axis. This can result in glucocorticoid insufficiency if the exogenous glucocorticoid therapy is stopped abruptly.

1.2.1.2 Corticosteroid-binding carrier proteins

Glucocorticoid bioavailability is also regulated by its interaction with carrier proteins. Approximately 95% of secreted cortisol is bound to carrier proteins; 80-90% to corticosteroid-binding globulin (CBG) and 10-15% to albumin (Lewis *et al.*, 2005). The remaining 5% is free to diffuse across cell membranes and bind to intracellular receptors. According to the 'free hormone hypothesis' (Mendel, 1989),

steroid hormones bound to carrier proteins are biologically inactive and provide a reservoir of inactive circulating hormone. Therefore, corticosteroid-binding carrier proteins regulate the amount of free glucocorticoid available for receptor-mediated action. In addition, there is a slight diurnal variation in plasma levels of CBG, which fluctuates in the opposite direction to glucocorticoid diurnal variation, thereby accentuating the diurnal profile of free cortisol (Hsu *et al.*, 1988; Lewis *et al.*, 2006).

1.2.1.3 Pre-receptor glucocorticoid metabolism

Metabolic inactivation of glucocorticoids provides an additional control of glucocorticoid activity. The 11β-hydroxysteroid dehydrogenase (11βHSD) isoenzymes interconvert active glucocorticoids, such as cortisol (corticosterone in rodents), and their inactive counterpart, cortisone (11-dehydrocorticosterone in rodents) (Figure 1.4). Both cortisol and cortisone are then metabolised in the liver, first by the A-ring reductases followed by several oxidation, hydroxylation and conjugation reactions. The resultant metabolites, 5α – and 5β-tetrahydrocortisol and 5β-tetrahydrocortisone, are excreted in the urine and are often used as biomarkers of glucocorticoid metabolism (Aranoff *et al.*, 1980). The 11βHSD isoenzymes are now appreciated to play important roles in the tissue-specific regulation of glucocorticoid action, rather than just in the clearance of glucocorticoids.

1.2.1.3.1 *11βHSD1*

11βHSD1 has the ability to interconvert glucocorticoids in both directions, but mainly catalyses the reductase reaction *in vivo* (Seckl *et al.*, 2001), regenerating active hormone from inert 11-keto metabolites. These results are supported by studies in 11β-HSD1$^{-/-}$ mice, which cannot convert 11-dehydrocorticosterone to corticosterone *in vivo* (Kotelevtsev et al., 1997). 11β-HSD1 is under complex regulatory control. Factors that influence its expression and activity include inflammatory cytokines, growth factors, sex steroids, insulin and glucocorticoids themselves (Tomlinson *et al.*, 2004). 11βHSD1 is widely expressed, notably in tissues rich in GR: liver, lung, adipose, brain, VSMCs, gonads, anterior pituitary and adrenal cortex (Tomlinson *et al.*, 2004). This suggests that its physiological role is to amplify local glucocorticoid concentrations in glucocorticoid target tissues, thereby maintaining adequate ligand exposure to the relatively low-affinity GR (Seckl *et al.*,

2001). Indeed, there is increasing evidence of the role that 11βHSD1 plays in glucocorticoid-mediated processes such as: gluconeogenesis (Kotelevtsev *et al.*, 1997) and insulin sensitivity (Walker *et al.*, 1995) in the liver; adipocyte differentiation in the adipose tissue (Bujalska *et al.*, 1999); cognitive function in the brain (Yau *et al.*, 2001); and negative feedback regulation of the HPA axis (Kotelevtsev *et al.*, 1997). Furthermore, enhanced 11βHSD1 activity has been implicated in some common clinical syndromes including obesity and type 2 diabetes mellitus (Seckl *et al.*, 2001). 11βHSD1 is therefore an exciting potential therapeutic target for the treatment of the metabolic syndrome. Indeed, based on animal studies (Alberts *et al.*, 2002), promising results have been reported from a phase II clinical trial, which has shown selective 11βHSD1 inhibition to lower glucose levels, improve insulin resistance, lower fasting cholesterol and LDL levels in patients with type II diabetes (Rosenstock *et al.*, 2010).

1.2.1.3.2 *11βHSD2*

Conversely, 11βHSD2 mainly catalyses the dehydrogenase reaction, converting active glucocorticoids to their 11-keto metabolites. In addition to endogenous cortisol, 11βHSD2 possesses the ability to inactive the synthetic glucocorticoids dexamethasone and prednisolone and also reduce their 11-dehydro metabolites (Best *et al.*, 1997; Diederich *et al.*, 2002; Siebe *et al.*, 1993). 11βHSD2 is highly expressed in mineralocorticoid target tissues: kidney, colon, and salivary glands (Walker et al., 2003). Mutations in 11βHSD2 gene are seen in patients with the congenital syndrome of apparent mineralocorticoid excess (SAME) (Dave-Sharma et al., 1998) and 11βHSD2$^{-/-}$ mice have similar features of glucocorticoid-mediated mineralocorticoid excess, including sodium retention, hypokalaemia, and salt-dependent hypertension (Kotelevtsev et al., 1999). It is, therefore, believed that the major role of 11βHSD2 is to protect the mineralocorticoid receptor (MR) from illicit occupation by glucocorticoids. Co-localisation with 11βHSD2 explains why MR, which has similar affinities for cortisol and aldosterone (Funder, 2007), preferentially binds aldosterone, despite a 1,000 fold higher circulating cortisol concentration (Ferrari, 2010).

It has also been noted that 11βHSD2 is expressed in tissues that are not classic mineralocorticoid targets. For example, high levels of 11βHSD2 are present in the placenta, where MR is not abundant. Its role in this tissue is believed to be to protect the foetus from the relatively high levels of maternal glucocorticoids (Edwards et al., 1993; Meaney et al., 2007). Indeed, in humans and in animal models, prenatal inhibition of 11βHSD2 reduces birth weight and causes offspring hyperglycemia, hypertension, increased HPA axis reactivity, and increased anxiety-related behaviour (Harris *et al.*, 2010). In addition, cardiac 11βHSD2 may prevent fibrosis caused by glucocorticoid-mediated MR activation (Glorioso *et al.*, 2005; Konishi *et al.*, 2003). The role of vascular 11βHSD2 in modulating the vascular effects of glucocorticoids is discussed below (section 1.2.2.4)

1.2.1.4 Receptor activation

Glucocorticoids exert their effects by interacting with intra-cellular glucocorticoid (low affinity type II) receptors (GR) and mineralocorticoid (high affinity type I) receptors (MR), both of which are members of the nuclear hormone receptor super family of ligand-activated transcription factors (Parker, 1993). While GRs are ubiquitously expressed, MRs are only expressed in select tissues and are often protected from activation by glucocorticoids by co-localisation of 11βHSD2. Thus, glucocorticoids exert most of their physiological effects through GR. In the absence of glucocorticoids, GR is bound to a large protein complex that includes two subunits of the heat shock protein Hsp90, which maintains the receptor in an inactive state. Upon glucocorticoid binding, Hsp90 dissociates and the active ligand/receptor complex dimerises and translocates rapidly to the nucleus (Figure 1.5). Within the nucleus the complex binds to DNA at consensus sites termed glucocorticoid response elements (GRE) in the 5'-upstream promoter region of glucocorticoid-sensitive genes. The result is either to repress or induce the transcription of the target gene. Co-activators and co-repressors provide additional control over the tissue-specific pattern of response to GR activation. There are believed to be 10-100 genes in each cell that are directly regulated by GR, but many genes are indirectly regulated through an interaction with other transcription factors, including activator protein-1 (AP-1) and NFκB (Barnes, 1998).

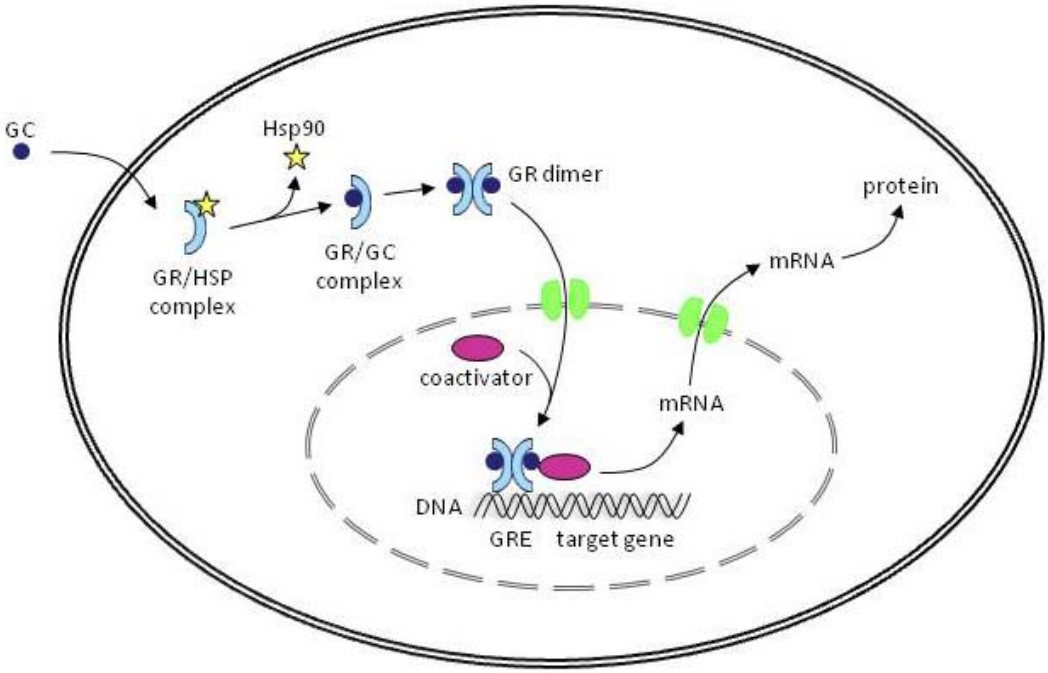

Figure 1.5: Mechanism of action of glucocorticoids in target cells.
Glucocorticoids (GC) enter the cell and bind to the cytoplasmic glucocorticoid receptor (GR), stimulating the release of the heat shock protein (Hsp) 90. The receptor/hormone complex then dimerises and enters the nucleus. The receptor complex then binds glucocorticoid response elements (GRE) in the DNA, modulating specific gene expression with the help of coactivators and corepressors.

As previously mentioned, GRs are ubiquitously expressed; however, levels of both messenger ribonucleic acid (mRNA) and protein vary between cell and tissue types. This contributes significantly to tissue-specific sensitivity to glucocorticoids as cellular sensitivity is directly proportional to the receptor concentration (Oakley *et al.*, 1993). Perinatally, GR levels are programmed by environmental manipulations, including neonatal stress (de Kloet *et al.*, 1990) or *in utero* dexamethasone administration (Cleasby *et al.*, 2003). However, in adults there is dynamic auto-regulation of GR levels by glucocorticoids, which mediates short-term control over glucocorticoid sensitivity. In most cells glucocorticoids can promote GR down-regulation, which consequently reduces the span of cellular responsiveness to glucocorticoids (Bellingham *et al.*, 1992). Ligand-induced GR down-regulation is mediated by both a reduction in GR gene expression (Oakley *et al.*, 1993) and an increase in proteasome-mediated GR degradation (Wallace *et al.*, 2001).

Although glucocorticoids are understood to exert their physiological effects through nuclear hormone receptors, there is increasing evidence that they have additional non-genomic effects. These rapid effects do not involve interaction with genes but are instead mediated by the interaction of glucocorticoids with specific membrane receptors (Gametchu *et al.*, 1999; Stellato, 2004; Tasker *et al.*, 2006). For example, glucocorticoids have been shown to inhibit smooth muscle contraction in the trachea via nongenomic actions that are not blocked by the intracellular GR antagonist mifepristone (Sun *et al.*, 2006). In the heart, glucocorticoids induce endothelial NO production from nitric oxide synthase (NOS) via activation of the Akt intracellular signalling pathways (Hafezi-Moghadam *et al.*, 2002). However, the physiological relevance of these non-genomic responses to glucocorticoids remains uncertain (Tasker *et al.*, 2006).

1.2.1.5 Pharmacological therapy

Clinically, glucocorticoid administration is used predominately as physiological replacement in glucocorticoid deficiency and, in higher doses, as an anti-inflammatory or immunosuppressant. Replacement therapy tends to use glucocorticoids with both GR and MR activity, for example hydrocortisone (the synthetic form of cortisol). However, these steroids are limited by their high

bioavailability and short half-life and so require doses which produce supra-physiological circulating concentrations in the first few hours after administration (Howlett, 1997). Importantly, exogenous glucocorticoids also cannot easily replicate the diurnal rhythm of endogenous cortisol secretion. Anti-inflammatory therapy usually employs the synthetic glucocorticoids prednisolone (GR and MR agonist) and dexamethasone (GR agonist) (Coghlan *et al.*, 2003). While both of these synthetic compounds are substrates for the 11βHSD isoenzymes, dexamethasone is relatively protected from dehydrogenation (Best *et al.*, 1997), which is likely to increase its bioavailability. The therapeutic use of glucocorticoids is limited by a range of systemic side effects mediated through the ubiquitously expressed GR, including osteoporosis, dyslipidaemia, hypertension, hyperglycaemia and peptic ulcers (Moghadam-Kia *et al.*, 2010).

1.2.2. **Physiological actions**

Endogenous glucocorticoids have a wide-range of homeostatic functions in the body, regulating a number of important developmental and metabolic processes, modulating inflammation, as well as influencing the cardiovascular system. Given the range and complexity of glucocorticoid physiology, their effects are highly sensitive to context (for example, physiological vs supraphysiological levels, MR- vs GR-mediated action and acute vs chronic exposure) and thus can be difficult to predict. However, the importance of glucocorticoids, and their homeostasis, is clearly demonstrated in patients with adrenal disease. A deficiency in glucocorticoid production, Addison's disease, is characterised by muscle weakness, depression, loss of weight, low blood pressure and hypoglycaemia (Ten *et al.*, 2001) and susceptibility to Addisonian 'crisis' at times of intercurrent illness. Glucocorticoid deficiency can also occur on abrupt withdrawal of chronic glucocorticoid treatment. This occurs due to suppression of the HPA axis, and endogenous glucocorticoid production, by chronic high circulating exogenous glucocorticoid levels. Conversely, Cushing's syndrome is caused by glucocorticoid excess, which can result from chronic steroid treatment (Souverein *et al.*, 2004; Wei *et al.*, 2004), Cushing's disease, caused by a pituitary gland adenoma that secretes excessive levels of ACTH which subsequently elevates cortisol (Colao *et al.*, 1999; Etxabe *et al.*, 1994), or an adrenal adenoma that secretes excessive levels of cortisol (Stratakis *et al.*, 2007).

Characteristics of Cushing's syndrome include thinning of skin, poor wound healing, obesity, diabetes, hypertension, dyslipidaemia, mood disturbances and increased CVD event rate (Newell-Price *et al.*, 2006).

1.2.2.1 Developmental effects

During development, glucocorticoids play an important role in regulating foetal growth and organ maturation in preparation for extra-uterine life. GR is expressed in most tissues from mid-gestation onwards, as well as in the placenta and foetal membranes (Cole *et al.*, 1995). MR expression is more limited and is only present at later gestational stages (Brown *et al.*, 1996). Correspondingly, there is a rise in cortisol levels during late pregnancy, which parallels increased maturity of foetal organs (Smith *et al.*, 1974). Glucocorticoid treatment is often used to accelerate lung development in foetuses at risk of pre-term delivery (San Feliciano *et al.*, 2011). However, excess foetal exposure to glucocorticoids can have a detrimental influence on early life programming, increasing the risk of developing diabetes and obesity in adulthood (Reynolds, 2010). Placental 11βHSD2 is crucial in protecting the foetus from excessive exposure to maternal glucocorticoids (Edwards *et al.*, 1993).

1.2.2.2 Metabolic effects

The main metabolic effects of glucocorticoids occur in the liver, adipose tissue, pancreas and brain, in response to stressors (starvation, physical and psychological stress). Glucocorticoids oppose the effects of insulin and increase conversion of stored energy (glycogen, triglycerides and protein) to available energy (glucose and free fatty acids). Glucocorticoids also oppose insulin-mediated reduction of central appetite (Chavez *et al.*, 1997), stimulating the intake of fat (Castonguay, 1991) and sugar (Epel *et al.*, 2000). In addition, glucocorticoids inhibit the secretion of insulin from pancreatic β-cells (Lambillotte *et al.*, 1997; Ling *et al.*, 1998). Glucocorticoids also increase the hepatic release of fatty acids and glucose as energy by increasing protein catabolism and gluconeogenesis, while decreasing liver mitochondrial β-oxidation (Morton *et al.*, 2001). The aim of the metabolic effects of endogenous glucocorticoids is to increase energy availability to the skeletal muscles and brain at times of stress, to enhance 'fight or flight' (Walker, 2007). Although glucocorticoids are useful in adapting to short-term stress, longer term glucocorticoid excess has

maladaptive metabolic consequences including obesity, dyslipidaemia and diabetes mellitus, as characterised in Cushing's syndrome (Newell-Price *et al.*, 2006). The contrast between short-term weight loss and long-term weight gain exemplifies the context-sensitivity of glucocorticoid action.

1.2.2.3 Anti-inflammatory and immunosuppressive effects

Glucocorticoids have potent anti-inflammatory and immunosuppressive properties, which make them highly effective agents in controlling inflammatory diseases, including asthma, rheumatoid arthritis, inflammatory bowel disease and autoimmune diseases, as well as in the prevention of transplant rejection.

Glucocorticoids control inflammation by attenuating many aspects of the inflammatory process by a GR-mediated increase of the transcription of anti-inflammatory genes and decrease of the transcription of inflammatory genes. GR are expressed in endothelial cells (Oishi *et al.*, 2011) and inflammatory cells, notably macrophages (Liu *et al.*, 1999), which have a key role in inflammatory processes. For example, glucocorticoids increase the synthesis of the anti-inflammatory cytokine IL-10, which inhibits the transcription of many pro-inflammatory cytokines, chemokines and inflammatory enzymes (Wang *et al.*, 1995). In addition, glucocorticoids induce the transcription of the IL-1 receptor antagonist (Levine *et al.*, 1996) and IL-1 receptor 2, which binds IL-1 but has no signalling capacity (Colotta *et al.*, 1993), thus reducing the activity of the pro-inflammatory cytokine IL-1. Although the up-regulation of these mediators will contribute to the anti-inflammatory effects of glucocorticoids, the down-regulation of pro-inflammatory mediators is likely to be the most significant mechanism by which glucocorticoids hinder inflammatory processes. For example, glucocorticoids inhibit the transcription of several pro-inflammatory cytokines (IL-1β, IL-2, IL-3, IL-4, IL-5, IL-6, IL-11, IL-13, TNF-α and M-CSF) and chemokines (IL-8, RANTES (regulated upon activation, normal T cell expressed and secreted), MCP-1, MCP-3, MCP-4 and macrophage inflammatory protein-1α (MIP-1α)) (reviewed in (Barnes, 1998)). The result is the attenuation of the recruitment of immune cells, such as neutrophils, monocytes, T-lymphocytes and granulocytes, to the site of inflammation, and the inhibition of their activation and proliferation.

Glucocorticoids also inhibit the transcription of the inflammatory enzyme inducible NOS (iNOS) in macrophages (Di Rosa *et al.*, 1990), perhaps by inhibiting the most important transcription factor regulating iNOS gene transcription, NFκB (Barnes, 1998). In addition, glucocorticoids inhibit the expression of endothelial adhesion molecules, further contributing to the inhibition of immune cell recruitment to the site of inflammation. This may in part be due to their inhibitory effects on the cytokines that induce adhesion molecule expression (IL-1β and TNF-α), but glucocorticoids may also directly inhibit the transcription of the genes encoding ICAM-1 and E-selectin (Cronstein *et al.*, 1992). Furthermore, these hormones regulate the maturation of monocytes into highly phagocytic macrophages (Giles *et al.*, 2001), and enhance the phagocytosis of apoptotic leukocytes (Liu *et al.*, 1999), promoting the resolution of inflammation (Heasman *et al.*, 2003).

It should be noted that physiological levels of glucocorticoids exert both pro- and anti-inflammatory effects. It has been proposed that at low circulating levels, glucocorticoids exert primarily permissive effects on inflammation. As circulating levels increase to the high end of the normal diurnal range, glucocorticoids become stimulatory. Higher circulating levels of glucocorticoids, such as in times of stress or following pharmacological administration, potently inhibit inflammation (Yeager *et al.*, 2004). This is another example of the context-sensitivity of glucocorticoid action.

1.2.2.4 Cardiovascular effects

Functional GR and MR are expressed in cardiovascular tissues, including VSMCs (Dhawan et al., 2007; Krug et al., 2010), endothelial cells (Nguyen Dinh Cat et al., 2010; Oishi et al., 2011) and cardiomyocytes (Latouche et al., 2010; Sun et al., 2008), supporting the idea that glucocorticoids interact directly with the cardiovascular system. Indeed, glucocorticoids have diverse effects on cardiovascular tissues influencing tone, vascular development, inflammation and vascular lesion formation (section 1.2.3). In addition, both 11βHSD1 and 11βHSD2 are expressed in VSMCs (Hatakeyama et al., 1999) and endothelial cells (Brem et al., 1998), suggesting that pre-receptor glucocorticoid metabolism may influence steroid action within the vessel wall.

1.2.2.4.1 *Blood pressure homeostasis*

Physiological levels of endogenous glucocorticoids are required to sustain normal blood pressure and fluid volume, in response to stimuli such as shock. These steroids increase blood pressure by mechanisms that are incompletely understood, but are likely to involve renal, cardiac and vascular actions. For example, glucocorticoids play an important role in the regulation of fluid and electrolyte balance, by modulating renal sodium retention and thus plasma volume. This is likely to be mediated indirectly by glucocorticoids influencing the production of angiotensinogen by the liver (Brasier *et al.*, 1996), AVP in the hypothalamus (Raff, 1987) and atrial natriuretic peptide (ANP) by cardiac myocytes (Shields et al., 1988). They can also regulate cardiac output by influencing contractility and work performance of the heart (Pirpiris *et al.*, 1993).

Importantly, glucocorticoids are also believed to have direct effects on vascular tone, enhancing contractility of the vessel wall and thus peripheral vascular resistance (Yang *et al.*, 2004b). Glucocorticoids increase vasoconstriction by: (1) increasing the secretion of the vasoconstrictors angiotensin II (Mendelsohn et al., 1982), endothelin-1 (Morin et al., 1998) and erythropoietin (Kelly et al., 2000); (2) augmenting the sensitivity of VSMCs to vasoconstrictors such as angiotensin II and noradrenaline (Ullian, 1999); (3) up-regulating the angiotensin II receptor (Sato *et al.*, 1994); and (4) down-regulating the expression of the Na^{+}/Ca^{2+} exchanger in VSMCs, increasing intracellular Ca^{2+} and promoting contraction (Smith *et al.*, 1994). Furthermore, glucocorticoid-mediated enhanced constriction may be secondary to impaired endothelium-dependent relaxation. Indeed, glucocorticoids can attenuate endothelial-dependent vasodilatation to acetylcholine (Mangos *et al.*, 2000) and reduce the release of vasodilatory agents such as NO (Whitworth *et al.*, 2002), PGI_2 (Grunfeld et al., 1986) and prostaglandin E_2 (PGE_2) (Handa *et al.*, 1984) from endothelial cells. Although glucocorticoids play an important role in blood pressure homeostasis, elevated levels are associated with hypertension. The mechanisms behind glucocorticoid-induced hypertension are complex and not fully elucidated. Although not essential, renal MR agonism has been suggested to play a role (Smets *et al.*, 2010). Indeed, 11βHSD2 deficiency in SAME (Ferrari, 2010) and in mice

(Kotelevtsev *et al.*, 1999) results in glucocorticoid-induced MR activation and hypertension. There is, however, increasing evidence to suggest a non-renal mechanism contributes to glucocorticoid-induced hypertension, mediated by direct effects on endothelial cells and VSMCs (Ullian, 1999).

1.2.2.4.2 *Angiogenesis*

Angiogenesis, the growth of new blood vessels from pre-existing vasculature, is a complex process regulated by many activators and inhibitors. It is a crucial process during embryonic development, as well as during wound healing and in the female reproductive tract in adults. However excessive angiogenesis has been associated with a number of diseases including cancer, diabetic retinopathies and rheumatoid arthritis (Carmeliet, 2003). The ability of glucocorticoids to inhibit angiogenesis has been confirmed *in vitro*, *in vivo* and in tumour-bearing animals (Folkman *et al.*, 1983; Logie *et al.*, 2010; Small *et al.*, 2005). In addition, genetic deletion of 11βHSD1 has been shown to enhance angiogenesis both *in vitro* and *in vivo* (Small *et al.*, 2005). Despite considerable research, the mechanisms behind glucocorticoids' anti-angiogenic properties are incompletely understood. However, there are several possible pathways through which glucocorticoids may inhibit angiogenesis: (1) modification of cytokine production; (2) inhibition of leukocyte interaction with the endothelium; (3) inhibition of protease activity; (4) degradation of extracellular matrix; (5) inhibition of growth factor activity; (6) inhibition of the arachidonic acid cascade; (7) impairment of vessel maturation and stability; and (8) non-transcriptional effects (reviewed in (Hadoke *et al.*, 2006)). It has been suggested that glucocorticoid-mediated inhibition of angiogenesis is independent of GR and MR (Crum *et al.*, 1985). However, others have shown it to be GR-dependent (Logie *et al.*, 2010; Small *et al.*, 2005).

1.2.2.4.3 *Intra-vascular inflammation*

As their anti-inflammatory actions proceed through GR-mediated interactions within blood vessels and inflammatory cells (section 1.2.2.3), glucocorticoids have the potential to directly attenuate intra-vascular inflammation. For example, glucocorticoids decrease expression of endothelial adhesion molecules, cytokines

and chemokines, and so directly inhibit the recruitment of immune cells such as neutrophils and macrophages into the vasculature (reviewed in (Barnes, 1998)). In addition, as well as being expressed in VSMCs (Hatakeyama et al., 1999) and endothelial cells (Brem et al., 1998), 11βHSD1 is expressed in inflammatory cells such as T-lymphocytes (Zhang *et al.*, 2005a) and activated macrophages (Thieringer *et al.*, 2001), suggesting that pre-receptor glucocorticoid metabolism may contribute to regulation of intra-vascular inflammation. The anti-inflammatory influence of glucocorticoids on the vascular inflammatory conditions associated with CVD is discussed in detail below.

1.2.3. **Glucocorticoids and CVD**

1.2.3.1 Glucocorticoids and CVD risk factors

While physiological levels of endogenous glucocorticoids play an important role in adaptive responses to stressors, excess circulating glucocorticoid levels are maladaptive. The detrimental consequences of hypercortisolaemia include metabolic and cardiovascular complications such as obesity, hypertension, dyslipidaemia, hyperglycaemia and insulin resistance (Newell-Price *et al.*, 2006). These symptoms parallel with features of the metabolic syndrome, a cluster of risk factors associated with a high risk for CVD and type 2 diabetes mellitus (Thomson et al., 2007). Indeed, CVD is the main cause of mortality in Cushing's patients (Pivonello *et al.*, 2008; Ross *et al.*, 1982). Non-Cushing's hypercortisolaemia, for example in those predisposed to HPA hyperactivity by early life programming (Seckl, 2004) or those receiving exogenous glucocorticoid replacement therapy, is also associated with obesity, dyslipidaemia and diabetes (Filipsson *et al.*, 2006; Reynolds, 2010). In addition, chronic glucocorticoid therapy for inflammatory conditions is limited by a number of adverse side effects including the metabolic and cardiovascular complications associated with an increase risk of CVD (Moghadam-Kia *et al.*, 2010; van Raalte *et al.*, 2009).

1.2.3.2 Glucocorticoids and atherosclerosis

The influence of glucocorticoids on atherosclerosis is complex and incompletely understood. In addition to their effects to induce systemic risk factors for CVD, glucocorticoids also have a plethora of local actions on the vascular wall, some of

which may contribute to the pro-atherosclerotic effects of glucocorticoids. For example dexamethasone enhances formation and accumulation of cholesterol esters in human smooth muscle cells (Petrichenko *et al.*, 1997) and macrophages (Cheng *et al.*, 1995; Yang *et al.*, 2004a), as well as inhibit cholesterol efflux from macrophages (Ayaori *et al.*, 2006). In addition, prednisolone has been shown to delay endothelial migration and cytoskeletal rearrangement, thus inhibiting endothelial wound repair (Fyfe *et al.*, 1995). Endothelial NO availability can also be disturbed by dexamethasone-induced augmentation of reactive oxygen species (ROS) production (Iuchi *et al.*, 2003).

However, glucocorticoids can also mediate a number of anti-atherosclerotic processes in the vessel wall including the potent anti-inflammatory effects (section 1.2.2.3) that glucocorticoids are primarily utilised for clinically. Furthermore, dexamethasone inhibits incorporation of modified LDL into macrophages (Asai *et al.*, 1993; Chono *et al.*, 2006) and foam cell formation (Tauchi *et al.*, 2000) *in vitro* as well as reducing macrophage growth induced by ox-LDL (Sakai *et al.*, 1999). Thus, glucocorticoids have the potential to prevent lipid accumulation in the intima, a crucial process in the pathogenesis of atherosclerosis. In addition, dexamethasone increases circulating high density lipoprotein (HDL), an atheroprotective lipoprotein (Saladin *et al.*, 1996). Dexamethasone, hydrocortisone and prednisolone also have an inhibitory effect on VSMC proliferation (Voisard *et al.*, 1994) and dexamethasone have been shown to inhibit VSMC migration (Goncharova *et al.*, 2003), both of which contribute to the progression of atherosclerosis. Therefore, the net effect of glucocorticoids on atherosclerotic lesion development is likely a balance of their systemic influences and their local pro- and anti-atherosclerotic effects (Figure 1.6) and, thus, is likely sensitive to context.

In pre-clinical studies, dexamethasone administration has consistently been shown to inhibit atherogenesis both in rabbits (Asai et al., 1993; Makheja et al., 1989; Naito et al., 1992) and in mice (Tauchi *et al.*, 2001), attributed to the anti-inflammatory properties of the steroids. However, this beneficial influence of glucocorticoid therapy on atherogenesis does not translate into the clinic and there is concern that

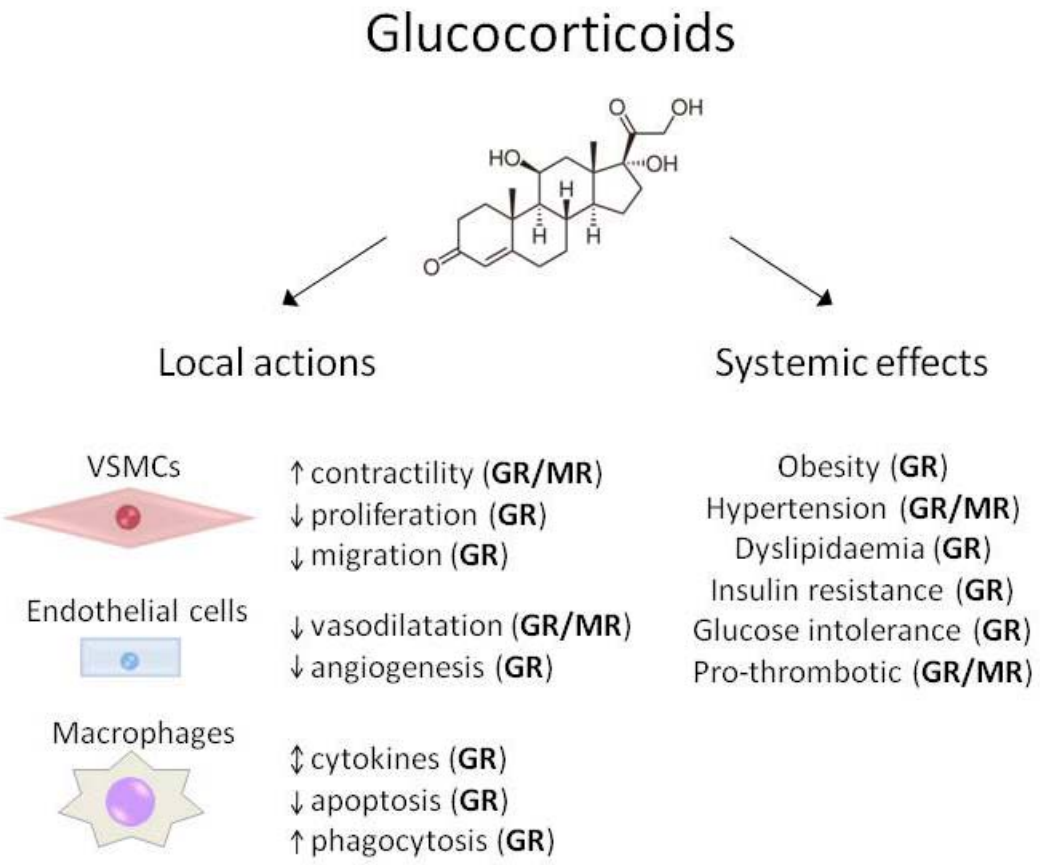

Figure 1.6: Systemic vs local effects of glucocorticoids on the cardiovascular system. Glucocorticoids can interact locally with endothelial cells, vascular smooth muscle cells (VSMCs) and macrophages, thereby modulating vascular function, structure and response to inflammation. Glucocorticoids also have systemic effects on non-vascular organs, such as the liver, adipose and kidneys, which are associated with increased risk of cardiovascular disease. These actions are mediated through the glucocorticoid receptor (GR) and the mineralocorticoid receptor (MR).

anti-inflammatory glucocorticoid therapy will augment atherogenesis in patients with inflammatory diseases (Maxwell *et al.*, 1994). Indeed, glucocorticoid administration is associated with an increased prevalence of carotid artery atheroma, visualised by ultrasound, in patients with rheumatoid arthritis (del Rincon *et al.*, 2004). Pharmacoepidemiological studies have also found a positive correlation between glucocorticoid therapy and cardiovascular events, particularly an increase in the incidence of heart failure and MI (Davis *et al.*, 2007; Solomon *et al.*, 2006; Souverein *et al.*, 2004; Wei *et al.*, 2004). Intriguingly, the effect of glucocorticoids was not altered by adjustment for components of the metabolic syndrome (Souverein *et al.*, 2004; Wei *et al.*, 2004), confirming that the influence of glucocorticoids on cardiovascular outcome is not mediated exclusively by the known systemic metabolic risk factors. However, it continues to be difficult to dissect the influence of exogenous glucocorticoids from the underlying inflammatory conditions, which may themselves be pro-atherogenic.

As with chronic glucocorticoid therapy, endogenous glucocorticoid excess is also associated with an increase in CVD risk factors, in man. Although few studies have investigated the incidence of cardiovascular events, Cushing's patients have been shown to have intimal thickening and a higher incidence of atherosclerotic plaques than controls, visualised by echo-Doppler ultrasonography (Faggiano *et al.*, 2003), even 5 years after the removal of the tumour responsible for glucocorticoid excess (Colao *et al.*, 1999). In addition, higher plasma cortisol in response to stress has been associated with coronary artery stenosis, quantified by angiography (Alevizaki *et al.*, 2007). This is supported by animal studies that have reported social stress to increase atherogenesis (Bernberg *et al.*, 2008; Okwusidi *et al.*, 1991; Shively *et al.*, 2009).

The pro-atherosclerotic effect of endogenous glucocorticoids is further supported in murine models of glucocorticoid deficiency, in which prevention of pre-receptor generation of glucocorticoids by inhibition of 11βHSD1 attenuates atherosclerotic lesion development (Hermanowski-Vosatka *et al.*, 2005; Nuotio-Antar *et al.*, 2007). Similarly, adrenalectomy inhibited aortic lesion development in a rat model of atherosclerosis (Iams *et al.*, 1977).

1.2.3.3 Glucocorticoids and neointimal proliferation

Glucocorticoids clearly have the potential to inhibit neointimal proliferation due to their potent anti-inflammatory properties (section 1.2.2.3). Indeed, glucocorticoids have been shown to attenuate the inflammatory response to vascular injury by inhibiting leukocyte accumulation following cuff placement (Hagihara *et al.*, 1991) or balloon-injury in rabbits (Poon *et al.*, 2001), possibly by reducing the expression of MCP-1 (Poon *et al.*, 2001). Also, glucocorticoids reduce the release of cytokines, including IL-6, IL-13, MCP-1, RANTES, TGF-β and TNF-α, after stenting in rabbits, measured using a cytokine array (Ribichini *et al.*, 2007c). In addition to their anti-inflammatory properties, glucocorticoids can directly inhibit VSMC processes which are involved in neointimal proliferation. For example, glucocorticoids inhibit VSMC migration (Goncharova *et al.*, 2003; Ribichini *et al.*, 2005) and proliferation (Berk *et al.*, 1988; Voisard *et al.*, 1994) *in vitro*, and inhibit release of PDGF (a growth factor implicated in both the induction of migration and the expression of inflammatory chemoattractant molecules (Marmur *et al.*, 1992)) from VSMCs, following vascular injury (Nakano *et al.*, 1993).

Importantly, glucocorticoids also have a number of properties which could promote vascular cell proliferation. For example, they can stimulate the release of growth factors, such as endothelin-1, from VSMCs (Morin *et al.*, 1998) and inhibit the production and action of NO, a potent inhibitor of cell proliferation (Whitworth *et al.*, 2002). In addition, glucocorticoids can stimulate the expression of angiotensin-converting enzyme (ACE) in VSMCs (Fishel *et al.*, 1995) and in endothelial cells (Mendelsohn *et al.*, 1982), thus increasing the production of angiotensin II; a stimulant of VSMC growth both *in vitro* (Berk et al., 1989) and *in vivo* (Griffin *et al.*, 1991). Furthermore, glucocorticoids have been shown to prevent endothelial healing, through delayed endothelial migration and cytoskeletal rearrangement (Fyfe *et al.*, 1995), which may contribute to continued inflammation and VSMC migration and proliferation. Thus, the overall influence of glucocorticoids on neointimal proliferation will depend on the balance between the anti-inflammatory/anti-proliferative effects and the pro-proliferative effects of the steroids, which will be context-specific.

In pre-clinical studies, glucocorticoid administration has consistently been shown to inhibit neointimal development in a number of animal models, including the rat (Guzman *et al.*, 1996; Nagasaki *et al.*, 2004; Villa *et al.*, 1994), rabbit (Hagihara *et al.*, 1991; Petrik *et al.*, 1998; Valero *et al.*, 1998; Van Put *et al.*, 1995) and mouse (Pires *et al.*, 2005). In addition, glucocorticoid-coated stents inhibited neointimal proliferation in the dog femoral artery (Strecker *et al.*, 1998) and in the pig coronary artery (Wang *et al.*, 2005c). Following the success of these animal studies, glucocorticoids have been trialled as anti-restenotic agents in the clinic, both as systemic treatment alongside PCI and as local treatment in the form of DES. Oral therapy with high-dose prednisone for 45 days gave positive results in the IMPRESS trials, with a significant reduction in MACCE, TLR and angiographic restenosis, in patients with elevated systemic markers of inflammation following PCI (Ribichini *et al.*, 2005; Versaci *et al.*, 2002). However, while oral glucocorticoid treatment has advantages of being low cost and easy to administer and control, there are contraindications including diabetes mellitus, severe arterial hypertension and peptic ulcers. In addition, high-dose glucocorticoid treatment can result in adverse effects such as gastric pain, impaired glucose tolerance, worsened hypertension and, occasionally, neutropenia (Ribichini *et al.*, 2007a). Local glucocorticoid delivery, in the form of dexamethasone-eluting stents (DexES), has the advantage of avoiding the systemic secondary effects of steroids, while releasing a high dose of steroid at the site of the target lesion. Unfortunately, although there have been some positive clinical outcomes and/or angiographic results with DexES (Han *et al.*, 2006; Jimenez-Valero *et al.*, 2007; Liu *et al.*, 2003; Patti *et al.*, 2005), there are a number of studies describing DexES as having no effective anti-proliferative actions in acute coronary syndromes (Hoffmann *et al.*, 2004b; Pesarini *et al.*, 2009), no benefit over BMS in patients with stable angina (Gaspardone *et al.*, 2006; Hoffmann *et al.*, 2004a), and an association with relatively high restenosis rates in patients with diabetes mellitus (van der Hoeven *et al.*, 2008).

While there has been an assortment of investigations into the effects of exogenous glucocorticoids on neointimal proliferation, there do not appear to be any reports detailing the influence of endogenous glucocorticoids. However, two studies carried

out in this department, have investigated the effect of endogenous glucocorticoids on neointimal proliferation through manipulation of 11βHSD1. Inhibition or genetic deletion of 11βHSD1 was shown to reduce neointimal lesion development following intra-luminal wire injury in ApoE$^{-/-}$ mice, suggesting endogenous glucocorticoids are in fact pro-restenotic (Iqbal, 2010). However, a similar study using C57Bl/6 mice, described manipulating 11βHSD1 to have no effect on neointimal proliferation following wire-injury (Macdonald, 2007). The conflicting results between these two studies might be attributed to metabolic disturbances caused by ApoE deficiency.

1.2.3.4 Thrombotic effects of glucocorticoids

Although it is widely accepted that inflammation causes thrombosis and thrombosis stimulates inflammation (section 1.1.4.4) anti-inflammatory glucocorticoids have well-described pro-thrombotic properties. Indeed, a hypercoagulable state and increased incidence of thromboembolic complications are reported in Cushing's syndrome (Boscaro *et al.*, 2002; La Brocca *et al.*, 1997). This hypercoagulable state is mainly attributed to an increase in clotting factors, including FV, FVIII, FIX, FXI, FXII and prothrombin (Dal Bo Zanon *et al.*, 1983; Patrassi *et al.*, 1985; Sjoberg *et al.*, 1976), as well as an inhibition of fibrinolysis via an increase in PAI-1 and α_2-antiplasmin (Patrassi *et al.*, 1985; Patrassi *et al.*, 1992). Glucocorticoid treatment in healthy individuals (Brotman *et al.*, 2006) and in patients following organ transplant surgery (Patrassi *et al.*, 1995; Sartori *et al.*, 1999) is also associated with increased coagulation and reduced fibrinolytic activity (Patrassi *et al.*, 1997; Patrassi *et al.*, 1995; Sartori *et al.*, 1999). These results are complemented by *in vivo* studies in rats which report reduced fibrinolysis following dexamethasone treatment (van Giezen *et al.*, 1994; van Giezen *et al.*, 1992), and a number of *in vitro* studies which describe a dexamethasone-induced increase in PAI-1 mRNA and protein levels in a number of different human and animal cell lines (Fukumoto *et al.*, 1992; Halleux *et al.*, 1999; Ma *et al.*, 2002; Yamamoto *et al.*, 2004).

In addition to influencing the coagulation and fibrinolysis factors, glucocorticoids may also promote thrombosis by modulating endothelial function. Excess circulating glucocorticoids in Cushing's patients or with glucocorticoid administration have been reported to increase circulating levels of vWF (Fatti *et al.*, 2000; Jilma *et al.*,

2005; Sartori *et al.*, 1999) and p-selectin (Jilma *et al.*, 2005), changes likely to increase platelet adhesion to the endothelium. These results are complemented by *in vitro* demonstrations that glucocorticoids increase production of vWF by cultured human and animal endothelial cells (Graf *et al.*, 1990; Huang *et al.*, 1995; Yamamoto *et al.*, 2004).

A number of (often contradictory) studies, report an influence of glucocorticoids on platelet function. van Giezen *et al* showed that dexamethasone inhibits platelet aggregation in rats, thus suggesting an anti-coagulant outcome (van Giezen *et al.*, 1994; van Giezen *et al.*, 1992). Conversely, methyl prednisolone has successfully been used clinically to reverse clopidogrel-related inhibition of platelet aggregation (Qureshi *et al.*, 2008) and dexamethasone has been shown to block inhibition of platelet aggregation by activated macrophages *in vitro* (Pinto *et al.*, 1993). In addition, increased circulating concentrations of cortisol have been described to increase platelet aggregation in *ex vivo* animal vessels (Fantidis, 2010). However, whether glucocorticoids can exert these effects by directly modulating platelet function is not fully understood, considering glucocorticoids mediate many of their effects through GR-mediated *de novo* mRNA and protein synthesis and platelets are anuclear and so incapable of synthetic activity. However, functional GR has been shown to be expressed in human platelets and glucocorticoids may modulate platelet function through non-genomic pathways (Moraes *et al.*, 2005). Alternatively, the influence of glucocorticoids on platelets may be mediated indirectly though their modulation of inflammatory cytokine and chemokine release and of endothelial function.

1.3 Hypothesis and Aims

Vascular lesion development arises from an inflammatory and proliferative response to vascular wall injury. Glucocorticoid hormones have widely-recognised anti-inflammatory and anti-proliferative properties which appear to make them ideal candidates for inhibition of vascular lesion development. Indeed, glucocorticoids are currently being trialled clinically as anti-restenotic agents and administration of glucocorticoids to experimental animals inhibits the growth of vascular lesions in some models. However, a previous study in this department found that inhibition of neointimal lesion formation by administration of dexamethasone was obscured by excessive thrombosis at the site of injury. In addition, chronic glucocorticoid excess in patients (either as a result of Cushing's syndrome or chronic treatment) is associated with increased cardiovascular disease. The influence of glucocorticoids on vascular lesion development, therefore, remains incompletely understood and appears to be highly sensitive to context.

The overall objective of this PhD was to explore the influence of endogenous and exogenous glucocorticoids on atherosclerotic lesion development and neointimal proliferation. Based on clinical evidence, this thesis addresses the hypothesis that glucocorticoids are pro-atherosclerotic and anti-restenotic.

It is therefore proposed:

- removal of endogenous glucocorticoids by adrenalectomy will attenuate atherosclerotic lesion development yet augments neointimal proliferation.

- glucocorticoid administration will augment atherosclerotic lesion development yet inhibits neointimal proliferation.

In order to address these hypotheses, the specific aims of the work described in this thesis were to:

1. determine the influence of physiological levels of endogenous glucocorticoids and the impact of a pharmacological dose of an exogenous glucocorticoid on atherosclerotic lesion development in $ApoE^{-/-}$ mice fed a western diet.

2. determine the role of physiological levels of endogenous glucocorticoids and the impact of pharmacological doses of an exogenous glucocorticoid on neointimal lesion development following intra-luminal wire injury of the mouse femoral artery.

3. elucidate the mechanism behind the local thrombus formation associated with exogenous glucocorticoid-induced inhibition of fibro-proliferative neointimal lesion development.

Chapter 2

Materials and methods

2.1 Animals

All animal experiments were performed in accordance with the Animals (Scientific Procedures) Act (UK), 1986 and with local ethical committee approval. All non-genetically-modified mice were of the inbred C57Bl/6J strain purchased from Harlan Laboratories, UK. All ApoE knockout ($ApoE^{-/-}$) mice (C57Bl/6J background) were bred in-house. All PAI-1 knockout ($PAI\text{-}1^{-/-}$) mice were imported from The Jackson Laboratory, ME, USA. Mice were bred and housed at the University of Edinburgh Biomedical Research Facility at Little France in a controlled 12hr light/dark cycle environment, at room temperature (RT; defined as 21 ± 2°C) and 50% humidity. Animals were allowed free access to standard laboratory chow (Special Diet Services, UK) and drinking water, unless otherwise stated.

2.2 In vivo techniques/treatments

2.2.1. Adrenalectomy

Mice were randomised to undergo bilateral adrenalectomy, with sham adrenalectomy used as a control, as described by de Jong *et al* (de Jong *et al.*, 2007), to assess the effect of endogenous glucocorticoids on vascular lesion development

2.2.1.1 Animal preparation

Mice were weighed, and anaesthetised by inhalation of isoflurane (4%; Merial Animal Health Ltd., UK) in an exposure chamber. Upon loss of consciousness, the animals were transferred onto a heated pad to maintain body temperature, where administration of anaesthetic (2% isoflurane in oxygen) was maintained via a nose cone. The animals were given a subcutaneous injection of analgesic (0.05mg/kg of bodyweight buprenorphine; Alstoe Animal Health, UK) prior to commencing the surgery. All surgeries were performed under a surgical microscope using aseptic technique: all surgical instruments were sterilised in a bead steriliser prior to surgery.

2.2.1.2 Adrenal gland removal, wound closure and recovery

Mice were placed in a prone position before an area in the centre of the back was shaved and a 15mm longitudinal skin incision was made. The mice were then rotated onto their right side and a small incision was made in the muscle above the spleen.

The left adrenal gland was then identified, isolated and removed cleanly. The procedure was repeated on the right side. Following closure of the skin incision with metal clips, the animals were ear notched for identification and were transferred to a clean cage to recover from anaesthesia. After surgery, all animals were allowed free access to 0.9% w/v saline as their drinking water, to restore salt balance.

2.2.2. **Femoral artery injury**

Intra-luminal injury was inflicted on murine femoral arteries to induce neointimal hyperplasia. This was achieved by the application of the intra-luminal wire-injury model, described by Sata *et al.* (Sata *et al.*, 2000).

2.2.2.1 Animal preparation and femoral artery isolation

Mice were anaesthetised and prepared for surgery as described above (section 2.2.1.1). The inner surface of the left hind limb was shaved and a 5mm skin incision was made at the top of the leg. The rectus femoris and vastus medialis muscles were separated by blunt dissection to expose the femoral neurovascular bundle. The femoral artery and vein were isolated from the nerve both proximally and distally to the femoropopliteal bifurcation. Temporary ligatures (6-0 silk suture; Fine Science Tools, UK), looping the artery and vein, were positioned proximal and distal to the popliteal branch point to allow control of blood flow in the femoral artery and vein.

2.2.2.2 Wire injury

The popliteal artery was isolated from the adjacent vein and ligated distally with 6-0 silk suture. Tension was placed upon this ligature to bring the popliteal artery up into the plane of the femoral artery and both arteries were cleared of peri-adventitial connective tissue by blunt dissection. The popliteal artery was dilated with 1% w/v lignocaine (1% lidocaine hydrochloride; Hamlen Pharmaceuticals Ltd., UK), as necessary. A 0.014” diameter straight sprung angioplasty guide wire (Cook Inc., IN, USA) was then inserted through a transverse arteriotomy in the isolated popliteal artery, approximately 2mm distal to the femoropopliteal bifurcation. The proximal temporary ligature was loosened to allow the wire to be advanced approximately 1.5cm into the femoral artery towards the iliac artery. The wire was left in place for 30 seconds before being removed. On withdrawal, the proximal temporary ligature was re-tensioned and a further permanent ligature was positioned immediately

proximal to the arteriotomy site. The two temporary ligatures were removed, restoring blood flow to the femoral artery and reperfusing the injured area. The skin incision was then closed using interrupted sutures with a 6-0 silk ligature (Mersilk; Ethicon, UK), before the animals were transferred to a clean cage to recover from anaesthesia.

2.2.3. **Administration of drugs**

2.2.3.1 Systemic glucocorticoid administration

The synthetic glucocorticoid dexamethasone (dex) was administered to investigate the effects of exogenous glucocorticoids on vascular lesion development. *In vivo*, dex is a potent and relatively selective GR agonist (Kim *et al.*, 1998). Dex (Sigma-Aldrich, UK) was dissolved in absolute ethanol at a concentration of 1mg/mL before being diluted in the animals' standard drinking water to achieve doses of 0.1 and 0.8mg/kg/day, through monitoring the animals' weight and water consumption.

2.2.3.2 Western diet administration

A high cholesterol "Western" diet was used to accelerate atherosclerotic lesion development in ApoE$^{-/-}$ mice. The diet (0.21% cholesterol, 21% fat, D12079B; Research Diets Inc., USA) was stored at 2-4ºC until administered to the animals *ad libitum* for 12 weeks.

2.2.4. **Tail cuff plethsmography**

Systolic blood pressure was determined using the technique of tail cuff photo-plethysmography (Cervenka *et al.*, 2003). This technique involves monitoring blood flow through a rodent's tail by light transmittance (inversely proportional to tail volume) at a point distal to an inflating/deflating pressurised cuff. Systolic blood pressure is designated as the cuff inflation pressure at which changes in tail volume, and therefore blood flow, are quenched.

To ensure sufficient tail blood flow, mice were placed in a 40ºC chamber for 10 minutes immediately prior to the procedure. Mice were transferred to a restraint positioned above a heated pad and an integrated pressure cuff/photosensor sleeve (Harvard Apparatus, UK) was placed around the base of the tail. Degree of restraint

and position of the cuff were adjusted until a regular cyclical tail volume trace, representing the pulse, was reached. Pulse traces were recorded while four inflate/deflate pressure cycles were performed. Systolic blood pressure was calculated as the mean measurement of the four deflate-cycles only. Once adequate pressure measurements were acquired mice were returned to their cages.

2.2.5. **Tail tip bleeding time**

Tail tip bleeding time was measured as an *in vivo* parameter of combined plasma- and platelet-mediated blood coagulation. Mice were anaesthetised by inhalation of 4% isoflurane in an exposure chamber. Upon loss of consciousness, the animals were transferred onto a heated pad, to maintain body temperature, where administration of anaesthetic (2% isoflurane in oxygen) was maintained via a nose cone. The tail was dipped in 37ºC water for 1 minute before 0.5cm from the tip of the tail was excised using a scalpel. The tail wound was immediately placed in a pre-warmed Eppendorf of 0.9% w/v saline at 37ºC and time until bleeding ceased was recorded.

2.2.6. **Perfusion fixation**

Chemical fixatives are used to preserve tissue from degradation, prevent growth of microorganisms and maintain tissue structure, allowing storage and analysis of biological samples. Aldehyde fixatives, such as formalin, achieve fixation by the formation of methylene crosslinks between tissue amino groups. Perfusion of whole animals not only allows rapid and even delivery of fixative to all organs but also provides rigidity to blood vessels to maintain their luminal dimensions once excised.

Mice were terminally anaesthetised with an intra-peritoneal injection of sodium pentobarbital (80mg/kg of bodyweight, Ceva Animal Health Ltd, UK). Following onset of deep anaesthesia, as determined by loss of pedal withdrawal reflex, a bilateral thoracotomy and transverse sternotomy were made. At this point, blood was collected from the right ventricle of the heart using a 23 gauge needle and syringe. For delivery of perfusate, a 23 gauge needle was advanced 4mm through the left ventricular wall and secured. A further incision was made in the right atrial wall to allow perfusate to run off. Phosphate-buffered saline (PBS; 24 mL; 1 tablet per 200mL deionised water to give phosphate buffer (0.01 M) containing KCl (2.7 mM)

and NaCl (137 mM), pH 7.4; Sigma-Aldrich, UK) containing 10U/mL heparin (Leo Laboratories, UK), was delivered to the left ventricle at a constant rate (6mL/min) by a peristaltic pump (Gilson, UK). Ideally, a constant (physiological) pressure should have been used to prevent any vascular damage. Immediately after perfusion with heparinised PBS, 10% neutral buffered formalin (24mL; Sigma-Aldrich, UK) was delivered to the left ventricle. Adequate fixation was determined by blanching of the liver and muscle rigidity. Following perfusion, the animal was immersed in 10% neutral buffered formalin for a further 48 hours to ensure full fixation.

2.3 Ex vivo techniques

2.3.1. Semi-quantitative atherosclerosis scoring

The high cholesterol-fed ApoE$^{-/-}$ mouse model of atherosclerosis has sites of the arterial tree that are predisposed to atherosclerotic plaque development: aortic root, lesser curvature, brachiocephalic artery, origin of the left carotid artery and left subclavian artery, origins of the renal arteries and the femoral artery branches. To determine the distribution of plaque within the animals, the lesion size at the predisposed sites was semi-quantitatively scored.

Following perfusion fixation (section 2.2.6), the arterial tree was dissected out as a whole and cleaned of connective tissue before being stored in 70% v/v ethanol (Fisher Scientific, UK). The arterial tree was then pinned on a Sylgard plate (prepared in a petri dish with Sylgard 184 silicone elastomer kit; Dow Corning, MI, USA). Microscopic evaluation of the entire tree was carried out by an independent individual blinded to treatment groups and the areas predisposed to atherosclerotic plaque development were semi-quantitatively scored from 1-5 where 1: no plaque, 2: small plaque, 3: large plaque, 4: extensive plaque, 5: extensive plaque with outward remodelling. Following evaluation, the trees were returned to 70% v/v ethanol.

2.3.2. Optical projection tomography

Optical projection tomography (OPT) is a 3-dimensional imaging technique with similarities to optical coherence tomography (OCT), but providing images of greater resolution and at a lower cost (Sharpe *et al.*, 2002). The current gold standard

examination of blood vessels by histology offers superior resolution to OPT but 3D reconstructions of 2D sections is time-consuming, labour-intensive and destructive. OPT allows quick and reproducible 3-dimensional quantifications of blood vessels, with the added advantage of being non-destructive, allowing further analysis with standard histology (Kirkby *et al.*, 2011). Briefly, an ultraviolet source illuminates the rotating specimen, suspended in a refractive index-matching solution, through a filter selective for a specific excitation wavelength. Photons emitted by endogenous fluorophores in the specimen are focussed through an emission filter to the detector. The multiple single projections covering 360º of sample rotation are reconstructed using a modified computed tomography back-projection algorithm to produce a 3D image.

2.3.2.1 Tissue preparation, sample embedding and mounting

Arteries to be analysed by OPT were excised from mice following trans-cardiac perfusion fixation with 10% neutral buffered formalin (section 2.2.6), cleared of connective tissue and stored in 70% v/v ethanol. Low melting point agarose (Invitrogen Ltd., UK) was dissolved in distilled water to 1.5% w/v at 90ºC and allowed to cool to 40-50ºC before being filtered through Whatman 113V paper (GE Healthcare, UK) to eliminate particulate contaminants. Each artery was suspended vertically in 40mL of agarose solution and rapidly cooled to <20ºC to allow the agarose to set. Agarose blocks were glued to magnetic OPT mounts with cyanoacrylate adhesive (Henkel, UK) so that the artery lay in the axis of the mount. The mounted blocks were trimmed to a conical shape to minimise back-reflection of light within the plane of scanning. Mounted samples were dehydrated in absolute methanol (Fisher Scientific, UK) for >24 hours before being cleared in the refractive index matching solution BABB (34% v/v benzyl alcohol, 66% v/v benzyl benzoate; both Acros Organics) for >24 hours.

2.3.2.2 Scanning and tomographic reconstruction

Mounts with samples attached were secured in the scanning chamber by magnetic attachment. Under white light the sample position was adjusted until the sample revolved about its own axis in the centre of the field of view. Optical magnification was set to 1 pixel = 5.5μm and 1 pixel = 7μm for aortic arch and femoral arteries,

respectively. To scan, samples were illuminated by a UV source with 425/40nm band-pass excitation filter and 475nm low-pass emission filter (GFP1 filter). The exposure time was adjusted to maximise the quality of the resulting image; typically ~650ms. Raw data were acquired by automated capture of projection images (1024x1024 pixels) at rotation increments of 0.9º to give 400 images covering 360º.

After scanning, mounted arteries were cleared of BABB by immersion in absolute methanol for >24 hours. Tissues were removed from mounts and trimmed of excess agarose before being processed for histology as described in section 2.4.

Following manual evaluation of focus and rotational misalignment of projection images using Data Viewer software (Skyscan, Belgium), computed tomographic reconstructions were calculated using NRecon software (Skyscan, Belgium). For each dataset, rotational misalignment was then corrected for.

2.3.2.3 Quantification

Reconstructed OPT tomographs were quantified using CTan software (Skyscan, Belgium). For each scan, a region of interest along the length of the artery was defined; the full length of the brachiocephalic artery in the aortic arch and 4mm immediately proximal to the femoropopliteal bifurcation in the femoral artery. To quantify lesion size, for every 50^{th} cross-section scan-line within the region of interest, the outline of the lesion was estimated and traced. This was possible due to the greater fluorescent signal emitted by the media than the intima and by observation of the luminal conformation. The lesion areas for the interleaved scan-lines were interpolated by the software and manually checked and corrected where required. Lesion volume was then calculated from the stack of cross-sectional areas by the software. To quantify lumen, the process was repeated, tracing the outline of the lumen area every 50^{th} scan-line and correcting the interpolated sections. From both sets of data, the total volume inside the internal elastic lamina was calculated and thus the proportion of this volume occupied by lesion, the volumetric "stenotic ratio", was calculated. As the 3-dimensional volumetric data are calculated from a stack of 2-dimensional cross-section areas, the maximum cross-sectional area of lesion can be found, as can the corresponding lumen cross-sectional area.

2.4 Histological techniques

2.4.1. Tissue preparation, paraffin embedding and microtomy

The aim of tissue processing is to remove water from the tissue and replace it with a solidifying medium, most commonly paraffin wax, to enable the cutting of sufficiently thin sections for subsequent analysis of morphology and composition. Formalin-fixed samples were loaded into cassettes and processed to wax using a Tissue-Tek Vacuum Infiltration Processor (Sakura Finetek Europe, The Netherlands). Briefly, cassettes were dehydrated in graded concentrations of ethanol (50%, 70%, 95%, 100% v/v, each for 2 hours; Fisher Scientific, UK), cleared in xylene (two changes, each for 2 hours; Fisher Scientific) and immersed in molten paraffin wax at 60ºC (three changes, each for 2 hours, Thermo-Shandon, UK). Each step was performed under vacuum and with agitation to accelerate infiltration of solvent/wax. After processing, samples were positioned in molten paraffin wax-filled embedding moulds and cooled rapidly on a Tissue-Tek Cryo-console (Sakura Finetek Europe, The Netherlands) to form solid blocks.

Paraffin blocks were cut into sequential 4μm thick sections using a Leitz 1512 microtome (Leica Microsystems, Germany). Immediately after cutting, ribbons of sections were floated onto a 40ºC water bath (Sakura Finetek Europe, The Netherlands) to stretch and smooth the sections before being mounted on Superfrost Plus electrostatically-coated microscope slides (VWR International, UK). Slides were baked at 37ºC overnight to ensure adherence of the sections to the slides. Brachiocephalic arteries were entirely sectioned and retained from the brachiocephalic bifurcation to the right carotid/subclavian bifurcation. In contrast, femoral arteries were sectioned in a repeated manner, where 20 sections were mounted on 10 slides (2 per slide) then the following 20 sections (80μm) were discarded. Sectioning in this manner was continued until the remaining vessel was morphologically normal (i.e. uninjured) under microscopic evaluation. For vessels for which OPT scans had previously been acquired, sectioning was localised to the region of artery containing the largest area of lesion.

2.4.2. **United States trichrome staining**

For routine examination and morphometric analysis tissue sections were stained using the "United States trichrome" (UST) method (Hadoke *et al.*, 1995) using an automated stainer (Varistain Gemini, Thermo-Shandon, UK). This technique combines an elastin stain (Gomori's aldehyde fuschin) with Gomori's Trichrome stain, delineating collagen (green), elastin (purple) and cells (red with black nuclei).

Gomori's aldehyde fuschin was prepared by dissolving pararosaniline (Sigma, UK) to 1% w/v in 60% v/v ethanol. To this, 1% v/v hydrochloric acid (HCl; VWR International, UK) and 2% v/v fresh paraldehyde (Sigma-Aldrich, UK) were added, and the mixture was allowed to blue at RT for at least two days, to allow reaction of pararosaniline and acetaldehyde. The solution was vacuum filtered before use. Gomori's trichrome was prepared in distilled water by the addition of 0.6% w/v phosphotungstic acid (Sigma-Aldrich, UK), 0.6% w/v chromotrope 2R (Sigma-Aldrich, UK), 0.3% w/v fast green FCF (Sigma-Aldrich, UK) and, after vigorous mixing, 1% v/v acetic acid (Fisher Scientific, UK). The solution was filtered before use. Weigert's iron haematoxylin was prepared by mixing equal volumes of Weigert's solution A and B (Bios Europe, UK) immediately before use. Acidified potassium permanganate solution (0.3% w/v potassium permanganate in 0.3% v/v sulphuric acid) was prepared from solutions of 1% w/v potassium permanganate (Sigma-Aldrich, UK) and 3% v/v sulphuric acid (Fisher Scientific, UK).

Sections were de-waxed in xylene and rehydrated through graded alcohols (both Fisher Scientific, UK) before being treated with acidified potassium permanganate and decolourised in 2% oxalic acid (Sigma-Aldrich, UK). Sections were then placed in the Gomori's aldehyde fuschin, to stain the elastin, and differentiated in 70% v/v ethanol. After being rinsed in running tap water, nuclei were counter-stained with Weigert's iron haemotoxylin and blued in running tap water. Sections were then placed in 5% w/v phosphotungstic acid, to displace previously applied dyes from collagen fibres, and rinsed in distilled water. In the final staining step, sections were immersed in Gomori's trichrome to stain cytoplasm and collagen and then rinsed in 0.2% v/v acetic acid. The sections were then dehydrated through graded alcohols and

cleared in xylene. Coverslips were mounted with the synthetic resin mountant DPX (Fisher Scientific, UK) either by hand or with an automated coverslipping machine (Consul, Thermo-Shandon, UK). The full staining protocol is detailed in Table 2.1.

2.4.3. **Picrosirius red staining**

Lesion collagen content was evaluated with picrosirius red staining which specifically stains collagen fibres pink/red (Puchtler *et al.*, 1973). Sections were de-waxed in xylene (2 x 5 min) and rehydrated through graded alcohols (each for 2 min) and rinsed in running tap water (5 min) before being immersed in picrosirius red solution for 2 hours. The staining solution was prepared by dissolving the collagen stain Direct Red 80 (Sigma-Aldrich, UK) and plasma counter-stain Fast Green FCF (Sigma-Aldrich, UK) in saturated aqueous picric acid (Sigma-Aldrich, UK), each to 1% w/v. Sections were then briefly rinsed in tap water before being dehydrated and coverslipped as described above (section 2.4.2). Photomicrographs of picrosirius red-stained sections were quantified by colour deconvolution (section 2.4.7.5).

2.4.4. **Photomicrograph acquisition**

Colour photomicrographs of histologically-stained sections of arteries were taken to allow analysis of lesion size and composition. Images were captured with a CoolSNAP colour camera (Photometrics, AZ, USA) coupled to a Axioskop light microscope (Carl Zeiss, UK), under 10X objective magnification, via a MicroColour liquid crystal RGB filter (Cambridge Research and Instrumentation Inc., MA, USA) using MCID Basic 7.0 software (Imaging Research Inc., ON, Canada).

2.4.5. **Morphometric analysis**

Morphometric analysis was performed on UST-stained sections. Measurements of area (μm^2) inside the EEL, area inside the IEL and luminal area were recorded using Photoshop CS3 Extended software (Adobe Systems Inc, CA, USA). Potential tissue distortion was not taken into account during lumen quantification. From these measurements the medial area (area inside EEL – area inside IEL) and intimal area (area inside IEL – luminal area) could be calculated. The section with the largest intimal area was chosen to represent each artery. Additional morphometric analysis parameters of intima/media ratio and stenotic ratio were calculated.

Table 2.1: United States trichrome staining protocol

Step	Reagent	Duration
1	Xylene	2 x 5 min
2	100% v/v ethanol	2 x 5 min
3	95% v/v ethanol	1 x 5 min
4	Running tap water	1 x 5 min
5	0.3% w/v potassium permanganate in 0.3% v/v sulphuric acid	1 x 1 min
6	Running tap water	1 x 1 min
7	2% v/v oxalic acid	1 x 5 s
8	70% v/v ethanol	1 x 5 min
9	Gomori's aldehyde fuchsin	1 x 5 min
10	70% v/v ethanol	1 x 2 min
11	Running tap water	1 x 5 min
12	Weigert's iron haematoxylin	1 x 5 min
13	5% w/v phosphotungstic acid	1 x 5 min
14	Running tap water	1 x 2 min
15	Gomori's trichrome	1 x 20 min
16	0.2% v/v acetic acid	1 x 1 min
17	95% v/v ethanol	1 x 1 min
18	100% v/v ethanol	2 x 2 min
19	Xylene	2 x 2 min

2.4.6. **Lipid content measurement**

An estimation of the extracellular lipid content of the brachiocephalic arteries was also calculated from UST stained sections. As lipid is removed from sections during the staining process, extracellular lipid content was quantified from the acellular clefts seen in the UST stained sections. These have been show to represent areas of extracellular lipid pooling prior to the vessels being processed (Figure 2.1), as previously described by Shiomi *et al* (Shiomi *et al.*, 2008). The white acellular clefts were identified using a semi-automated colour deconvolution process (section 2.4.7.5) and their areas calculated with Photoshop CS3 Extended software. The lipid content was measured in the representative section containing the largest plaque and was expressed a percentage of plaque area.

2.4.7. **Immunohistochemistry**

Immunohistochemistry involves the localisation of antigens in tissue sections by the use of specific antibodies. The antigen-antibody interaction can be visualised by fluorescence or enzymatic development of a chromogenic substrate, usually following several amplification steps. Representative sections containing the maximum cross-section of lesion for each artery were immunohistochemically-stained to assess the cellular and protein composition of the lesions.

2.4.7.1 Slide preparation

All immunohistochemical procedures followed the following preparation protocol. Slides were first baked for 30 minutes at 55ºC to ensure adherence of the mounted paraffin sections. Slides were then de-waxed in xylene (2 x 5 min) and rehydrated through graded alcohols (100%: 2 x 5 mins, 70% v/v: 1 x 5 min) before being rinsed in running tap water (5 min) and transferred to PBS. Slides were then installed in Sequenza coverplates (Thermo-Shandon, UK), trapping 80µl PBS between slide and coverplate. Sequenzas were flushed twice with PBS.

2.4.7.2 Smooth muscle α-actin staining

Following flushing with PBS, slides were incubated with 3% v/v H_2O_2 solution (Sigma-Aldrich, UK) to block endogenous peroxidise activity. After 5 min, slides were again flushed twice with PBS. Slides were then incubated with blocking

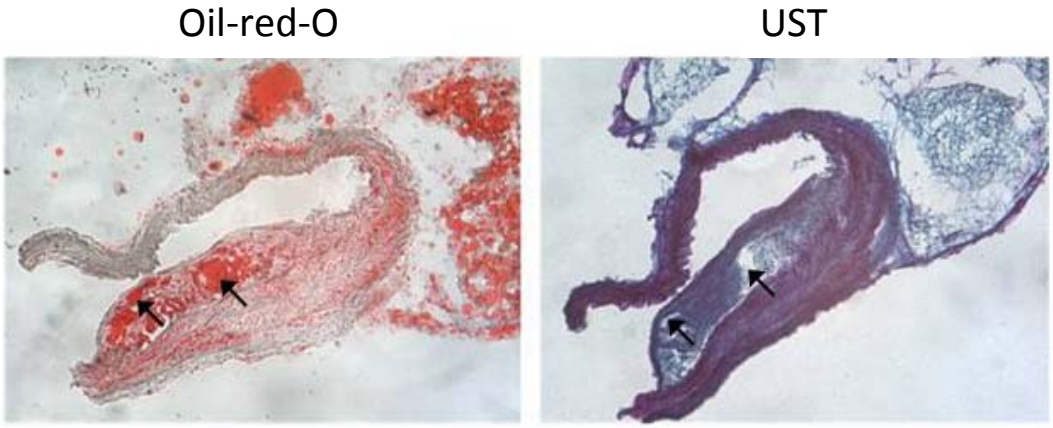

Figure 2.1: Comparison of Oil-red-O and United States trichrome staining to assess lipid distribution in the a-cellular clefts of atherosclerotic plaques.
Male ApoE$^{-/-}$ mice were fed a high (0.2%) cholesterol diet for 12 weeks to induce atherosclerotic lesion development. The brachiocephalic artery was excised and frozen before being cut into 10μm thick transverse sections. Serial sections were stained with Oil-red-O or United States trichrome (UST), the latter of which removes all lipid from the section. Comparison of these sections confirms the acellular clefts (black arrows) seen in the UST section approximate to intra-plaque lipid pools (black arrows) as seen in the Oil-red-O stain section. Original magnification: 100x.

solutions to reduce non-specific binding of primary antibodies: 60 min with PBS containing 2.5% w/v bovine serum albumin (BSA; Sigma-Aldrich, UK) and 2.5% w/v milk powder; followed by 30 min with PBS containing 1% w/v BSA and 20% v/v normal serum from the species in which the respective secondary antibody was raised, which in this case was goat. Without washing, mouse anti-mouse smooth muscle α-actin primary antibody (Sigma-Aldrich, UK), diluted 1/400 in PBS containing 1% w/v BSA, was applied to the Sequenza and incubated for 30 min at RT. Sections incubated with mouse ascities fluid (Sigma-Aldrich, UK), also diluted 1/400, served as negative controls. Sequenzas were then flushed 3 times with PBS before addition of goat anti-mouse IgG biotinylated secondary antibody (Vector Laboratories, UK), diluted 1/400 in PBS containing 1% w/v BSA. After 30 min at RT, the slides were washed 3 times with PBS. ExtrAvidin-Peroxidase (Sigma-Aldrich, UK), a conjugate of streptavidin and horseradish peroxidase, was diluted 1/200 in PBS containing 1% w/v BSA and incubated with the slides for 30 min at RT before the final 3 washes with PBS. Slides were removed from the Sequenzas and placed in PBS. The sites of immunoreactivity were determined with the horseradish peroxidise substrate diaminobenzidine (DAB; prepared according to manufacturer's instructions; Dako Cytomation Ltd, UK). Incubation time was determined by microscopic evaluation of a positive control slide. The reaction was quenched in tap water before the slides were counterstained with one dip in Harris's haematoxylin solution (Fisher Scientific, UK) and blued in running tap water for 5 min. Slides were then dehydrated through graded alcohols (70% v/v: 2 x 1 min, 100%: 1 x 1 min) to xylene (2 x 2 min) before being coverslipped with DPX.

2.4.7.3 Macrophage staining

Following flushing with PBS, slides were incubated with 3% v/v H_2O_2 solution for 5 min and then flushed twice with PBS. Slides were then incubated for 30 min with a blocking solution of PBS containing 1% w/v BSA and 20% v/v normal goat serum. Without washing, rat anti-mouse Mac2 primary antibody (Cedarlane Laboratories, Canada), diluted 1/6000 in PBS containing 1% w/v BSA, was applied to the Sequenza and incubated overnight at 4ºC. Sections incubated with rat $IgG_{2a,\kappa}$ (BD Pharmingen, UK), also diluted 1/6000, served as negative controls. Sequenzas were then flushed 3 times with PBS before addition of goat anti-rat IgG biotinylated

secondary antibody (Vector Laboratories, UK), diluted 1/400 in PBS containing 1% w/v BSA. After 30 min at RT, the slides were washed 3 times with PBS. ExtrAvidin-Peroxidase and DAB solution were applied before counterstaining, rehydration and coverslipping, as described above (section 2.4.7.2).

2.4.7.4 Fibrinogen staining

For fibrinogen staining, antigen-retrieval was required to break the protein cross-links, formed by formalin-fixation, masking the antigenic sites. To achieve this, 20µg/mL proteinase K (Roche Applied Science, UK) was applied to the sequenzas and incubated for 20 min at 37ºC and a further 20 min at RT. Following flushing with PBS, blocking solutions were applied: PBS containing 2.5% w/v BSA and 2.5% w/v milk powder for 60 min, followed by PBS containing 1% w/v BSA and 20% v/v normal goat serum for 30 min. Without washing, rat anti-human fibrinogen primary antibody (Dako UK Ltd, UK), diluted 1/200 in PBS containing 1% w/v BSA and 20% v/v goat serum, was applied to the Sequenza and incubated overnight at 4ºC. Sections incubated with rat IgG (Dako UK Ltd, UK), also diluted 1/200, served as negative controls. Sequenzas were then flushed 3 times with PBS before addition of 3% v/v H_2O_2 solution. After 10 min and 3 washes with PBS, goat anti-rat biotinylated secondary antibody (Vectastain ABC kit; Vector Laboratories, UK) was applied. After 30 min at RT, the slides were washed 3 times with PBS. The ABC solution (Avadin : biotinylated peroxidase complex; Vectastain ABC kit) was then added to the slides and incubated at RT for 30 min before being washed off with PBS. DAB solution was applied before counterstaining, rehydration and coverslipping, as described above (section 2.4.7.2).

2.4.7.5 Quantification

Quantification of immunoreactivity was carried out from photomicrographs of immuno-stained tissues, acquired as described in section 2.4.4. Positive DAB staining was identified using a semi-automated colour deconvolution process and their areas calculated with Photoshop CS3 Extended software. Immunoreactivity was expressed as a percentage of DAB stained area within lesion area, delineated as described in section 2.4.5. To avoid problems of inter-batch variability quantitative comparisons were only made between slides stained in parallel.

2.5 **Blood analyses**

2.5.1. **Plasma corticosterone**

Plasma samples from mice were analysed for corticosterone by competition radioimmunoassay to confirm the success of the adrenalectomy surgery. Samples were collected by tail tip into Microvette CB 300 EDTA tubes (Sarstedt Ltd, UK), immediately prior to sacrifice between 10am and 12pm, when corticosterone levels were elevated from the diurnal nadir at 8am (Holmes *et al.*, 1997).

Plasma samples were diluted 1/10 (sham animals) or 1/5 (adrenalectomised animals) in borate buffer (Boric acid (133mM), NaOH (180mM), HCl (0.35% v/v), BSA (0.5% w/v) pH 7.4; all Sigma-Aldrich, UK) and denatured (75ºC, 1 hour) to release corticosterone from its binding protein, corticosterone-binding globulin. The samples were centrifuged (16,000 x g, 5 min, RT) to pellet the debris. Denatured samples (20µl) were then added in duplicate to a 96 well plate. Corticosterone (Sigma-Aldrich, UK) standards of known concentration (0.3 - 320nM) were also added in duplicate to the plate. Borate buffer containing [$^3H_4$] corticosterone (1µl stock (62.2 Ci/mmol) in 6 mL borate buffer and adjusted to 5,000 cpm; GE Healthcare, UK) and rabbit anti-corticosterone primary antibody (diluted 1/15000; kindly provided by C. Kenyon) were added to each well, mixed and incubated (2 hours, RT). Following primary incubation, anti-rabbit secondary antibody linked to scintillation proximity assay (SpA) beads (diluted according to manufacturer's instructions; GE Healthcare, UK) were then added to each well. The plate was sealed with anti-crosstalk film and inverted to mix. The plate was incubated (16 hours, RT, dark) before the radioactivity in each well was counted in a beta counter. A standard curve of the proportion of bound [^{3}H] corticosterone (B/B_0) against the standard corticosterone concentrations (Figure 2.2) was plotted and the level of corticosterone in each sample determined by interpolation from the standard curve. Finally, the result was multiplied by 5 (adrenalectomised animals) or 10 (sham animals) to account for the initial dilution of each plasma sample.

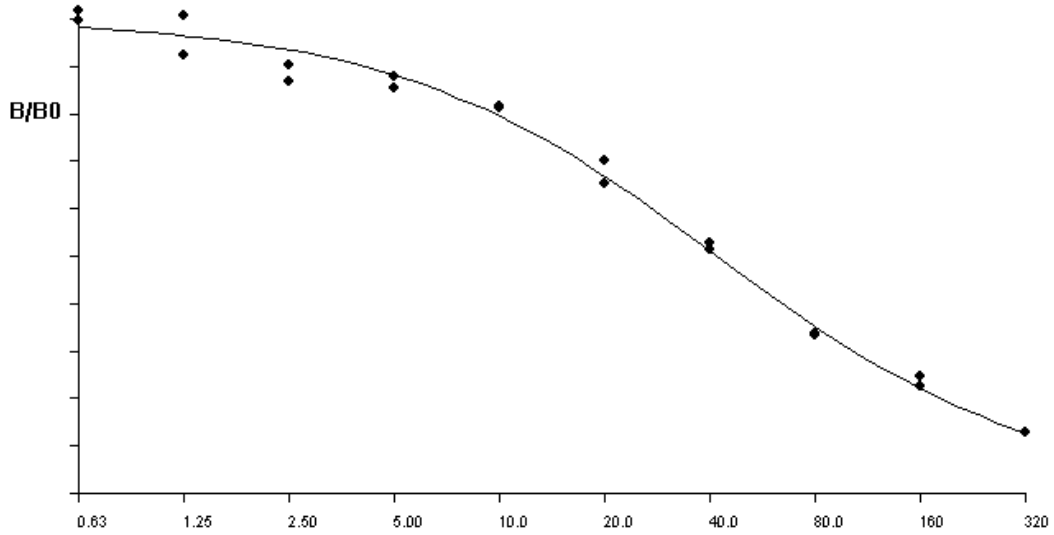

Figure 2.2: Example of a corticosterone assay standard curve.
Proportion bound [$^3H_4$] corticosterone (B/B_0; y-axis) decreases as displaced by increasing concentrations of competing unlabelled corticosterone (x-axis). The graph points were fitted with a sigmoidal concentration-response curve, constructed using AssayZap software (Biosoft, UK). Duplicates of standards were deemed acceptable if the coefficient of variation <10%. The corticosterone concentration of unknown samples was determined from their B/B_0 by interpolation against the standard curve.

2.5.2. **Serum lipids**

Serum samples were analysed for total cholesterol and triglyceride levels by colourimetric assay. Briefly, samples were incubated with reagents containing specific enzymes which sequentially hydrolyse and oxidise cholesterol and triglycerides to produce hydrogen peroxide (H_2O_2). In the final reaction, catalysed by peroxidase, the H_2O_2 reacts to form a chromophore (quinoneimine dye).

Blood was collected by cardiac puncture into clean tubes and allowed to clot on ice before being centrifuged (8,000 x g, 10 min, 4ºC). The supernatant (serum) was removed into a fresh tube. Serum samples (neat) were added in triplicate to a 96-well microtitre plate. Cholesterol or triglyceride standards of known concentration (0.97 - 27.16mM and 0.57 - 7.91mM, respectively; Thermo Scientific, UK) were also added in triplicate to the plate. Cholesterol or Triglyceride reagent (Thermo Scientific, UK) was then added to their respective plates and incubated (37ºC, 5 min). Following incubation, the absorbance was read at 500 and 600nm. The absorbance (A) at 500nm is proportional to the concentration of cholesterol or triglyceride in the original sample. Absorbance at 600nm was subtracted as plate background. A standard curve of $A_{500} - A_{600}$ against the standard concentrations was plotted (Figure 2.3) and the concentration of cholesterol or triglyceride in each sample was interpolated from the standard curve.

2.5.3. **Plasma fibrinolytic factors**

Platelet-poor plasma samples (PPP) were analysed for the fibrinolytic factors PAI-1 and tPA using enzyme-linked immunosorbent assay kits (ELISA; Innovative Research, MI, USA). Briefly, ELISAs involve the target antigen being immobilised, usually by a capture antibody coated and dried on a microtiter plate, followed by detection using specific antibodies. The antigen-antibody interaction can be visualised by enzymatic development of a chromogenic substrate, often following an amplification step. Platelet-poor plasma was used as platelets are a source of PAI-1 (Loscalzo *et al.*, 1995) and so may misrepresent the *in vivo* levels at time of collection.

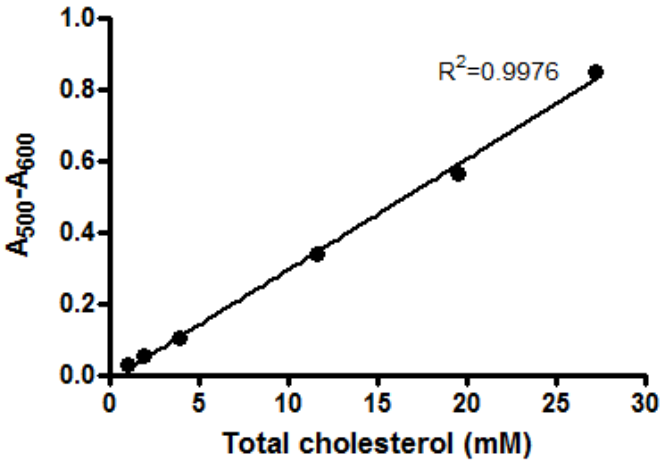

Figure 2.3: Example of total cholesterol assay standard curve.
The relative absorbance of cholesterol standards at 500nm-600nm increases with increasing concentration of cholesterol. The graph points were fitted by linear regression analysis using Prism 5.01 software (GraphPad software, CA, USA). Triplicates of standards were deemed acceptable if coefficient of variance < 10%. Standard curves were deemed acceptable if $R^2 > 0.98$. The cholesterol concentration of unknown samples was determined from their A_{500}-A_{600} by interpolation against the standard curve.

PPP samples were prepared as described in the relevant chapters (section 4.3.5, 5.3.4 and 6.3.5). Samples diluted 1:4 with blocking buffer (3% w/v BSA in TBS buffer; Tris base (100mM), NaCl (150mM), pH 7.4; both Sigma-Aldrich, UK) and added (100µl) to the 96-well plate provided with each kit, prepared for specific antigen capture (Table 2.2). PAI-1 or tPA standards of known concentration (0.05 - 50ng/mL; 100µl) were also added in duplicate to the plate. The plate was shaken (300rpm, 30 min) and washed (300µl wash buffer provided, three times). Following antigen capture, the appropriate primary antibody (Table 2.2) was added (100µl) to each well and the plate was shaken and washed, as before. The appropriate secondary antibody, conjugated to horseradish peroxidise (HRP), was then added (100µl) to each well, shaken and washed, as before. Following secondary incubation, tetramethylbenzidine (TMB) HRP substrate was then added (100µl) to each well and the plate was agitated for 2-10 min. 0.5M H_2SO_4 (Fisher Scientific, UK) was added (50µl) to each well to quench the reaction before the plate was mixed thoroughly and the absorbance was read immediately at 450nm. A standard curve of A_{450} against the standard concentrations (Figure 2.4) was plotted and the levels of PAI-1 or tPA in each sample were determined by interpolation from the standard curve. The result was multiplied by 4 to account for the initial dilution of each sample.

2.5.4. **Flow Cytometry**

Platelet activation status was determined using flow cytometry. Briefly, a beam of light is directed onto a hydrodynamically-focussed stream of platelet-rich plasma (PRP). Detectors positioned in line with and perpendicular to the light beam pick up forward scatter (FSC) and side scatter (SSC), respectively. FSC correlates with the cell volume and SSC depends on the inner complexity of the cell. Platelets have a unique FSC and SSC, which allows their identification (Sintnicolaas *et al.*, 1991). In addition, a fluorescently-labelled antibody against CD41 (glycoprotein IIb), a constitutively-expressed surface protein, can be used to further isolate the platelet population. Activated platelets can be identified by their expression of p-selectin, distinguished using a fluorescently-labelled antibody against CD62P (Braun *et al.*, 2008). On passing the light beam, the fluorescent labels are excited into emitting a detectable wavelength and the geometric mean fluorescence intensity (GMFI) was quantified.

Table 2.2: Details for specific ELISA protocols.

Target antigen (Catalogue no.)	Antigen capture	Primary antibody
PAI-1 total (IMPAIKT-TOT)	Mouse anti-mouse PAI-1 antibody	Polyclonal anti-mouse PAI-1 antibody
PAI-1 active (IMPAIKT)	Human uPA	Polyclonal anti-mouse PAI-1 antibody
tPA total (IMTPAKT-TOT)	Anti-mouse tPA antibody	Monoclonal anti-mouse tPA antibody
tPA active (MTPAKT)	Biotinylated PAI-1 (requires addition to plate)	Monoclonal anti-mouse tPA antibody

PAI-1: plasminogen activator inhibitor-1, tPA: tissue plasminogen activator. All ELISA kits were purchased from Innovative Research, MI, USA.

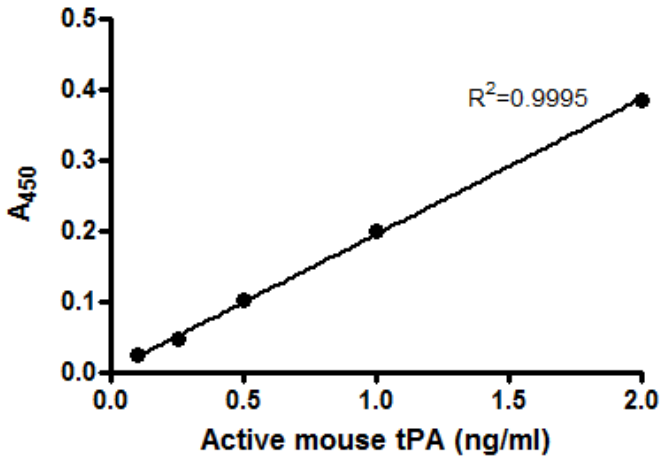

Figure 2.4: Example of active mouse tPA ELISA standard curve.
The relative absorbance of tPA standards at 450nm increases with increasing concentration of tPA. The graph points were fitted by linear regression analysis using Prism 5.01 software (GraphPad software, CA, USA). Duplicates of standards were deemed acceptable if the coefficient of variation was <10%. Standard curves were deemed acceptable if $R^2 > 0.98$. The tPA concentration of unknown samples was determined from their A_{450} by interpolation from the standard curve.

2.5.4.1 Sample preparation

Fresh PRP was prepared from citrated blood, collected from the vena cava, by centrifugation (120 x g, 5 min, RT) (section 4.3.5). PRP was diluted 1:20 with Hanks' basic saline (Sigma-Aldrich, UK). Appropriate antibodies were prepared in Hanks' basic saline as described (Table 2.3). 10µl of each antibody preparation was incubated with 10µl diluted PRP at RT for 20 min. A positive control for platelet activation was also prepared by pre-incubating the PRP with 10µM ADP and 2mM Ca^{2+}. The cells were then fixed with 1% v/v formaldehyde in Hanks' buffered saline (300µl) in preparation for flow cytometry.

2.5.4.2 Flow cytometric analysis

Flow cytometry was performed on a FACSCalibur (Becton Dickinson, UK) and analysed using FlowJo software version 7.5 (Tree Star Inc., OR, USA). FSC/SSC characteristics were used to gate the platelets population (Figure 2.5A). A total of 10,000 gated events were collected. To further isolate the platelets, only CD41 positive cells were included in the analysis (Figure 2.5B). The geometric mean fluorescence intensity (GMFI) was quantified for CD62P-expressing platelets (Figure 2.5C), representing their activation status.

2.6 Molecular Biology

2.6.1. Genotyping ApoE$^{-/-}$ mice

ApoE-deficient mice were originally created by homologous recombination (Plump *et al.*, 1992; Zhang *et al.*, 1992), producing a disrupted "knockout" allele. The genotype of ApoE$^{-/-}$ mice, bred to use in these studies, was confirmed by polymerase chain reactions (PCR) using specific primers and the enzyme *Taq* DNA polymerase. The PCR products were then separated by size using gel electrophoresis, from which wild-type and knockout alleles can be identified.

2.6.1.1 DNA extraction from tail tips

DNA was extracted from tail tip samples from ApoE$^{-/-}$ mice using the Qiagen DNeasy Tissue Kit (Qiagen, UK). Tail tips (~5mm) were lysed in Buffer ATL (180µl) with proteinase K (20µl) overnight in a rotating incubator at 56ºC. The samples were then vortexed (15s) before Buffer AL (200µl) was added and mixed

Table 2.3: Details for flow cytometry antibody preparations.

Stain	Antibody (supplier)	Hanks' volume
Control	-	10µl
CD41	PE rat anti-mouse CD41 (1µl; Serotec, UK)	9µl
CD62P	FITC rat anti-mouse CD62P (1µl; BD Biosciences, UK)	9µl
Double	PE rat anti-mouse CD41 (1µl) + FITC rat anti-mouse CD62P (1µl)	8µl
CD62P isotype control	PE rat anti-mouse CD41 (1µl) + FITC rat IgG1 λ (1µl; BD Biosciences, UK)	8µl

PE: R-phycoerythrin, FITC: Fluorescein isothiocyanate.

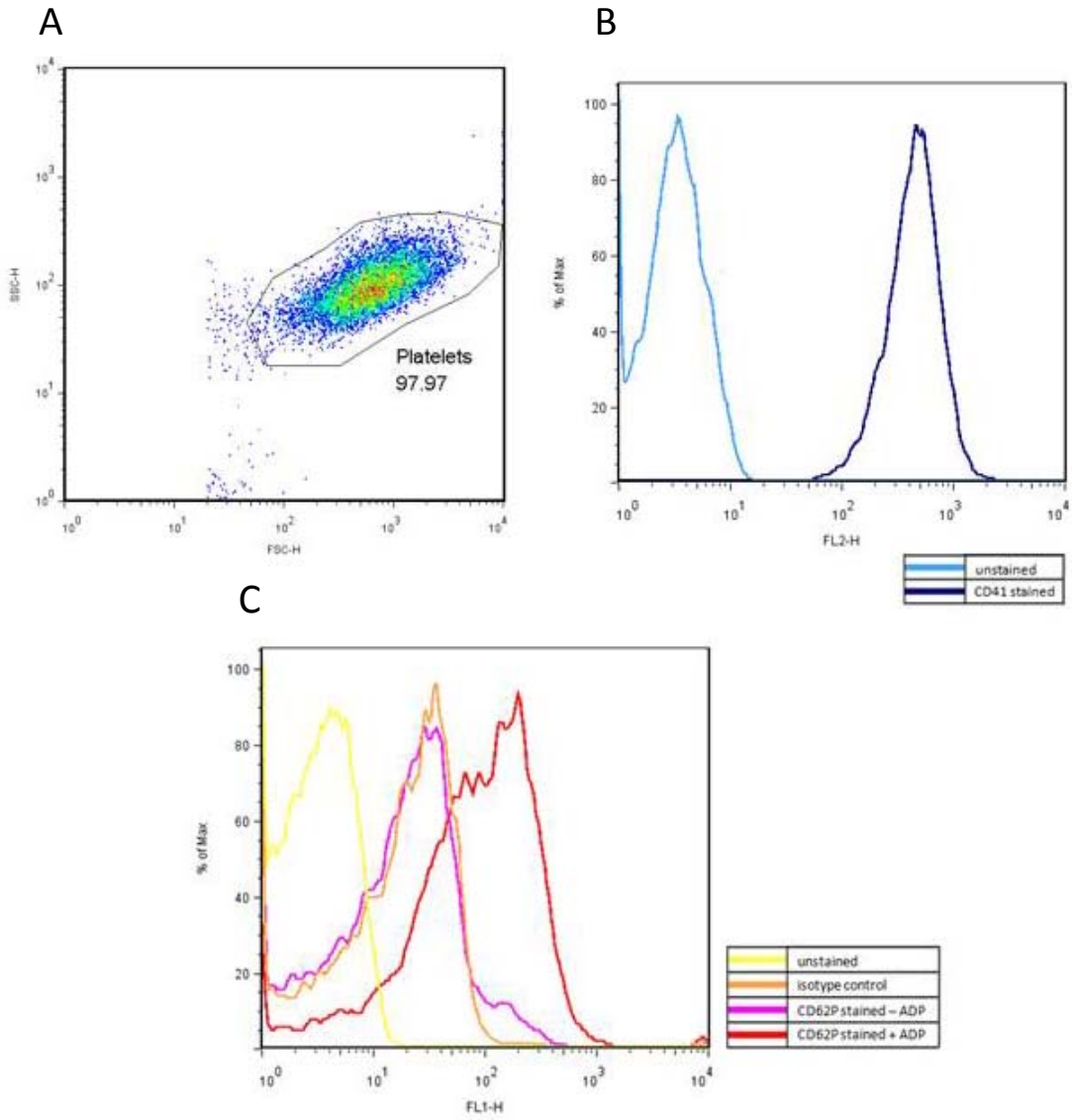

Figure 2.5: Assessment of platelet activation status by flow cytometry.
Platelet activation status was assessed by flow cytometric analysis of p-selectin expression. Platelets were gated by FSC/SSC characteristics. In this example, 97.97% of original events were within the platelet gate (A). 10,000 gated events were then analysed. Platelets were further identified by their expression of the platelet specific antigen CD41 (B). Platelet activation was identified by their expression of p-selectin (CD62P), tested with a positive (+ADP) and negative (-ADP) control (C). An isotype control for the anti-CD62P antibody was used to identify non-specific binding. Platelet activation status was expressed as the geometric mean fluorescence intensity (GMFI) of CD62P-stained platelets.

by vortexing (15s). Ethanol (absolute; 200µl) was then added for optimal column binding, and mixed by vortexing (15s). Each sample was then loaded into the DNeasy Mini spin column, subjected to centrifugation (6,000 x g, 1 min, RT) and the eluate was discarded. The column was then washed with Buffer AW1 (500µl) and the eluate was discarded following centrifugation (6,000 x g, 1 min, RT). The column was further washed with Buffer AW2 (500µl) and the eluate discarded following centrifugation (20,000 x g, 3 min, RT). The spin column was then placed in a fresh 2mL collecting tube and subjected to centrifugation (20,000 x g, 1 min, RT) to dry the spin column membrane and ensure no ethanol is carried over during DNA elution. The spin column was then placed in a fresh 1.5mL Eppendorf before Buffer AE (200µl) was added and incubated at RT for 1 min. DNA was eluted by centrifugation (6,000 x g, 1 min, RT). Eluted DNA was then stored at 4ºC.

2.6.1.2 Polymerase chain reaction (PCR)

PCR was carried out using the Invitrogen *Taq* DNA polymerase system (Invitrogen Ltd., UK). DNA samples (1.5µl) and primer mix (0.3mM each; Apo E Forward: AAC TTA CTC TAC ACA GGA TGC C, Apo E Reverse: CGT CAT AGT GTC CTC CAT CAG TGC; Invitrogen Ltd., UK) were pre-heated to 94ºC before 22µl "mastermix" was added, with a reaction composition of:

$MgCl_2$ (4.5mM)
1x PCR Buffer
dNTP mixture (0.5mM each)
Taq DNA polymerase (1 unit)
Nuclease-free water

Two controls were prepared as above; one with water instead of DNA to identify any contaminating DNA, and one with $ApoE^{+/-}$ DNA to represent both the wild-type and transgene alleles. Samples were heated for initial denaturation (94ºC, 3 min), then underwent 32 cycles of PCR amplification, which consisted of denaturation (94ºC, 35 s), annealing (58ºC, 1 min) and elongation (72ºC, 2 min). Samples were then incubated for an additional 3 min at 72ºC to ensure optimal elongation of products to full length. Upon completion of the PCR programme, samples were cooled to 4ºC.

2.6.1.3 Gel electrophoresis

PCR products were separated by electrophoresis on an agarose (Lonza, UK) gel (1% w/v in 1x TAE buffer; Tris-base (40mM), Acetic acid (0.01% v/v), EDTA (1mM), pH 8.0; all Sigma-Aldrich, UK) containing SYBR safe DNA dye (1:10,000; Invitrogen Ltd., UK). DNA samples (25µl) were prepared by adding loading dye (1µl; Promega, WI, USA). Prepared samples (26µl) were electrophoresed on the gel (140V, 1hr) alongside a 1Kb DNA ladder (Invitrogen Ltd., UK). The gel was then photographed under UV light at λ260nm to allow visualization of PCR product bands. The wild-type *Apoe* allele product was 584bp and the transgene *Apoe* allele product was 1500bp. Animals were confirmed as ApoE knockout mice if there was a clear transgene band and no wild-type band (Figure 2.6).

2.6.2. **mRNA quantification**

The transcript (mRNA) abundance of specific genes of interest was quantified using quantitative real time PCR (qPCR). Briefly, following extraction from the tissue of interest, total RNA was reverse transcribed to cDNA by the enzyme reverse transcriptase. Total cDNA then underwent qPCR using specific primers, allowing exponential amplification of the cDNA sequence of interest by the enzyme *Taq* DNA polymerase. The specialised 5' to 3' exonuclease activity of *Taq* DNA polymerase allows the use of fluorescent probes to quantify the amplification. The mRNA levels of the genes of interest were assessed relative to the mRNA levels of reference genes, to control for reverse transcription efficiency (Zhu *et al.*, 2005).

2.6.2.1 RNA extraction from lung

RNA was extracted from lung using the Qiagen RNeasy Mini Kit (Qiagen Ltd, UK). Tissue (~30mg) was homogenised in 600µl Buffer RLT (lysis buffer) with 10µl β-mercaptoethanol per mL, in order to denature ribonucleases released during cell lysis. The samples were subjected to centrifugation (16,000 x g, 3 min, RT). The supernatant was removed into an equal volume of 70% v/v ethanol and mixed for optimal column binding. This solution was then loaded into the RNeasy spin column, subjected to centrifugation (8,000 x g, 15 s, RT) and the eluate was discarded. The column was then washed with Buffer RW1 (700µl) and the eluate was discarded following centrifugation (8,000 x g, 15s, RT). Two further wash steps were

Figure 2.6: Example of ApoE$^{-/-}$ genotyping PCR product assessment by gel electrophoresis. PCR products were separated on a 1% gel at 100V for 1 hour, alongside a 1Kb DNA ladder. The wild-type *Apoe* allele product was 584bp and the transgene *Apoe* allele product was 1500bp. Animals were confirmed as ApoE knockout mice if there was a clear transgene band and no wild-type band, as with these 6 samples. – : negative control, + : positive control with DNA from ApoE$^{+/-}$ mice.

performed using Buffer RPE (500µl) followed by centrifugation (8,000 x g, 15s and 2 min, respectively, RT) and eluate discarding, to ensure no ethanol was carried over during RNA elution. The spin column was then placed in a fresh 2mL collecting tube and subjected to centrifugation (16,000 x g, 1 min, RT) to eliminate any Buffer RPE carryover. The spin column was then placed in a fresh 1.5mL Eppendorf before RNase-free water (30µl) was added and RNA eluted by centrifugation (8,000 x g, 1 min, RT). The eluate was added back to the column and for a further centrifugation (8,000 x g, 1 min, RT) to enhance the final RNA concentration. Eluted RNA was stored at -80°C. The RNA quality check (section 2.6.2.5) revealed there was no genomic DNA contamination.

2.6.2.2 RNA extraction from liver

RNA was extracted from liver as described above (section 2.6.2.1). The RNA quality check (section 2.6.2.5) revealed DNA contamination and so RNA samples underwent additional DNA-*free* (Applied Biosystems, CA, USA) treatment to eliminate genomic DNA. DNase 1 buffer (10x; 5µl) and rDNase 1 (1µl) were added to 50µl of extracted RNA and mixed gently. The samples were incubated at 37ºC for 20-30 min before DNase Inactivation Reagent (5µl) was added. The samples then underwent centrifugation (8,000 x g, 1.5 min, RT) and the supernatant, containing the RNA was transferred to a fresh tube. RNA was stored at -80ºC.

2.6.2.3 RNA extraction from heart

RNA was extracted from heart as described above (section 2.6.2.1) with the following modifications. Tissue (~30mg) was homogenised in 1mL Qiazol (Qiagen Let, UK), followed by incubation (5 min, RT) with chloroform (300µl; Rathburn Chemicals Ltd, UK). This alternative lysis protocol is deemed more appropriate for fibrous tissue, such as the heart, allowing better penetration of RNase inhibitors. The samples were then subjected to centrifugation (16,000 x g, 3 min, 4ºC). The top aqueous phase containing the RNA was removed into an equal volume of 70% v/v ethanol before being loaded onto the RNeasy spin column. An additional on-column DNase digestion step, carried out to eliminate genomic DNA: DNase 1 incubation mix (80µl; prepared as 10µl DNase 1 stock in 70µl Buffer RDD) was added directly onto the spin column membrane and incubated at RT for 15 mins. The column was

then washed again with Buffer RW1 (350µl) and the eluate was discarded following centrifugation (8,000 x g, 15s, RT). The protocol then continued as described above (section 2.6.2.1). Eluted RNA was stored at -80°C.

2.6.2.4 RNA quantification

RNA was quantified using a NanoDrop Spectrophotometer (Thermo Fisher, UK). The concentration of RNA was determined by the absorbance at 260nm wavelength (A_{260}) using Beer's law. The purity was assessed by the ratio A_{260}:A_{280} which was deemed acceptable if between 1.9 and 2.1, as suggested in the NanoDrop Manual (Thermo Fisher, UK).

2.6.2.5 RNA quality

Quality of RNA was assessed by electrophoresis on an agarose (Lonza, UK) gel (1.5% w/v in 0.5x TBE buffer; Tris-borate (89mM), EDTA (2mM) pH 8.0; all Sigma-Aldrich, UK) containing SYBR safe DNA dye (1:10,000; Invitrogen Ltd., UK). RNA samples (2µl) were prepared by adding loading dye (10µl; Promega, WI, USA; diluted 1:4 in RNase-free water). Prepared samples (12µl) were electrophorosed on the gel (100V, 1hr) before the gel was photographed under UV light (λ260nm) to allow visualization of RNA bands. RNA integrity was deemed satisfactory if sharp, clear 28S and 18S ribosomal RNA (rRNA) bands were present without smearing (Figure 2.7).

2.6.2.6 Reverse transcription polymerase chain reaction (RT-PCR)

Total RNA (500ng) was reverse transcribed using a Reverse Transcription System (Promega, UK). Each RNA sample was diluted to 57ng/µl in RNase-free water. RNA samples (8.7µl; 500ng) were denatured by incubation at 72ºC for 10 min, centrifuged for 10s to return sample to bottom of tube and returned to ice. To each denatured RNA sample, 11.3µl "mastermix" was added, with a reaction composition of:

$MgCl_2$ (5mM)
1x RT buffer (2µl)
dNTP mixture (1mM each)
Recombinant RNasin® Ribonuclease Inhibitor (1u/µl)
AMV (avian myeloblastosis virus) RT polymerase (15u/µg)
Random primers (0.25µg)
Nuclease-free water

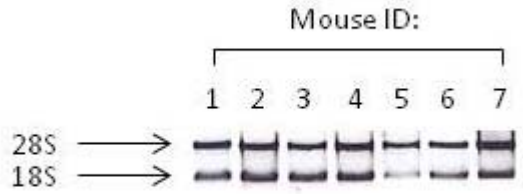

Figure 2.7: Example of RNA quality assessment by gel electrophoresis.
Eluted RNA was separated on a 1.5% gel at 100V for 1 hour. RNA integrity was assessed on the basis of 18S and 28S ribosomal RNA (rRNA) bands. RNA integrity was deemed satisfactory if sharp, clear 28S and 18S rRNA bands were present without smearing, and if 28S rRNA band was approximately twice as intense as 18S rRNA band, as with these 7 samples.

Two negative controls were prepared, as above, one with water instead of RNA (to identify any RNA contamination in reagents) and one without the reverse transcriptase enzyme (in order to detect the presence of contamination by genomic DNA (-veRT)). Samples were incubated at RT for 10 min, to allow annealing and extension of primers, followed by 15 min at 42ºC, to allow the reverse transcriptase to transcribe single-stranded RNA into double-stranded cDNA, and 5 min at 95ºC, to inactivate the enzymes. The resultant cDNA was stored at -20ºC.

2.6.2.7 Quantitative real time PCR (qPCR)

Abundance of mRNA was assessed using a LightCycler® 480 platform (Roche Applied Science, UK). Primers (Table 2.4; Invitrogen Ltd., UK) were designed to match intron-spanning probes within the Roche Universal Probe Library (UPL). It was not possible to design primers within the UPL system for some genes so commercially designed assays were used (Table 2.4; *Taq*Man® Gene Expression Assays; Applied Biosystems (ABI), UK). cDNA samples, including the –veRT sample, were diluted (1 in 20) in LightCycler H_2O (Roche Applied Science, UK) and 2µl were added to each well in triplicate. Standards were generated by serial dilution (1/4 – 1/512) of pooled cDNA from each sample and also added (2µl) in triplicate to the plate. A negative control containing water instead of cDNA was prepared to identify any cDNA contamination. To each standard and sample, 8µl "mastermix" was added.

UPL primers "mastermix" reaction composition:

Roche Probes Master (5µl)
Forward primer (0.2µM)
Reverse primer (0.2µM)
Probe (0.1µM)
LightCycler H_2O

ABI *Taq*Man® Gene Expression Assays "mastermix" reaction composition:

Roche Probes Master (5µl)
1x primer/probe assay mix
LightCycler H_2O

Table 2.4: Details of qPCR primers for use with Roche Universal Probe Library (UPL) and TaqMan® Gene Expression Assays from ABI.

Gene Accession No.		Primer sequence	UPL probe number
Serpine1 (PAI-1) NM_008871.2	For Rev	AGG ATC GAG GTA AAC GAG AGC GCG GGC TGA GAT GAC AAA	69
Plat (tPA) NM_008872.2	For Rev	GCC TGG GCA GAC ACA ATT A ATC ACA TGG CAC CAA GGT C	9
F8 (Factor VIII) NM_007977.2	For Rev	AGA TAC ACT TAC CCT GTT CCC ATT ACC CCA AGA CCC ATA GAC CT	2
Vwf (vWF) NM_011708.3	For Rev	GAG GAG GCC TGC ACT CAG GAC CCA GGT CTC CAG GAA CT	58
Plg (Plasminogen) NM_008877.3	For Rev	CCT GGC AAA TCA GCC TTA GA CCC ACT CTG GGG CTA TTA AA	56
Tbp (TATA box-binding protein) NM_013684.3	For Rev	GGG AGA ATC ATG GAC CAG AA GAT GGG AAT TCC AGG AGT CA	97
Rb18s (18s) NR_003278.1	For Rev	CTC AAC ACG GGA AAC CTC AC CGC TCC ACC AAC TAA GAA CG	78
		ID of TaqMan® Gene Expression Assays purchased from ABI	
Ppia (Cyclophilin) NM_008907.1		Mm02342430_gl	
Actb (β-actin) NM_007393.3		Mm01215647_gl	

For: forward, Rev: reverse, PAI-1: plasminogen activator inhibitor-1, tPA: tissue plasminogen activator, vWF: von Willebrand factor.

The plate was spun (800 x g, 2 min, 4ºC) to ensure contents were at the bottom of the wells. Samples were heated for initial denaturation and activation (95ºC, 5 min), then underwent 50 cycles of PCR amplification, which consisted of denaturation (95ºC, 10s), annealing and elongation (60ºC, 30s). Upon completion of the PCR programme, samples were cooled (40ºC, 30s). Amplification curves of cycle number against fluorescence were plotted. The crossing point (Cp) was calculated as the maximum point of the second derivative of the amplification curve. Triplicates of standards were deemed acceptable if the standard deviation of the Cp was < 0.5 cycles. Negative controls were deemed acceptable if >10 Cp higher than the lowest standard. Standard curves were deemed acceptable if reaction efficiency was between 1.7 and 2.1. A standard curve of Cp against log "concentration" (serial dilutions of pooled samples) for each gene was generated (Figure 2.8) and the mRNA "concentrations" of unknown samples were determined by interpolation from the standard curve. The mRNA abundance of the gene of interest was presented as ratio to reference gene(s). Reference genes did not vary between treatments.

2.7 Statistics

All statistical analysis was performed using Prism 5.01 software (GraphPad software, CA, USA). Comparisons between OPT and histological methods were performed by linear regression, and subsequent F-testing to determine if the slope deviates from a hypothetical value of 1.0 (Chapter 3). For comparison of physiological levels of endogenous glucocorticoid or exogenous glucocorticoid treatment with control, adrenalectomised mice (Chapter 3 and 4) or comparison of exogenous glucocorticoid treatment with vehicle treatment (Chapter 5), statistical analysis was performed by one-way analysis of variance (ANOVA) with Dunnett's post-hoc test. For comparison of the effects of exogenous glucocorticoids in C57Bl/6 mice and PAI-$1^{-/-}$ mice (Chapter 6), statistical analysis was performed by two-way ANOVA with Bonferroni's post hoc test. In all studies, n refers to the number of individual animals from which data were acquired.

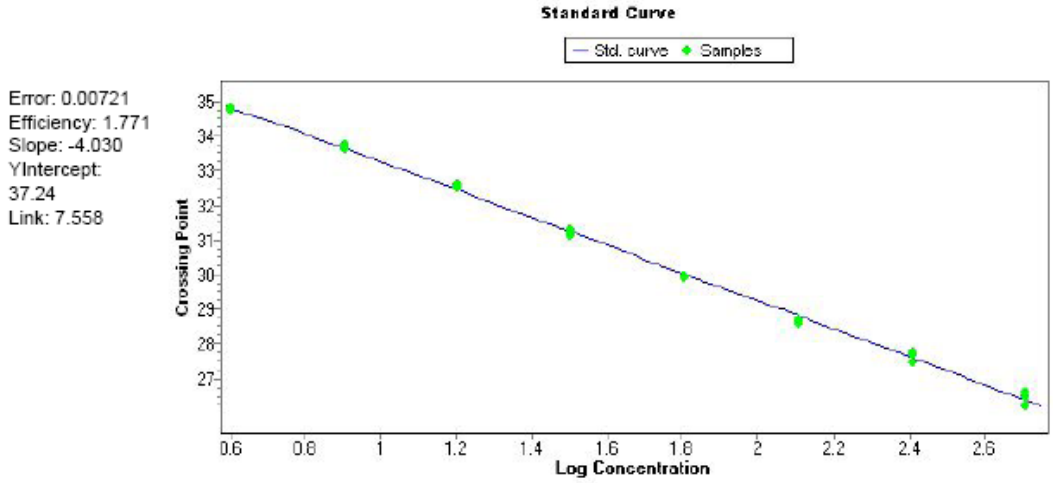

Figure 2.8: Example of qPCR standard curve.
The crossing point (Cp) decreases as log concentration of mRNA increases. Graph points were fitted with a straight line using Lightcycler 480 Software, Version 1.5 (Roche Applied Science, UK). Triplicates of standards were deemed acceptable if the standard deviation of the Cp was < 0.5 cycles. Standard curves were deemed acceptable if reaction efficiency was between 1.7 and 2.1. The mRNA concentration of unknown samples was determined from their Cp by interpolation from the standard curve. The mRNA levels of the target genes were quantified relative to the mRNA levels of appropriate housekeeping genes.

Chapter 3

Influence of glucocorticoids on atherosclerosis in the mouse

3.1 Introduction

The influence of glucocorticoids on atherosclerosis is imperfectly understood and unpredictable. On one hand, glucocorticoids are associated with adverse systemic effects on the cardiovascular system, such as dyslipidaemia (Becker *et al.*, 1988; Curtis *et al.*, 1982; Tauchmanova *et al.*, 2002), hypertension (Whitworth *et al.*, 2001) and hyperglycaemia (Delaunay *et al.*, 1997; Tounian *et al.*, 1997). In contrast, they also have potentially beneficial direct effects on the vascular wall, attenuating inflammation (Liu *et al.*, 1999; Yamada *et al.*, 1993) and smooth muscle cell migration and proliferation (Goncharova *et al.*, 2003; Voisard *et al.*, 1994), both of which are necessary for progression of atherosclerosis. Clinically, glucocorticoid excess, whether as a result of chronic glucocorticoid treatment or in patients with spontaneous Cushing's syndrome, is associated with enhanced cardiovascular disease (Colao et al., 1999; Etxabe et al., 1994; Souverein et al., 2004; Wei et al., 2004). This premise is further supported by the finding that inhibition of 11βHSD1, thereby reducing availability of active corticosterone in glucocorticoid target tissues, is anti-atherogenic in mice (Hermanowski-Vosatka *et al.*, 2005; Nuotio-Antar *et al.*, 2007) and adrenalectomy inhibits aortic lesion development in a rat model of atherosclerosis (Iams *et al.*, 1977). There has also been one study describing a pro-atherosclerotic effect of glucocorticoids in $ApoE^{-/-}$ mice fed a standard chow diet (Tous *et al.*, 2006). Despite this evidence that glucocorticoids are pro-atherogenic, other animal studies have suggested that systemic glucocorticoid treatment protects against atherosclerosis, at least in rabbits (Asai et al., 1993; Makheja et al., 1989; Naito et al., 1992). Therefore, the influence of glucocorticoids on lesion development remains unclear. Elucidating these effects will improve our understanding of the role of glucocorticoid activity in regulating atherogenesis and the therapeutic potential of glucocorticoids as a treatment for, or as a target in, cardiovascular disease.

The majority of *in vivo* atherosclerosis research has used rabbits as their primary animal model. The use of mice has, however, become more popular following the development of the $ApoE^{-/-}$ mouse (Plump *et al.*, 1992; Zhang *et al.*, 1992). Currently, the most commonly used murine model of atherosclerosis, both within our laboratory and elsewhere, combines the $ApoE^{-/-}$ mouse with high cholesterol,

"Western" diet to further accelerate plaque development. For example, Hermanowski-Vosatka *et al* used this model to show that pharmacological inhibition of 11βHSD1 (reducing pre-receptor generation of active glucocorticoid) ameliorates metabolic syndrome and prevents development of atherosclerotic lesions (Hermanowski-Vosatka *et al.*, 2005). Therefore, the Western-diet fed ApoE$^{-/-}$ mouse was chosen for the investigation described in this chapter.

Histological examination of atherosclerotic plaques dates back to the 1950s (Wanscher *et al.*, 1951) and remains the gold standard for lesion quantification as it allows detailed analysis of lesion cross sectional size and composition. Nevertheless, histology is labour intensive and is restricted to 2-dimensional analysis, thereby limiting information of plaque volume. The alternative, *en face* measure of atherosclerosis, which involves staining and quantifying lipid deposition within the aorta (Ko *et al.*, 2009; Mulvihill *et al.*, 2010), are limited by the inability to inspect lesion thickness or cellular composition. Visualising arteries in 3-dimensions, and from that considering volumetric parameters of lesion development, would allow a more robust and sensitive measure than the traditionally used 2-dimensional techniques (McAteer *et al.*, 2004). *Ex vivo* magnetic resonance imaging (MRI) and micro computed tomography (CT) have been applied to the study of murine atherosclerosis (Langheinrich *et al.*, 2004; McAteer *et al.*, 2004), but offer limited resolution and require long acquisition times. Optical coherence tomography (OCT) has been used successfully to visualise and quantify atherosclerosis in mice (Cilingiroglu *et al.*, 2006), but it is yet to be reported to enable 3-dimensional quantification of atherosclerotic plaques. Optical projection tomography (OPT) was originally described for the imaging of mouse embryos (Alanentalo *et al.*, 2007; Sharpe *et al.*, 2002) and has since been utilised to allow 3-dimensional visualisation and quantification of murine neointimal lesions (Kirkby *et al.*, 2011). OPT has, for the first time, successfully been implemented here in the visualisation of atherosclerotic plaques in the murine brachiocephalic artery. This technique allows 3-dimensional quantification of the aortic arch and plaques within, a feat almost impossible by standard histology.

3.2 Hypothesis and Aims

The work described in this chapter addresses the hypothesis that glucocorticoids are pro-atherogenic. It is therefore proposed that removal of endogenous glucocorticoids (adrenalectomy) inhibits, whilst glucocorticoid administration augments, lesion development in atherosclerosis-prone mice. In order to address this hypothesis, the specific aims of the work described in this chapter were to:

- optimise the use of optical projection tomography for improved quantification of murine atherosclerotic plaques.
- determine whether surgical removal of the adrenal glands reduced lesion development in $ApoE^{-/-}$ mice fed a western diet.
- determine whether chronic administration of the synthetic glucocorticoid dexamethasone increased lesion development in adrenalectomised $ApoE^{-/-}$ mice fed a western diet.

3.3 Methods

3.3.1. Animals

Male ApoE$^{-/-}$ mice (bred in-house at the Biomedical Research Facility, Little France, Edinburgh, UK) aged 5 weeks and weighing 17-23 grams were used in this study. A tissue sample from each mouse was analysed to confirm genotype (section 2.6.1).

3.3.2. Adrenalectomy

In order to investigate endogenous glucocorticoids mice were randomised to undergo either bilateral adrenalectomy or sham adrenalectomy (section 2.2.1).

3.3.3. Administration of drugs

Adrenalectomised mice were provided with 0.9% w/v NaCl in their drinking water. Vehicle (absolute ethanol) or the synthetic glucocorticoid dexamethasone (dex; 0.1mg/kg/day; section 2.2.3.1) were administered by addition to the drinking water. Animals that had undergone sham adrenalectomy were provided with vehicle in their standard drinking water. Drug administration commenced immediately after adrenalectomy/sham surgery and continued for 13 weeks (Figure 3.1). One week after surgery all animals were started on a high cholesterol (0.2%) Western Diet. Body weight and water intake were monitored throughout and used to titre the dex required to ensure the appropriate dose was administered.

3.3.4. Tissue collection

At the end of the 13-week treatment period the animals were fasted overnight, before blood was collected by tail tip and by cardiac puncture onto wet ice. The blood collected by tail tip was centrifuged (8,000 x g, 10min, 4ºC) and the plasma (supernatant) was removed into a fresh Eppendorf tube. The blood collected by cardiac puncture was allowed to clot on wet ice before being centrifuged (8,000 x g, 10min, 4ºC) and the serum (supernatant) was removed into a fresh tube. Plasma and serum samples were snap frozen on dry ice and stored at -80ºC. The mice were then perfusion fixed under terminal anaesthesia (section 2.2.6). The whole animal was then stored in 10% formalin for a minimum of 2 days to ensure complete fixation.

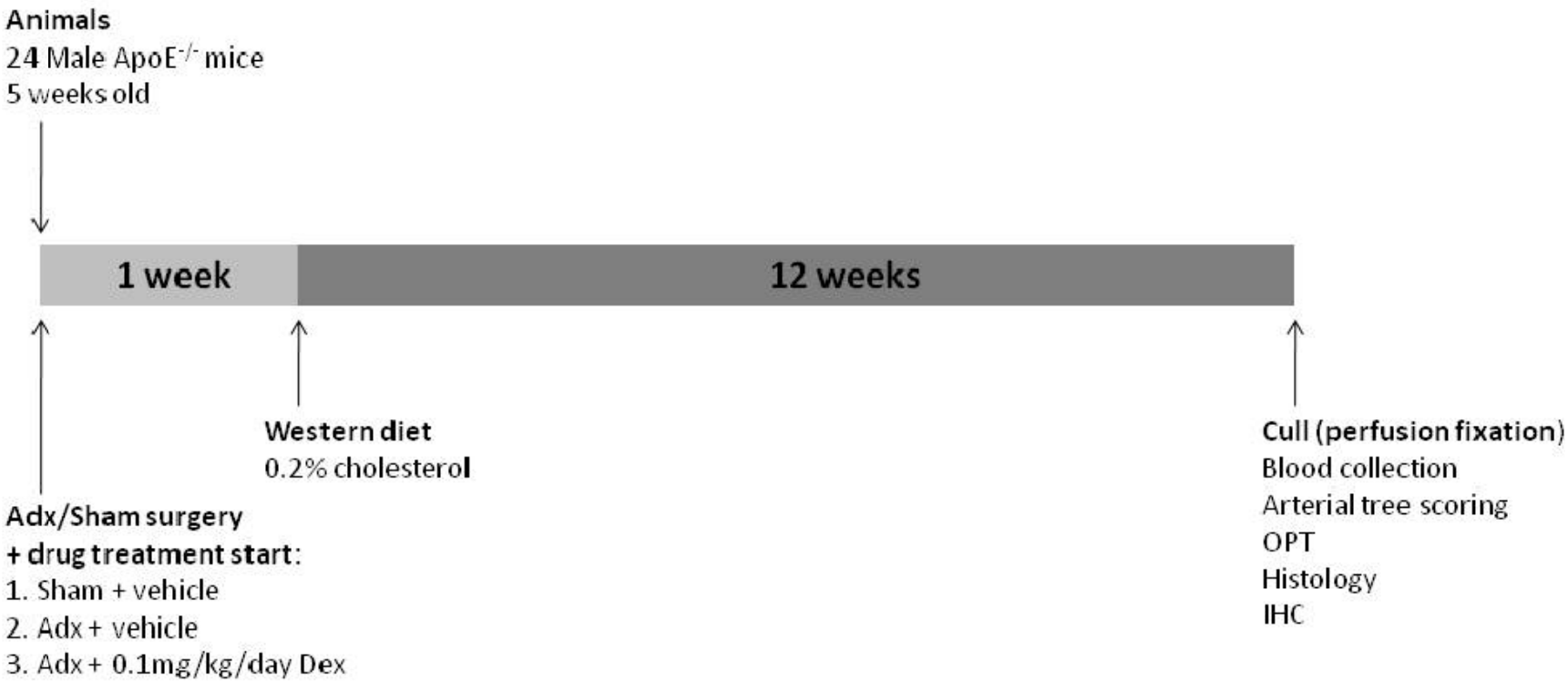

Figure 3.1: Study protocol to determine the effects of glucocorticoids on the development of atherosclerosis.
Experiments were conducted in male, 5 week old ApoE$^{-/-}$ mice. Animals were randomised to undergo adrenalectomy (adx) or sham surgery (n=8). Adrenalectomised animals were provided with 0.9% saline containing either vehicle (absolute ethanol; n=8) or dexamethasone (dex; 0.1mg/kg/day; n=8) in their drinking water for the remainder of the experimental period. One week following surgery all animals were placed on a high cholesterol (0.2%) western diet for 12 weeks. At the end of the experimental period mice were culled by perfusion fixation and the arterial tree was excised for examination of atherosclerotic plaque development by semi-quantitative scoring, optical projection tomography (OPT), histology and immunohistochemistry.

The arterial tree (consisting of aorta, carotid, subclavian, iliac and femoral arteries) was dissected free and cleaned of connective tissue before being stored in 70% ethanol. Organs (liver, kidneys, spleen, heart, adrenals and thymus) were removed and cleaned of connective tissue and weighed. They were then stored in 10% neutral buffered formalin for a further 24 hours before being transferred to 70% ethanol.

3.3.5. **Measurement of blood components**

3.3.5.1 Plasma corticosterone levels

Plasma spun from blood collected by tail tip immediately prior to sacrifice was used to assess corticosterone levels using a radioimmunoassay (section 2.5.1), to confirm successful removal of the adrenal glands.

3.3.5.2 Serum cholesterol and triglyceride levels

Serum spun from blood collected by cardiac puncture was used to assess cholesterol and triglyceride levels using respective colourimetric assays (section 2.5.2). Sera collected from chow-fed C57Bl/6 mice were used as controls for diet and genotype.

3.3.6. **Atherosclerotic plaque analysis**

3.3.6.1 Semi-quantitative scoring

To gain an insight into the extent of lesion development in $ApoE^{-/-}$ mice a semi-quantitative method was used to gauge lesion development and severity. The dissected arterial trees were semi-quantitatively scored (1-5) for lesion size at the predisposed sites (aortic root, lesser curvature, brachiocephalic artery, origin of the left carotid artery and left subclavian artery, origins of the renal arteries and the femoral artery branches) for atherosclerotic plaque development in high cholesterol fed $ApoE^{-/-}$ mice, where 1: no plaque, 2: small plaque 3: large plaque, 4: extensive plaque, 5: extensive plaque with outward remodelling (section 2.3.1).

3.3.6.2 Optical Projection Tomography (OPT)

Once scored, the aortic arch (and its major branches) was isolated from the vascular tree and embedded in agarose for analysis by OPT (section 2.3.2). Briefly, after dehydration in methanol (24 hours) and clearing in a refractive index-matching solution of BABB (24 hours), the arch was scanned under UV light using a Bioptonics OPT tomograph. Computed tomography reconstructions were calculated

by filtered back-projection of raw data using NRecon software. This imaging technique provides a 3-dimensional image of the arch and the atherosclerotic plaques within. Volumetric measurements of the brachiocephalic artery were acquired by manual tracing of the estimated outline of the plaque and lumen, respectively, using CTan software.

3.3.6.3 Histology

Following acquisition of OPT scans, the aortic arch was prepared for histological analysis by washing in methanol before standard processing and embedding in paraffin wax (section 2.4.1). The specimen was then cut into 4μm thick transverse sections through the entire brachiocephalic artery from the carotid-subclavian bifurcation to the ascending aorta. Transverse sections at 80μm intervals along the brachiocephalic artery were stained with United States trichrome stain (section 2.4.2). Photographs of the sections were taken using a light microscope coupled to a colour camera and image analysis system (MCID Basic 7.0 software; section 2.4.4). The plaque area and lumen area in each section were measured using Photoshop CS3 software (section 2.4.5). The section with the largest area of plaque was chosen to represent each arterial sample.

3.3.6.4 Composition

The cellular composition of the atherosclerotic plaques was investigated using histological staining and immunohistochemistry on sections of the artery adjacent to the section identified as having the largest plaque. Smooth muscle cell content was assessed using an alkaline-phosphatase conjugated monoclonal primary antibody against smooth muscle cell α-actin (section 2.4.7.2). A monoclonal rat anti-mouse primary antibody against Mac-2 (clone M3/38) was used to determine the macrophage content of plaques (section 2.4.7.3). The collagen content of the plaques was assessed using Picrosirius Red staining (section 2.4.3). In addition, the extracellular lipid content of the plaques was estimated by quantification of the acellular clefts seen in the UST stained sections. These have been shown to represent pools of extracellular lipid in unprocessed tissue sections (section 2.4.6).

3.3.7. **Statistics**

All statistical analysis was performed by one-way ANOVA with Dunnett's post-hoc test for comparison of physiological levels of endogenous glucocorticoid or exogenous glucocorticoid treatment with control, adrenalectomised mice. Comparisons between OPT and histological methods were performed by linear regression, and subsequent F-testing to determine if the slope deviates from a hypothetical value of 1.0. Statistical analysis of all data was performed using GraphPad Prism 4.0 software.

3.4 Results

3.4.1. Body weights

There were no differences in the weights of the animals at the start of the experiment. All animals gained weight steadily throughout the 13 week experimental period (Figure 3.2A), following early weight loss after adrenalectomy surgery. All animals lost weight at the final reading as they were fasted overnight prior to sacrifice. Adrenalectomy had no significant effect on body weight, whilst dex treatment inhibited the animals' weight gain ($p<0.05$) in comparison to the adx group (Figure 3.2B). By the end of the protocol, the surgical incisions had healed fully and the fur had re-grown in all animals. Food intake was consistent between the three groups averaging at approx. 23g per mouse per week. The average dex intake was 0.10±0.004mg/kg/day.

3.4.2. Organ weights

Adrenalectomy had no effect on organ weights, whereas dex treatment reduced thymus weight ($p<0.01$; Figure 3.3A), and increased left kidney weight ($p<0.05$; Figure 3.3B). Although a similar pattern was seen in the right kidney, the difference was not significant (Figure 3.3C). There were no significant changes seen in the other organs collected (liver, heart and spleen; Figure 3.4).

3.4.3. Plasma corticosterone levels

Both adrenalectomised groups had significantly reduced corticosterone levels compared with sham adrenalectomised mice (Figure 3.5). It is important to note that adrenalectomy did not completely abolish circulating corticosterone level.

3.4.4. Serum cholesterol and triglyceride levels

Serum cholesterol and triglyceride levels were measured in blood collected *post mortem* by cardiac puncture. When compared with chow-fed C57Bl/6 mice, sham ApoE$^{-/-}$ mice on a Western diet had a 20-fold increase in cholesterol (Figure 3.6A) and 2-fold increase in triglycerides (Figure 3.6B). Neither adrenalectomy nor dex treatment caused any significant change in serum lipid levels (Figure 3.6A and B).

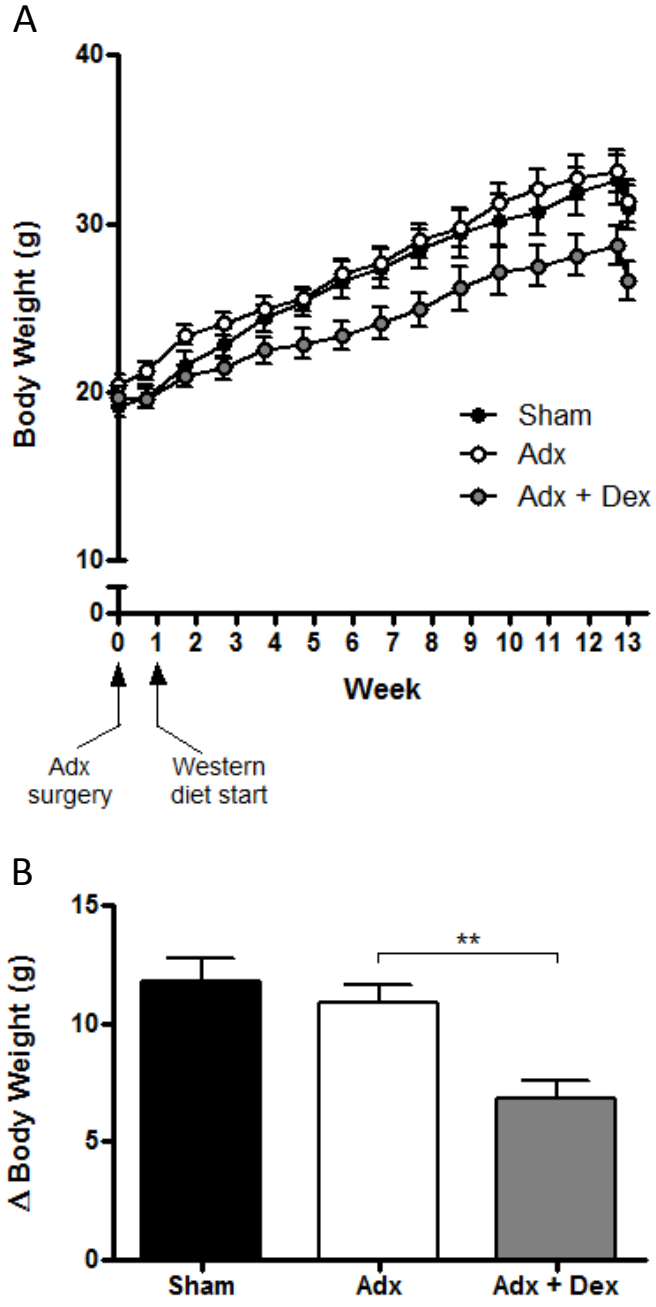

Figure 3.2: Weight changes induced by adrenalectomy and dexamethasone treatment.
Mice were randomised to undergo sham or adrenalectomy (adx) surgery. Adx animals were supplied with 0.9% saline with either vehicle or dexamethasone (dex; 0.1mg/kg/day) as their drinking water. Atherosclerotic lesion development was accelerated by provision of a high cholesterol (0.2%) western diet. (A) Body weight was measured regularly throughout the 13 week experimental period. Mice in the three different groups had similar body weights at the start of the experiment and all animals gained weight steadily throughout the 13 week experimental period following an early weight loss after adx surgery and a final weight loss due to fasting overnight prior to sacrifice. (B) Change in body weight from the start to the end of the experimental period was also calculated. Adx had no significant effect on weight gain, whereas weight gain was reduced in dex-treated animals. All data expressed as mean±SEM, n=8. Data were analysed by one way ANOVA with Dunnett's post hoc test vs adx. **p<0.01.

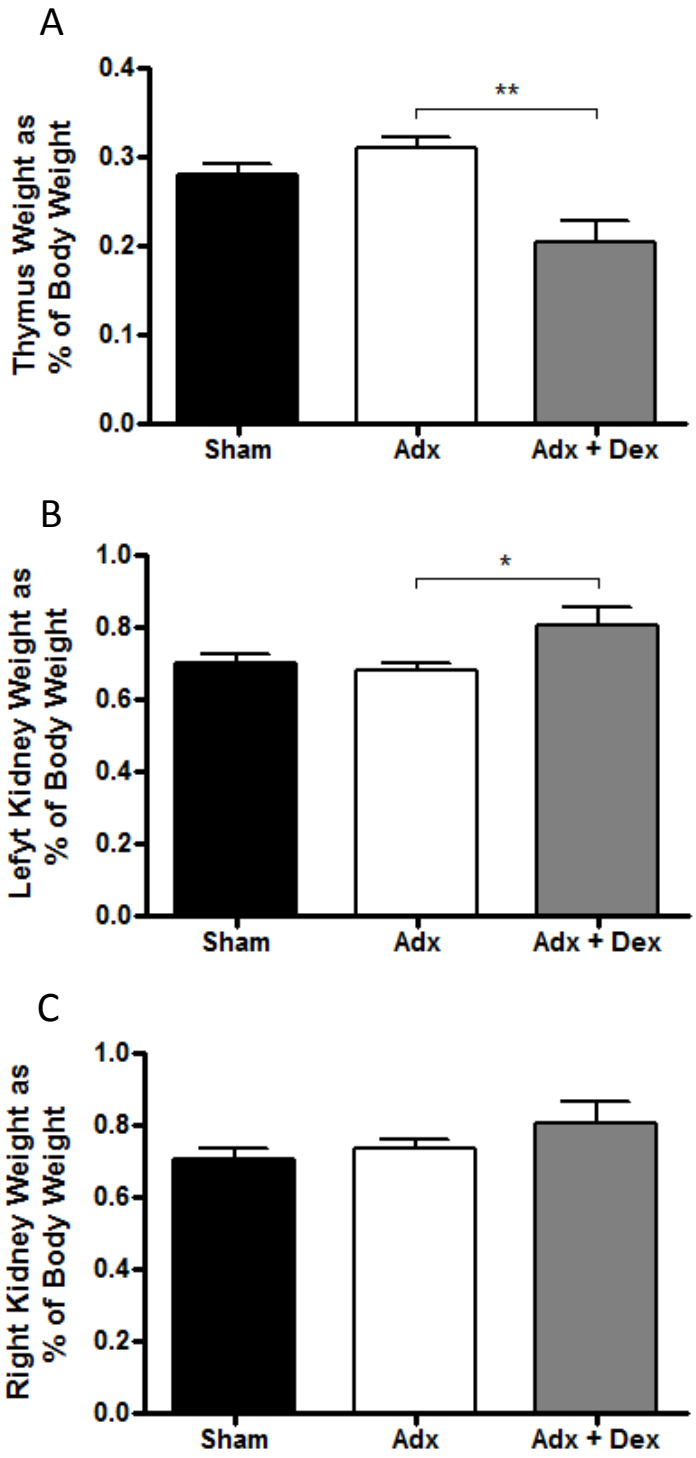

Figure 3.3: Organ weight changes induced by adrenalectomy and dexamethasone treatment. Mice were randomised to undergo sham or adrenalectomy (adx) surgery. Adx animals were supplied with 0.9% saline supplemented with either vehicle or dexamethasone (dex; 0.1mg/kg/day) as their drinking water. Atherosclerotic lesion development was accelerated by provision of a high cholesterol (0.2%) western diet. Organs were weighed upon sacrifice. Adx had no effect on any organ weight. In contrast, dex treatment caused a reduction in thymus weight (A) and an increase in left kidney weight (B). This effect was mirrored in the right kidney but did not reach significance (C). Data expressed as mean±SEM, n=8. Data were analysed by one-way ANOVA with Dunnett's post hoc test vs adx. * $p<0.05$, ** $p<0.01$.

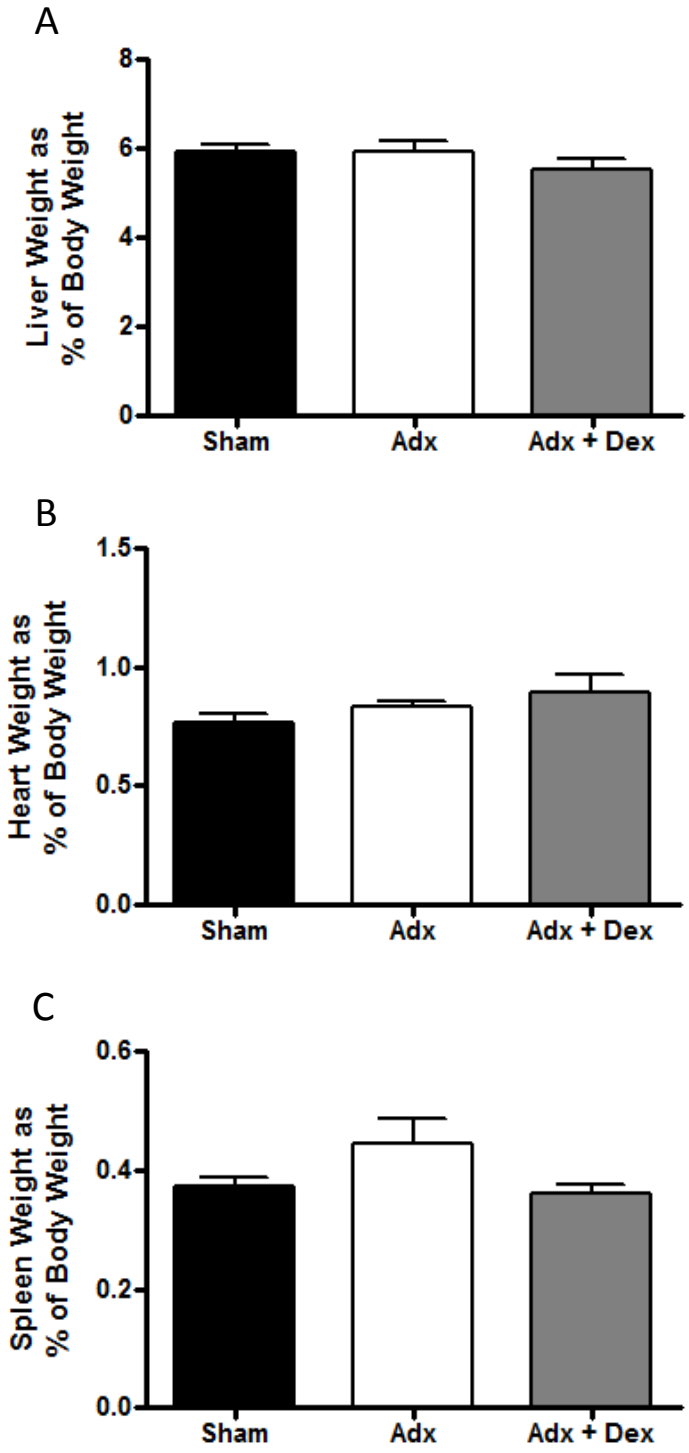

Figure 3.4: Organ weight changes induced by adrenalectomy and dexamethasone treatment. Mice were randomised to undergo sham or adrenalectomy (adx) surgery. Adx animals were supplied with 0.9% saline supplemented with either vehicle or dexamethasone (dex; 0.1mg/kg/day) as their drinking water. Atherosclerotic lesion development was accelerated by provision of a high cholesterol (0.2%) western diet. Organs were weighed upon sacrifice. Neither adx nor dex influenced liver, heart or spleen weight. Data expressed as mean±SEM, n=8. Data were analysed by one-way ANOVA with Dunnett's post hoc test vs adx.

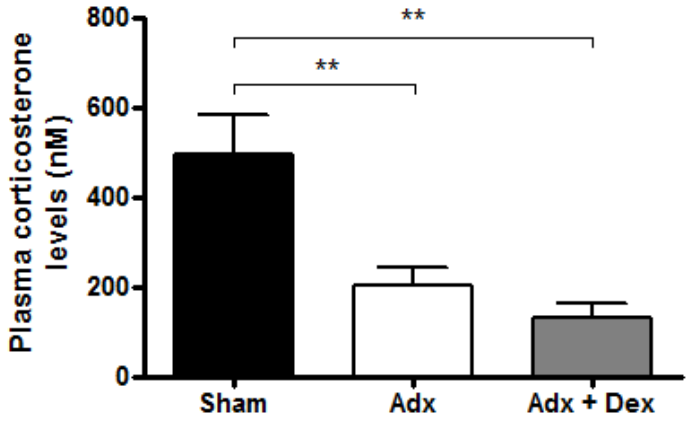

Figure 3.5: Plasma corticosterone levels in sham and adrenalectomised animals.
Mice were randomised to undergo sham or adrenalectomy (adx) surgery. Adx animals were supplied with 0.9% saline with either vehicle or dexamethasone (dex; 0.1mg/kg/day) as their drinking water. Atherosclerotic lesions development was accelerated by provision of a high cholesterol (0.2%) western diet. Plasma corticosterone levels were measured in tail-tip plasma by radioimmunoassay. Both groups that underwent adrenalectomy had significantly lower plasma corticosterone levels when compared with sham animals. Data expressed as mean±SEM, n=8. Data were analysed by one-way ANOVA with Dunnett's post hoc test vs sham, **$p<0.01$.

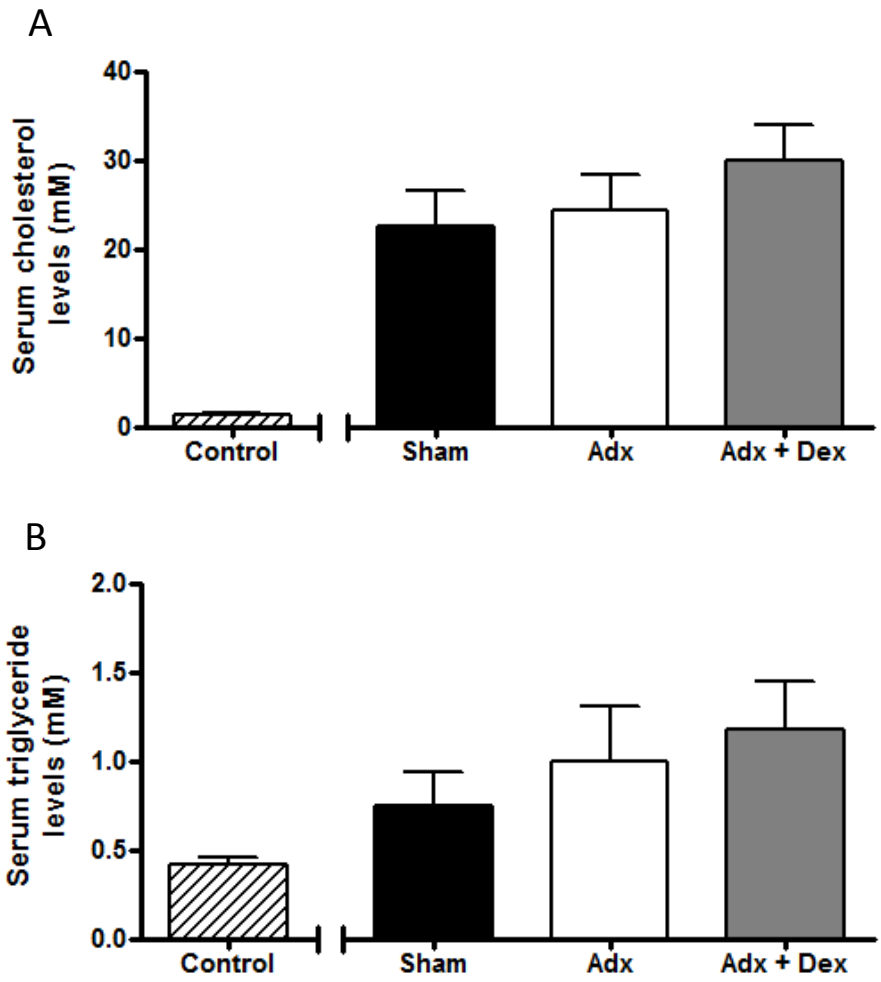

Figure 3.6: Impact of adrenalectomy and dexamethasone treatment on serum cholesterol and triglyceride levels.
Mice were randomised to undergo sham or adrenalectomy (adx) surgery. Adx animals were supplied with 0.9% saline with either vehicle or dexamethasone (dex; 0.1mg/kg/day) as their drinking water. Atherosclerotic lesion development was accelerated by provision of a high cholesterol (0.2%) western diet. Neither adx nor dex treatment had any significant effect on serum cholesterol (A) or triglyceride (B) levels. However, compared with chow-fed control C57Bl6 mice (striped bars), the combination of genotype and western diet increase both cholesterol (A) and triglyceride (B) levels. All data expressed as mean±SEM, n=8 (controls n=6). Data were analysed by one-way ANOVA with Dunnett's post hoc test vs adx.

3.4.5. **Atherosclerotic plaque development**

3.4.5.1 Semi-quantitative scoring

All animals exhibited visible atherosclerotic plaques in the lesser curvature of the aorta, the brachiocephalic artery and the origins of the left common carotid artery and the left subclavian artery (Figure 3.7). The brachiocephalic artery consistently exhibited the most extensive plaque burden. Neither adrenalectomy nor dex treatment significantly altered the lesion burden at any of the 8 areas (Table 3.1). Scores were higher at all sites in the dex-treated animals but this difference did not achieve significance.

3.4.5.2 Optical projection tomography (OPT)

3.4.5.2.1 *Validation of OPT*

Optical projection tomography imaging of atherosclerotic plaques proved very successful. Atherosclerotic plaques were clearly visible in both the raw images and in back-projected reconstructions in the expected anatomical distribution, comprising lesions in the lesser curvature of the arch, the brachiocephalic artery and at the origins of the left common carotid and left subclavian arteries (Figure 3.8A). In cross section, these plaques were typically eccentric in morphology and could easily be distinguished from the media due to its greater fluorescent signal. Similarly, the lumen could be distinguished from the vessel by its absence of signal (Figure 3.8B).

To validate the interpretation of OPT reconstructions, cross-sectional areas of atherosclerotic plaque within the brachiocephalic artery were quantified from serial histological sections and corresponding 2D tomographic planes within the OPT reconstructions of the same vessels. Not only were there striking similarities between the histological sections and OPT virtual sections (Figure 3.8C), but also clear, significant correlation between the two measurement modalities (R^2=0.85; Figure 3.9A). More importantly, the slope of these relationships between histological and OPT measurements did not significantly deviate from 1 (p=0.88). Bland-Altman analysis revealed a small but positive bias in OPT-derived measurements (Figure 3.9B), possibly reflecting shrinkage of these large vessels during histological

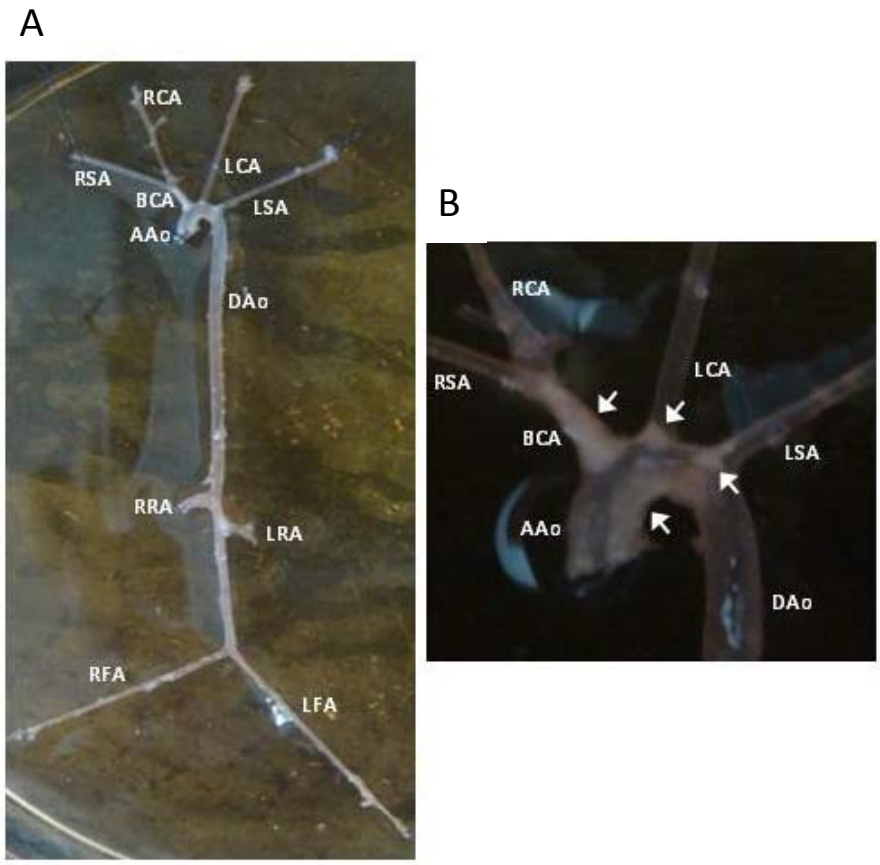

Figure 3.7: **Example of arterial tree used to assess atherosclerotic plaque distribution.** Perfusion-fixed, arterial trees from ApoE-/- mice, fed a western diet for 12 weeks, were excised and used to assess atherosclerotic plaque distribution. Plaque size was semi-quantitatively scored (1-5) at sites predisposed to atherosclerotic plaque development (A); right subclavian artery (RSA), right carotid artery (RCA), left carotid artery (LCA), left subclavian artery (LSA), brachiocephalic artery (BCA), ascending aorta (AAo), descending aorta (DAo), right renal artery (RRA), left renal artery (LRA), right femoral artery (RFA), left femoral artery (LFA). A higher power image of the arch region (B) allows clear identification of the atherosclerotic plaques (white arrows) in their expected anatomical distribution.

Table 3.1: Semi-quantitative scoring of lesion size at sites within the arterial tree.

Site	Sham	Adx	Adx + Dex
n	8	8	8
Aortic Root	0.3 ± 0.2	1.1 ± 0.2	1.3 ± 0.3
Inner curvature	0.9 ± 0.2	1.4 ± 0.2	1.8 ± 0.3
Brachiocephalic artery	2.8 ± 0.3	2.4 ± 0.3	2.8 ± 0.3
Root of left carotid artery	1.9 ± 0.3	1.7 ± 0.3	2.3 ± 0.3
Root of left subclavian artery	1.7 ± 0.3	1.4 ± 0.3	2.3 ± 0.3
Root of renal branches	0.5 ± 0.2	0.8 ± 0.2	1.1 ± 0.3
Right femoral artery	1.0 ± 0.3	0.7 ± 0.2	1.3 ± 0.5
Left femoral artery	0.9 ± 0.3	0.6 ± 0.4	0.5 ± 0.4
TOTAL	9.5 ± 0.5	9.0 ± 1.2	11.8 ± 1.6

Mice were randomised to undergo sham or adrenalectomy (adx) surgery. Adx animals were supplied with 0.9% saline, supplemented with either vehicle or dexamethasone (dex; 0.1mg/kg/day), as their drinking water. Atherosclerotic lesion development was accelerated by provision of a high cholesterol (0.2%) western diet before isolation of the arterial tree. Areas of the arterial tree predisposed to atherosclerotic plaque development were semi-quantitatively scored 1-5 where 1: no plaque, 2: small plaque 3: large plaque, 4: extensive plaque, 5: extensive plaque with outward remodelling. Neither adx nor dex treatment significantly altered the score at any of the 8 areas, although the dexamethasone-treated animals consistently averaged the highest score, with the exception of the left femoral artery. All data expressed as mean±SEM, n=8. Data were analysed by one-way ANOVA with Dunnett's post hoc test.

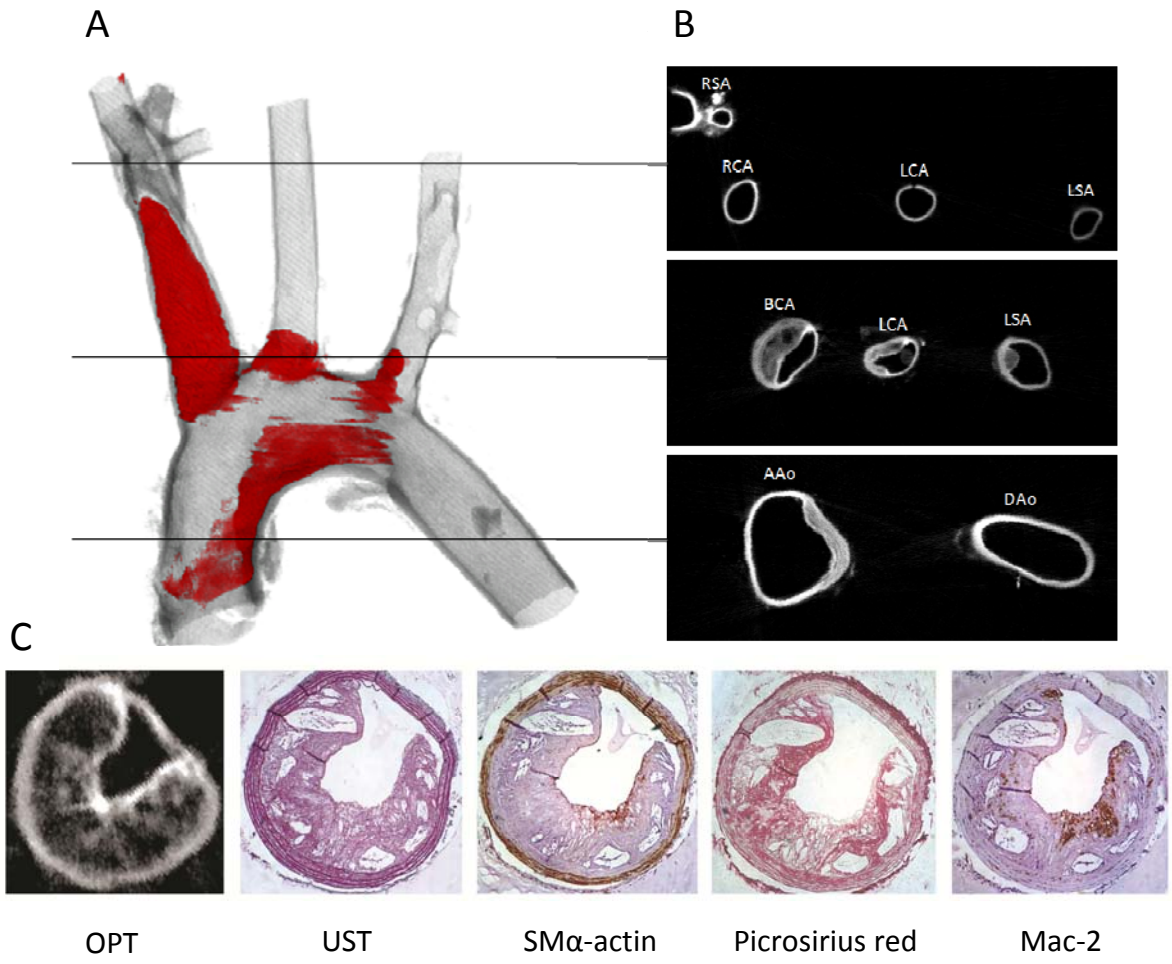

Figure 3.8: Optical projection tomographic (OPT) imaging of atherosclerotic plaques in the mouse aortic arch.
Perfusion-fixed, aortic arches from ApoE$^{-/-}$ mice, fed a western diet for 12 weeks, were subjected to optical projection tomographic scanning. In non-tomographic images of the aortic arch, atherosclerotic plaques were clearly visible (highlighted in red) in the expected anatomical distribution comprising lesions in the lesser curvature of the arch, the brachiocephalic artery and at the origins of the left common carotid and left subclavian arteries (A). In reconstructed virtual cross-sections, plaques were visible with the same distribution and can easily be distinguished from the media due to its greater fluorescent signal (B). Regions within the plaque devoid of fluorescence are thought to represent intra-plaque lipid pools, which would be removed during histology preparation. These virtual cross sections possess striking similarity to histological, United States trichrome (UST)-stained sections from the same region of the same artery (C). Successful analysis of the brachiocephalic artery by standard histology and immunochemistry confirmed the non-destructive nature of this technique (C). RSA: right subclavian artery; RCA: right carotid artery; LCA: left carotid artery; LSA: left subclavian artery; BCA: brachiocephalic artery; AAo: ascending aorta; DAo: descending aorta; SMα-actin: smooth muscle α-actin.

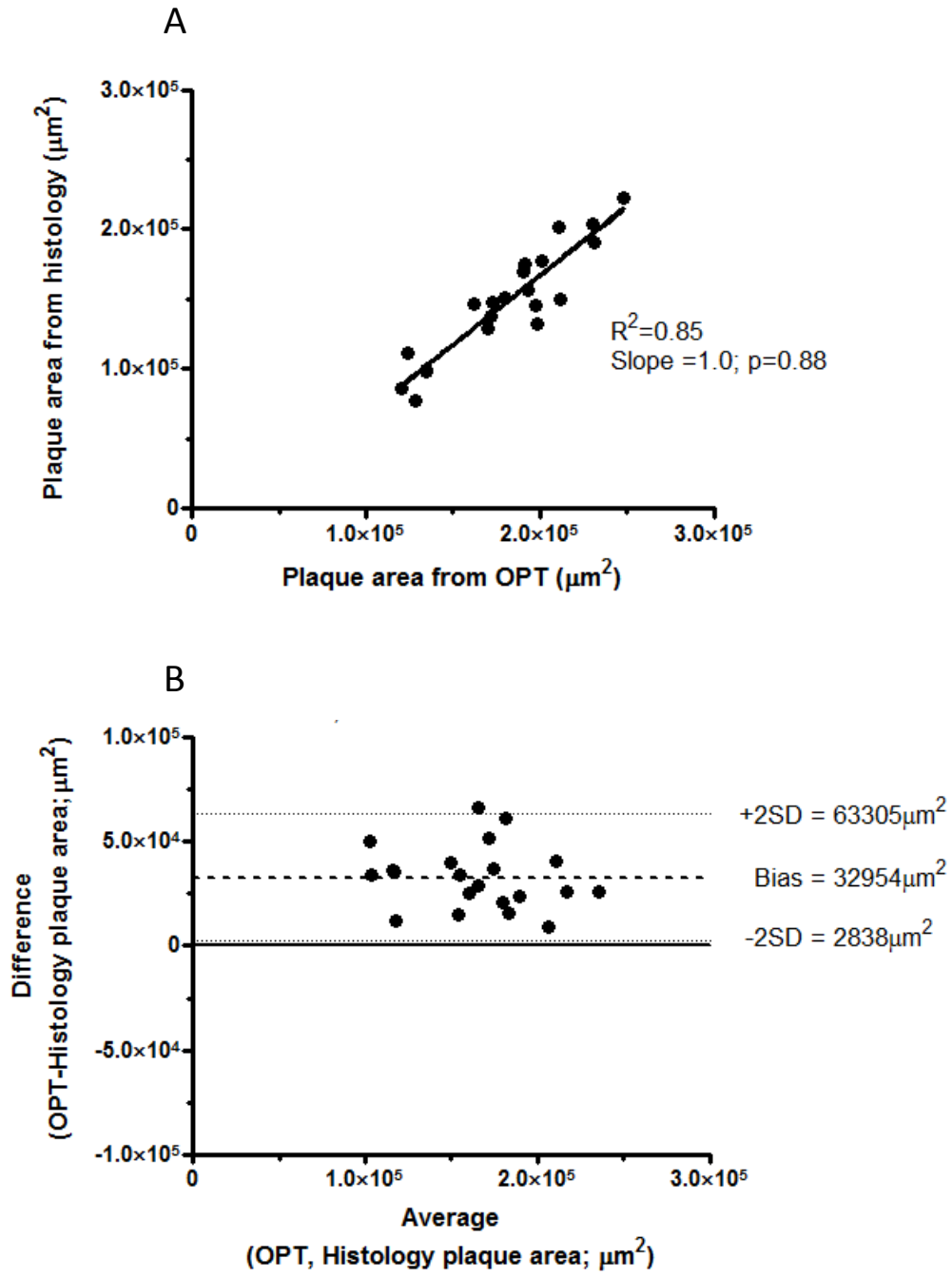

Figure 3.9: **Comparison of optical projection tomography (OPT) and histological methods for 2D analysis of brachiocephalic plaque size.**
Perfusion-fixed, aortic arches from ApoE$^{-/-}$ mice, fed a western diet for 12 weeks, were subjected to optical projection tomographic scanning before histological analysis of the same vessels. Comparison of 2D measures of brachiocephalic artery atherosclerotic plaque area derived from OPT scans and histological sections of the same area by linear regression showed a strong correlation and that the slope of relationship did not differ from 1 (A). Bland-Altman analysis indicates that OPT measurements have a consistent positive bias (B). n=21.

processing. Crucially, however, this bias was independent of plaque size indicating that measurements made in this way are comparable within and between vessels. It was also confirmed that the OPT imaging procedure did not compromise subsequent analysis of lesion composition. In vessels previously subjected to OPT scanning, immunohistochemical staining for markers of smooth muscle (smooth muscle α-actin) and macrophages (Mac2), and histological staining for collagen (picro-sirius red) all occurred with an intensity and distribution (Figure 3.8C) consistent with previous work with this model (Van Herck *et al.*, 2009).

While 2D comparisons of OPT and histology provide crucial validation, the novel potential of OPT is to allow 3D, volumetric analysis. After optimising the protocol for volumetric quantification for use in atherosclerotic arteries, plaque volumes were successfully recorded (0.18 ± 0.018 mm^3; n=8). The coefficient of variation (4.79%, n=4) indicated that these measurements were highly reproducible.

3.4.5.2.2 *Plaque quantification by OPT*

The brachiocephalic trunk in all three groups contained extensive atherosclerotic plaques. Adrenalectomy had no effect on the plaque volume or maximum cross-sectional area. In contrast, dex increased the volume of plaque ($p<0.05$; Figure 3.10A), subsequently increasing the volumetric stenotic ratio ($p<0.05$; Figure 3.10B) and reducing the volumetric luminal ratio ($p<0.05$; Table(a)). However, the maximum cross-sectional area of the plaque, and corresponding lumen area, was unaffected by dex (Figure 3.11A and B). Analysis of the cross-sectional profile of the plaque revealed that dex augmented the cross-sectional area of the plaque over the majority of the artery, thereby accounting for the increase in plaque volume despite no change in maximum cross-sectional area (Figure 3.11C).

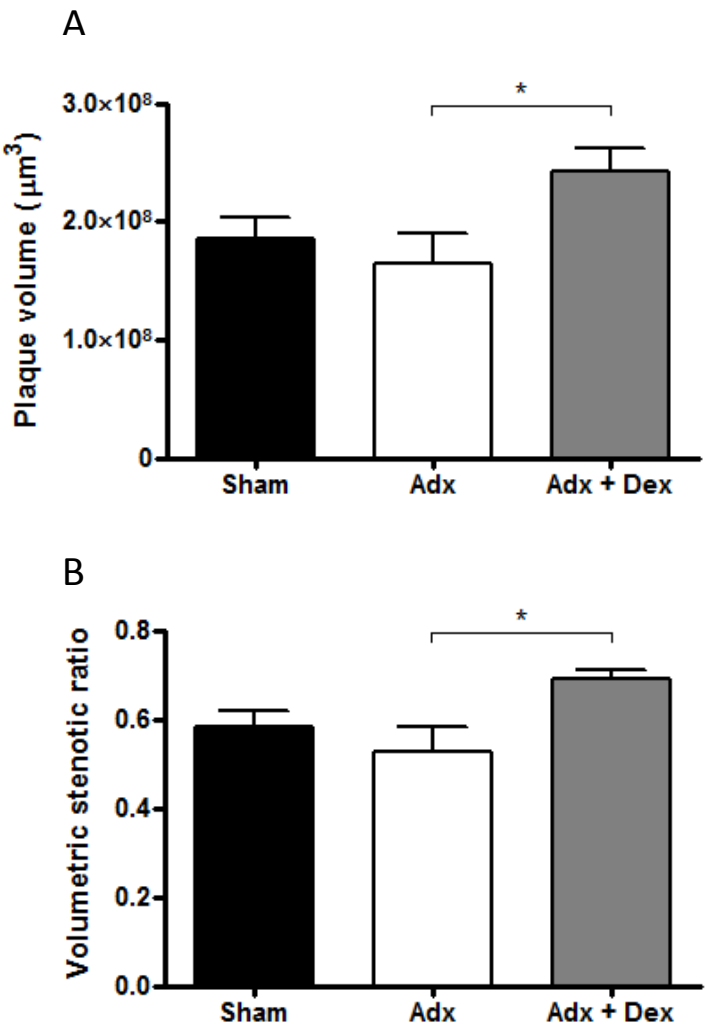

Figure 3.10: Impact of adrenalectomy and dexamethasone treatment on brachiocephalic plaque volume, as assessed by optical projection tomography (OPT).
Mice were randomised to undergo sham or adrenalectomy (adx) surgery. Adx animals were supplied with 0.9% saline with either vehicle or dexamethasone (dex; 0.1mg/kg/day) as their drinking water. Atherosclerotic lesion development was accelerated by provision of a high cholesterol (0.2%) western diet before isolation and OPT scanning. Plaque volumes were quantified from reconstructed tomograms and expressed as absolute volume (A) and as the volumetric stenotic ratio; plaque volume as proportion of volume inside internal elastic lamina (IEL; B). Adx had no influence on plaque volume. Dex treatment significantly increased absolute plaque volume (A) and volumetric stenosis (B). All data expressed as mean±SEM, n=6-8. Data were analysed by one-way ANOVA with Dunnett's post hoc test vs adx, * $p<0.05$.

Table 3.2: Impact of adrenalectomy and dexamethasone treatment on the size and composition of brachiocephalic atherosclerotic plaques.

Measurement	Sham	Adx	Adx + Dex
n	8	6	7
(a) 3D Morphometry (OPT)			
Plaque volume ($x10^7 \mu m^3$)	18.6 ± 1.7	16.5 ± 2.5	**24.3 ± 1.9***
Luminal volume ($x10^7 \mu m^3$)	13.3 ± 1.4	14.8 ± 2.1	10.7 ± 0.7
Volume inside IEL ($x10^7 \mu m^3$)	31.9 ± 2.1	31.3 ± 2.6	35.0 ± 2.2
Volumetric stenotic ratio	0.58 ± 0.04	0.53 ± 0.06	**0.69 ± 0.02***
(b) 2D Morphometry (OPT)			
Plaque max area ($x10^4 \mu m^2$)	21.2 ± 1.2	21.3 ± 1.8	24.3 ± 1.6
Luminal area ($x10^4 \mu m^2$)	6.9 ± 1.6	7.7 ± 1.2	6.3 ± 1.3
Area inside IEL ($x10^4 \mu m^2$)	28.1 ± 1.5	29.1 ± 1.7	30.7 ± 1.1
Stenotic ratio	0.76 ± 0.05	0.73 ± 0.04	0.79 ± 0.04
(c) 2D Morphometry (Histology)			
Plaque max area ($x10^4 \mu m^2$)	13.6 ± 0.9	14.9 ± 2.1	16.2 ± 1.6
Medial area ($x10^4 \mu m^2$)	10.2 ± 0.9	11.7 ± 1.4	8.6 ± 0.4
Intima/Media ratio	1.4 ± 0.1	1.3 ± 0.1	**1.9 ± 0.1****
Luminal area ($x10^4 \mu m^2$)	10.0 ± 0.8	10.3 ± 1.2	7.4 ± 0.8
Area inside IEL ($x10^4 \mu m^2$)	23.6 ± 1.0	25.2 ± 2.6	23.6 ± 1.7
Stenotic ratio	0.57 ± 0.03	0.58 ± 0.05	0.68 ± 0.04
(d) Composition (Histology/IHC)			
Smooth Muscle α-actin (%)	2.9 ± 0.3	3.0 ± 0.2	2.9 ± 0.4
Collagen (%)	29.4 ± 2.7	25.6 ± 3.0	30.9 ± 3.9
Lipid (%)	27.8 ± 2.0	25.7 ± 2.8	26.0 ± 1.0
Mac-2 (%)	10.6 ± 2.0	11.7 ± 3.0	**3.8 ± 0.9***

Mice were randomised to undergo sham or adrenalectomy (adx) surgery. Adx animals were supplied with 0.9% saline supplemented with either vehicle or dexamethasone (dex; 0.1mg/kg/day) as their drinking water. Atherosclerotic lesion development was accelerated by provision of a high cholesterol (0.2%) western diet before isolation and examination of the brachiocephalic artery by optical projection tomography (a and b), histology (c and d) and immunohistochemistry (d). Adx had no influence on any parameter measured. Dex treatment augmented plaque volume, increasing the volumetric stenotic ratio and thereby reducing the volumetric luminal ratio (a). Dex treatment did not influence the cross-sectional area of the plaque as measured by OPT (b) or histology (c), but did reduce macrophage content of the plaque as measured by immunohistochemistry (d). All data expressed as mean±SEM, n=6-8. Data were analysed by one-way ANOVA with Dunnett's post hoc test vs adx, * $p<0.05$.

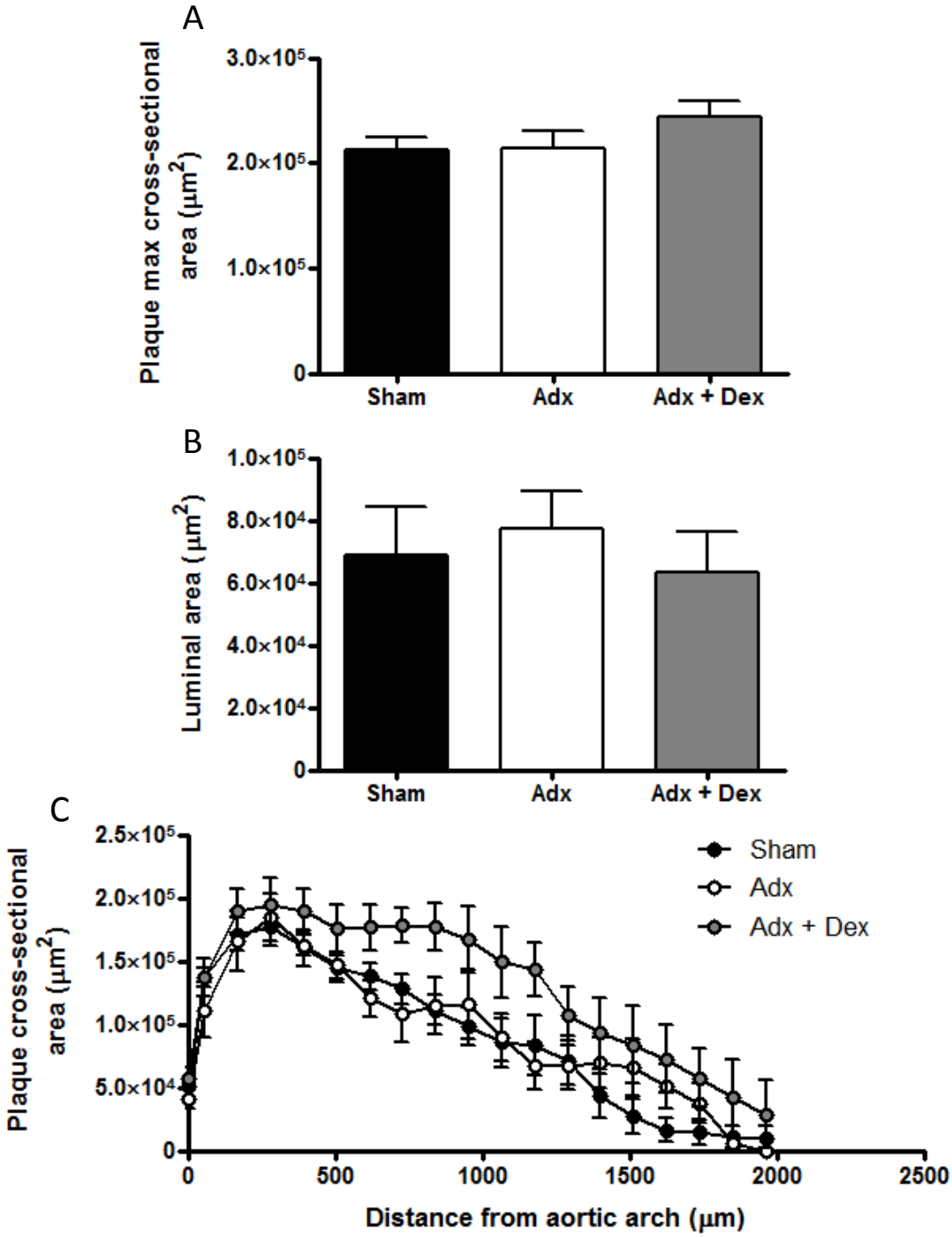

Figure 3.11: **Impact of adrenalectomy and dexamethasone treatment on brachiocephalic plaque and lumen cross-sectional area, as assessed by optical projection tomography (OPT).** Mice were randomised to undergo sham or adrenalectomy (adx) surgery. Adx animals were supplied with 0.9% saline with either vehicle or dexamethasone (dex; 0.1mg/kg/day) as their drinking water. Atherosclerotic lesions development was accelerated by provision of a high cholesterol (0.2%) western diet before isolation and OPT scanning. Plaque and lumen cross-sectional areas were quantified from reconstructed tomograms. Neither adx nor dex treatment influenced the max cross-sectional area of the plaque (A) or corresponding lumen cross-sectional area (B). However, analysis of the cross-sectional profiles of the plaque (C) revealed that dex treatment, but not adx, increased the cross-sectional area of the plaque along most of the artery. All data expressed as mean±SEM, n=6-8. A and B were analysed by one-way ANOVA with Dunnett's post hoc test vs adx.

3.4.5.3 Plaque quantification by histology

Histological analysis of the brachiocephalic artery allowed quantification of the maximum cross-sectional area of the plaque. Consistent with 2-D OPT measurements, neither adrenalectomy nor dex treatment had any significant influence on the maximum cross-sectional area of the plaque (Figure 3.12A) or corresponding lumen area (Figure 3.12B). It is worth noting that, although neither the plaque nor medial areas were significantly altered by dex treatment, the intima/media ratio was significantly increased ($p<0.01$; Table 3.2(c)).

3.4.5.4 Plaque composition

3.4.5.4.1 *Smooth muscle*

Neither adrenalectomy nor dex treatment had any effect on the smooth muscle content of the atherosclerotic plaques, as assessed by immunohistochemical staining against smooth muscle α-actin. The plaques from all three groups contained approximately 3% smooth muscle (Figure 3.13A).

3.4.5.4.2 *Collagen*

Similarly, neither adrenalectomy nor dex had any influence on the collagen content of the atherosclerotic plaques, as assessed by picrosirius red staining. The collagen content within the plaques was approximately 30% (Figure 3.13B).

3.4.5.4.3 *Macrophages*

Macrophage content was assessed using immunohistochemical staining against Mac-2 protein. Adrenalectomy had no influence, while dex significantly reduced the number of macrophages within the atherosclerotic plaques ($p<0.05$; Figure 3.13C).

3.4.5.4.4 *Lipid*

The lipid content of the lesion was represented by the acellular clefts that remain in the plaque post-histological processing. Neither adrenalectomy nor dex altered the lipid content of the plaques (Figure 3.13D).

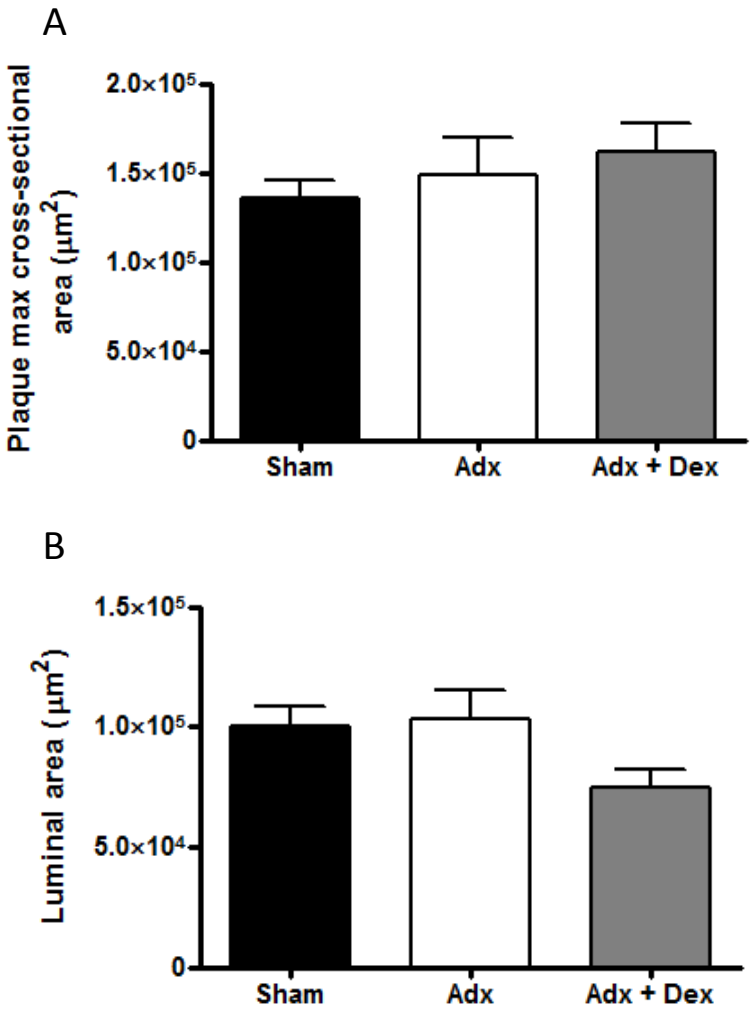

Figure 3.12: Impact of adrenalectomy and dexamethasone treatment on brachiocephalic plaque and lumen cross-sectional area, as assessed by histology.
Mice were randomised to undergo sham or adrenalectomy (adx) surgery. Adx animals were supplied with 0.9% saline supplemented with either vehicle or dexamethasone (dex; 0.1mg/kg/day) as their drinking water. Atherosclerotic lesion development was accelerated by provision of a high cholesterol (0.2%) western diet before isolation and optical projection tomography scanning. Plaque and lumen cross-sectional areas were quantified by histological analysis. Neither adx nor dex treatment influenced the max cross-sectional area of the plaque (A) or corresponding lumen cross-sectional area (B). All data expressed as mean±SEM, n=6-8. Data were analysed by one-way ANOVA with Dunnett's post hoc test vs adx.

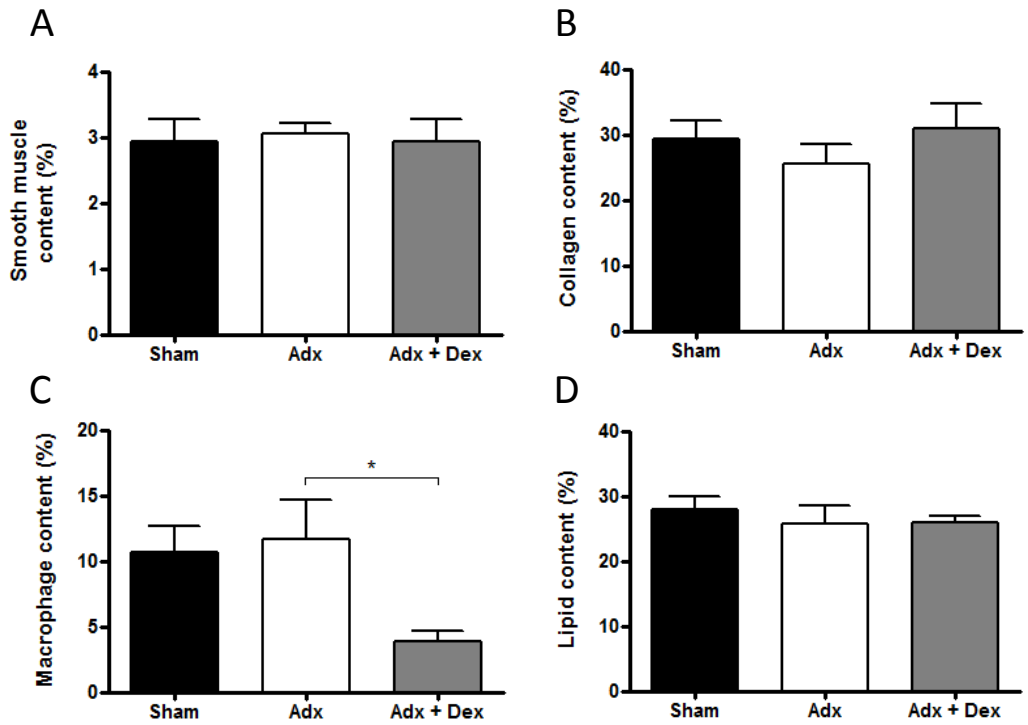

Figure 3.13: **Impact of adrenalectomy and dexamethasone treatment on brachiocephalic plaque composition, as assessed by histology and immunohistochemistry.**
Mice were randomised to undergo sham or adrenalectomy (adx) surgery. Adx animals were supplied with 0.9% saline supplemented with either vehicle or dexamethasone (dex; 0.1mg/kg/day) as their drinking water. Atherosclerotic lesion development was accelerated by provision of a high cholesterol (0.2%) western diet before isolation and analysis. Composition was quantified at the point of largest lesion as determined by histological analysis. Smooth muscle and macrophage content were assessed using immunohistochemistry, collagen content was assessed by picrosirius red staining and lipid content was quantified from United States trichrome stained sections. Neither adx nor dex treatment influenced the smooth muscle (A), collagen (B) or lipid (D) content of the plaque. Dex treatment, but not adx, reduced the macrophage content of the plaque (C). All data expressed as percentage of total area of plaque; mean±SEM, n=6-8. Data were analysed by one-way ANOVA with Dunnett's post hoc test vs adx, * $p<0.05$.

3.5 Discussion

The work described in this chapter addresses the hypothesis that glucocorticoids are pro-atherogenic. The results obtained suggest that physiological levels of endogenous glucocorticoids do not influence atherogenesis in this murine model. In contrast, exogenous glucocorticoids do indeed augment the development of atherosclerosis.

3.5.1. Endogenous glucocorticoids and atherosclerosis

3.5.1.1 Manipulating endogenous glucocorticoids

A number of different methods can be utilised to determine the influence of endogenous glucocorticoids on physiological or pathophysiological processes in animals. As the aim of this investigation was to determine the effects of physiological levels of endogenous glucocorticoids on atherosclerotic plaque development, the approach adopted was global removal of glucocorticoids by adrenalectomy, which has not been described previously in the mouse.

In order to confirm the success of the adrenalectomy surgery and to monitor the animals' welfare, physiological parameters including plasma corticosterone levels, body weight and organ weights were measured. All animals that underwent adrenalectomy had significantly reduced plasma corticosterone levels. It is acknowledged that bilateral adrenalectomy fails to completely eliminate circulating corticosterone, usually retaining around 30-50% (Dubuc *et al.*, 1986; Jacobson, 1999; Makimura *et al.*, 2000; Vrang *et al.*, 2002), comparable with the levels found in this investigation. One possible explanation as to the source of the remaining corticosterone includes adrenal remains post-adrenalectomy. Upon sacrifice, all animals were scrutinised for the presence of adrenal remains or regenerated adrenal material and found to have none. An alternative source of corticosterone could be adrenal rest cells; cortical tissue separate from the adrenal glands. Although relatively well-defined in humans (Claahsen-van der Grinten *et al.*, 2009; Linder *et al.*, 2009), adrenal rest cells have only once been described in mice. Val *et al* identified a novel population of adrenal-like cells in the testis of male mice, which

respond to ACTH and secrete corticosterone (Val *et al.*, 2006). Perhaps these adrenal-like testicular cells are the source of corticosterone in the adrenalectomised mice in the current study. However, detailed analysis of the testes would be required to confirm such a speculation. In addition, it is well known that dex administration is a potent inhibitor of ACTH release through negative-feedback on the HPA axis (Cole *et al.*, 2000) and would therefore prevent corticosterone release from these potential adrenal rests. However, in the current study, dex-treated mice retained around 25% of their circulating corticosterone levels following bilateral adrenalectomy. Therefore, adrenal rests cannot account for all of the remaining circulating corticosterone.

As has been previously shown (de Jong *et al.*, 2007; Ingram *et al.*, 2005; Makimura *et al.*, 2003), adrenalectomy had no effect on the animals' body weight over the experimental period. Conversely, the thymus weight was expected to increase following removal of the adrenals as has been described in a number of murine studies (Jacobson, 1999; Pruett *et al.*, 2004; Reber *et al.*, 2007). However, in this study there was no significant change in the weight of the organ in comparison to the sham animals. Another group has reported a similar lack of effect on thymus weight following adrenalectomy in mice (Kawiak *et al.*, 1996). Thus, the adrenalectomy surgery was considered a success, with no evidence of remaining adrenal tissue, significantly reduced circulating corticosterone levels and healthy mice.

Although bilateral adrenalectomy is a frequently-used technique to determine the role of glucocorticoids on physiological and pathophysiological processes (Haluzik *et al.*, 2002; Lim *et al.*, 2007; Vrang *et al.*, 2002), it has some important limitations. Firstly, removal of the adrenal glands from mice eliminates not only the release of glucocorticoids but also the release of the other adrenal-derived hormones including mineralocorticoids and catecholamines. Therefore, care must be taken, when analysing the effects of adrenalectomy, not to assume they are solely due to the loss of glucocorticoids. Secondly, abolition of mineralocorticoid release requires the animals to be maintained on 0.9% saline in their drinking water for the remainder of their lives to ensure appropriate salt balance (Tordoff, 1996).

3.5.1.2 Impact of manipulating endogenous glucocorticoids on atherogenesis.

Despite the majority of previous work concluding that endogenous glucocorticoids are pro-atherogenic, the results from this investigation suggest that a reduction of endogenous glucocorticoids to approx. 25% of normal levels has no effect on atherogenesis, influencing neither plaque burden nor composition. One explanation for this observation is that the additional removal of mineralocorticoids and catecholamines by adrenalectomy could themselves be influencing atherogenesis and, thereby, obscuring the effect of removing glucocorticoids. However, there is substantial evidence that mineralocorticoids themselves are also pro-atherogenic. Administration of aldosterone (Keidar *et al.*, 2004) or deoxycorticosterone acetate (Weiss *et al.*, 2008) to ApoE$^{-/-}$ mice exacerbates atherosclerotic lesion development. This effect is confirmed by the finding that MR blockade (Suzuki *et al.*, 2006; Takai *et al.*, 2005), inhibition of ACE (Weiss *et al.*, 2008) or antagonism of angiotensin-receptor 1 (Keidar *et al.*, 2004) reduces the pro-atherosclerotic effects of mineralocorticoids. In addition, as described above, excessive activation of MR by glucocorticoids in 11βHSD2/ApoE double knock out (DKO) mice, has been shown to severely augment atherogenesis (Deuchar *et al.*, 2011). Therefore, removal of mineralocorticoids alongside glucocorticoids by adrenalectomy would be anticipated to reduce MR-mediated augmentation of atherosclerosis. During an acute stress response, catecholamines are released from the adrenal medulla in addition to glucocorticoids being released from the adrenal cortex. Therefore, stress-induced atherosclerosis also implicates catecholamines as pro-atherosclerotic (Black *et al.*, 2002). Although, little has been reported on the specific effects of catecholamines on atherosclerosis, one study has described an increase in plaque development in ApoE$^{-/-}$ mice by norepinephrine administration (Weiss *et al.*, 2001). In addition, doxazocin (an alpha-1 adrenoceptor antagonist) has been reported to reduce atherosclerotic lesion development in high cholesterol-fed rabbits (Swindell *et al.*, 1993) and reduce intima-media thickness in males with peripheral atherosclerotic disease (Hoogerbrugge *et al.*, 2002). Therefore, removal of catecholamines alongside glucocorticoids and mineralocorticoids by adrenalectomy would be anticipated to further attenuate the development of atherosclerosis.

It is widely accepted that elevated circulating lipid levels correlate with increased cardiovascular disease in the clinic. A similar correlation is acknowledged in mice (Temel *et al.*, 2007). Indeed, the reduction in atherosclerosis by inhibition of 11βHSD1 described by Hermanowski *et al* and Nuotio-Antar *et al* was accompanied by reduced circulating lipid levels in both cases (Hermanowski-Vosatka *et al.*, 2005; Nuotio-Antar *et al.*, 2007). In the current study, adrenalectomy had no influence on circulating cholesterol or triglyceride levels, which may in part account for adrenalectomy having no effect on atherogenesis. Unfortunately, there is very little published on the effect of adrenalectomy on circulating lipids in mice to help indicate further if this finding is comparable with other studies. A single study demonstrated that adrenalectomy had no effect on plasma triglyceride levels in mice (Haluzik *et al.*, 2002) but cholesterol levels were not reported.

As well as not influencing the lipid profile in mice, adrenalectomy also had no influence on the composition of the plaque. It is surprising that removing endogenous glucocorticoids had a negligible influence on the macrophage content, considering these steroids are important modulators of immune cell function (Rickard *et al.*, 2009). However, as monocyte-derived macrophages play a crucial role in the development of atherosclerosis (Libby, 2002), this may also contribute to the lack of effect on atherogenesis by adrenalectomy. It has previously been reported that macrophage-specific GR inactivation has no effect of atherogenesis in mice (Preusch *et al.*, 2008), supporting the conclusion that endogenous glucocorticoids have little influence on atherosclerosis through their macrophage-specific effects.

Therefore, despite considerable evidence suggesting that endogenous glucocorticoids are pro-atherosclerotic, adrenalectomy had no effect on atherosclerotic plaque development in $ApoE^{-/-}$ mice. This suggests that physiological levels of endogenous glucocorticoids have a limited role in the regulation of atherogenesis in the mouse.

As adrenalectomy did not influence any glucocorticoids-sensitive systemic parameters; body weight, thymus weight, serum lipid levels, or local effects; lipid accumulation, inflammatory content of the plaque, the lack of effect on atherogenesis

is not completely inexplicable. However, the mechanism behind which atherogenesis is unaffected by adrenalectomy remains to be elucidated. Certainly, it is required that the role of mineralocorticoids and catecholamines in atherosclerosis be accounted for. This could be elucidated by replacing physiological levels of mineralocorticoids and/or catecholamines to adrenalectomised animals. However, it would be challenging to pharmacologically mimic adrenal physiology, in particular the diurnal patterns of adrenal hormone secretion. Perhaps, to further determine the influence of endogenous glucocorticoids on atherosclerosis development, a different approach is necessary. The use of endothelial- and VSMC-specific $GR^{-/-}$ mice could provide crucial information on the influence of endogenous glucocorticoids in atherosclerosis and indicate the potential role of the endothelium and smooth muscle cells in the mechanism. Also, additional investigation into the role of pre-receptor metabolism of glucocorticoids by the 11βHSD1 enzyme would certainly help elucidate the role of endogenous glucocorticoids in atherogenesis. However, a more constructive approach may be to model endogenous glucocorticoid excess. One currently used method of investigating glucocorticoid excess is ACTH administration, modelling Cushing's Disease (Bailey *et al.*, 2009; Dunbar *et al.*, 2010). ACTH stimulates corticosterone release from the adrenal glands, resulting in hypercorticosteronism. This model has been used previously to investigate the influence of glucocorticoids on atherosclerosis in the 1960s using dogs and rats (Rosenfeld *et al.*, 1960; Wexler *et al.*, 1960). Both studies concluded an augmentation of atherosclerosis by ACTH administration. It would be of interest to further investigate the effect of ACTH administration on atherosclerosis using our more modern models of the disease and analytical techniques to help further elucidate the role of endogenous glucocorticoids on atherosclerosis development.

3.5.2. **Exogenous glucocorticoids and atherosclerosis**

3.5.2.1 Systemic glucocorticoid treatment

Several different glucocorticoids could have been used for administration to mice. Hydrocortisone (Moraes-Fontes *et al.*, 2009), prednisone (Wissing *et al.*, 2010) and prednisolone (Frijters *et al.*, 2010) have been used previously to assess the influence of glucocorticoids on physiological and pathophysiological processes in mice. Dex

was chosen for the investigation described in this chapter as it is the glucocorticoid most commonly used for medium- and long-term systemic administration in mice (Brack *et al.*, 1997; Gunin *et al.*, 2003). Use of dex, therefore, allows direct comparisons with these studies. Dex has also been used in a number of studies investigating the effects of glucocorticoid administration on atherosclerosis in rabbits (Asai *et al.*, 1993; Naito *et al.*, 1992) and mice (Tous *et al.*, 2006). In addition, dex is used clinically for its anti-inflammatory and immunosuppressant properties, for example in rheumatoid arthritis (Cole, 2006). As dex is a GR-selective glucocorticoid, its use also allows distinction of GR-mediated effects of glucocorticoids on atherosclerosis. Dex was administered in drinking water to reduce any stress to the animals and allow a consistent dose throughout the day (Gunin *et al.*, 2003). The dose of 0.1mg/kg/day was selected as it is similar to the doses of dex used in previous rabbit studies (Asai *et al.*, 1993; Naito *et al.*, 1992) and consistent with the low dose used in the neointimal proliferation study, described in Chapter 4. Ideally, circulating dex levels would have been assayed to confirm the dose received. Unfortunately, this was not practical with the length of the study, number of animals and the cost of running the assay. However, dex intake was calculated regularly and the dose provided in the water bottles was adjusted to account for changes in drinking habbits and body weight to maintain an average of 0.1mg/kg/day.

Dex was administered to adrenalectomised mice to allow distinction of the effects of exogenous glucocorticoids on atherosclerosis, without the added complication of endogenous glucocorticoids and mineralocorticoids in the circulation. It is important to note that 0.1mg/kg/day is a pharmacological dose of dex and thus was not used as a replacement for physiological levels of corticosterone that were removed by adrenalectomy. Future investigations could consider assessing the effect of glucocorticoid administration on atherogenesis in mice with intact adrenal glands.

Dex treatment caused a significant inhibition of weight gain and reduced the weight of the glucocorticoid-sensitive thymus, confirming that this dose of dex was pharmacologically active in the animals. These systemic side effects are well documented in the mouse (Pires *et al.*, 2005). The animals recovered fully from

surgery and remained outwardly healthy, with appropriate food and water intake. These observations suggest that the dose and method of administration of dex were appropriate to induce the expected pharmacological effects, whilst maintaining healthy animals.

3.5.2.2 Impact of exogenous glucocorticoids on atherogenesis

Clinically, glucocorticoid excess may induce or exacerbate several known cardiovascular risk factors, including: hypertension (Mangos *et al.*, 2003), hypercholesterolaemia (Curtis *et al.*, 1982) and glucose intolerance (Tounian *et al.*, 1997). Moreover, there is clinical evidence that prolonged corticosteroid therapy is associated with enhanced cardiovascular disease (Souverein *et al.*, 2004; Wei *et al.*, 2004). However, it is difficult to distinguish between the effects of the exogenous glucocorticoid and the underlying disease for which the therapy is required, on atherogenesis in these patients. Thus, we turn to animal studies to help further elucidate the influence of exogenous glucocorticoids on atherosclerosis. The majority of experimental data have been generated in the cholesterol-fed rabbit model (Bailey *et al.*, 1973; Friedman *et al.*, 1964). These largely contradict clinical observations, reporting that steroid-treated rabbits exhibit less atherosclerosis, probably as a result of the potent anti-inflammatory effects of glucocorticoids (Asai *et al.*, 1993; Naito *et al.*, 1992). However, it is important to note that the lesions that develop in the cholesterol-fed rabbit model tend to be fatty streaks rather than complex advanced lesions, as described by Asai *et al* and Naito *et al*. Conversely, one animal study describes an increase in aortic atherosclerosis in dex-treated $ApoE^{-/-}$ mice on a normal chow diet (Tous *et al.*, 2006), suggesting that the $ApoE^{-/-}$ mouse is a better model of human atherosclerosis than the cholesterol-fed rabbits.

Based on clinical observations, it was hypothesised that exogenous glucocorticoid treatment would increase the development of atherosclerosis in cholesterol-fed $ApoE^{-/-}$ mice. Data acquired from OPT analysis demonstrated that systemic dex treatment did indeed increase atherosclerotic plaque volume in the brachiocephalic artery. Further analysis, including histological methods, revealed that the increase in plaque volume was not represented in the max cross-sectional area of plaque. Therefore, changes in plaque burden by dex administration would have been missed

if standard histological analysis alone had been used. These results support the value of the 3-dimensional visualisation provided by OPT in allowing a more detailed analysis of lesion size.

The effect of glucocorticoids on atherosclerotic lesion development is likely to be a balance between the predominantly pro-atherosclerotic systemic effects of steroid treatment (Curtis *et al.*, 1982; Delaunay *et al.*, 1997; Whitworth *et al.*, 2001) and the primarily anti-atherosclerotic local actions of steroids on the vasculature (Goncharova *et al.*, 2003; Jilma *et al.*, 2000; Liu *et al.*, 1999). Indeed, the anti-atherosclerotic effects of glucocorticoids in rabbits were attributed to their potent anti-inflammatory actions. This would inhibit recruitment and proliferation of macrophages (Asai *et al.*, 1993; Naito *et al.*, 1992) in the arterial wall and, thereby, reduce the formation of foam cells. Somewhat counter-intuitively, in the current investigation, dex significantly reduced the macrophage content of the plaque, despite the increase in plaque volume. Interestingly, in the study by Tous *et al,* which also describes an increase in atherosclerosis by dex, the treatment did not reduce macrophage content of the lesions (Tous *et al.*, 2006). This conflict may be explained by Tous *et al* using a 3-fold lower dose of dex than in this study. Nevertheless, the current result does suggest that dex-mediated augmentation of atherogenesis is independent of macrophage numbers.

It could be postulated that, whilst dex is having the expected local "anti-atherosclerotic" effect, the detrimental systemic effects of steroid treatment are prevailing, tipping the balance to favour atherosclerosis development. These systemic effects could include hypertension, dyslipidaemia and disturbances in glucose homeostasis. Although blood pressure was not measured in this investigation, it is well-established that glucocorticoids induce hypertension (Mangos *et al.*, 2003) and, specifically, that dex induces hypertension in the mouse (Goodwin *et al.*, 2010). In addition, the study described in chapter 5 demonstrates that the dose of dex used in this investigation (0.1mg/kg/day) induces hypertension after 3 weeks of treatment in male, adult C57Bl/6 mice (section 5.4.3). Therefore, it is highly likely that the dex-treated mice in the current investigation have elevated blood pressure.

Exogenous glucocorticoids have long been known to increase circulating lipid levels in the clinic (Becker *et al.*, 1988; Brotman *et al.*, 2005; Curtis *et al.*, 1982) and in animal studies (Cole *et al.*, 1982; Makheja *et al.*, 1989; Pinheiro *et al.*, 2009). Indeed, Tous *et al* found that dex-treated mice had increased hyperlipidaemia over controls, with a significant increase in plasma cholesterol concentration (Tous *et al.*, 2006). However, in the current study, dex treatment barely (and not significantly) increased circulating cholesterol or triglyceride levels. This result was complimented by dex having no effect on the lipid content of the plaques, suggesting the steroid treatment had no influence on lipid accumulation or clearance from the arterial wall. Therefore, these findings suggest that hyperlipidaemia cannot account for the pro-atherosclerotic effect of dex. However, before completely discounting the effects on lipids, it would be of interest to break down the total circulating cholesterol levels into pro-atherosclerotic LDL and anti-atherosclerotic HDL fractions (Rader *et al.*, 2005). If the LDL levels are significantly increased over HDL levels, this would indicate an atherogenic lipid profile, despite the total cholesterol levels remaining unaltered by dex treatment. Unfortunately, there were insufficient volumes of blood samples remaining to carry out this more detailed assay in this investigation.

Finally, metabolic disturbances in glucose homeostasis could play a role in the atherogenic effects of dex. Glucocorticoids are known to play a substantial role in the development of the metabolic syndrome (Anagnostis *et al.*, 2009), which is associated with an increased risk of type 2 diabetes mellitus and vascular disease. More specifically, dex administration has been shown to cause glucose intolerance in mice (Gounarides *et al.*, 2008). Metabolic parameters were not assessed in this investigation but it would be of interest to determine whether this course of dex is sufficient to induce glucose intolerance and insulin resistance significant enough to exacerbate atherosclerotic lesion development. It is notable that Tous *et al* found normal glucose tolerance in their dex-treated ApoE$^{-/-}$ mice. However, as previously mentioned, they did use a 3-fold lower dose of dex so their result may not predict the metabolic status of the mice in the current study. Nevertheless, they found an increase in atherosclerosis despite no glucose intolerance, suggesting that metabolic disturbances cannot fully account for dex-mediated augmentation of atherosclerosis.

In conclusion, exogenous glucocorticoid treatment significantly augmented atherosclerotic plaque development in brachiocephalic arteries of western diet fed $ApoE^{-/-}$ mice. The mechanism behind this effect remains to be elucidated but appears to be independent of circulating lipid levels and macrophage numbers. This study supports the conclusion of Tous *et al*. that the $ApoE^{-/-}$ mouse model is a more clinically-relevant model of atherosclerosis than the cholesterol-fed rabbit. Therefore, it would be of great interest to utilise this model to expand our understanding of the mechanism behind the pro-atherosclerotic effects of glucocorticoid treatment.

3.5.3. **Optical projection tomography**

Optical projection tomography (OPT) has successfully been utilised in this investigation to allow reproducible quantification of atherosclerotic plaque and lumen volumes as well as corresponding cross-sectional areas. In addition, as OPT is non-destructive, standard histological and immunohistochemical analysis of the arteries can be carried out to allow both comparison with OPT and generation of further information regarding plaque composition. Qualitative similarities between images produced by OPT and those subsequently produced by histological analysis of the same vessel were striking and were confirmed by strong correlations between cross-sectional measurements. It should be noted that there was a small but positive bias, meaning that the OPT-derived measurements were consistently larger than those derived by histology. This inconsistency likely reflects shrinkage of these large vessels during histological processing, supporting the advantage of OPT over histology alone. Crucially, this bias was independent of plaque size, indicating that measurements made in this way are comparable within and between vessels.

OPT offers a number of benefits over the conventional histological analysis used by so many. Not only is histology time-consuming and labour intensive, it also typically limits quantification to one snap-shot of the vessel where the largest cross-sectional area of the plaque is present, although some investigators do laboriously quantify serial section to gain a more representative measure of lesion size. Conversely, OPT is a more rapid technique that requires less preparation time. In addition, OPT allows a full 3-dimensional description of plaque volume and distribution which adds

greater power to determine the effects of intervention and may allow detection of more subtle changes in plaque development, as exemplified in this investigation. Given the unproven nature of this technique, full histological analysis was carried out following OPT scan acquisition. In future, OPT can be used to quantify plaque volume and distribution and therefore reduce the histological requirement to complimentary selective analysis of only the regions containing the largest lesion.

As with any technique, OPT has some disadvantages. As the traditional refractive index matching solution used for OPT imaging is a lipid solvent, the extracellular lipid pools within the plaques were removed prior to scanning. A potential alternative solution could be glycerol, which, as a polar solution, may allow preservation of the lipid pools. However, as has been suggested for *ex vivo* MRI of atherosclerotic arteries (McAteer *et al.*, 2004), the removal of lipid may provide a means of quantifying the extracellular lipid pools within the plaques by measurement of the holes that remain after solvent treatment. Certainly, the volume of these empty regions can be measured by OPT, but further optimisation will be required to standardise the quantification parameters, specifically the grey-level thresholding, to delineate the lipid from the plaque.

As mentioned previously, this is the first time OPT has been described for the analysis of murine atherosclerotic lesions. Additionally, in this department, OPT has been successfully applied to the visualisation and quantification of neointimal lesions in the femoral artery of mice (Kirkby *et al.*, 2011). These successes support OPT's prospect as a novel technique, which can transform the way in which vascular lesions are analysed in animal models.

3.5.4. **Summary**

In summary, optical projection tomography has been successfully used to allow 3-dimensional visualisation and quantification of atherosclerotic plaques in the mouse, providing a much needed improvement on the standard histological techniques used currently. Using this technique, it has been shown that exogenous glucocorticoids are indeed pro-atherosclerotic, whereas physiological levels of endogenous glucocorticoids appear to play a limited role in atherogenesis.

Chapter 4

Influence of glucocorticoids on neointimal proliferation in the mouse

4.1 Introduction

Despite the conflicting evidence on the effects of glucocorticoids on atherogenesis, the effects of these steroids on neointimal proliferation following vascular injury is somewhat clearer. Certainly, there have been many investigations into the effects of exogenous glucocorticoids on neointimal proliferation. However, there do not appear to be any reports detailing the influence of endogenous glucocorticoids.

Glucocorticoids clearly have the potential to inhibit neointimal proliferation due to their potent anti-inflammatory properties (Liu *et al.*, 1999; Yamada *et al.*, 1993) and ability to directly inhibit smooth muscle cell migration and proliferation (Goncharova *et al.*, 2003; Voisard *et al.*, 1994). Indeed, glucocorticoid administration has been shown to inhibit neointimal development in a number of animal models, including the rat (Guzman *et al.*, 1996; Nagasaki *et al.*, 2004; Villa *et al.*, 1994) and rabbit (Hagihara *et al.*, 1991; Petrik *et al.*, 1998; Valero *et al.*, 1998; Van Put *et al.*, 1995). In addition, glucocorticoid-coated stents inhibited neointimal proliferation in the dog femoral artery (Strecker *et al.*, 1998) and in the pig coronary artery (Wang *et al.*, 2005c). There are a limited number of studies in the mouse, with one study describing both local and systemic dex treatment reducing neointima formation after cuff placement around the femoral artery (Pires *et al.*, 2005). A recent study from this department concluded that both systemic dex and local cortisol treatment reduced neointimal proliferation following femoral artery wire-injury in mice (Macdonald, 2007). Therefore, there is a plethora of evidence from animal studies to support the contention that exogenous glucocorticoids attenuate neointimal proliferation.

Glucocorticoids have since been trialled as anti-restenotic agents in the clinic, with systemic treatment alongside PCI showing positive results (Ribichini *et al.*, 2007b; Ribichini *et al.*, 2005; Versaci *et al.*, 2002). However, there are contraindications to oral glucocorticoid therapy, including diabetes mellitus, severe arterial hypertension and peptic ulcers, as well as adverse effects such as gastric pain, impaired glucose tolerance and worsened hypertension (Ribichini *et al.*, 2007a). In addition,

glucocorticoid administration augments atherogenesis in mice, as reported in Chapter 3 (section 3.5.3.2). Another important complication of glucocorticoid therapy is an increased risk of thrombosis, thought to be partly attributable to increased activity of the coagulation cascade and reduced fibrinolytic activity (Brotman *et al.*, 2006; Jilma *et al.*, 2005; Patrassi *et al.*, 1995; Sartori *et al.*, 1999). Indeed, MacDonald *et al* describe increased local thrombus following systemic dex treatment in their murine femoral artery wire-injury model (Macdonald, 2007). Local glucocorticoid delivery, in the form of DexES, has the advantage of avoiding the systemic secondary effects of steroids, while releasing a high dose of steroid at the site of the target lesion. Unfortunately, although there have been some positive clinical outcomes and/or angiographic results with DexES (Han *et al.*, 2006; Jimenez-Valero *et al.*, 2007; Liu *et al.*, 2003; Patti *et al.*, 2005), there are a number of studies describing DexES as having no effective anti-proliferative actions in acute coronary syndromes (ACS) (Hoffmann *et al.*, 2004b; Pesarini *et al.*, 2009), no benefit over bare metal stents (BMS) in patients with stable angina (Gaspardone *et al.*, 2006; Hoffmann *et al.*, 2004a), and an association with relatively high restenosis rates in patients with diabetes mellitus (van der Hoeven *et al.*, 2008).

Therefore, evidence from pre-clinical and human studies using systemic treatment suggests that exogenous glucocorticoids do have anti-restenotic effects, albeit with a number of contraindications and adverse effects. Unfortunately, DexES have not provided the advancement in the prevention of restenosis that was hoped for in the clinic. Therefore, elucidating the mechanisms of the anti-restenotic effects and adverse effects of systemic glucocorticoid therapy may help improve the therapeutic potential of these steroids as a treatment for the prevention of restenosis.

While there has been an assortment of investigations into the effects of exogenous glucocorticoids on neointimal proliferation, there do not appear to be any reports detailing the influence of endogenous glucocorticoids. However, two studies (unpublished), carried out in this department, have investigated the effect of endogenous glucocorticoids on neointimal proliferation through manipulation of the enzyme 11β-hydroxysteroid dehydrogenase type 1 (11βHSD1), the enzyme

responsible for the conversion of inactive 11-dehydrocorticosterone to active corticosterone. Inhibition or genetic deletion of 11βHSD1 was shown to reduce neointimal development following intra-luminal wire injury in ApoE$^{-/-}$ mice, suggesting endogenous glucocorticoids are in fact pro-restenotic. However, a similar study using C57Bl/6 mice, described manipulating 11βHSD1 to have no effect on neointimal proliferation following wire-injury. The conflicting results between these two studies are attributed to metabolic disturbances caused by ApoE deficiency. There are a number of alternative methods available for manipulating endogenous glucocorticoids, which could add clarity to the role of these steroids in neointimal proliferation. Bilateral adrenalectomy is one such method, commonly used to globally remove endogenous glucocorticoids thereby allowing investigation into their role in physiological and pathophysiological processes (de Jong *et al.*, 2007; Haluzik *et al.*, 2002). Improving our understanding of the complex role of endogenous glucocorticoids in neointimal proliferation, using adrenalectomy, may enable further advancement in the treatment of restenosis.

There are many well-described murine models of neointimal proliferation, including: intra-luminal wire injury (Lindner *et al.*, 1993; Sata *et al.*, 2000), carotid artery ligation (Kumar *et al.*, 1997b), electrical injury (Carmeliet *et al.*, 1997c) and perivascular ferric chloride injury (Schafer *et al.*, 2002). Previous studies in this laboratory investigating the role of glucocorticoids in neointimal proliferation utilised the wire injury model of acute vascular injury. This is a well-characterised model of neointimal proliferation, first described by Sata *et al.* (Sata et al., 2000). It involves the insertion of an angioplasty guidewire into the femoral artery via a small muscular side-branch. The wire stretches the vessel, causing endothelial denudation and extensive medial damage. The resulting healing process produces a smooth muscle-rich neointimal lesion. This model was used in this investigation to maintain consistency and allow direct comparisons to be made with the previous studies.

4.2 Hypothesis and Aims

The work described in this chapter addresses the hypothesis that glucocorticoids attenuate neointimal proliferation. It is, therefore, proposed that removal of endogenous glucocorticoids (adrenalectomy) augments, whilst glucocorticoid administration reduces, neointimal proliferation following arterial injury in mice. In order to address this hypothesis, the specific aims of the work described in this chapter were to:

- determine whether surgical removal of the adrenal glands increased lesion development following intra-luminal wire injury in mice.
- determine whether chronic administration of the synthetic glucocorticoid dexamethasone reduced lesion development following intra-luminal wire injury in adrenalectomised mice.

4.3 Methods

4.3.1. Animals

Male C57Bl/6 mice (Harlan Olac, UK) aged 10-14 weeks and weighing 26-34 grams were used in this study.

4.3.2. Adrenalectomy

In order to investigate endogenous glucocorticoids mice were randomised to undergo either bilateral adrenalectomy or sham adrenalectomy (section 2.2.1).

4.3.3. Administration of drugs

Adrenalectomised (adx) mice were provided with 0.9% NaCl in their drinking water. Vehicle (absolute ethanol) or the synthetic glucocorticoid dexamethasone (dex; 0.1 or 0.8 mg/kg/day; section 2.2.3.1) were administered by addition to the drinking water or saline, as appropriate. Drug administration commenced immediately after adrenalectomy/sham surgery and continued for 4 weeks (Figure 4.1).

4.3.4. Femoral artery injury

One week following adrenalectomy/sham and the start of drug administration, the mice were subjected to femoral artery injury (section 2.2.2). Briefly, an angioplasty wire was inserted into the artery to induce neointimal hyperplasia (Sata *et al.*, 2000).

4.3.5. Tissue collection

At the end of the 4-week experimental period a tail tip blood sample was collected, spun to plasma and stored as described previously (section 3.3.4). The mice were then killed by asphyxiation in CO_2 and arteries (aorta and femorals) and organs were collected and weighed.The aorta, femoral arteries, a lobe of the liver, the left kidney and adrenals were fixed in 10% neutral buffered formalin for 24 hours before being transferred into 70% ethanol. The remainder of the liver, the heart, right kidney, spleen and thymus were snap frozen and stored at -80°C.

Figure 4.1: Study protocol to determine the effects of glucocorticoids on neointimal proliferation.
Experiments were conducted in male, 10-12 week old C57Bl/6 mice. Animals were randomised to undergo adrenalectomy (adx) or sham surgery (n=8). Adrenalectomised animals were provided with 0.9% saline with either vehicle (absolute ethanol; n=8) or dexamethasone (dex; 0.1 or 0.8mg/kg/day; n=8) in their drinking water for the remainder of the experimental period. One week following surgery all animals underwent femoral artery injury surgery to induce neointimal hyperplasia and were maintained for a further 3 weeks. At the end of the experimental period mice were culled by CO_2 asphyxiation and the femoral arteries were excised and fixed for examination of neointimal lesion development by histology and immunohistochemistry.

4.3.6. **Measurement of plasma corticosterone levels**

Plasma spun from blood collected by tail tip immediately prior to sacrifice was used to assess corticosterone levels using a radioimmunoassay (section 2.5.1), to confirm successful removal of the adrenal glands.

4.3.7. **Neointimal lesion analysis**

4.3.7.1 Quantification

The injured femoral arteries were processed, embedded in paraffin and cut into 4μm thick transverse sections (section 2.4.1). Sets of twenty serial sections (80μm) were collected every 160μm along the entire artery. One section every 160μm along the artery was stained with the United States trichrome (section 2.4.2). Photomicrographs were taken using a light microscope coupled to a colour camera and image analysis system (section 2.4.4). The area (μm^2) of lesion in each section was measured using Photoshop CS3 software (section 2.4.5). The section with the largest area of lesion was chosen to represent each arterial sample

4.3.7.2 Composition

The cellular composition of the neointimal lesions was investigated using histological staining and immunohistochemistry on serial sections at the point of maximum lesion area. Smooth muscle cell content was assessed using an alkaline-phosphatase conjugated monoclonal primary antibody against smooth muscle cell α-actin (section 2.4.7.2). A polyclonal rabbit anti-human primary antibody was used to determine the fibrinogen content of the lesions (section 2.4.7.4). A monoclonal rat anti-mouse primary antibody against Mac-2 was used to determine the macrophage content of the lesions (section 2.4.7.3).

4.3.8. **Statistics**

All statistical analysis was performed by one-way ANOVA with Dunnett's post-hoc test for comparison of physiological levels of endogenous glucocorticoid or exogenous glucocorticoid treatment with control, adrenalectomised mice. Statistical analysis of all data was performed using GraphPad Prism 4.0 software.

4.4 Results

4.4.1. Body weights

There was no significant difference in body weight at the start of the study. In the 4-week study, animals in all four groups showed an early weight loss after both the adrenalectomy and femoral artery injury surgeries (Figure 4.2A). Adrenalectomy had no significant effect on body weight, whereas dex caused a dose-dependent reduction in body weight (low dose dex: $p<0.05$, high dose dex: $p<0.01$; Figure 4.2B). The average dose of dex received was 0.09±0.002mg/kg/day (low dose) and 0.80±0.04mg/kg/day (high dose).

4.4.2. Organ weights

Adrenalectomy slightly reduced thymus weight ($p<0.05$) and dex treatment significantly decreased thymus weight in a dose-dependent manner (low and high dose dex: $p<0.01$; Figure 4.3A). Dex treatment also resulted in a dose-dependent decrease in spleen weight (low and high dex: $p<0.001$; Figure 4.3B). High dex treatment also induced a significant increase in heart weight ($p<0.05$; Figure 4.3C). There were no significant changes in the weight of other organs collected (kidneys and liver; Figure 4.4).

4.4.3. Plasma corticosterone levels

Unfortunately, there were insufficient plasma volumes available from some animals, including the entire sham group. Plasma samples were therefore collected from intact control C57Bl/6 mice at the same time of day (between 10am and 12pm) and under the same conditions to illustrate corticosterone levels in intact mice. All samples from adrenalectomised animals that were analysed, which included 6/8 animals in the adx group, 3/6 in the high dex group and 4/7 in the low dex group, had corticosterone levels 10-fold lower than controls, equivalent to diurnal nadir levels (Figure 4.5). It is important to note that adrenalectomy did not completely abolish circulating corticosterone levels.

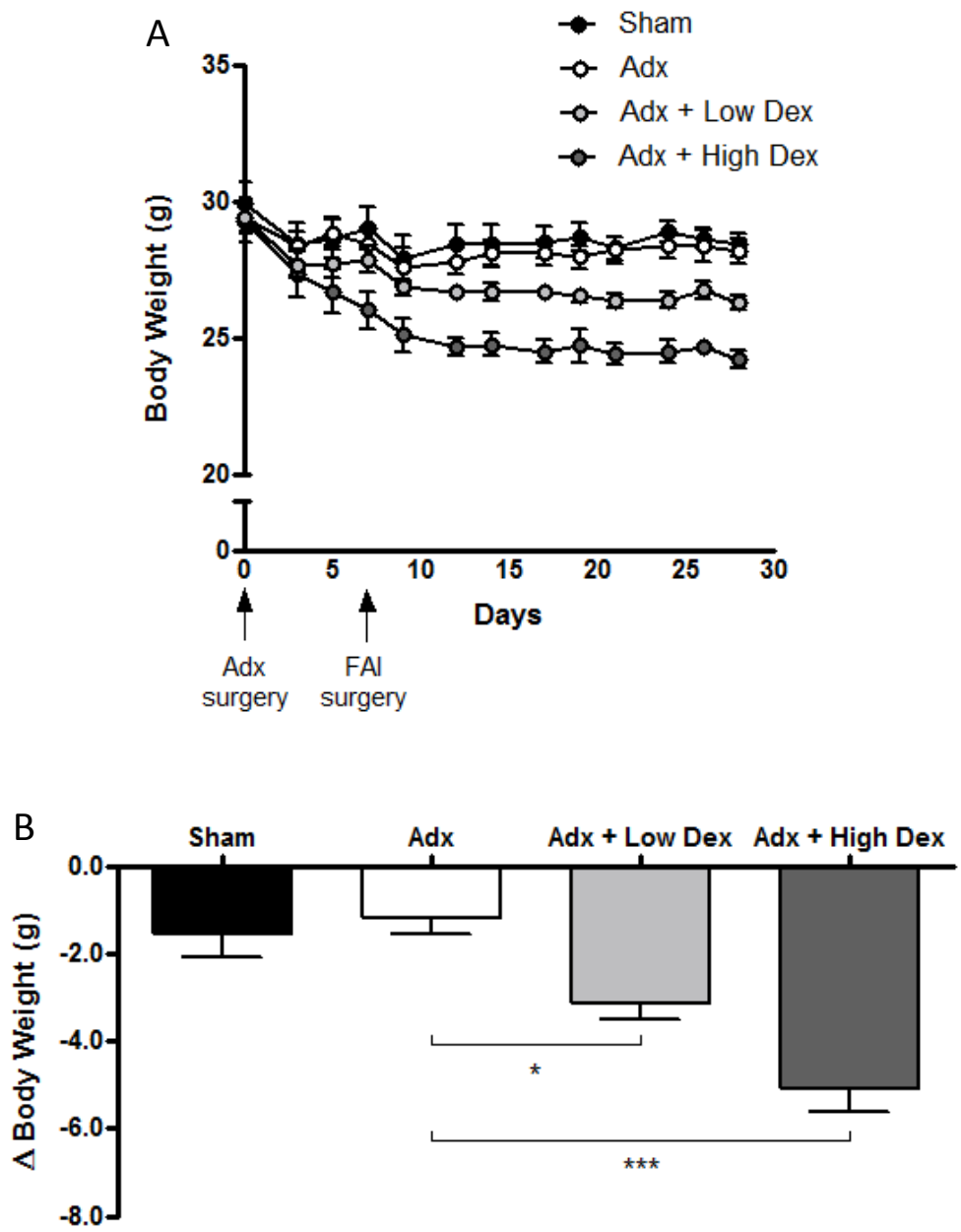

Figure 4.2: Weight changes induced by adrenalectomy and dexamethasone treatment.
Mice were randomised to undergo sham or adrenalectomy (adx) surgery. Adx animals were supplied with 0.9% saline with either vehicle or dexamethasone (dex; 0.1 or 0.8mg/kg/day) in their drinking water. Neointimal hyperplasia was induced by femoral artery wire- or ligation-injury (FAI). Body weight was measured regularly throughout the 4-week experimental period. There were no differences in the weights of the animals at the start of the experiment. All animals showed an early weight loss after both the adrenalectomy and femoral artery injury surgeries. Adx appeared to have no influence on body weight, whereas dex appeared to reduce body weight (A). Analysis of change in body weight from start to end of the experimental period confirmed that adx had no significant effect on weight, whilst dex treatment caused a dose-dependent reduction in body weight in comparison to the adx group (B). All data expressed as mean±SEM, n=6-8. Data were analysed by one way ANOVA with Dunnett's post hoc test vs adx. * $p<0.05$, ***$p<0.001$.

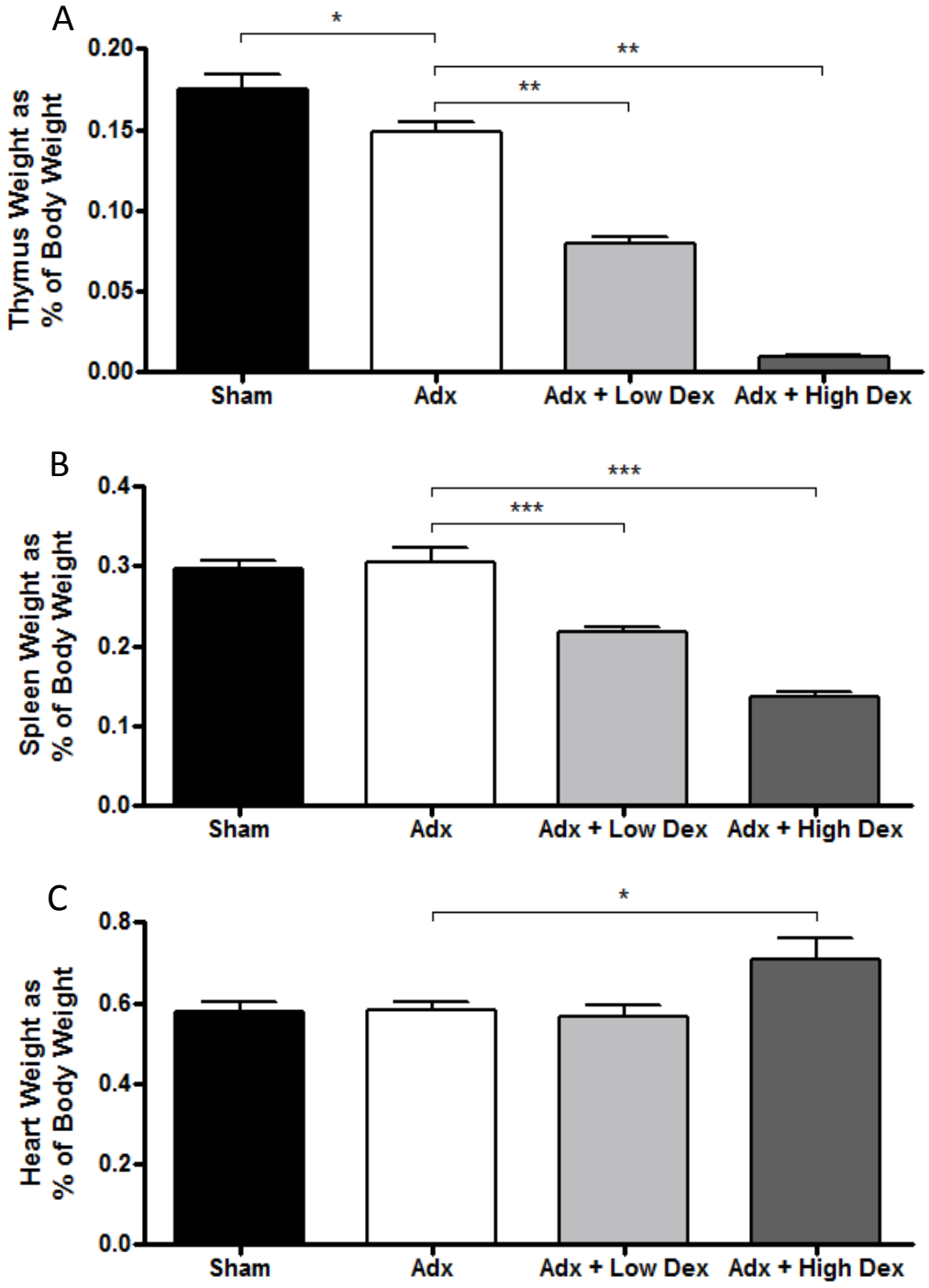

Figure 4.3: Organ weight changes induced by adrenalectomy and dexamethasone treatment. Mice were randomised to undergo sham or adrenalectomy (adx) surgery. Adx animals were supplied with 0.9% saline with either vehicle or dexamethasone (dex; 0.1 or 0.8mg/kg/day) in their drinking water. Neointimal hyperplasia was induced by femoral artery wire- or ligation-injury. Organs were weighed upon sacrifice. Adx reduced thymus weight but had no effect on any other organ (A). Dex treatment caused a dose-dependent reduction in both thymus (A) and spleen (B) weight. The high dose dex also increased heart weight (C). All data expressed as mean±SEM, n=6-8. Data were analysed by one way ANOVA with Dunnett's post hoc test vs adx. *$p<0.05$, **$p<0.01$, ***$p<0.001$.

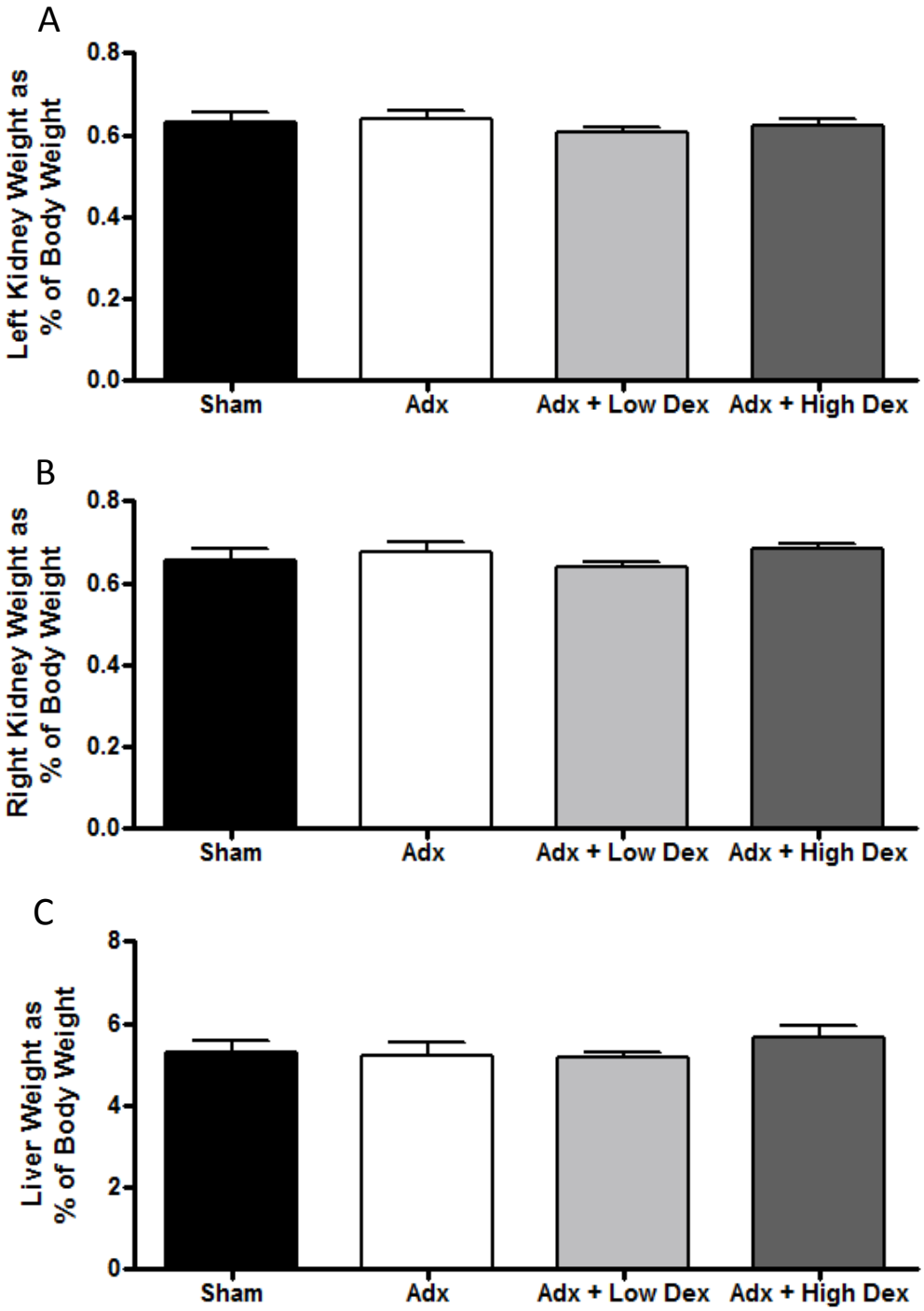

Figure 4.4: Organ weight changes induced by adrenalectomy and dexamethasone treatment. Mice were randomised to undergo sham or adrenalectomy (adx) surgery. Adx animals were supplied with 0.9% saline with either vehicle or dexamethasone (dex; 0.1 or 0.8mg/kg/day) in their drinking water. Neointimal hyperplasia was induced by femoral artery wire- or ligation-injury. Organs were weighed upon sacrifice. Neither adx nor dex influenced kidney and liver weight. All data expressed as mean±SEM, n=6-8. Data were analysed by one way ANOVA with Dunnett's post hoc test vs adx.

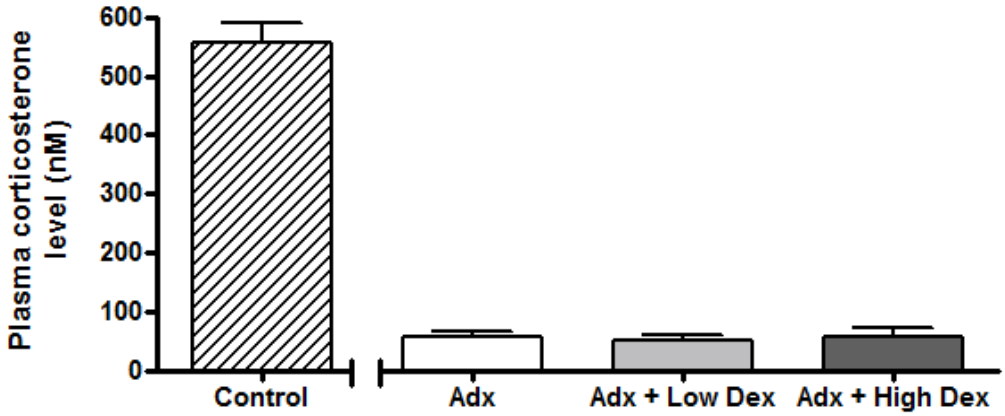

Figure 4.5: Plasma corticosterone levels in animals that underwent adrenalectomy.
Mice were randomised to undergo sham or adrenalectomy (adx) surgery. Adx animals were supplied with 0.9% saline with either vehicle or dexamethasone (dex; 0.1 or 0.8mg/kg/day) as their drinking water. Neointimal hyperplasia was induced by femoral artery wire- or ligation-injury. Plasma corticosterone levels were measured in tail-tip plasma by radioimmunoassay. Plasma samples from control C57Bl6 mice (striped bar) represent peak corticosterone levels in mice with intact adrenals. All adx mice measured had corticosterone levels 10-fold lower than control mice, equivalent to diurnal nadir levels. All data expressed as mean±SEM; Control: n=6, adx: n=6, adx + low dex, adx + high dex: n=3: n=4. Adx + low dex and adx + high dex were analysed by one way ANOVA with Dunnett's post hoc test vs adx.

4.4.4. **Neointimal lesion development**

4.4.4.1 Neointima quantification

Adrenalectomy and low dex had no effect on lesion size. High dex treatment appeared to reduce lesion size, but this did not reach significance (Figure 4.6A; Table 4.1). In addition, while the majority of neointimal lesions that developed in the sham, adx and low dex groups were fibro-proliferative in nature, most of the lesions that developed in the high dex group were acellular and appeared to be thrombotic in nature.

The sections were re-analysed, quantifying only the fibrous (cellular) part of the lesions. With this approach, adrenalectomy still had no effect on the size of fibrous lesions. The high dex resulted in a significant decrease in fibrous lesion size but this effect was not seen at the low dose (Figure 4.6B).

4.4.4.2 Neointima composition

4.4.4.2.1 *Smooth muscle and fibrinogen*

Immunohistochemical staining against smooth muscle α-actin revealed that lesions which developed in the sham, adx and low dex groups were relatively rich in smooth muscle, containing 45-65% smooth muscle. In the high dex group, staining was limited to the fibrous regions and made up only 17% of the lesions, although this reduction did not reach statistical significance (Figure 4.7). Immunohistochemical staining against fibrinogen further suggested that the non-fibrous components are thrombotic in nature (Figure 4.8).

4.4.4.2.2 *Macrophages*

The macrophage content of the lesions was assessed using immunohistochemical staining against Mac-2 protein. Neither adrenalectomy nor low dex treatment had any effect on macrophage content within the neointima, making up 11-15% of the lesion. Although the high dex treatment indicated a reduction in macrophage staining to <2%, this did not reach significance (Figure 4.9).

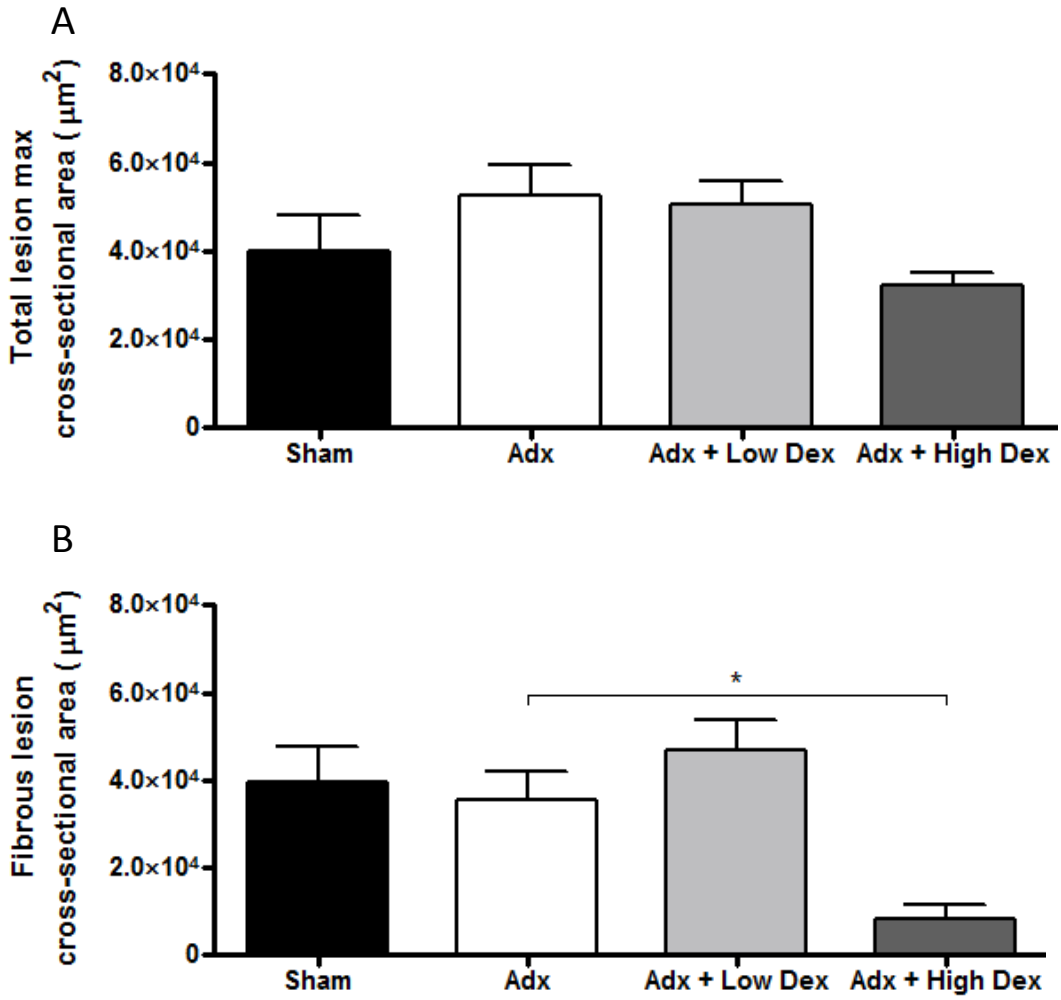

Figure 4.6: Impact of adrenalectomy and dexamethasone treatment on neointimal lesion development, as assessed by histology.
Mice were randomised to undergo sham or adrenalectomy (adx) surgery. Adx animals were supplied with 0.9% saline with either vehicle or dexamethasone (dex; 0.1 or 0.8mg/kg/day) as their drinking water. Neointimal hyperplasia was induced by femoral artery wire-injury. Neointima cross-sectional areas were measured at the point of largest lesion by histological analysis. Both total lesion (A) and fibrous lesion only (B) areas were quantified. Adx had no effect on lesion size. High dose dex appeared to reduce total lesion size (A), a tend that was not seen with the low dose, but this did not reach significance. The high dose dex did, however, reduce fibrous lesion size (B). Again this effect was not seen at the lower dose. All data expressed as mean±SEM, n=6-8. Data were analysed by one way ANOVA with Dunnett's post hoc test vs adx. *p<0.05.

Table 4.1: Impact of adrenalectomy and dexamethasone treatment on the size and composition of neointimal lesions.

Measurement	Sham	Adx	Adx + Low Dex	Adx + High Dex
n	8	7	6	6
(a) 2D Morphometry (Histology)				
Neointimal area ($x10^4 \mu m^2$)	4.0 ± 0.8	5.3 ± 0.7	5.1 ± 0.5	3.2 ± 0.3
Medial area ($x10^4 \mu m^2$)	1.5 ± 0.2	1.2 ± 0.1	1.8 ± 0.2	1.3 ± 0.2
Intima/Media ratio	3.2 ± 0.9	4.7 ± 0.7	3.0 ± 0.7	3.0 ± 0.4
(b) Composition (IHC)				
Smooth Muscle α-actin (%)	52.7 ± 9.3	45.6 ± 11.1	64.1 ± 6.7	16.7 ± 5.2
Macrophages (%)	14.4 ± 3.0	11.5 ± 3.4	16.4 ± 3.8	2.2 ± 0.4

Mice were randomised to undergo sham or adrenalectomy (adx) surgery. Adx animals were supplied with 0.9% saline with either vehicle or dexamethasone (dex; 0.1 or 0.8mg/kg/day) as their drinking water. Neointimal hyperplasia was induced by femoral artery wire-injury, before isolation and examination of the left femoral artery by histology (a) and immunohistochemistry (b). Adx had no influence on any parameter measured. Neither dose of dex significantly altered total lesion area (a). The high dose of dex appeared to reduce both smooth muscle content and macrophage content of the plaque, as measured by immunohistochemistry (b), but these trends did not reach significance. All data expressed as mean±SEM, n=6-8. Data were analysed by one way ANOVA with Dunnett's post hoc test vs adx.

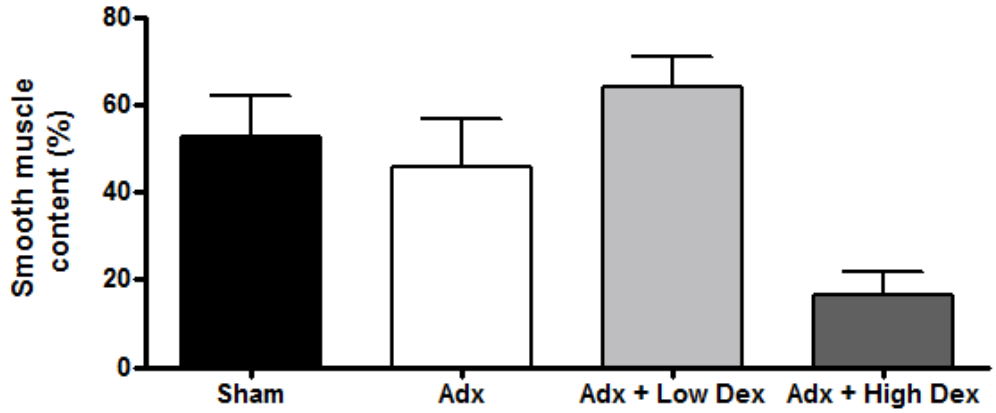

Figure 4.7: Impact of adrenalectomy and dexamethasone treatment on neointimal lesion smooth muscle content.
Mice were randomised to undergo sham or adrenalectomy (adx) surgery. Adx animals were supplied with 0.9% saline with either vehicle or dexamethasone (dex; 0.1 or 0.8mg/kg/day) as their drinking water. Neointimal hyperplasia was induced by femoral artery wire-injury. Composition was quantified at the point of largest lesion as determined by histological analysis. Smooth muscle content was assessed using immunohistochemistry. Lesions that developed in the sham, adx and low dex groups all strongly stained for smooth muscle α-actin. In the high dose dex group staining was limited to the fibrous regions and there was a trend towards a reduction in smooth muscle content, but this did not reach significance. Data expressed as mean±SEM, n=6-8. Data were analysed by one-way ANOVA with Dunnett's post hoc test vs adx.

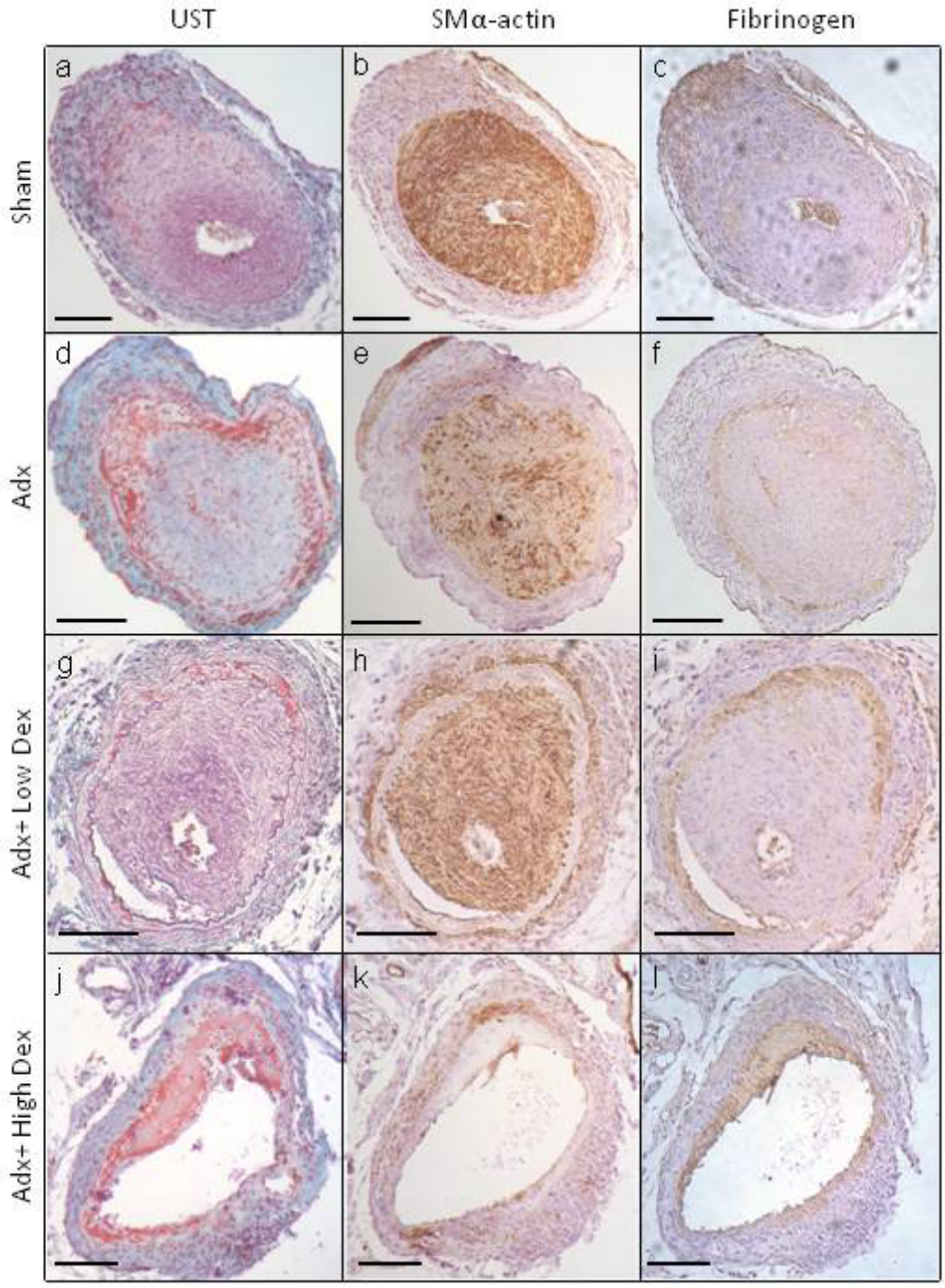

Figure 4.8: Composition of lesions formed after femoral artery wire-injury.
Mice were randomised to undergo sham or adrenalectomy (adx) surgery. Adx animals were supplied with 0.9% saline with either vehicle or dexamethasone (dex; 0.1 or 0.8mg/kg/day) as their drinking water. Neointimal hyperplasia was induced by femoral artery wire-injury. Composition was quantified at the point of largest lesion as determined by histological analysis. Smooth muscle (SMα-actin) and fibrinogen content was assessed using immunohistochemistry. Sham, adx and low dex-treated mice developed typical lesions, staining strongly for elastin (a, d, g) and smooth muscle (b, e, h). Whereas, high dex-treated animals developed lesions that were acellular, elastin-deficient and appeared to be thrombotic (j). In addition, these lesions did not stain for smooth muscle cells (k) and did stain for fibrinogen (l), confirming that these lesions are thrombotic in nature. Scale bar = 100μm.

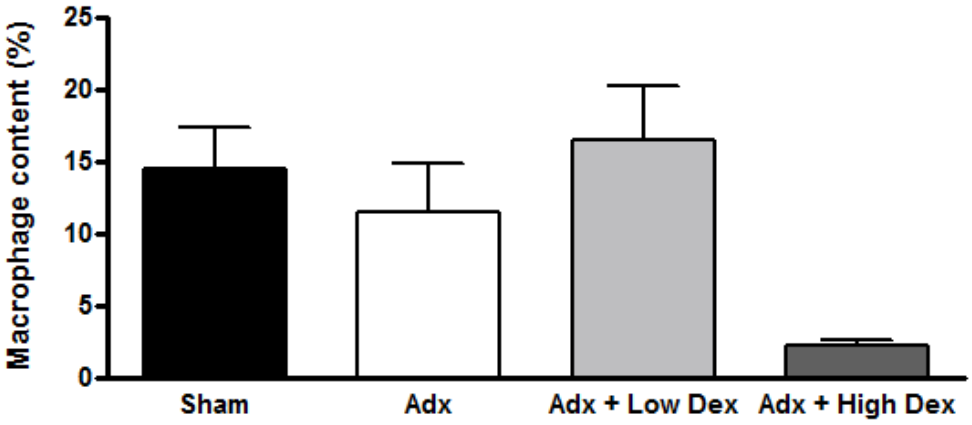

Figure 4.9: Impact of adrenalectomy and dexamethasone treatment on neointimal lesion macrophage content.
Mice were randomised to undergo sham or adrenalectomy (adx) surgery. Adx animals were supplied with 0.9% saline with either vehicle or dexamethasone (dex; 0.1 or 0.8mg/kg/day) as their drinking water. Neointimal hyperplasia was induced by femoral artery wire-injury. Composition was quantified at the point of largest lesion as determined by histological analysis. Macrophage was assessed using immunohistochemistry. Adx had no influence on the macrophage content of the lesions. High dose dex appeared to dramatically reduce the macrophage content, however this did not reach significance. This was not seen at the lower dose. Data expressed as mean±SEM, n=6-8. Data were analysed by one-way ANOVA with Dunnett's post hoc test vs adx.

4.5 Discussion

The work described in this chapter addresses the hypothesis that glucocorticoids attenuate neointimal proliferation. The results obtained suggest that physiological levels of endogenous glucocorticoids do not influence neointima development following intra-vascular injury. Conversely, high dose dex administration does indeed reduce fibrous neointima size but this effect is not seen at a lower dose. Although the high dex dose reduced fibrous lesion size, its ability to decrease the size of the overall lesion (and thus to reduce arterial narrowing) appears compromised by the stimulation of thrombosis at the site of injury.

4.5.1. Endogenous glucocorticoids and neointimal proliferation

4.5.1.1 Manipulating endogenous glucocorticoids

In order to confirm the success of the adrenalectomy surgery and to monitor the animals' welfare, physiological parameters (including plasma corticosterone levels, body and organ weights) were measured. All animals that underwent adrenalectomy had significantly reduced, but not abolished, plasma corticosterone levels. It is acknowledged that bilateral adrenalectomy fails to completely eliminate circulating corticosterone (Dubuc *et al.*, 1986; Jacobson, 1999; Makimura *et al.*, 2000; Vrang *et al.*, 2002). Potential explanations for this have been discussed previously (section 3.5.1.1), but the source of the remaining corticosterone remains to be elucidated.

As has been previously shown (de Jong *et al.*, 2007; Ingram *et al.*, 2005; Makimura *et al.*, 2003), and described in the previous chapter (section 3.4.1) adrenalectomy had no effect on the animals' body weight over the experimental period. Conversely, the thymus weight was expected to increase following removal of the adrenals as has been described in a number of murine studies (Jacobson, 1999; Pruett *et al.*, 2004; Reber *et al.*, 2007). However, in this study thymus weight was actually decreased slightly by adrenalectomy, in comparison to the sham animals. There have been no previous reports of such an effect and the mechanism behind it remains to be elucidated. Upon sacrifice, all animals were scrutinised for the presence of adrenal remains or regenerated adrenal material and found to have none. In addition, dex treatment did not reduce circulating corticosterone levels, as would be expected in

intact mice due to negative feedback regulation of the hypothalamic-pituitary-adrenal (HPA) axis (Kageyama *et al.*, 2009). This, therefore, supports the conclusion that the adrenalectomy surgery was a success, with no evidence of remaining adrenal tissue, significantly reduced circulating corticosterone levels and healthy mice.

4.5.1.2 Impact of manipulating endogenous glucocorticoids on neointimal proliferation

Despite evidence that glucocorticoids have the potential to inhibit neointimal proliferation (section 4.1), reducing endogenous glucocorticoids to approx. 25% of normal levels failed to influence lesion development in this investigation. Two previous studies (unpublished), carried out in this department, have investigated the effect of manipulating 11βHSD1 on neointimal proliferation in mice. Both inhibition and genetic deletion of 11βHSD1 has been shown to reduce neointimal development following intra-luminal wire injury in $ApoE^{-/-}$ mice, suggesting endogenous glucocorticoids are potentially pro-restenotic. However, a similar study using C57Bl/6 mice, described the same manipulations of 11βHSD1 to have no effect on neointimal proliferation following wire-injury. The conflicting results between these two studies are attributed to metabolic disturbances caused by ApoE deficiency. The results from the current investigation therefore complement the latter study, and as both of these studies were carried out in the same strain of mice and used the same model of vascular injury, confidence can be drawn in the mutual conclusion that physiological levels of endogenous glucocorticoids play a limited role in neointimal proliferation. It must be noted that an important difference between these studies is that inhibition or genetic deletion of 11βHSD1 will only influence endogenous glucocorticoids action in specific tissues, unlike adrenalectomy which will reduce endogenous glucocorticoid action globally.

As described in the previous chapter, the lack of effect of adrenalectomy on neointimal proliferation may be due to additional removal of mineralocorticoids and catecholamines, along with glucocorticoids, by adrenalectomy. A number of pre-clinical studies report that ACE inhibition and angiotensin II receptor (AT1R) blockade prevent neointimal proliferation following balloon injury in the carotid artery of rats (Clozel *et al.*, 1993; Osterrieder *et al.*, 1991; Powell *et al.*, 1989). This

may indicate a role for mineralocorticoids in promoting neointimal proliferation but direct effects of angiotensin II and AT1R (Strawn *et al.*, 2002) cannot be excluded. Consistent with these data, administration of aldosterone, the primary endogenous mineralocorticoid, increased neointimal proliferation following coronary artery angioplasty in pigs (Ward *et al.*, 2001). The clinical relevance of these findings is supported by the demonstration that high plasma aldosterone levels in patients correlate with restenosis 6 months after coronary stent implantation (Amano *et al.*, 2006). Similarly, norepinephrine has been shown to augment neointimal proliferation following vascular balloon injury (Erami *et al.*, 2002; Zhang *et al.*, 2001). This effect has not only been attributed to haemodynamic changes, but also to direct alpha-1-adrenoceptor (α1AR) activation of VSMC growth, with evidence that antagonists of α1AR inhibit neointimal proliferation in similar models (Fingerle *et al.*, 1991; O'Malley *et al.*, 1989; Vashisht *et al.*, 1992; Zhang *et al.*, 2001). Therefore, removal of mineralocorticoids and catecholamines by adrenalectomy would be expected to reduce neointimal proliferation in the current investigation. Perhaps the beneficial effect of removing mineralocorticoids and catecholamines is counteracting the potential detrimental effects of removing the anti-inflammatory glucocorticoids.

As well as having no influence on the size of neointimal lesions, adrenalectomy appeared to have no influence on lesion composition, with similar macrophage and smooth muscle content to the lesions in the sham-operated animals. It had been anticipated that macrophage numbers may have increased in lesions from adrenalectomised mice as glucocorticoids can play a key anti-inflammatory role in the vasculature (Liu *et al.*, 1999; Ruetten *et al.*, 1997). However, as macrophages play a crucial role in the development of neointimal proliferation (Hui, 2008), the lack of effect of adrenalectomy on macrophage content may explain the lack of effect on overall neointima size. Macrophage infiltration has been shown to peak at day 7 following wire injury and then decline steadily as the inflammation resolves (Macdonald, 2007). As the lesions in this study were assessed at day 21, perhaps any influence of adrenalectomy on macrophage infiltration was missed. To further investigate this hypothesis, ideally day 7 lesions would be analysed.

In summary, to further determine the influence of endogenous glucocorticoids on neointimal proliferation, perhaps a different approach is necessary. The use of vascular-specific $GR^{-/-}$ mice could provide crucial information on the influence of endogenous glucocorticoids and indicate the potential role of the endothelium and smooth muscle cells in the mechanism. Also, additional investigation into the role of pre-receptor metabolism of glucocorticoids by the 11βHSD1 enzyme would help clarify the conflicting results currently described and help elucidate the role of endogenous glucocorticoids in restenosis. However, a more constructive approach may be to model endogenous glucocorticoid excess. One currently used method of investigating glucocorticoid excess is ACTH administration, modelling Cushing's Disease (Bailey *et al.*, 2009; Dunbar *et al.*, 2010). It would be of interest to utilise this technique in our model of intimal hyperplasia to investigate more specifically the role of endogenous glucocorticoids on neointimal proliferation.

4.5.2. **Exogenous glucocorticoids and neointimal proliferation**

4.5.2.1 Systemic glucocorticoid treatment

As described previously, dex was chosen for the investigation described in this chapter as it is the glucocorticoid most commonly used for medium- and long-term systemic administration in mice (Brack *et al.*, 1997; Gunin *et al.*, 2003). In addition, dex is the most commonly used glucocorticoid in previous studies describing the effect of glucocorticoid treatment on neointimal lesion formation in animals (Hagihara *et al.*, 1991; Karim *et al.*, 1997; Van Put *et al.*, 1995; Villa *et al.*, 1994). Use of dex, therefore, allows direct comparison with this previous work. Dex has also been trialled clinically for its anti-restenotic effects in DexES. For the experiments described in this chapter, dex was administered in drinking water to reduce any stress to the animals and allow a consistent dose throughout the day (Gunin *et al.*, 2003), of either 0.1 or 0.8mg/kg/day.

Dex administration commenced immediately following adrenalectomy to allow the dose to equilibrate before arterial injury. The treatment was continued for the full three weeks following injury so as to maintain the influence of the steroid throughout the development of the lesion. Limiting the treatment to before the injury may well

alter the outcome on lesion development, as well as limit the systemic side effects. With this in mind, modifying the time-course of treatment may bring some additional insight into the mechanisms behind the influence of dex on neointimal proliferation. In addition, mice receiving dex were also adrenalectomised to allow distinction of the effects of exogenous glucocorticoids on neointimal proliferation, without the added complication of endogenous glucocorticoids and mineralocorticoids in the circulation. A previous study in this department had assessed the effects of glucocorticoid administration on neointimal proliferation in mice with intact adrenal glands, the results of which are discussed below.

The dose-dependent weight loss and reduction in size of glucocorticoid-sensitive organs confirms that both doses of dex were pharmacologically active in the animals. These systemic side effects of dex are well documented in the mouse (Pires *et al.*, 2005). In addition, the high dose of dex increased heart weight. This could be an indication of hypertrophy of the heart as a consequence of hypertension. Blood pressure was not measured in these mice but glucocorticoids are known to induce hypertension in rodents (Goodwin *et al.*, 2008; Whitworth *et al.*, 2001; Zhang *et al.*, 2004). Indeed, the investigation described in Chapter 5 confirms that the same doses of dex (0.1 and 0.8mg/kg/day) show an increase in systolic blood pressure after two weeks treatment, in intact C57Bl/6 mice (section 5.4.3).

4.5.2.2 Impact of exogenous glucocorticoids on neointimal proliferation

It was hypothesised that the high dose of dex (0.8mg/kg/day; chosen as it is comparable to doses used in other long-term dex studies in mice (Blyth *et al.*, 1998; Gunin *et al.*, 2003)) would reduce fibrous neointimal lesion formation. There was the additional expectation of possible development of alternative thrombotic lesion instead, as shown by Macdonald *et al*. in a similar previous study carried out in this department. The lower concentration of dex (0.1mg/kg/day) was therefore included, with the hypothesis that it would retain the inhibition of fibrous lesion development, whilst avoiding some of the adverse side effects seen in animals on a higher dose of dex, including thrombotic lesion development.

Interestingly, the low dex dose had no significant influence on lesion size. Despite changes in body weight and glucocorticoid-sensitive organs, the low dose appeared to be too low to influence neointimal lesion development. Conversely, the high dose of dex did indeed cause a dramatic reduction in fibrous neointima size. Pre-clinical *in vivo* studies have consistently described glucocorticoid treatment to reduce neointimal proliferation in a number of animal models, including the rat (Guzman *et al.*, 1996; Nagasaki *et al.*, 2004; Villa *et al.*, 1994) and rabbit (Hagihara *et al.*, 1991; Petrik *et al.*, 1998; Valero *et al.*, 1998; Van Put *et al.*, 1995). This effect is attributed to the potent anti-inflammatory properties of glucocorticoids (Liu *et al.*, 1999; Yamada *et al.*, 1993) and their potential to inhibit smooth muscle cell migration and proliferation (Goncharova *et al.*, 2003; Voisard *et al.*, 1994). Indeed, the lack of effect of the low dose of dex on neointimal size was accompanied by no change in the inflammatory component of the lesions, as measured by macrophage content, nor the smooth muscle content of the lesions.

A reduction in inflammatory cells within the neointima was expected as glucocorticoids are known to repress macrophage infiltration (Jilma *et al.*, 2000; Yamada *et al.*, 1993) and accumulation (Hagihara *et al.*, 1991). It should be noted, as described above, that macrophage infiltration peaks at day 7 in this model of neointimal proliferation. As this study is investigating lesion development at day 21, the conditions are not optimal for studying macrophage numbers and behaviour. To further address the effect of dex treatment on macrophage infiltration, assessment of lesions at an early time point, day 2, as well as at the expected peak infiltration, day 7, would be useful. In addition, at these time points a more comprehensive assessment of inflammation could be carried out using additional markers for macrophages (F4/80) (D'Elia *et al.*, 2009; Naghavi *et al.*, 2003), neutrophils (Ly6G) (Fridlender *et al.*, 2009; Gahring *et al.*, 2010) and T-lymphocytes (CD3) (Naghavi *et al.*, 2003) in flow cytometry for whole blood analysis and immunohistochemistry for lesion analysis.

Considering the anti-migratory and anti-proliferative effects of glucocorticoids are relatively well established, it is surprising that the VSMC content of the lesions was not significantly reduced. However, in order to fully understand the influence of dex on the VSMCs in this model of intimal hyperplasia, the somewhat controversial issue of the source of the VSMCs must be addressed. Medial apoptosis following injury questions the suggestion that VSMCs migrate from the media. There have been alternative indications that they differentiate from the circulating bone marrow-derived inflammatory cells which infiltrate the vasculature during the initial response to injury (Sahara *et al.*, 2007; Sata *et al.*, 2002; Tanaka *et al.*, 2003). However, there are critics of this proposal who claim to have refuted the existence of bone marrow-derived smooth muscle cells in vascular lesion, suggesting methodological discrepancies account for the confusion (reviewed in (Bentzon *et al.*, 2010b)). If indeed the VSMCs are sourced from circulating progenitors, the anti-inflammatory properties of dex may be directly altering the smooth muscle cell content. This is all speculation and would require investigation before any conclusions could be drawn.

Notably, it was identified that many of the lesions in the high dex group had areas within the lesion that were acellular, devoid of elastin and appeared to be thrombotic, confirming the previous observation of MacDonald *et al*. Further compositional analysis of the lesions confirmed that the smooth muscle cells in the high dex lesions were limited to the fibrous part of the lesion, whilst the thrombotic areas of lesion stained strongly for fibrinogen, further confirming that these regions are of alternative, thrombotic composition. This thrombotic side effect was sufficient to mask the reduction in size of fibro-proliferative lesions. Consequently, vessel occlusion in high dex-treated animals was similar to controls. But, importantly, the thrombotic nature of the lesion will render it less stable than a smooth muscle-rich neointima, with the potential to instigate acute thrombotic events. With dex being used clinically as an anti-restenotic agent, it is crucial to elucidate the mechanism behind which dex is inducing this type of lesion. It is important to note that the thrombotic areas of lesion were not exclusive to the high dex group. This suggests that dex is not inducing atypical thrombotic lesion development as such, but instead may be modulating normal lesion progression.

In 1992, Schwartz *et al* postulated a hypothesis for the mechanism of neointimal proliferation following vascular injury, based on observations in the porcine coronary injury model (Schwartz *et al.*, 1992a). In his hypothesis there are three stages in neointimal lesion formation; thrombotic (stage I), cellular recruitment (stage II) and proliferative (stage III). It is suggested that the thrombotic stage occurs immediately after, and as a direct consequence of, endothelial damage. This leads to formation of a thrombus composed of aggregated platelets, fibrin and trapped erythrocytes. The second stage of healing comprises cellular recruitment into the thrombus itself. Firstly, re-endothelialisation occurs at the thrombus/blood boundary, followed by recruitment of monocytes (later macrophages) and lymphocytes. The macrophages are responsible for thrombolysis (by secreting fibrinolytic enzymes) and phagocytosis of thrombus components. The cellular infiltrates, as well as the thrombus, are likely to secrete growth factors and chemo-attractants which facilitate further recruitment of cells (including VSMCs). The final stage involves cellular proliferation as the thin fibrous cap of VSMCs thickens and elaboration of extracellular matrix, eventually resulting in a mature, smooth muscle-rich neointima. This hypothesised model has been adapted for the specifics of the injury used in this study (Figure 4.10) and implemented as a potential explanation of the effects dex may have on neointimal proliferation. A more detailed explanation of the proposed pathogenesis of neointimal hyperplasia is described in Chapter 1 (section 1.1.3.1).

The results described in this chapter suggest that administration of dex is impeding the progression of arterial healing past stage I. Therefore, the lesions observed in the high dex group are immature lesions with a significant thrombotic component. A number of mechanisms could be suggested to explain such a dex-mediated augmentation of the thrombotic stage and impediment of the progression to stages II and III. Firstly, it is well-described that glucocorticoid excess induces a hypercoagulable state in both the clinic and in animal studies. More specifically, glucocorticoid excess has been shown to increase coagulation, with augmented clotting factor levels (Brotman *et al.*, 2006; Patrassi *et al.*, 1985; Sartori *et al.*, 1999), while additionally attenuating fibrinolysis with increased levels of PAI-1(Patrassi *et al.*, 1995; Patrassi *et al.*, 1992; Sartori *et al.*, 1999; van Giezen *et al.*, 1992).

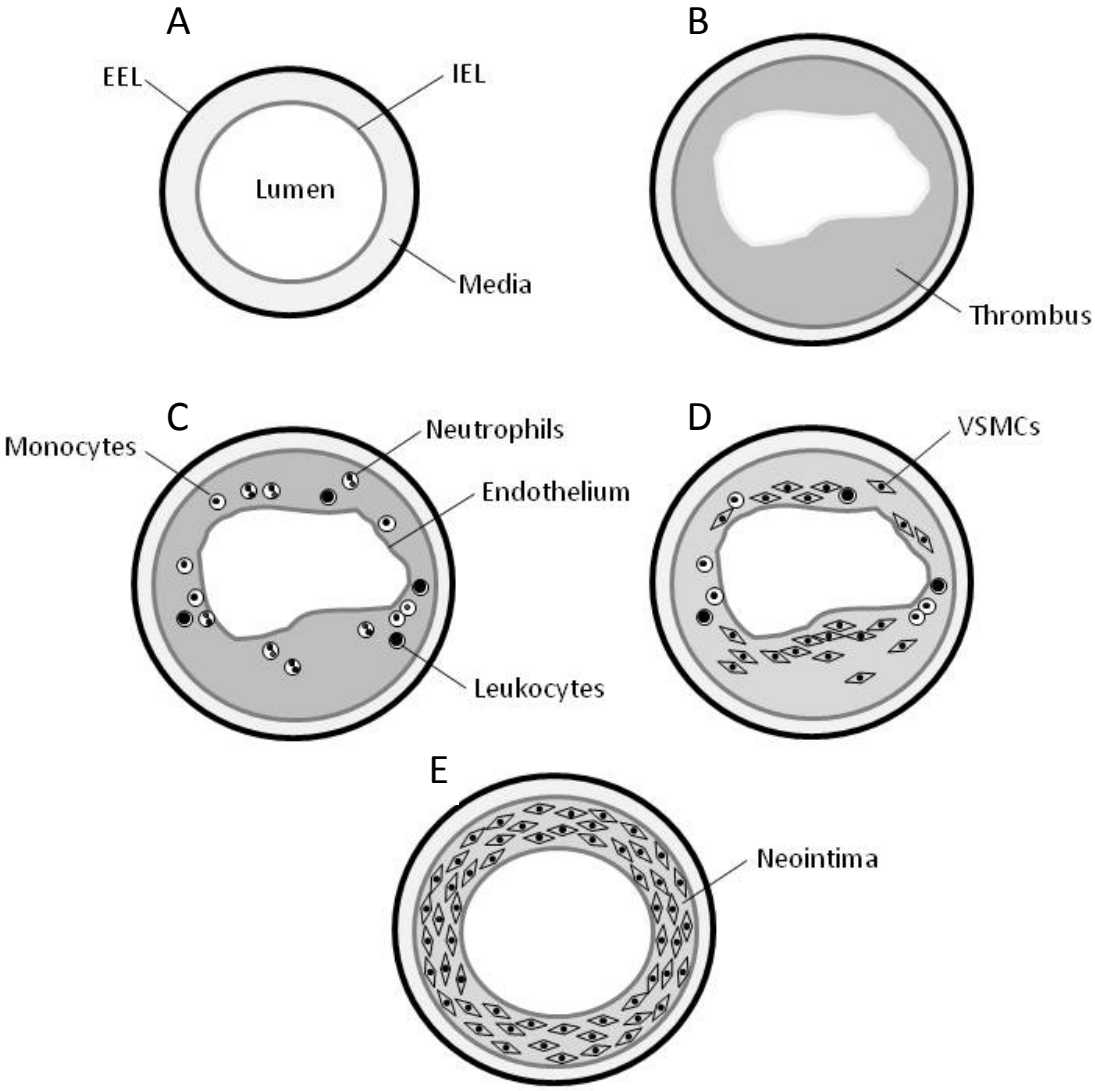

Figure 4.10: Schematic hypothesis of the mechanism of neointima formation.
A: pre-injured vessel. B: following intra-luminal wire injury the vessel has been stretched and denuded resulting in acute thrombosis within minutes of injury. C: Neutrophils infiltrate the thrombus within 24 hours of injury, followed by monocytes and leukocytes within 4 days. D: Smooth muscle cells begin to infiltrate roughly 6 days post-injury. The source of these smooth muscle cells is under debate, but there is a suggestion that they differentiate from the inflammatory cells (Tanaka *et al.*, 2003). E: The neointima is completely formed within 21 days. EEL: external elastic lamina.;IEL: Internal elastic lamina; VSMCs: vascular smooth muscle cells.

Therefore, there is evidence that dex treatment is likely to stabilise the thrombus formed by the wire-injury in the current investigation. Secondly, the potent anti-inflammatory properties of glucocorticoids can not only inhibit infiltration (Poon *et al.*, 2001) and proliferation (Asai *et al.*, 1993) of monocyte/macrophages at the site of injury, reducing further inflammatory cell recruitment (Prescott *et al.*, 1989; Yamada *et al.*, 1993), but also prevent monocyte/macrophage-mediated lysis, through release of tPA (Kung *et al.*, 1993), and clearance, by phagocytosis (Shantsila *et al.*, 2009), of the thrombus. In addition, if inflammatory cells are a source of smooth muscle cells in vascular lesions, as had been suggested (Sahara *et al.*, 2007; Tanaka *et al.*, 2003), the anti-inflammatory properties of dex may also directly contribute to reduced VSMC content of lesions. Thirdly, the anti-migratory effects of glucocorticoids are also well reported. They have been shown to inhibit VSMC migration (Goncharova *et al.*, 2003; Pross *et al.*, 2002) and also to prevent trans-migration of neutrophils through the blood vessel wall (Cronstein *et al.*, 1992; Pitzalis *et al.*, 2002). Finally, glucocorticoids have the potential to inhibit the cellular proliferative stage III as they have been shown to prevent proliferation of VSMCs *in vitro* (Bitzer *et al.*, 2004; Voisard *et al.*, 1994).

Ideally, all aspects described above would be investigated to fully elucidate the mechanism behind glucocorticoid-mediated thrombus formation following intra-luminal wire injury. In the interest of time, it was decided to focus on the influence of dex on the potential stabilisation of the thrombotic stage I, as this was deemed the most likely candidate to provide elucidation of the mechanism behind dex-mediated local thrombosis.

4.5.3. **Summary**

In summary, physiological levels of endogenous glucocorticoids appear to play a limited role in neointimal proliferation. Conversely, a high dose of exogenous glucocorticoid inhibited fibro-proliferative neointimal lesion development, but was associated with local thrombosis at the site of injury. In order to elucidate the mechanism behind this thrombotic effect, the influence of dex on thrombogenicity was investigated. The results of this investigation are described in Chapter 5.

Chapter 5

Influence of glucocorticoid administration on thrombogenicity in the mouse

5.1 Introduction

The work described in the previous chapter suggests that high dose glucocorticoid treatment reduces neointimal proliferation following arterial injury in mice, but is associated with increased local thrombosis. It is postulated that this may be in part due to stabilisation of the initial thrombotic stage during neointimal lesion development, thus preventing lesion progression. There is a great deal of clinical evidence to suggest glucocorticoids are pro-thrombotic. For example, a hypercoagulable state and increased incidence of thromboembolic complications are reported in Cushing's patients (Boscaro *et al.*, 2002; La Brocca *et al.*, 1997), attributable to increased circulating clotting factors and reduced fibrinolytic activity. Similarly, transplant patients receiving chronic immunomodulatory steroid therapy have an increased coagulation and decreased fibrinolytic potential (Patrassi *et al.*, 1995; Sartori *et al.*, 1999). Although the pro-coagulant effects of glucocorticoids in man are well-described, less is understood with regard to the influence of glucocorticoids on platelet function, with very little having been reported.

Importantly, there are also limited reports on the *in vivo* influence of glucocorticoids on thrombogenicity in rodents, with only evidence in rats (van Giezen *et al.*, 1994; van Giezen *et al.*, 1992). In these studies, the authors describe a dose-dependent effect of dex, suggesting that low doses attenuate thrombosis (primarily by inhibition of platelet aggregation), but this effect is lost at higher doses as a result of decreased fibrinolytic activity. Consequently, as with many glucocorticoid effects, the influence of dex on thrombogenicity appears to be sensitive to dose. Therefore, clarifying the influence of both doses of dex used in the previous chapter on thrombogenicity in mice may explain why the benefits of lesion prevention were lost as a result of excessive local thrombosis in high dose dex-treated mice.

5.2 Hypothesis and aims

The work described in this chapter addresses the hypothesis that high dose dex is pro-thrombotic, which may account for the thrombotic lesion development observed following arterial injury. In order to address this hypothesis, the work described in this chapter aims to determine the influence of high dose (0.8mg/kg/day) and low dose (0.1mg/kg/day) dex on thrombogenicity. Thus, the specific aims of this work were to determine whether administration of dex to mice *in vivo* influenced:

- bleeding time
- the activation status of platelets
- the activity of the coagulation cascade
- the activity of the fibrinolytic system

5.3 Methods

5.3.1. Animals

Male C57Bl/6 mice (Harlan Olac, UK) aged 10-14 weeks and weighing 26-34 grams were used in this study.

5.3.2. Administration of drug

Mice were randomised to receive either dex (0.1 or 0.8mg/kg/day; section 2.2.3.1) or vehicle in their drinking water for 5 weeks (Figure 5.1).

5.3.3. Blood pressure measurements

All mice had their systolic blood pressure monitored using tail cuff plethysmography (Pollock *et al.*, 1993) (section 2.2.4) at days 14, 21 and 28 following commencement of treatment.

5.3.4. Tissue collection

At the end of the 5-week experimental period the mice were anaesthetised by isoflurane inhalation before their tail bleeding time was assessed as described (Schwer *et al.*, 2001) (section 2.2.5). Blood was then collected from the vena cava into 3.8% sodium citrate and centrifuged (120 x g, 5 min, RT) to separate platelet rich plasma (PRP), for immediate flow cytometric analysis. The remaining PRP was centrifuged (10,000 x g, 1 min, RT) to gain platelet poor plasma (PPP), which was snap frozen and stored at -80ºC. After collection and weighing, a lobe of the liver, the left kidney, adrenal glands and femoral arteries were fixed in 10% neutral buffered formalin for 24 hours before being transferred to 70% ethanol. The remainder of the liver, the heart, aorta, lungs, right kidney, spleen and thymus were snap frozen and stored at -80°C.

5.3.5. Assessment of platelet activation

The activation status of the platelets was assessed using flow cytometry (section 2.5.4). Briefly, the platelets were stained with a generic platelet marker (anti-CD41 conjugated to the fluorochrome PE) to allow a platelet-only population to be

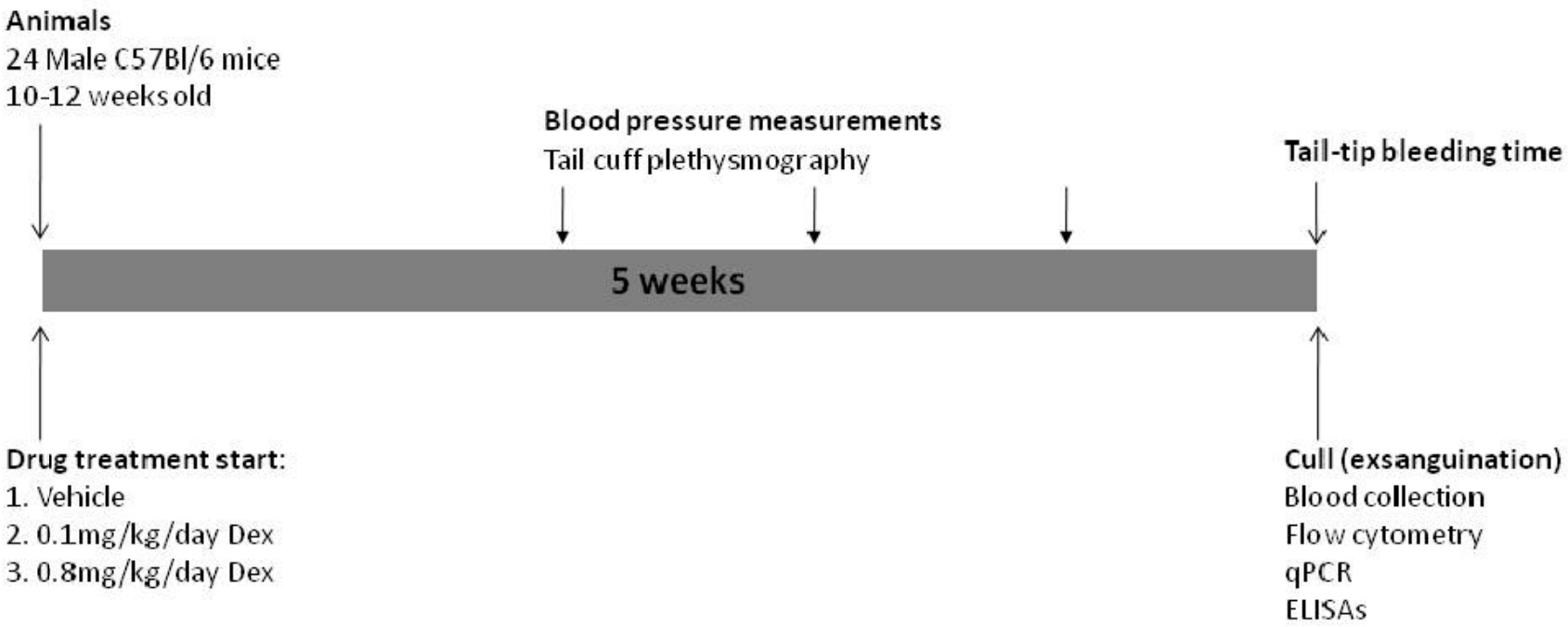

Figure 5.1: Study protocol to determine the effects of glucocorticoids on thrombotic potential.
Experiments were conducted in male, 12-14 week old C57Bl/6 mice. Animals were randomised to receive either vehicle (absolute ethanol; n=8) or dexamethasone (dex; 0.1 or 0.8mg/kg/day; n=8) in their drinking water for 5 weeks. Blood pressure measurements were acquired at days 14, 21 and 28. At the end of the experimental period mice had the tail-tip bleeding time recorded before being culled by exsanguination. Blood collected was used to assess platelet activation and measure clotting factor levels. A variety of tissues were also collected for assessment of clotting factor gene expression.

considered. The platelets were also stained with a marker for p-selectin (anti-CD62P conjugated to FITC) (Braun *et al.*, 2008). A positive control for platelet activation was also prepared using 10μM ADP to activate the platelets *ex vivo* (Cornelissen *et al.*, 2010). During flow cytometry acquisition, platelets were gated by their forward scatter (FSC) and side scatter (SSC) characteristics and further identified by the expression of CD41. Activated platelets were identified by the expression of p-selectin (CD62P) on their surface and quantified using the geometric mean fluorescence intensity (section 2.5.4).

5.3.6. **Assessment of mRNA levels**

Total RNA was extracted from the liver, lung and heart, and reverse transcribed to cDNA using reverse transcription polymerase chain reaction (RT-PCR). Total cDNA then underwent quantitative real-time PCR (qPCR) to assess mRNA abundance of specific clotting factor and fibrinolytic factor genes. Factor VIII (FVIII), von Willebrand factor (vWF), plasminogen, plasminogen activator inhibitor-1 (PAI-1) and tissue plasminogen activator (tPA) mRNA levels were assessed relative to reference genes (cyclophilin, β-actin, TATA-binding protein (TBP) and 18s) (section 2.6.2).

5.3.7. **Measurement of plasma fibrinolytic factors**

Plasma concentrations of total PAI-1 protein, active PAI-1 protein, total tPA protein and active tPA protein were quantified using ELISA kits with defrosted PPP collected from the vena cava (section 2.5.3).

5.3.8. **Statistics**

All statistical analysis was performed by one-way ANOVA with Dunnett's post-hoc test for comparison of treatment groups with the vehicle-treated group. Statistical analysis of all data was performed using GraphPad Prism 4.0 software.

5.4 Results

5.4.1. Body weights

There was no significant difference in body weights at the start of the study (Figure 5.2A). Dex administration caused a dose-dependent reduction in body weight (low and high dose dex $p<0.01$; Figure 5.2B). The average dex intake was 0.13±0.009mg/kg/day (low dose) and 0.82±0.02mg/kg/day (high dose).

5.4.2. Organ weights

Dex administration dose-dependently reduced both thymus weight (low dex: $p<0.05$, high dex: $p<0.01$; Figure 5.3A) and spleen weight (low and high dose dex: $p<0.01$; Figure 5.3B). High dex also increased liver weight compared with the vehicle-treated animals ($p<0.05$; Figure 5.3C). This effect was not seen at the low dose. There were no significant differences seen in the other organs collected (heart and kidneys; Figure 5.4).

5.4.3. Systolic blood pressure

The vehicle-treated animals showed no significant changes in systolic blood pressure between day 14 and day 28 of the experimental period, maintaining a pressure of around 125mmHg (Figure 5.5). Conversely, dex caused a dose-dependent increase in blood pressure with the high dose causing a significant increase (to 150mmHg) by day 14 ($p<0.01$). The low dose dex had no influence on blood pressure at day 14 but did cause a significant increase (to 140mmHg) by day 21 ($p<0.05$; Figure 5.5).

5.4.4. Tail-tip bleeding time

Dex dose-dependently reduced tail-tip bleeding time with the high dose reaching significance ($p<0.05$; Figure 5.6).

5.4.5. Platelet activation status

Neither low nor high dose dex influenced p-selectin expression on platelets (Figure 5.7). The p-selectin expression in the three test groups was 4-fold lower than the positive control for activated platelets (+ADP; Figure 5.7B).

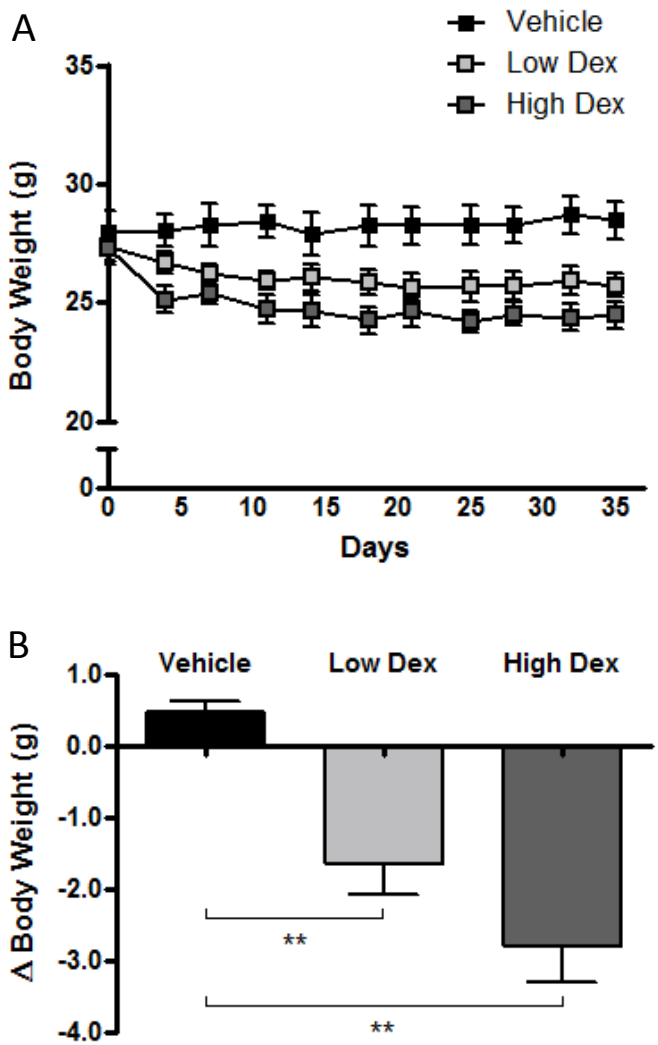

Figure 5.2: Weight changes induced by dexamethasone treatment.
Mice were randomised to receive either vehicle or dexamethasone (dex; 0.1 or 0.8mg/kg/day) in their drinking water. Body weight was measured regularly throughout the 5-week experimental period. There were no differences in the weights of the animals at the start of the experiment (A). Dex treatment appeared to dose-dependently reduce body weight. Analysis of change in body weight from start to end of the experimental period confirmed that dex treatment caused a dose-dependent reduction in body weight in comparison to the vehicle group (B). All data expressed as mean±SEM, n=6-7. Weight change was analysed by one way ANOVA with Dunnett's post hoc test vs vehicle. **$p<0.01$.

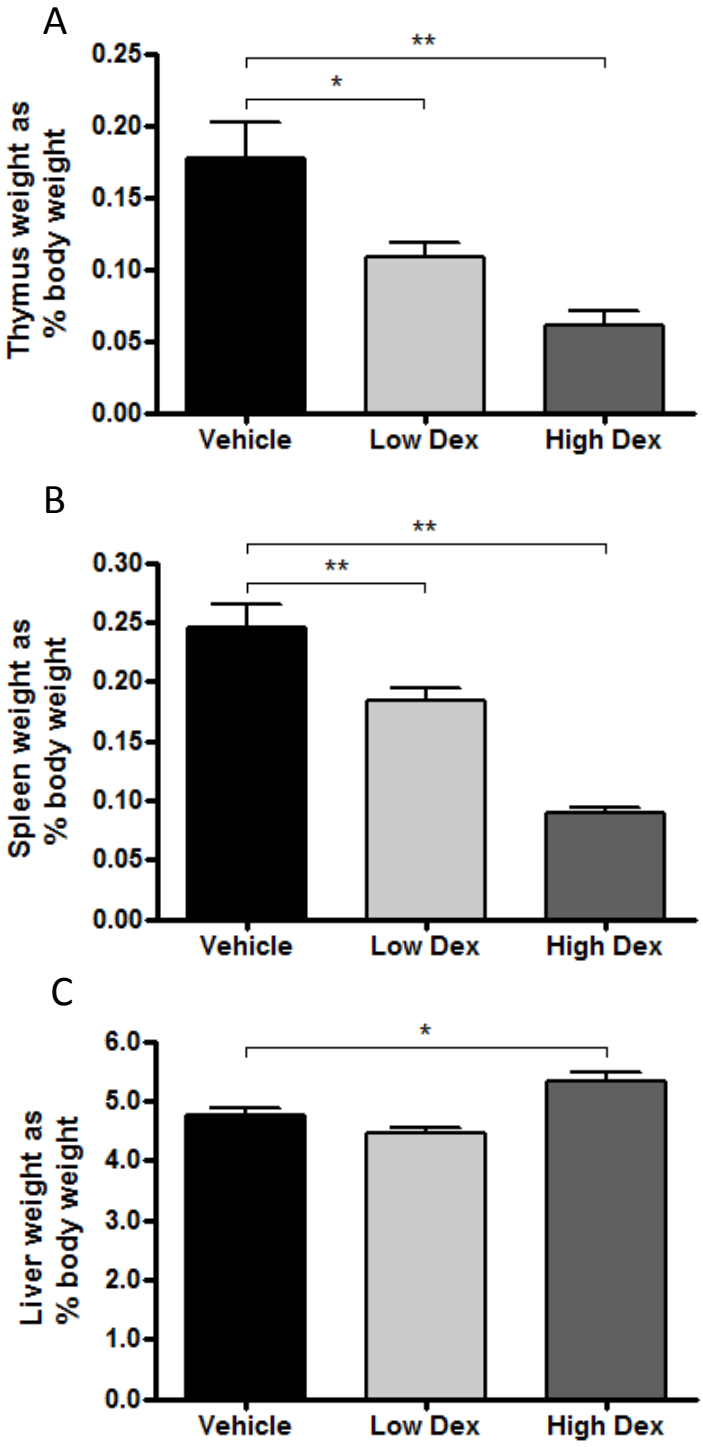

Figure 5.3: Organ weight changes induced by dexamethasone treatment.
Mice were randomised to receive either vehicle or dexamethasone (dex; 0.1 or 0.8mg/kg/day) in their drinking water. Organs were weighed upon sacrifice. Dex treatment caused a dose-dependent reduction in both thymus (A) and spleen (B) weight. The high dose dex also increased liver weight (C). All data expressed as mean±SEM, n=6-7. Data were analysed by one way ANOVA with Dunnett's post hoc test vs vehicle. *p<0.05, **p<0.01.

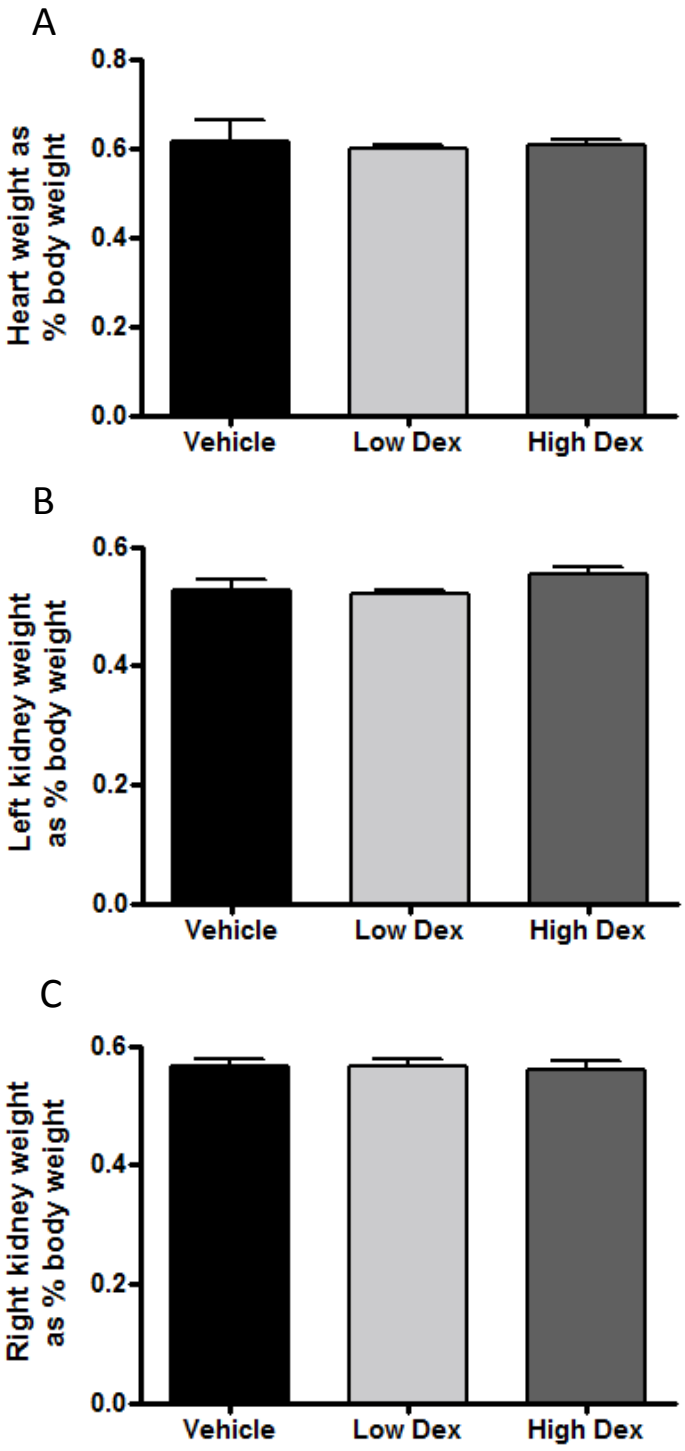

Figure 5.4: Organ weight changes induced by dexamethasone treatment.
Mice were randomised to receive either vehicle or dexamethasone (dex; 0.1 or 0.8mg/kg/day) in their drinking water. Organs were weighed upon sacrifice. Dex had no influence on heart or kidney weight. All data expressed as mean±SEM, n=6-7. Data were analysed by one way ANOVA with Dunnett's post hoc test vs vehicle.

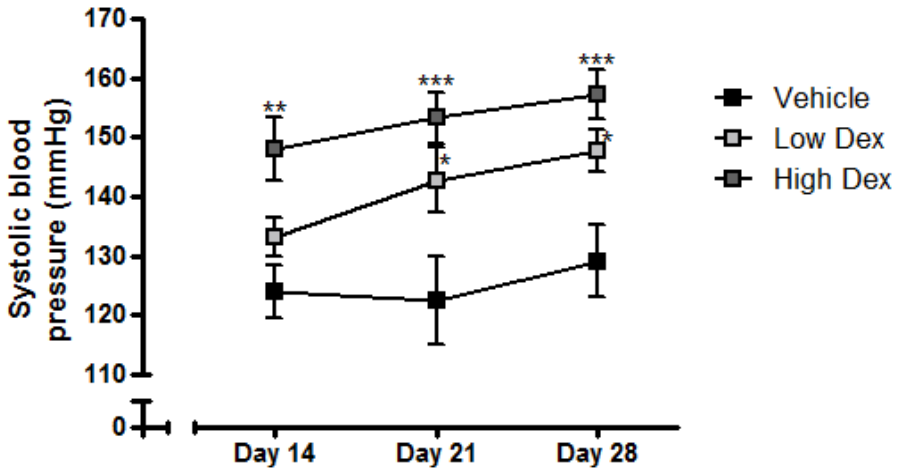

Figure 5.5: The impact of exogenous glucocorticoids on systolic blood pressure.
Mice were randomised to receive either vehicle or dexamethasone (dex; 0.1 or 0.8mg/kg/day) in their drinking water. Systolic blood pressure was measured weekly from day 14 by tail cuff plethysmography. Dex dose-dependently increased systolic blood pressure with the high dose significantly increasing blood pressure above vehicle by day 14 and the low dose by day 21. Data expressed as mean±SEM, n=6-7. Data were analysed by two-way ANOVA with Bonferroni post hoc test vs vehicle. * $p<0.05$, ** $p<0.01$, *** $p<0.001$.

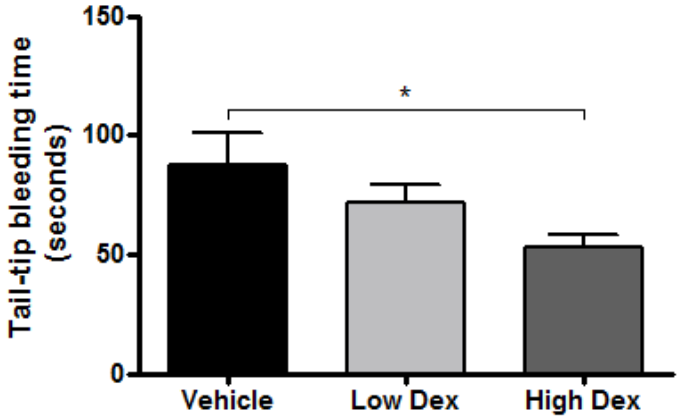

Figure 5.6: The impact of exogenous glucocorticoids on tail-tip bleeding.
Mice were randomised to receive either vehicle or dexamethasone (dex; 0.1 or 0.8mg/kg/day) in their drinking water. Tail-tip bleeding time was measured under anaesthesia at the end of the 5-week experimental period. The low dose of dex had no significant effect, whereas the high dose significantly reduced the bleeding time of the mice. Data expressed as mean±SEM, n=6-7. Data were analysed by one-way ANOVA with Dunnett's post hoc test vs vehicle. * $p<0.05$.

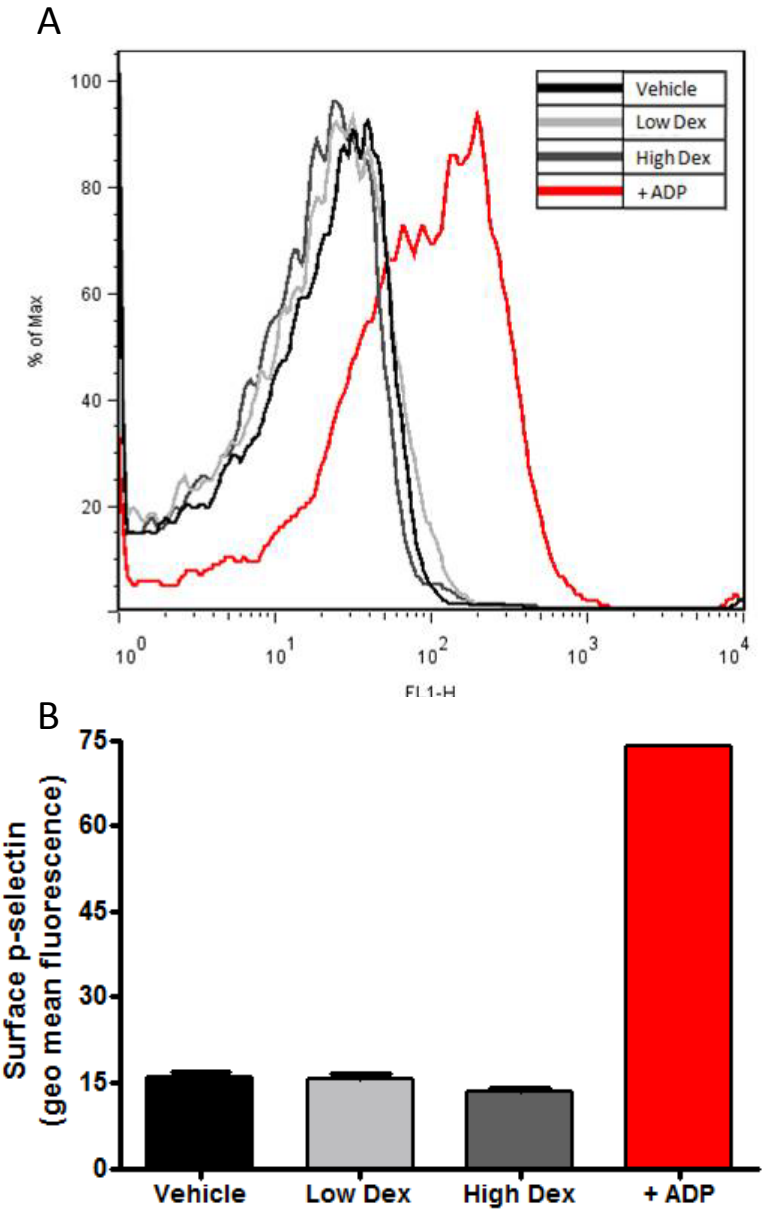

Figure 5.7: The impact of dexamethasone treatment on platelet activation status.
Mice were randomised to receive either vehicle or dexamethasone (dex; 0.1 or 0.8mg/kg/day) in their drinking water. Platelet activation status was assessed by flow cytometric analysis of p-selectin expression. Platelets were gated by FSC/SSC characteristics and further identified by their expression of the platelet specific antigen CD41. Platelet activation was identified by their expression of p-selectin (CD62P; A) and quantification of the geometric mean fluorescence intensity (GMFI; B). Neither dose of dex influenced the p-selectin expression on platelets. 10μM ADP was used as a positive control for activated platelets. Data expressed as mean±SEM, n=5-6, except control n=1. Data were analysed using one-way ANOVA with Dunnett's post hoc test vs vehicle

5.4.6. **Coagulation factor gene expression**

5.4.6.1 Factor VIII

Low dose dex reduced mRNA levels of FVIII in the lung ($p<0.05$) and heart ($p<0.05$), but not in the liver (Figure 5.8A). The high dose of dex had no significant effect in any tissue (Figure 5.8A).

5.4.6.2 vWF

Neither dose of dex affected mRNA levels of vWF in the liver and heart. It is worth noting that the abundace of vWF in the liver was particularly low in all three groups, thus making changes difficult to observe. There was, however, a dose-dependent reduction in vWF mRNA levels in the lung with the response to the high dose reaching significance ($p<0.01$; Figure 5.8B).

5.4.7. **Fibrinolytic factor gene expression**

5.4.7.1 Plasminogen

Plasminogen gene expression was too low to be detected by qPCR in the heart or lung. In the liver, low dose dex significantly increased plasminogen mRNA levels ($p<0.05$; Figure 5.9A). This increase was not seen with the high dose.

5.4.7.2 PAI-1

PAI-1 mRNA levels were too low to be detected in the liver. In the lung, neither dose of dex affected the mRNA levels, while in the heart the high dose only increased PAI-1 gene expression ($p<0.05$; Figure 5.9B).

5.4.7.3 tPA

tPA gene expression was too low to be detected in the liver. In the lung, dex treatment caused a dose-dependent increase in tPA mRNA levels with the high dose reaching significance ($p<0.05$; Figure 5.9C). Interestingly in the heart, dex treatment caused a dose-dependent decrease in tPA mRNA levels, with the high dose reaching significance ($p<0.05$; Figure 5.9C).

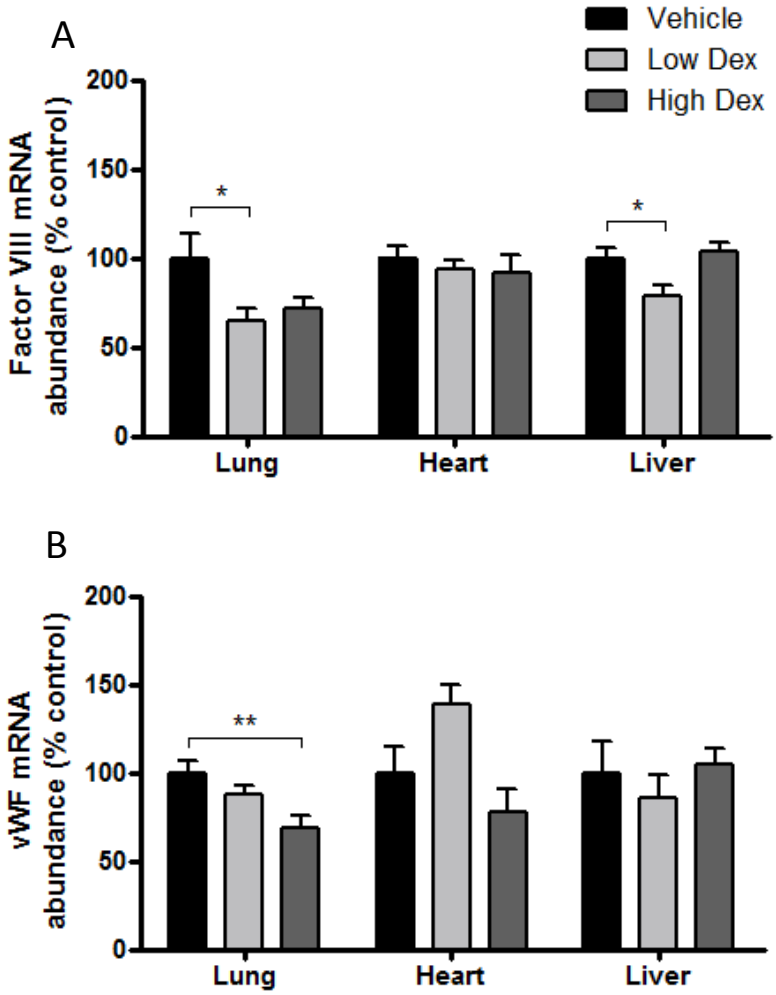

Figure 5.8: The impact of dexamethasone treatment on mRNA abundance of coagulation factor genes.
Mice were randomised to receive either vehicle or dexamethasone (dex; 0.1 or 0.8mg/kg/day) in their drinking water. Organs were collected and the mRNA levels of coagulation factor genes were assessed by qPCR relative to reference genes; β-actin (lung), TBP (TATA box-binding protein), cyclophilin and 18s (heart) and TBP, cyclophillin and β-actin (liver). Low dex treatment reduced mRNA levels of Factor VIII in the lung and heart but not in the liver, whereas, high dex had no significant effect on Factor VIII expression in any organ (A). Neither dose of dex affected mRNA levels of vWF in the liver or heart (B). However, there was a dose-dependent reduction in vWF mRNA levels in the lung, with the response to high dose dex reaching significance (B). Data expressed as mean±SEM, n=6-7. Data were analysed by one-way ANOVA with Dunnett's post hoc test vs vehicle. *$p<0.05$, **$p<0.01$. vWF: von Willebrand factor.

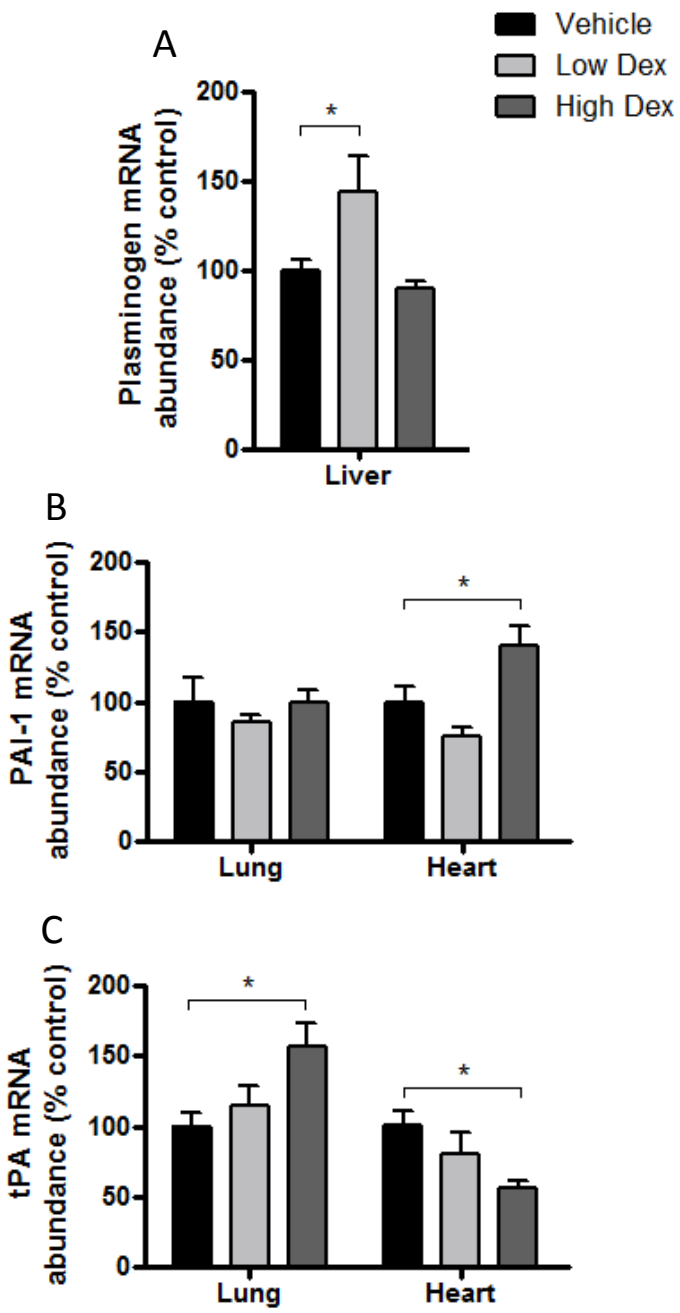

Figure 5.9: The impact of dexamethasone treatment on mRNA abundance of fibrinolysis factor genes.
Mice were randomised to receive either vehicle or dexamethasone (dex; 0.1 or 0.8mg/kg/day) in their drinking water. Organs were collected and the mRNA levels of fibrinolysis factor genes were assessed by qPCR relative to reference genes; β-actin (lung), TBP (TATA box-binding protein), cyclophillin and 18s (heart) and TBP, cyclophillin and β-actin (liver). Low dex only increased mRNA levels of plasminogen in the liver (A). Neither dose of dex affected mRNA levels of PAI-1 in the lung while the high dose only increased levels in the heart (B). There was a dose-dependent increase in tPA mRNA levels in the lung and a dose-dependent decrease in levels in the heart (C). Data expressed as mean±SEM, n=6-7. Data were analysed by one-way ANOVA with Dunnett's post hoc test vs vehicle. *$p<0.05$. PAI-1: plasminogen activator inhibitor-1, tPA: tissue plasminogen activator.

5.4.8. **Plasma fibrinolytic factor levels**

5.4.8.1 PAI-1

Plasma levels of total PAI-1 antigen and active PAI-1 antigen were both unaffected by low dose dex. However, the high dose dex increased the total PAI-1 antigen 3.5 fold ($p<0.001$; Figure 5.10A) and the active PAI-1 antigen 3 fold ($p<0.001$; Figure 5.10B).

5.4.8.2 tPA

Plasma levels of total tPA antigen and active tPA antigen were both unaffected by high dose dex. Interestingly, the low dose dex increased the active tPA antigen almost 2 fold ($p<0.05$; Figure 5.11B), while having no significant influence on the total tPA antigen level.

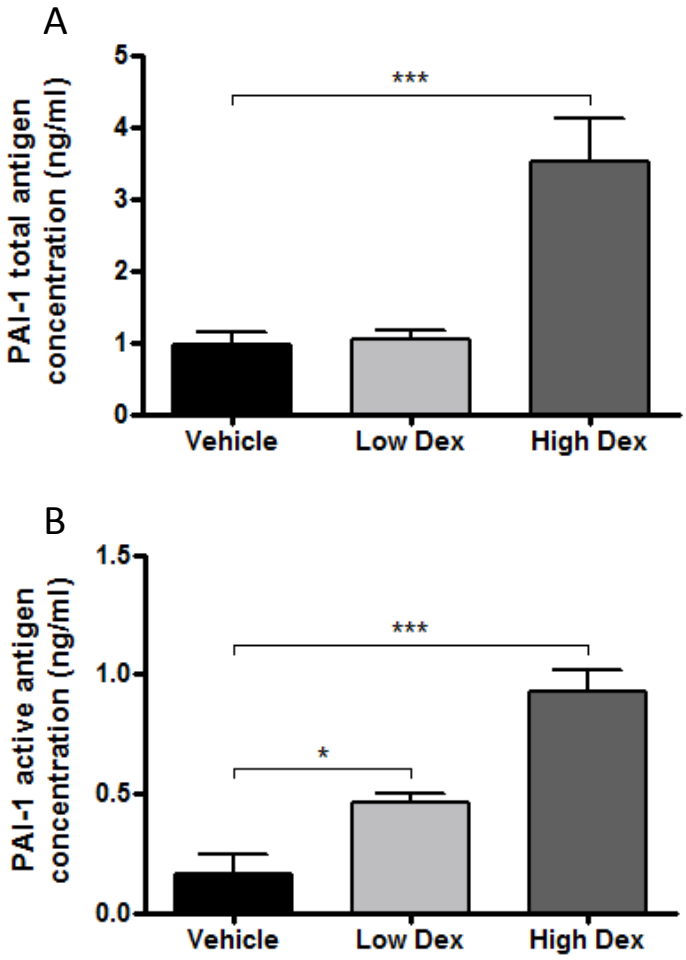

Figure 5.10: The impact of dexamethasone treatment on PAI-1 antigen levels in the plasma. Mice were randomised to receive either vehicle or dexamethasone (dex; 0.1 or 0.8mg/kg/day) in their drinking water. Total PAI-1 and active PAI-1 antigen levels were measured in the plasma by ELISA. Low dex had no influence on either total PAI-1 or active PAI-1 antigen levels. High dex greatly increased both total PAI-1 (A) and active PAI-1 (B) antigen levels in the plasma. Data expressed as mean±SEM, n=6-7. Data were analysed by one-way ANOVA with Dunnett's post hoc test vs vehicle. ***p<0.001. PAI-1: plasminogen activator inhibitor-1.

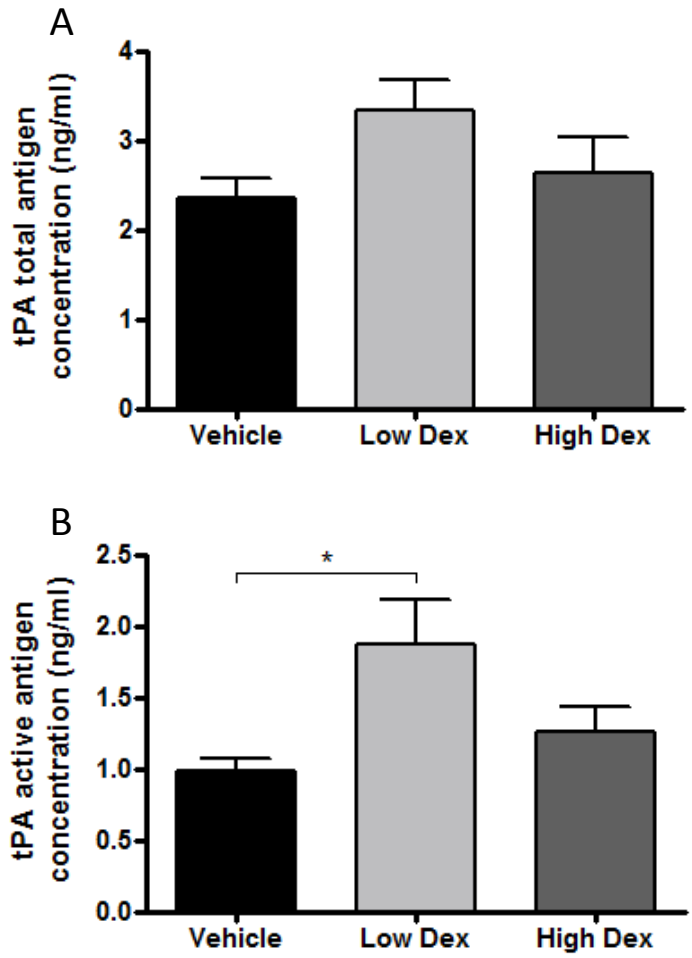

Figure 5.11: The impact of dexamethasone treatment on tPA antigen levels in the plasma. Mice were randomised to receive either vehicle or dexamethasone (dex; 0.1 or 0.8mg/kg/day) in their drinking water. Total tPA and active tPA antigen levels were measured in the plasma by ELISA. Neither dose of dex had any influence on the total tPA antigen levels (A). Low dose dex greatly increased both active tPA antigen levels (B) but this increase was not seen with the high dose. Data expressed as mean±SEM, n=6-7. Data were analysed by one-way ANOVA with Dunnett's post hoc test vs vehicle. *$p<0.05$. tPA: tissue plasminogen activator.

5.5 Discussion

The work described in this chapter addresses the hypothesis that high dose dex is pro-thrombotic. The results obtained suggest that high dose dex does indeed induce a systemic pro-thrombotic state, possibly as a result of increased PAI-1 activity. The low dose dex had no effect of thrombogenicity.

Consistent with the previous investigation (Chapter 4), the dose-dependent weight loss and reduction in size of glucocorticoid-sensitive organs confirms that both doses of dex were pharmacologically active in the animals. The high dose dex also induced a small increase in liver weight. Hepatomegaly could be indicative of liver steatosis, the retention of lipid in the liver, which has been shown to be induced by glucocorticoid excess, both in humans (Farrell, 2002; Stravitz *et al.*, 2003) and in rodents (Letteron *et al.*, 1997; Pinheiro *et al.*, 2009; Severino *et al.*, 2002).

It is well documented that glucocorticoids induce hypertension in rodents (Goodwin *et al.*, 2008; Whitworth *et al.*, 2001; Zhang *et al.*, 2004). Blood pressure was not measured in the previous study (Chapter 4) to prevent any additional stress to the animals, which may have influenced neointimal proliferation. The study described in this chapter, therefore, provided an opportunity to confirm the effect of dex on blood pressure in a similar experimental protocol. The results confirm a dose-dependent increase in systolic blood pressure following dex administration. Traditionally, glucocorticoids have been believed to induce hypertension by MR activation in the kidney. However, along with the selectivity of dex for GR, there is growing evidence that this is not the primary mechanism underlying this form of hypertension (Goodwin *et al.*, 2010). It has been suggested that disruption of the endothelial nitric oxide system is involved in glucocorticoid-induced hypertension (Whitworth *et al.*, 2001), but the precise mechanism remains incompletely understood.

A crucial finding from this investigation is the dose-dependent reduction in tail-tip bleeding times in mice treated with dex. Tail-tip bleeding time is a well-established, albeit relatively crude, method of assessing platelet function and coagulation enzyme defects (Lavelle *et al.*, 1998). For example, bleeding time is significantly increased in

mice administered aspirin (Yamamoto *et al.*, 2009) and mice deficient in Factor VIII (Lauer *et al.*, 2002). In the current investigation, reduced bleeding time indicates a systemic pro-thrombotic state in these mice, as a result of their high dose glucocorticoid treatment. This supports previous evidence that glucocorticoids increase the thrombogenicity of blood in patients and animals (Patrassi *et al.*, 1992; van Giezen *et al.*, 1994). A pro-thrombotic state could be produced via a number of mechanisms including those involving platelets, the endothelium and/or clotting factors. As tail-tip bleeding time cannot distinguish between these mechanisms, further explorations were carried out in order to clarify which are involved in glucocorticoid-mediated pro-thrombotic state.

Glucocorticoids have mixed effects on platelet activation and aggregation. van Giezen *et al* showed that dex inhibits platelet aggregation in rats, thus suggesting an anti-coagulant outcome (van Giezen *et al.*, 1994; van Giezen *et al.*, 1992). Conversely, methylprednisolone has successfully been used clinically to reverse clopidogrel-related inhibition of platelet aggregation (Qureshi *et al.*, 2008) and dex has been shown to block inhibition of platelet aggregation by activated macrophages *in vitro* (Pinto *et al.*, 1993); both these studies indicate a pro-coagulant capability of glucocorticoids. Direct assessment of platelet aggregation (using aggregometry) was considered impractical due to the low volume of plasma obtained from individual mice. As an alternative, platelet involvement was assessed using flow cytometry to investigate the activation status of platelets isolated from these mice. Expression of the adhesion molecule p-selectin (which is stimulated following activation) on the surface of platelets was used as a marker of platelet activation (Griesshammer *et al.*, 1999). Using this assay, dex administration had no influence on the activation status of circulating platelets. When compared with the control platelets, which were fully activated with ADP *ex vivo*, the number of platelets expressing p-selectin was 4-fold lower in all three test groups. Also, this method investigated the effects of glucocorticoid administration on “resting” platelet activation and not did not explore changes that glucocorticoid treatment may have had on the potential for platelets to activate. It would, therefore, be very interesting to pre-treat platelets with glucocorticoids *in vivo* and then assess their activation with agonists *in vitro*.

Investigation into the influence of dex on coagulation and fibrinolysis factor gene transcription did not reveal any striking changes which could explain the pro-thrombotic effect of the steroid. However, PAI-1 stood out due to the considerable increase in both the total and active circulating protein levels in response to high dose dex. Not only does this complement the dose-dependent increase in PAI-1 gene expression in the heart by dex, but it also complements many other *in vitro*, animal and clinical studies which have described a significant increase in total and active PAI-1 antigen levels with glucocorticoid treatment/excess (Ma *et al.*, 2002; Patrassi *et al.*, 1992; Sartori *et al.*, 1999; van Giezen *et al.*, 1994). An increase in PAI-1 protein strongly implies there is decreased fibrinolytic potential, which would likely contribute towards the pro-thrombotic state that we see in the high dose dex-treated mice. It is important to note that there was no increase in total or active PAI-1 protein in the low-dose group.

The influence of glucocorticoids on total tPA and active tPA protein levels are less clear. *In vitro* studies have concluded that dex administration increases tPA antigen in rat lymphocytes (Tsantarliotou *et al.*, 1999) and HUVEC culture medium (Huang *et al.*, 1995). However, clinical studies have reported inconsistent results, with Cushing's patients and healthy subjects receiving glucocorticoids having either increased (de Kruif *et al.*, 2007; Patrassi *et al.*, 1992) or unchanged tPA levels (Ambrosi *et al.*, 2000; Dover *et al.*, 2007). Thus the results from this study, describing no influence on total tPA levels by dex, support the latter clinical studies. However, the low dose dex did increased active tPA protein in the blood. This effect was not seen at the high dose. Perhaps dex induces an increase in tPA activity which is appreciable at the low dose but is inhibited by elevated PAI-1 levels at the high dose. However, the functional relevance of this dex-induced increase in tPA is unclear, as the low dose of dex had no influence on bleeding time.

In summary, the results from this investigation support the hypothesis that high dose dex is pro-thrombotic, while low dose dex had no influence on thrombogenicity, in this murine model. These results may explain the thrombotic lesions observed following arterial injury in high-dose dex-treated mice. It is proposed that this effect

is in part accounted for by a decrease in the activity of the endogenous fibrinolytic pathway, attributable to an increase in PAI-1. This hypothesis can be addressed by investigating the effects of genetic deletion of PAI-1 on dex-induced changes in neointimal proliferation. These studies are described in Chapter 6.

Chapter 6

Role of PAI-1 in dexamethasone-induced thrombosis following vascular injury

6.1 Introduction

The work described in the previous chapters suggests that elevated PAI-1 may be in part responsible for the effects of high dose dex on neointimal proliferation. Elevated PAI-1 levels would be expected to attenuate the endogenous fibrinolysis system, inhibiting the breakdown of thrombus by downstream plasmin and, therefore, may explain the increased presence of large semi-occlusive thrombi at the site of intra-arterial wire injury in high dose dex-treated mice. Indeed, PAI-1 has been implicated in acute coronary thrombosis, with elevated PAI-1 levels in patients with coronary artery disease, angina pectoris and recurrent myocardial infarction (Carmeliet *et al.*, 1993b).

However, a number of groups have reported evidence that PAI-1 itself is an important mediator of intimal hyperplasia in mice, albeit with discordant results. Some report that genetic deletion or pharmacological inhibition of PAI-1 decreases lesion development (Peng *et al.*, 2002; Ploplis *et al.*, 2001; Suzuki *et al.*, 2008; Zhu *et al.*, 2001), while others disagree, concluding that PAI-$1^{-/-}$ mice have increased lesion development (Carmeliet *et al.*, 1997b; de Waard *et al.*, 2002; Schafer *et al.*, 2006). Several different models of vascular injury were employed in these studies, including chemical injury, mechanical injury and electrical injury, which may be contributing to the variable results. Clearly, the exact role of the fibrinolytic system in vascular remodelling remains to be elucidated. Indeed, evidence from the clinic regarding the role of PAI-1 in restenosis is also conflicting: some studies found that elevated plasma PAI-1 levels were associated with increased risk of restenosis (Fornitz *et al.*, 2001; Huber *et al.*, 1992; Prisco *et al.*, 2001; Sakata *et al.*, 1996), while others reported a reduced risk of restenosis (Inoue *et al.*, 2003; Shah *et al.*, 1992; Strauss *et al.*, 1999).

In order to further elucidate the role of PAI-1 in neointimal proliferation and to test the hypothesis that PAI-1 is responsible for dex-mediated thrombosis following arterial injury, PAI-1 must be manipulated. The most obvious approach would be to reduce PAI-1 activity, by either genetic deletion of the *Serpine1* gene, resulting in

PAI-1$^{-/-}$ mice (Carmeliet *et al.*, 1993a; Carmeliet *et al.*, 1993b), or by use of the pharmacological inhibitor of PAI-1, tiplaxtinin (Elokdah *et al.*, 2004). Both approaches have their advantages and disadvantages. Genetic deletion of PAI-1 ensures an absence of circulating PAI-1 but may result in developmental abnormalities which could influence the outcome of the study. Pharmacological inhibition of PAI-1 by tiplaxtinin allows short-term manipulation of PAI-1 in parallel with dex treatment. However, it would require optimisation of dosage and administration regime, in addition to the risk of potential adverse side-effects. As the vast majority of studies investigating the role of PAI-1 in intimal hyperplasia use genetically-deficient mice, this was the approach chosen for this study. Reports on the characterisation of PAI-1$^{-/-}$ mice revealed that they develop normally, with a mild hyperfibrinolytic state and normal haemostasis (Carmeliet *et al.*, 1993a; Carmeliet *et al.*, 1993b).

6.2 Hypothesis and Aims

The work described in this chapter addresses the hypothesis that increased PAI-1 activity is responsible for dex-mediated thrombosis following vascular injury. It is, therefore, proposed that genetic deletion of PAI-1 prevents the thrombotic side effects of dex, while maintaining the anti-restenotic effects of steroid treatment. In order to address this hypothesis, the specific aims of the work described in this chapter were to:

- determine the role of PAI-1 in neointimal proliferation following intra-luminal wire injury in mice.
- determine whether genetic deletion of PAI-1 prevented dex-mediated thrombus formation following intra-luminal wire injury in mice.

6.3 Methods

6.3.1. Animals

Male C57Bl/6 mice (Harlan Olac, UK) and PAI-$1^{-/-}$ (C57Bl/6 background; The Jackson Laboratory, ME, USA) aged 19-21 weeks and weighing 26-34 grams were used in this study. It is important to note that these animals are not littermates.

6.3.2. Administration of drugs

All mice were randomised to receive either dexamethasone (dex; 0.8mg/kg/day) or vehicle (absolute ethanol) in their drinking water for 4 weeks (Figure 6.1).

6.3.3. Femoral artery injury

One week after commencement of drinking water treatments, the mice were subjected to unilateral femoral artery injury to induce neointimal hyperplasia (section 2.2.2).

6.3.4. Blood pressure measurements

All mice had their systolic blood pressure monitored with measurements acquired using tail cuff plethysmography (section 2.2.4) at weekly intervals following commencement of drinking water treatment.

6.3.5. Tissue collection

At the end of the 4-week study the mice were anaesthetised by isoflurane inhalation before their tail bleeding time was assessed (section 2.2.5). Blood was immediately collected by cardiac puncture into 3.8% sodium citrate (1:9) and spun (8,000 x g, 10 min, RT) and the plasma (supernatant) was snap frozen and stored at -80ºC. The mice were then perfusion fixed (section 2.2.6). Organs and femoral arteries were collected and stored as described previously (section 3.3.4).

6.3.6. Measurement of plasma fibrinolytic factors

Plasma concentrations of total PAI-1 protein, active PAI-1 protein, total tPA protein and active tPA protein were quantified using ELISA kits (section 2.9.4).

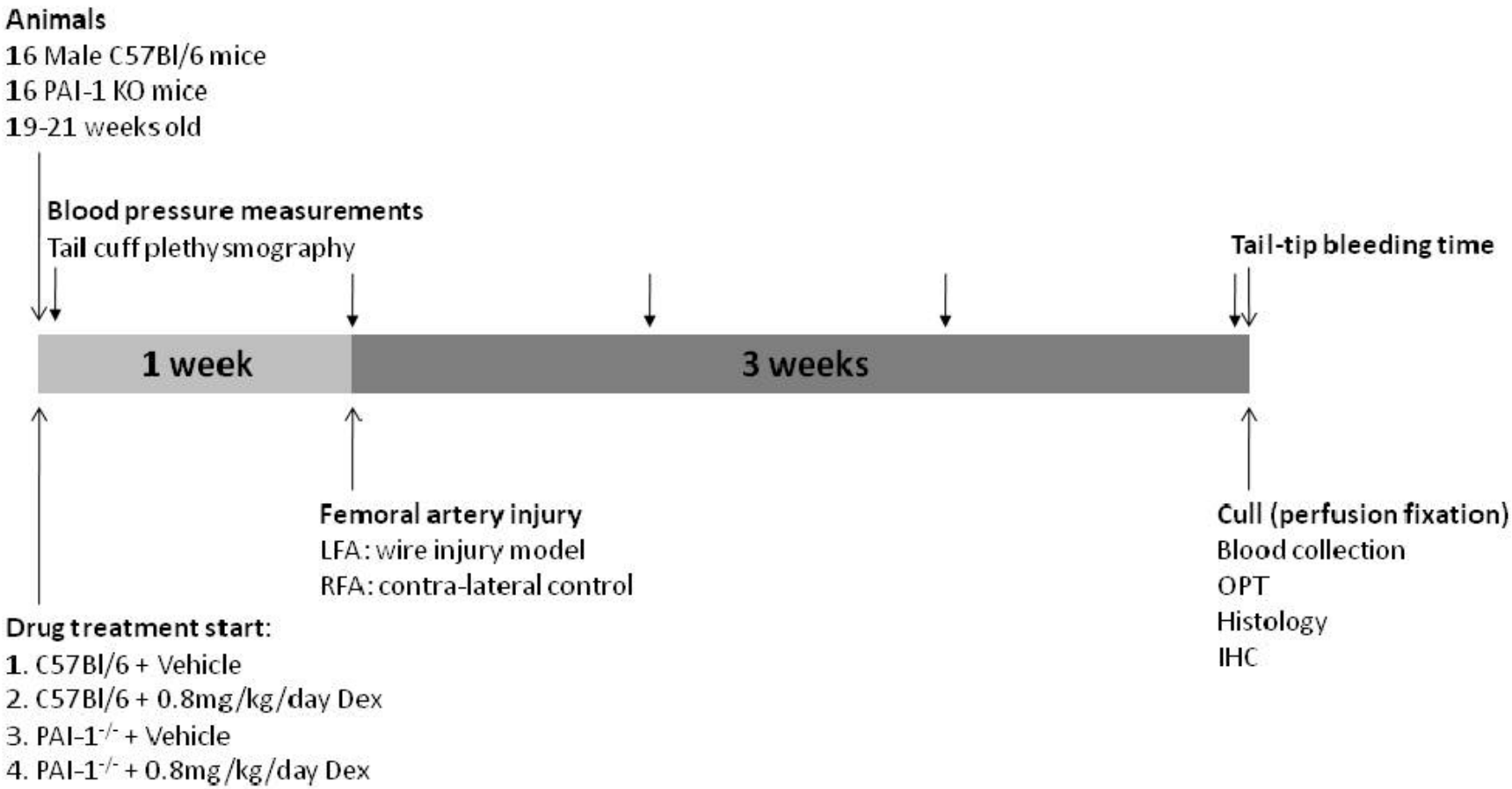

Figure 6.1: Study protocol to determine the influence of PAI-1 on glucocorticoid-mediated thrombus formation following intra-luminal wire injury. Experiments were conducted in male, 19-21 week old C57Bl/6 and PAI-$1^{-/-}$ mice. Animals were randomised to receive either vehicle (absolute ethanol; n=8) or dexamethasone (dex; 0.8mg/kg/day; n=8) in their drinking water for the 4-week experimental period. One week following surgery all animals underwent unilateral femoral artery injury surgery to induce neointimal hyperplasia and were maintained for a further 3 weeks. At the end of the experimental period mice were culled by perfusion fixation. The left femoral artery was excised for examination of neointimal lesion development by optical projection tomography (OPT), histology and immunohistochemistry.

6.3.7. **Neointimal lesion analysis**

6.3.7.1 Optical Projection Tomography (OPT)

Firstly, the femoral arteries were embedded in agarose for analysis by OPT (section 2.3.2). Briefly, after being dehydrated in methanol for 24 hours and cleared in BABB for a further 24 hours, the arteries were scanned under UV light using a Bioptonics OPT tomograph. Computed tomography reconstructions were calculated by filtered back-projection of raw data using NRecon software. Volumetric measurements of the femoral artery were acquired by manual tracing of the estimated outline of the plaque and lumen using CTan software.

6.3.7.2 Histology

Following acquisition of OPT scans, the femoral arteries were processed, embedded in paraffin and cut into 4μm thick transverse sections. Sets of twenty serial sections (80μm) were collected every 160μm along the entire artery. One section every 160μm along the artery were stained with United States trichrome stain (section 2.4.2). Photomicrographs were taken using a light microscope coupled to a colour camera and image analysis system (section 2.4.4). The area (μm^2) of lesion in each section was measured using Photoshop CS3 software (section 2.4.5). The section with the largest area of lesion was chosen to represent each arterial sample.

6.3.7.3 Composition

The cellular composition of the neointimal lesions was initially investigated using the United States trichrome-stained sections. Further immunohistochemical analysis was carried out on the section of the artery adjacent to the section identified as having the largest lesion. Smooth muscle cell content was assessed using an alkaline-phosphatase conjugated monoclonal primary antibody against smooth muscle cell α-actin (section 2.4.7.2).

6.3.8. **Statistics**

All statistical analysis was performed by two-way ANOVA with Bonferroni's post-hoc test to assess the effect of dex administration and the effect of PAI-1 deficiency, and any interaction between them. Statistical analysis of all data was performed using GraphPad Prism 4.0 software.

6.4 Results

6.4.1. Body weights

There were no differences in the weights of the animals at the start of the experiment. Animals in all 4 groups showed a weight loss following wire injury surgery (Figure 6.2A). Vehicle-treated PAI-$1^{-/-}$ mice appeared to recover fully by the end of the experimental period, while the C57Bl/6 mice maintained their post-surgery weight ($p<0.01$; Figure 6.2B), comparable with the previous study using C57Bl/6 mice (section 4.4.1). Dex administration caused a reduction in weight over the 4-week period in both C57Bl/6 mice ($p<0.01$) and PAI-$1^{-/-}$ mice ($p<0.001$; Figure 6.2B). The average doses of dex received were 0.84±0.02mg/kg/day (C57Bl/6 mice) and 0.84±0.03mg/kg/day (PAI-$1^{-/-}$ mice).

6.4.2. Organ weights

Genetic deletion of PAI-1 had no effect on any organ weight in vehicle-treated mice. In both C57Bl/6 and PAI-$1^{-/-}$ mice, dex induced a significant reduction in spleen weight ($p<0.001$ and $p<0.05$, respectively; Figure 6.3A) and thymus weight (both $p<0.001$; Figure 6.3B). There were no significant changes in the other organs collected (liver, kidneys, adrenals and heart; data not shown).

6.4.3. Systolic blood pressure

Vehicle-treated C57Bl6 and PAI-$1^{-/-}$ mice maintained steady blood pressures of around 110-115mmHg throughout the study, with no significant differences between the genotypes (Figure 6.4). Dex administration increased blood pressure from week 1 in both genotypes, reaching significance by week 2 (both $p<0.001$). By week 4 all dex-treated animals had a blood pressure of around 140mmHg (Figure 6.4).

6.4.4. Tail-tip bleeding time

Genetic deletion of PAI-1 had no effect on bleeding time in vehicle-treated mice. As previously reported in Chapter 4 (section 4.4.5.2), dex administration significantly reduced tail-tip bleeding time in C57Bl/6 mice ($p<0.01$; Figure 6.5). However, this reduction by dex was lost in the PAI-$1^{-/-}$ mice ($p>0.05$), but there was no significant interaction between genotype and treatment ($p=0.078$).

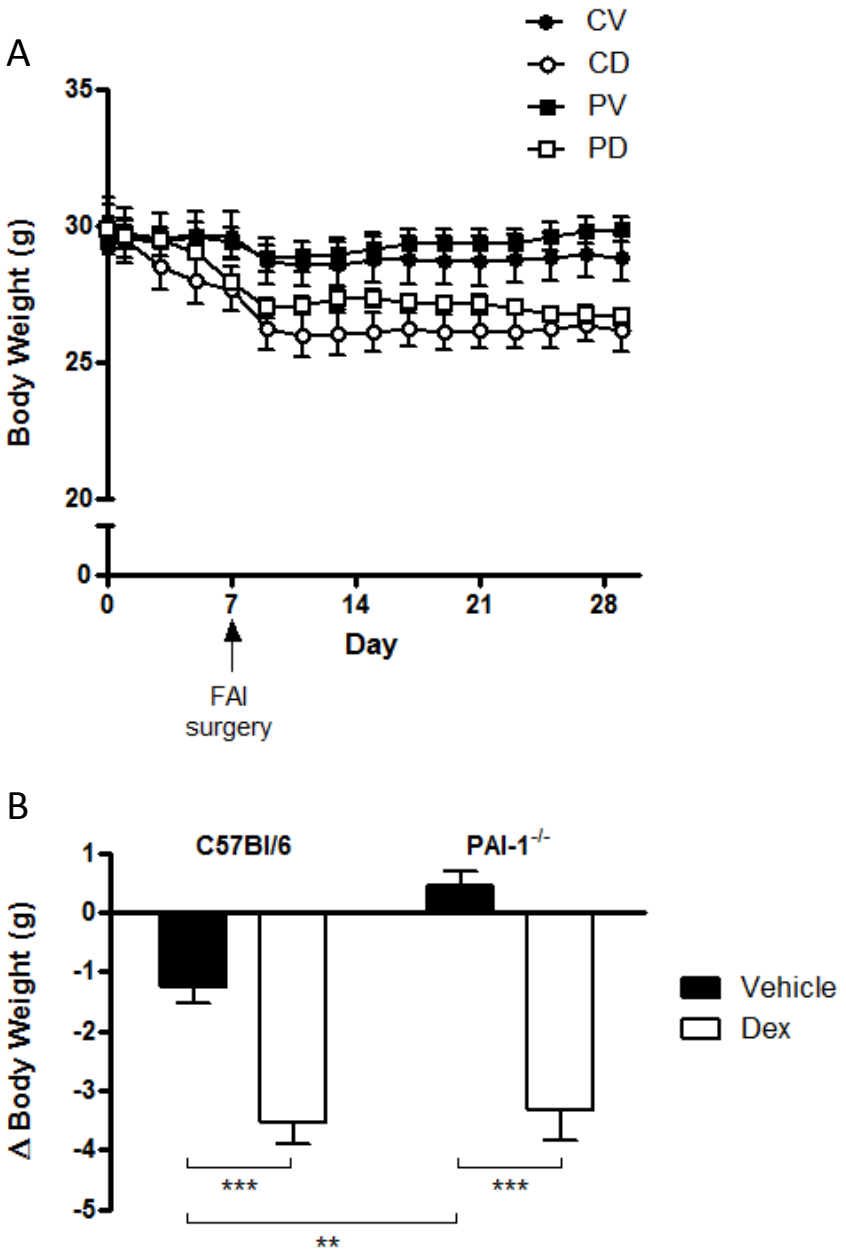

Figure 6.2: Weight changes induced by genotype and dexamethasone treatment.
C57Bl/6 and PAI-1$^{-/-}$ mice were randomised to receive either vehicle or dexamethasone (dex; 0.8mg/kg/day) in their drinking water. Neointimal hyperplasia was induced by femoral artery wire-injury (FAI). (A) Body weight was measured periodically throughout the 4-week experimental period. There were no differences in the weights of the animals at the start of the experiment. All animals showed a weight loss after the femoral artery injury surgery. (B) Change in body weight from start to end of the experimental period was also calculated. Vehicle-treated PAI-1$^{-/-}$ mice appeared to recover better from post-surgery weight loss than C57Bl/6 mice, whilst dex treatment caused a reduction in body weight in both genotypes. All data expressed as mean±SEM, n=6-8. Weight change analysed by two way ANOVA with Bonferroni post hoc test. ** $p<0.01$, ***$p<0.001$. CV: C57Bl/6 on vehicle, CD: C57Bl/6 on dex, PV: PAI-1$^{-/-}$ on vehicle, PD: PAI-1$^{-/-}$ on dex.

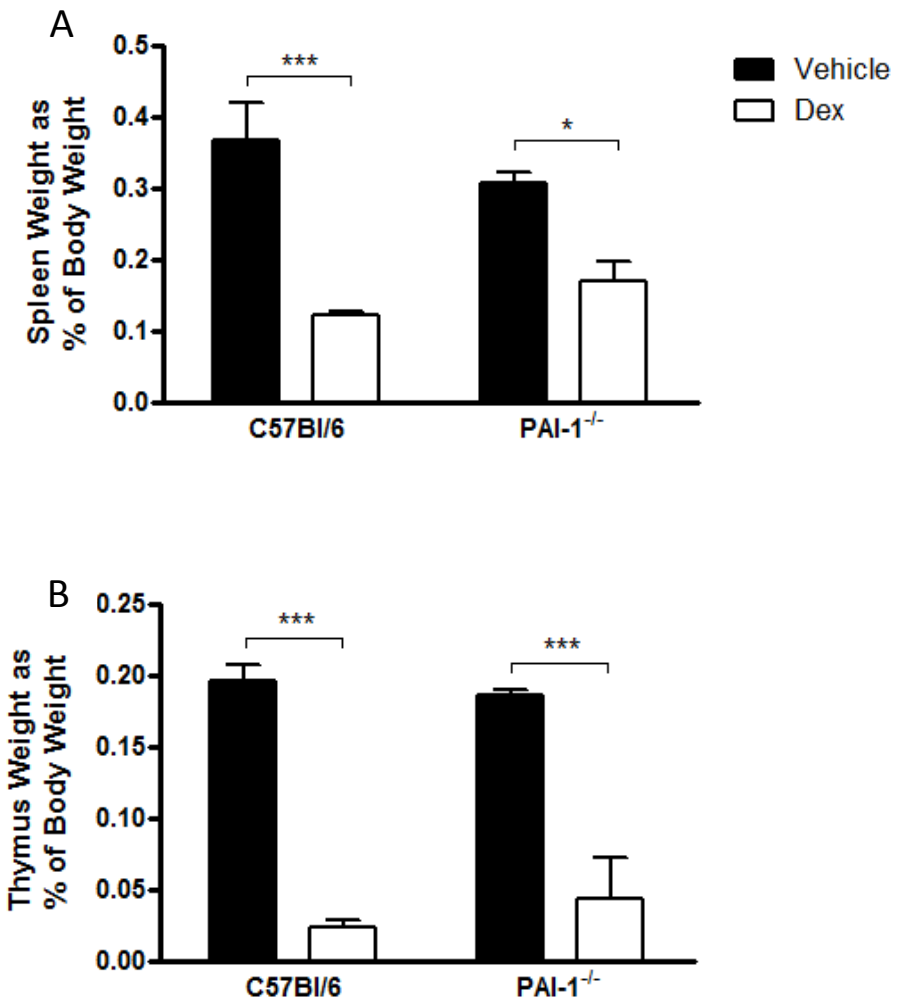

Figure 6.3: Organ weight changes induced by dexamethasone treatment.
C57Bl/6 and PAI-1$^{-/-}$ mice were randomised to receive either vehicle or dexamethasone (dex; 0.8mg/kg/day) in their drinking water. Neointimal hyperplasia was induced by femoral artery wire-injury. Organs were weighed upon sacrifice. Genotype had no influence on organ weight, whilst dex treatment caused a reduction in both spleen (A) and thymus (B) weight. All data expressed as mean±SEM, n=6-8. Data were analysed by two way ANOVA with Bonferroni post hoc test. * $p<0.05$, ***$p<0.001$.

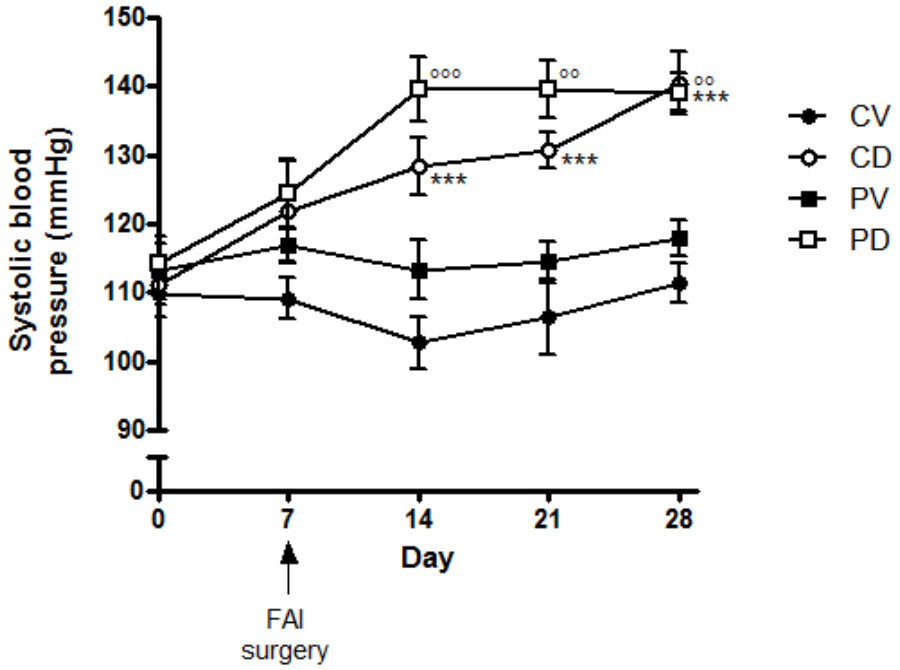

Figure 6.4: Systolic blood pressure changes induced by dexamethasone treatment.
C57Bl/6 and PAI-1$^{-/-}$ mice were randomised to receive either vehicle or dexamethasone (dex; 0.8mg/kg/day) in their drinking water. Neointimal hyperplasia was induced by femoral artery wire-injury (FAI). Systolic blood pressure was measured weekly by tail cuff plethysmography. Dex treatment significantly increased systolic blood pressure by day 14, in both genotypes. Data expressed as mean±SEM, n=5-8. Data were analysed by two way ANOVA with Bonferroni post hoc test. ***p<0.001 vs CV, ^{oo}p<0.01 vs PV, ^{ooo}p<0.001 vs PV. CV: C57Bl/6 on vehicle, CD: C57Bl/6 on dex, PV: PAI-1$^{-/-}$ on vehicle, PD: PAI-1$^{-/-}$ on dex.

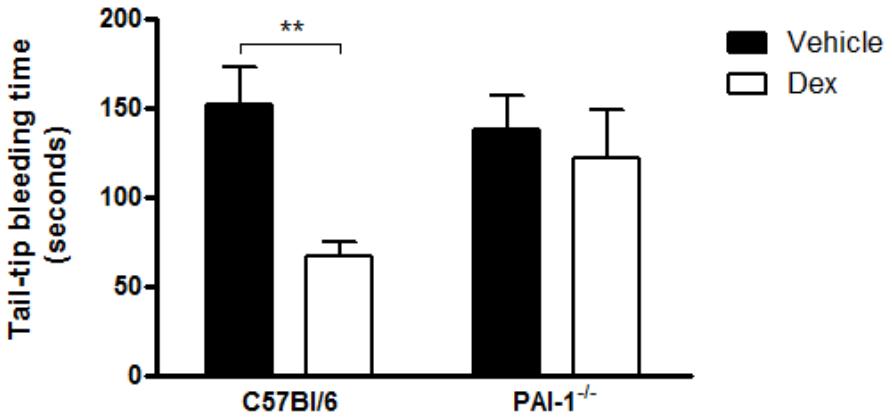

Figure 6.5: The impact of PAI-1 and dexamethasone treatment on tail-tip bleeding.
C57Bl/6 and PAI-$1^{-/-}$ mice were randomised to receive either vehicle or dexamethasone (dex; 0.8mg/kg/day) in their drinking water. Neointimal hyperplasia was induced by femoral artery wire-injury. Tail-tip bleeding time was measured under anaesthesia at the end of the 4-week experimental period. Tail tip bleeding time was not affected by genetic deletion of PAI-1 in vehicle treated animals. However, dex treatment significantly reduced the bleeding time in the C57Bl/6 mice only. Data expressed as mean±SEM, n=5-8. Data were analysed by two way ANOVA with Bonferroni post hoc test. **$p<0.01$.

6.4.5. **Plasma fibrinolytic factor levels**

6.4.5.1 PAI-1

Dex administration significantly increased circulating total ($p<0.001$; Figure 6.6A) and active ($p<0.001$; Figure 6.6B) PAI-1 levels in C57Bl/6 mice. No PAI-1 antigen was detected in PAI-$1^{-/-}$ mice.

6.4.5.2 tPA

Neither genetic deletion of PAI-1 nor dex administration had any significant effect on circulating total tPA levels (Figure 6.7). Unfortunately, the active tPA assay did not produce conclusive results as the data was very noisy. This is thought to be due to too many freeze-thaw episodes.

6.4.6. **Neointimal lesion development**

6.4.6.1 Neointima quantification by OPT

There were no differences, in any of the lesion or lumen parameters analysed, between the vehicle-treated C57Bl/6 and PAI-$1^{-/-}$ mice. Dex administration reduced absolute neointimal lesion volume, in both C57Bl/6 mice and PAI-$1^{-/-}$ mice (both $p<0.05$; Figure 6.8A). Interestingly, in the C57Bl/6 mice only, dex also reduced the total volume inside the internal elastic lamina (IEL; $p<0.05$; Figure 6.8B). Consequently, the volumetric stenotic ratio was unaffected by dex (Figure 6.8C). Conversely, dex had no effect on the total volume inside the IEL in PAI-$1^{-/-}$ mice (Figure 6.8B). Thus, lesion size was still reduced by dex when expressed as volumetric stenotic ratio ($p<0.05$; Figure 6.8C).

Dex administration significantly reduced the maximum cross-sectional area of lesion in the C57Bl/6 mice ($p<0.05$; Figure 6.9A), but not in the PAI-$1^{-/-}$ mice. This effect was lost when the lesion size was calculated as stenotic ratio (Figure 6.9B), as a result of dex treatment also reducing the area inside the IEL in the C57Bl/6 mice (Table 6.1(b)). Analysis of the cross-sectional profiles of the lesions revealed that dex treatment reduced lesion development consistently along the length of the artery, in both genotypes (Figure 6.9C).

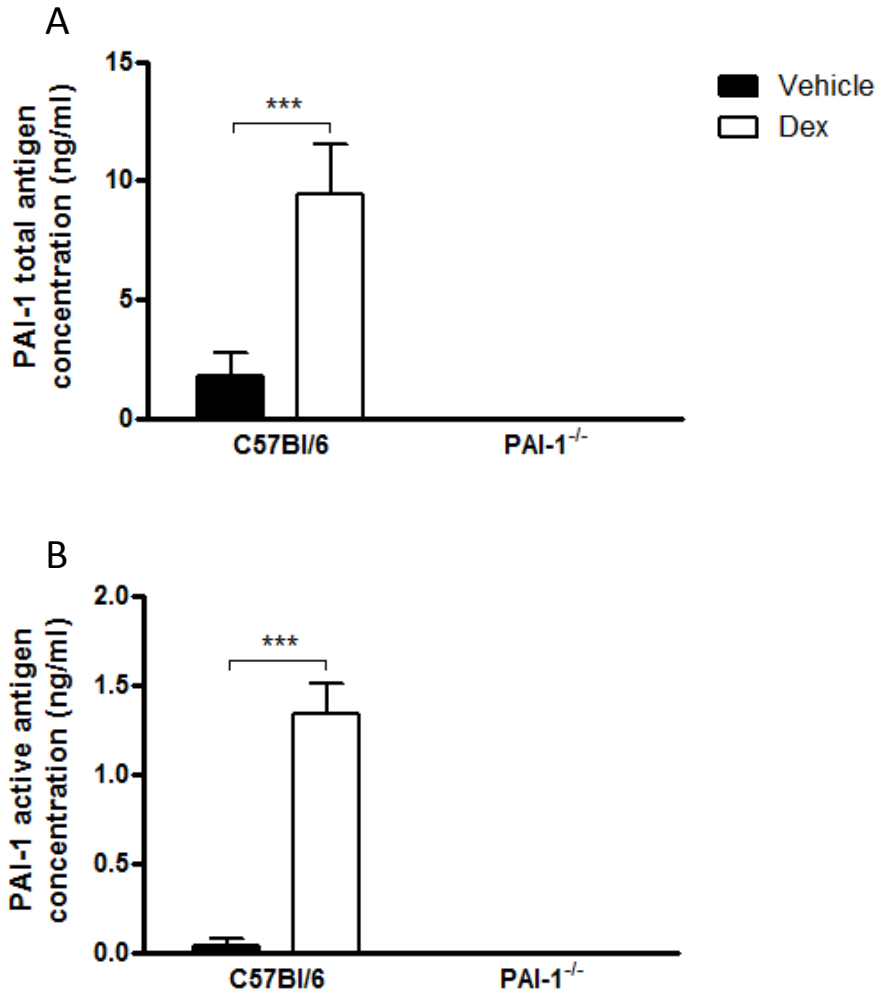

Figure 6.6: The impact of dexamethasone treatment on PAI-1 antigen levels in the plasma. C57Bl/6 and PAI-1$^{-/-}$ mice were randomised to receive either vehicle or dexamethasone (dex; 0.8mg/kg/day) in their drinking water. Neointimal hyperplasia was induced by femoral artery wire-injury. Total PAI-1 and active PAI-1 antigen levels were measured in the plasma by ELISA. Dex treatment greatly increased both total PAI-1 (A) and active PAI-1 (B) antigen levels in the plasma of C57Bl/6 mice. No PAI-1 antigen was detected in the plasma of PAI-1$^{-/-}$ mice. Data expressed as mean±SEM, n=6-8. Data were analysed by two way ANOVA with Bonferroni post hoc test. ***p<0.001.

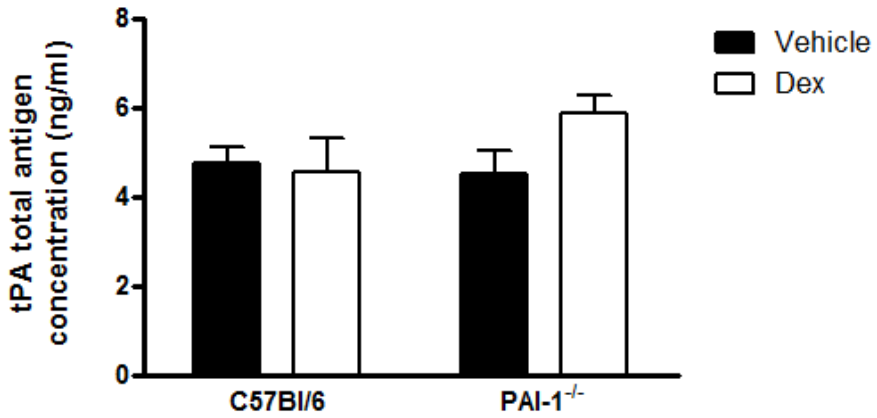

Figure 6.7: The impact of PAI-1 deletion and dexamethasone administration on tPA antigen levels in the plasma.
C57Bl/6 and PAI-$1^{-/-}$ mice were randomised to receive either vehicle or dexamethasone (dex; 0.8mg/kg/day) in their drinking water. Neointimal hyperplasia was induced by femoral artery wire-injury. Total tPA antigen levels were measured in the plasma by ELISA. Genetic deletion of PAI-1 had no effect on tPA levels. In addition, dex treatment had no significant effect on tPA antigen level in either genotype. Data expressed as mean±SEM, n=6-8. Data were analysed by two way ANOVA with Bonferroni post hoc test.

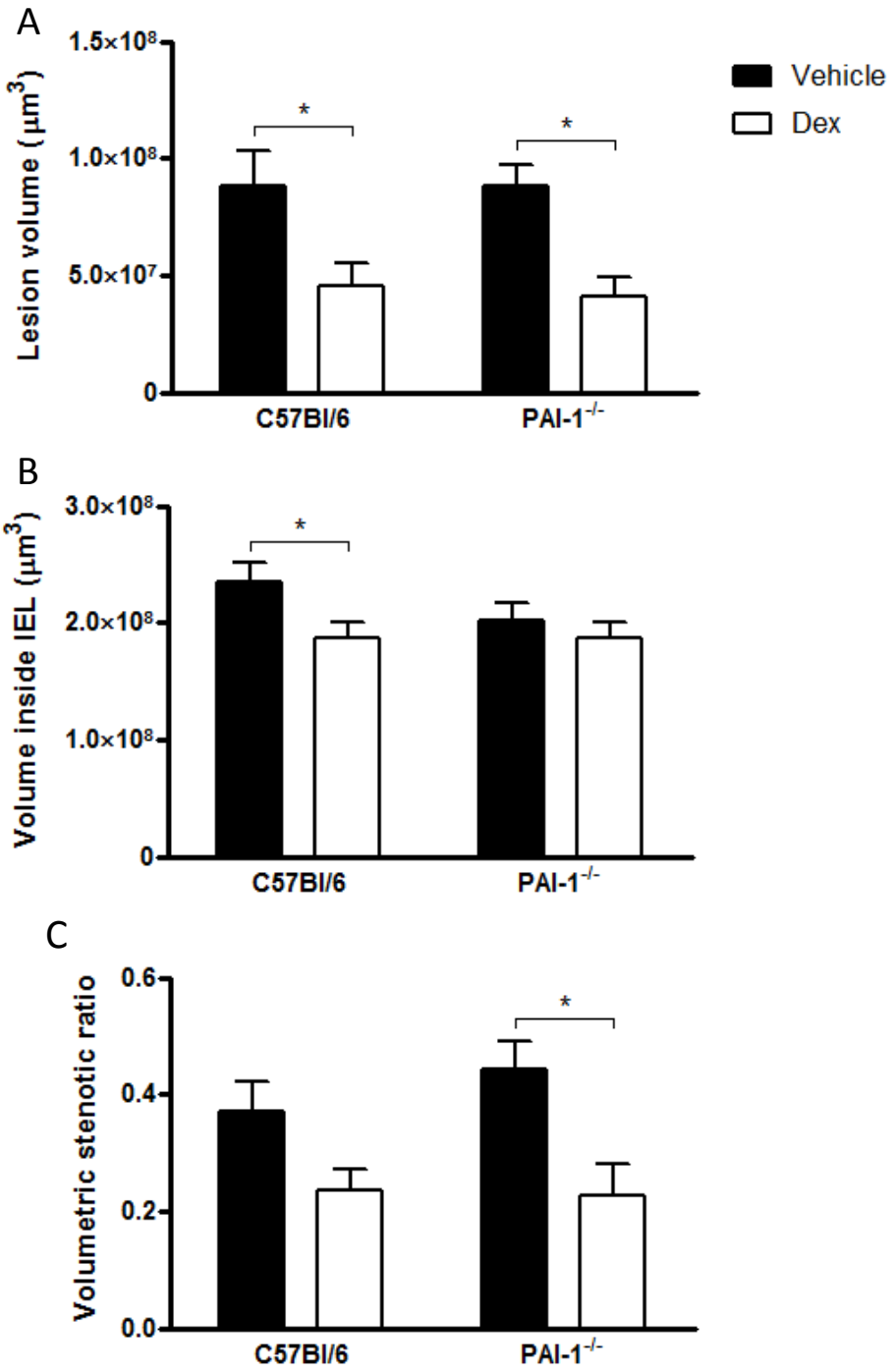

Figure 6.8: Impact of PAI-1 and dexamethasone treatment on neointimal lesion volume, as assessed by optical projection tomography (OPT).
C57Bl/6 and PAI-1$^{-/-}$ mice were randomised to receive either vehicle or dexamethasone (dex; 0.8mg/kg/day) in their drinking water. Neointimal hyperplasia was induced by femoral artery wire-injury, before isolation and OPT scanning. Lesion and lumen volumes were quantified from reconstructed tomograms and expressed as absolute volume (A and B, respectively) and as the volumetric stenotic ratio; plaque volume as proportion of volume inside internal elastic lamina (IEL; C). Dex treatment significantly reduced absolute lesion volume in both genotypes (A). Dex also increased the area inside the IEL in C57Bl/6 mice (B). Therefore, dex treatment reduced the volumetric stenotic ratio only in the PAI-1$^{-/-}$ mice (C). All data expressed as mean±SEM, n=6-8. Data were nalysed by two way ANOVA with Bonferroni post hoc test. *$p<0.05$.

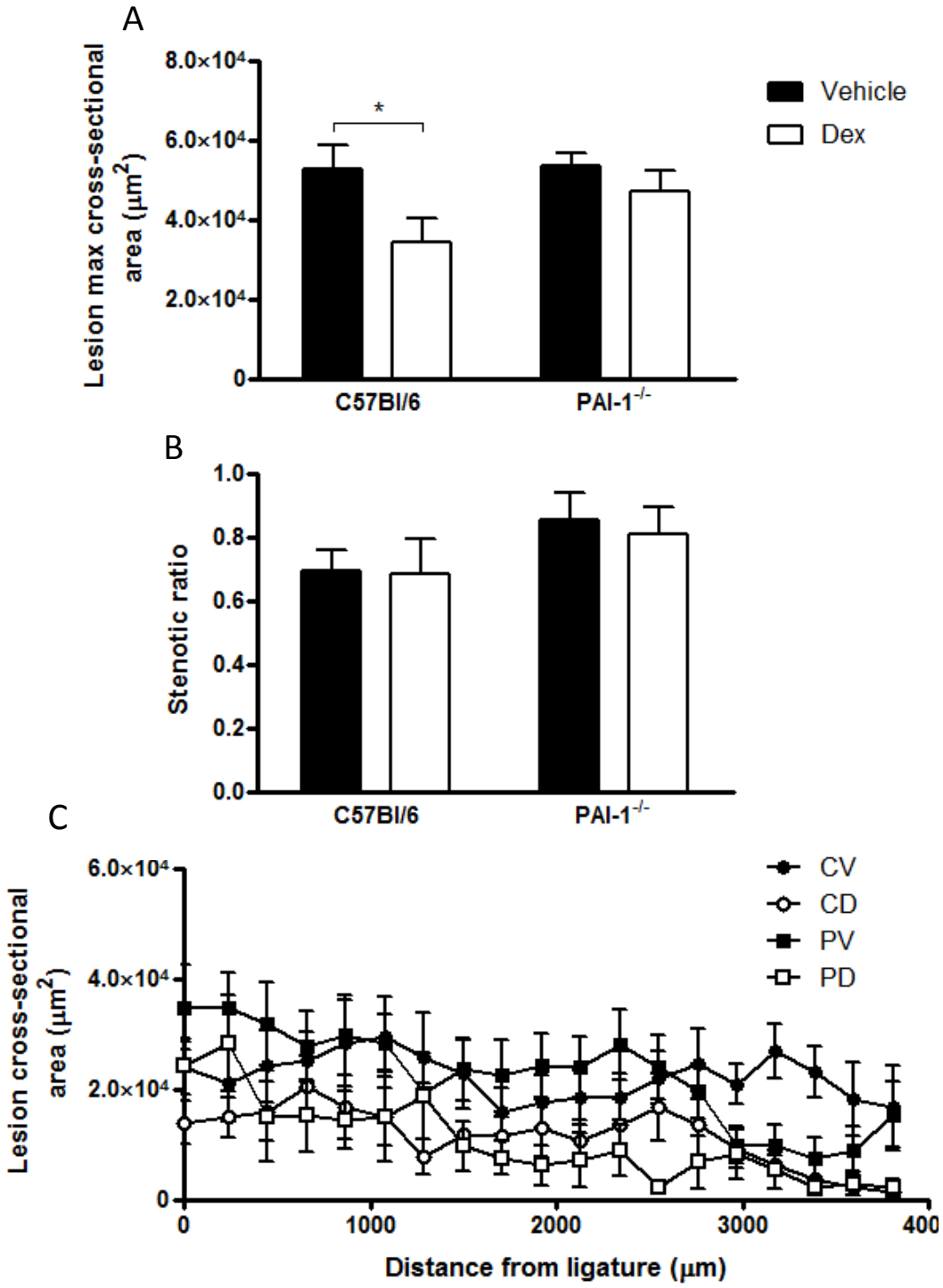

Figure 6.9: **Impact of PAI-1 and dexamethasone treatment on neointimal cross-sectional area, as assessed by optical projection tomography (OPT).**
C57Bl/6 and PAI-1$^{-/-}$ mice were randomised to receive either vehicle or dexamethasone (dex; 0.8mg/kg/day) in their drinking water. Neointimal hyperplasia was induced by femoral artery wire-injury, before isolation and OPT scanning. Lesion and lumen cross-sectional areas were quantified from reconstructed tomograms. Dex treatment reduced the absolute maximum cross-sectional area of the lesion only in the C57Bl/6 mice (A). This effect was lost when lesion size was expressed as stenotic ratio (B). Analysis of the cross-sectional profiles revealed that dex treatment reduced lesion development consistently along the length of the artery, in both genotypes (C). All data are expressed as mean±SEM, n=6-8. A and B were analysed by two way ANOVA with Bonferroni post hoc test. *$p<0.05$. CV: C57Bl/6 on vehicle, CD: C57Bl/6 on dex, PV: PAI-1$^{-/-}$ on vehicle, PD: PAI-1$^{-/-}$ on dex.

Table 6.1: Impact of PAI-1 deletion and dexamethasone treatment on the size and composition of neointimal lesions.

Measurement	C57Bl/6 + Vehicle	C57Bl/6 + Dex	PAI-1$^{-/-}$ + Vehicle	PAI-1$^{-/-}$ + Dex
n	8	7	6	6
(a) 3D Morphometry (OPT)				
Lesion volume (x10^{7}µm^3)	8.9 ± 1.5	**4.5 ± 1.0***	8.8 ± 0.9	**4.1 ± 0.8^o**
Luminal volume (x10^{7}µm^3)	14.7 ± 1.4	14.2 ± 0.8	11.4 ± 1.2	14.6 ± 1.7
Volume inside IEL (x10^{7}µm^3)	23.5 ± 1.7	**18.8 ± 1.3***	20.3 ± 1.4	18.7 ± 1.7
Volumetric stenotic ratio	0.37 ± 0.05	0.24 ± 0.04	0.44 ± 0.05	**0.23 ± 0.05^o**
(b) 2D Morphometry (OPT)				
Lesion area (x10^{4}µm^2)	5.3 ± 0.6	**3.4 ± 0.6***	5.3 ± 0.3	4.7 ± 0.5
Luminal area (x10^{4}µm^2)	2.5 ± 0.7	1.6 ± 0.6	1.2 ± 0.8	1.1 ± 0.5
Area inside IEL (x10^{4}µm^2)	7.8 ± 0.8	**5.1 ± 0.3****	6.5 ± 0.6	5.9 ± 0.3
Stenotic ratio	0.70 ± 0.06	0.68 ± 0.11	0.85 ± 0.08	0.81 ± 0.08
(c) 2D Morphometry (Histology)				
Neointimal area (x10^{4}µm^2)	3.1 ± 0.5	**1.5 ± 0.4***	3.3 ± 0.3	**1.3 ± 0.5^o**
Medial area (x10^{4}µm^2)	1.2 ± 0.2	1.0 ± 0.1	1.5 ± 0.3	0.9 ± 0.2
Intima/Media ratio	2.6 ± 0.7	1.8 ± 0.4	2.8 ± 0.2	3.2 ± 1.5
Luminal area (x10^{4}µm^2)	3.1 ± 0.6	3.4 ± 0.3	1.9 ± 0.7	4.2 ± 1.3
Area inside IEL (x10^{4}µm^2)	6.1 ± 0.3	4.9 ± 0.3	5.2 ± 0.5	5.4 ± 1.1
Stenotic ratio	0.50 ± 0.08	0.30 ± 0.06	0.72 ± 0.09	**0.37 ± 0.13^o**
(d) Composition (IHC)				
Smooth Muscle α-actin (%)	51.9 ± 5.2	**0.7 ± 0.3*****	53.6 ± 7.2	**1.9 ± 1.5^{ooo}**

C57Bl/6 and PAI-1$^{-/-}$ mice were randomised to receive either vehicle or dexamethasone (dex; 0.8mg/kg/day) in their drinking water. Neointimal hyperplasia was induced by femoral artery wire-injury, before isolation and examination of the left femoral artery by optical projection tomography (a and b), histology (c) and immunohistochemistry (d). Dex administration reduced absolute lesion size, as measured by OPT (a) and histology (c), and hugely reduced the smooth muscle cell content of lesions (d). PAI-1 deficiency had very little influence on neointimal lesion development (a, b, c) and composition (d). All data expressed as mean±SEM, n=6-8. Data were analysed by two way ANOVA with Bonferroni post hoc test. *p<0.05, **p<0.01, ***p<0.001 vs C57Bl/6 on Vehicle. ^{o}p<0.05, ^{oo}p<0.01, ^{ooo}p<0.001 vs PAI-1$^{-/-}$ on Vehicle.

6.4.6.2 Neointima quantification by histology

Dex administration reduced maximum cross-sectional area of lesion similarly in both C57Bl/6 and PAI-$1^{-/-}$ mice (both $p<0.05$; Figure 6.10). However, dex treatment only reduced the stenotic ratio in the PAI-$1^{-/-}$ mice ($p<0.05$; Table 6.1(c)). There was an indication that dex treatment also reduced the area inside the IEL in C57Bl/6 mice (ns; Table 6.1(c)), which may explain the loss of effect by dex when expressed as stenotic ratio.

6.4.6.3 Neointima composition

From evaluation of the UST stained sections it was clear that the lesions which developed in the vehicle-treated animals, of both genotypes, were elastin-rich and fibro-proliferative in nature (Figure 4.8a and e). Conversely, the lesions which developed in animals on dex treatment were acellular and elastin-deficient. This was observed both in C57Bl/6 (Figure 4.8c) and in PAI-$1^{-/-}$ (Figure 4.8g) mice. Further quantitative analysis of these sections confirmed that dex treatment vastly reduced the fibrous component of the lesion, in both genotypes (both $p<0.001$; Figure 6.10B).

Smooth muscle α-actin immunostaining verified that vehicle-treated mice developed lesions rich in smooth muscle (Figure 4.8b and f), while dex administration almost completely eliminated smooth muscle content of lesions in both C57Bl/6 and PAI-$1^{-/-}$ mice (Figure 4.8d and h, both $p<0.001$; Figure 6.12).

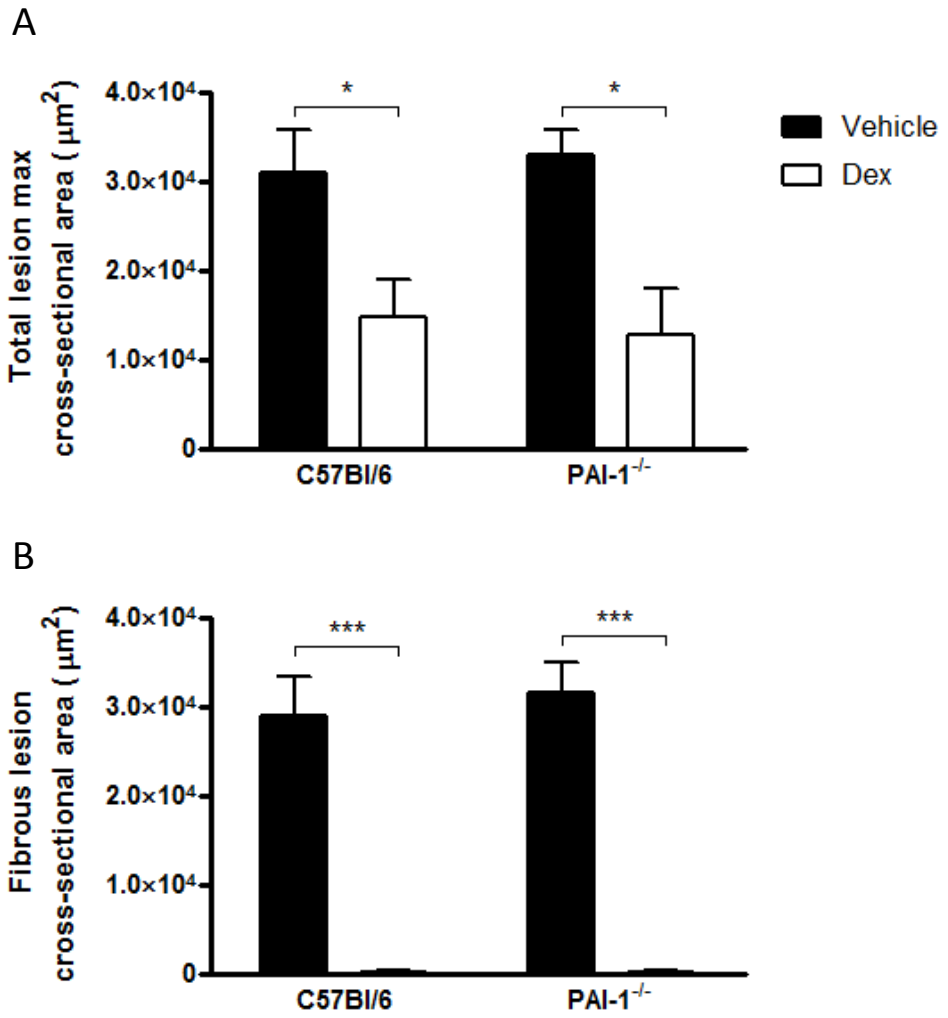

Figure 6.10: **Impact of PAI-1 and dexamethasone treatment on neointimal cross-sectional area, as assessed by histology.**
C57Bl/6 and PAI-1$^{-/-}$ mice were randomised to receive either vehicle or dexamethasone (dex; 0.8mg/kg/day) in their drinking water. Neointimal hyperplasia was induced by femoral artery wire-injury, before isolation and OPT scanning. Lesion and lumen cross-sectional areas were quantified by histological analysis. Dex treatment reduced the total maximum cross-sectional area of the lesion in both C57Bl/6 and PAI-1$^{-/-}$ mice (A). Furthermore, dex treatment appeared to almost completely eliminate any fibrous component of the lesion, in both C57Bl/6 and PAI-1$^{-/-}$ mice (B). All data expressed as mean±SEM, n=6-8. Data were analysed by two way ANOVA with Bonferroni post hoc test. *p<0.05, ***p<0.001.

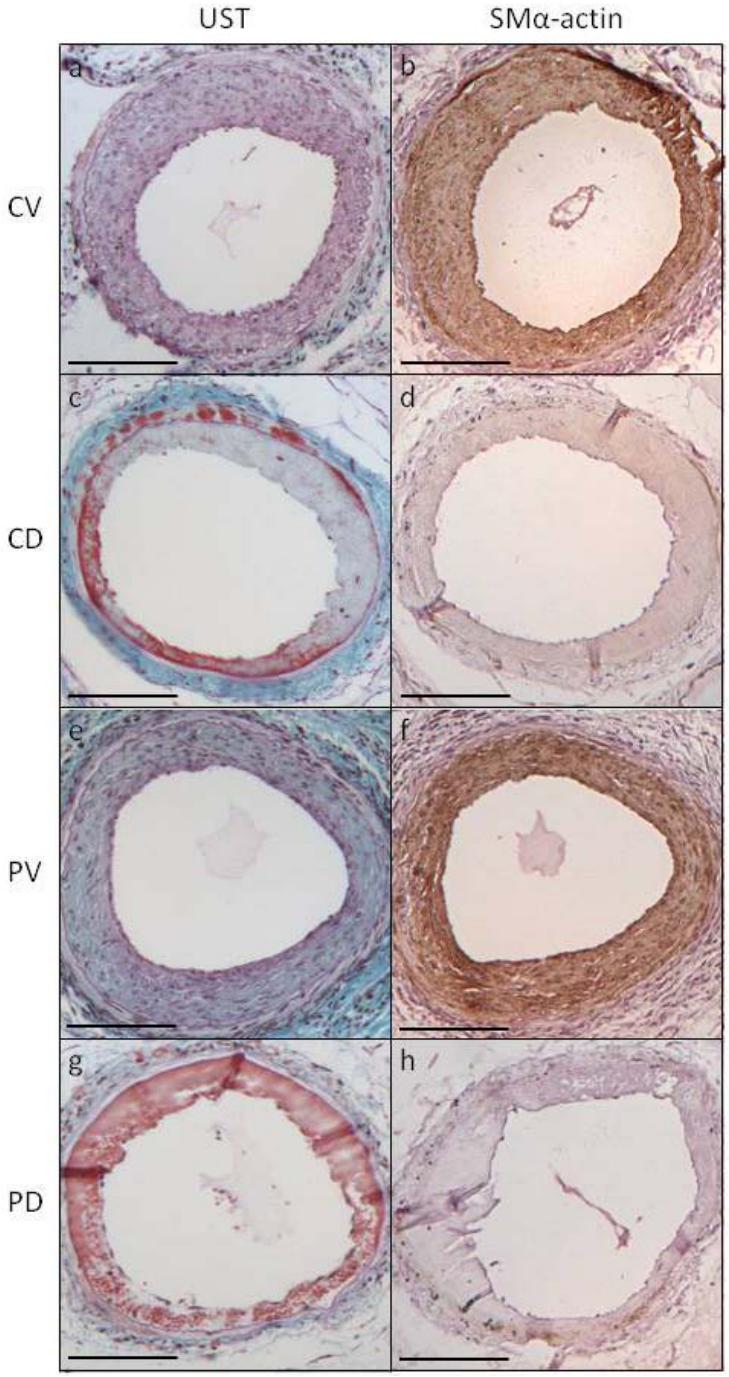

Figure 6.11: Composition of lesions formed after femoral artery wire-injury.
C57Bl/6 and PAI-1$^{-/-}$ mice were randomised to receive either vehicle or dexamethasone (dex; 0.8mg/kg/day) in their drinking water. Neointimal hyperplasia was induced by femoral artery wire-injury, before isolation and OPT scanning. Composition was quantified at the point of largest lesion as determined by histological analysis with United States trichrome (UST) staining. Smooth muscle content was assessed using immunohistochemistry against smooth muscle α-actin (SMα-actin). Vehicle-treated animals, from both genotypes (CV and PV), developed typical lesions (a, e), staining strongly for smooth muscle (b, f). Whereas, dex-treated animals, from both genotypes (CD and PD), developed lesions that were acellular and elastin-deficient as assessed by UST staining (c, g), and did not stain for smooth muscle cells (d, h). Scale bar = 100μm. CV: C57Bl/6 on vehicle, CD: C57Bl/6 on dex, PV: PAI-1$^{-/-}$ on vehicle, PD: PAI-1$^{-/-}$ on dex.

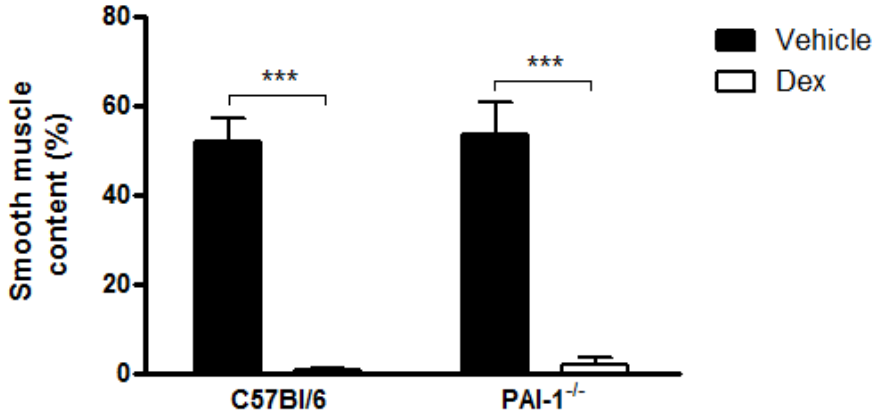

Figure 6.12: **Impact of PAI-1 deletion and dexamethasone treatment on neointimal smooth muscle cell content.**
C57Bl/6 and PAI-1$^{-/-}$ mice were randomised to receive either vehicle or dexamethasone (dex; 0.8mg/kg/day) in their drinking water. Neointimal hyperplasia was induced by femoral artery wire-injury, before isolation and OPT scanning. Lesion cross-sectional areas were quantified by histological analysis. Smooth muscle cell content was quantified at the point of largest lesion using immunohistochemistry. Dex treatment significantly reduced smooth muscle cell content of lesion in both C57Bl/6 and PAI-1 $^{-/-}$ mice. All data expressed as percentage of total area of plaque; mean±SEM, n=6-8. Data were analysed by two way ANOVA with Bonferroni post hoc test. ***p<0.001.

6.5 Discussion

The work described in this chapter addresses the hypothesis that increased PAI-1 activity is responsible for dex-mediated thrombosis following vascular injury. The results obtained suggest that PAI-1 plays a limited role in neointimal proliferation. Dex administration has been confirmed to increase local thrombus formation following vascular injury and increase circulating PAI-1. However, while increased PAI-1 does mediate the systemic pro-thrombotic effect of dex, it is not responsible for dex-mediated thrombotic response to injury.

6.5.1. PAI-1 and neointimal proliferation

6.5.1.1 PAI-$1^{-/-}$ mice

Plasminogen activator inhibitor-1 gene-deficient mice, purchased for use in this experiment, were confirmed to have no detectable PAI-1 antigen in their circulation. The knockout mice appeared to have no developmental abnormalities in comparison to C57Bl/6 control mice, with comparable starting body weights and organ weights. These results are consistent with the characterisation carried out by the group who first generated PAI-$1^{-/-}$ mice by homologous recombination (Carmeliet *et al.*, 1993a). They reported that disruption of the PAI-1 gene did not significantly influence organogenesis or development, with no apparent functional or histological abnormalities. Further, systolic blood pressure measurements taken throughout the experimental period were equivalent with the C57Bl/6 mice, which is consistent with previous reports (Kaikita *et al.*, 2001; Ma *et al.*, 2006).

PAI-1 is the endogenous inhibitor of the fibrinolytic pathway. Therefore, PAI-1 deficiency would be expected to augment fibrinolysis and the subsequent breakdown of thrombi. However, genetic disruption of PAI-1 also did not appear to impair haemostasis in this investigation, as assessed by tail-tip bleeding time, a measure of coagulation and fibrinolysis factor activity, among other things (Lavelle *et al.*, 1998). This result is supported by a previous report that tail-tip bleeding time and re-bleeding does not differ between wild type and PAI-$1^{-/-}$ mice (Carmeliet *et al.*, 1993b). These results suggest that PAI-1, and perhaps the entire fibrinolysis pathway, plays a limited role in haemostasis in healthy individuals. Interestingly,

delayed re-bleeding after trauma or surgery has been reported in patients with absent or reduced PAI-1 levels (Dieval *et al.*, 1991; Fay *et al.*, 1992; Lee *et al.*, 1993). A possible explanation of a milder hyperfibrinolytic state in mice may be the lower basal plasma levels of PAI-$1^{+/+}$ mice (~2ng/mL; consistent with level reported here in C57Bl/6 mice) than in humans (~10ng/mL) (Carmeliet *et al.*, 1993b).

Of interest, PAI-1 deficiency did not influence total tPA antigen concentration in the plasma. This result is supported by reports that two patients with absent or reduced PAI-1 levels have normal circulating tPA protein levels, with increased tPA activity (Fay *et al.*, 1992; Lee *et al.*, 1993). As PAI-1 inhibits tPA's activity at the protein level and not the gene level, changes in total tPA by PAI-1 deficiency would not be expected. Unfortunately, the tPA activity ELISA in the current investigation failed to produce conclusive results. Originally the assay did not work and on repeat the standard errors were such that the results were not reliable. This outcome may be a consequence of repeated freeze-thaw cycles leading to denaturation of the enzyme. Other studies using PAI-$1^{-/-}$ mice have, however, confirmed that tPA activity is increased using zymography analysis (Wang *et al.*, 2005a; Wang *et al.*, 2007b).

In conclusion, the PAI-$1^{-/-}$ mice were viable, healthy and had no detectable circulating PAI-1 protein. In addition, PAI-1 appeared to have no influence on physiological parameters or on haemostasis. Ideally, wild-type (PAI-$1^{+/+}$) littermates would have been used as controls in this investigation. However, due to cost and time constrains, this was not practical. Therefore, as the PAI-$1^{-/-}$ mice were generated on a C57Bl/6 background, C57Bl/6 mice were deemed the most appropriate alternative.

6.5.1.2 Impact of PAI-1 deficiency on neointimal proliferation

Genetic disruption of PAI-1 had no apparent influence on neointimal hyperplasia, as measured by OPT and histology. This conclusion is supported by previous studies which have found PAI-1 to have no effect on neointimal lesion development in a carotid artery ligation model (Kawasaki *et al.*, 2001) and an electrical model (Lijnen *et al.*, 2004) of vascular injury. However, there are a number of groups who have reported evidence that PAI-1 is indeed an important mediator of intimal hyperplasia

in mice, albeit with discordant results. Some report that genetic deletion or pharmacological inhibition of PAI-1 decreases lesion development (Peng *et al.*, 2002; Ploplis *et al.*, 2001; Suzuki *et al.*, 2008; Zhu *et al.*, 2001), while others directly disagree, concluding PAI-$1^{-/-}$ mice have increased lesion development (Carmeliet *et al.*, 1997b; de Waard *et al.*, 2002; Schafer *et al.*, 2006).

The conflicting conclusions on the influence of PAI-1 on lesion development may be explained by evidence that PAI-1 can potentially modulate neointimal proliferation by multiple mechanisms. PAI-1 may promote intimal hyperplasia by stabilising fibrin, which often forms following vascular injury, and which can then be invaded by VSMCs to form a neointima (Fay, 2004). This is supported by reports that hyperfibrinogenemic mice have increased neointimal lesion development (Kerlin et al., 2004) and depletion of circulating fibrinogen with the snake venom ancrod reduces lesion development (Kawasaki et al., 2001), following vascular injury. As well as by inhibiting tPA, PAI-1 may also stabilise fibrin and thrombin by inhibition of APC which would otherwise inhibit FVa and FVIIIa (Fay, 2004). In addition, PAI-1 increases proliferation of VSMCs as well as rendering them more resistant to apoptosis (Chen *et al.*, 2006), which could contribute to an increase in neointimal proliferation.

Conversely, PAI-1 may inhibit intimal hyperplasia by inhibiting urokinase uPA on the surface of VSMCs, and consequently, the formation of cell-associated plasmin, which is thought to be important in VSMC migration through extracellular matrices and across elastic laminae (Fay, 2004). This proposal is supported by reports that uPA deficiency and pharmacological inhibition of uPAR, but not tPA deficiency, inhibit neointimal proliferation in mice (Carmeliet *et al.*, 1997a; Quax *et al.*, 2001; Schafer *et al.*, 2002). Complementary to this, binding of PAI-1 to its cofactor vitronectin (VN), within the extracellular matrix, can competitively inhibit VSMC binding to VN (Czekay *et al.*, 2003; Deng *et al.*, 2001; Deng *et al.*, 1996) and, consequently, the migration of VSMCs through extracellular matrices (Stefansson *et al.*, 1996). Consistent with these results, one study has shown that VN deficiency attenuates neointimal proliferation after carotid artery ligation and chemical injury in

mice (Peng *et al.*, 2002). However, a similar study concluded that both VN deficiency and PAI-1 deficiency augment intimal hyperplasia in a carotid artery ligation model (de Waard *et al.*, 2002). The authors proposed that the inhibition is mediated by the capacity of PAI-1/VN complexes to inhibit thrombin (Naski *et al.*, 1993), a VSMC mitogen.

Clearly, PAI-1 has multiple functions in the vascular wall and on fibrin homeostasis, which makes predicting the outcome, and explaining the result, of manipulation of PAI-1 on neointima development very difficult. It has been proposed that the model of vascular injury, and more specifically the extent of thrombus initially formed, determines the outcome of the action of PAI-1 on the subsequent intimal hyperplasia (Fay, 2004). This may explain some of the different effects of manipulating PAI-1 reported with use of different models of vascular injury (Carmeliet *et al.*, 1997c; Kawasaki *et al.*, 2001; Lijnen *et al.*, 2004; Peng *et al.*, 2002; Ploplis *et al.*, 2001; Zhu *et al.*, 2001). Interestingly, all of these models employ perivascular injury, as opposed to the intra-luminal wire-injury model described in this study.

Perhaps, in the current investigation, the pro-fibrinolytic effects of PAI-1 deficiency were inhibiting neointimal proliferation, while the accelerating effect of PAI-1 deficiency on VSMC migration was augmenting neointimal proliferation, resulting in no net effect on lesion development, as reported, despite PAI-1 actively affecting intimal hyperplasia. Further mechanistic analysis would be required to confirm this proposal. Firstly, the significance of PAI-1's fibrin-stabilising ability could be tested by administration of recombinant α_2-antiplasmin to PAI-$1^{-/-}$ mice to restore the inhibition of plasmin activity, in a model of wire injury. Secondly, in the current investigation, lesions that developed in the PAI-$1^{-/-}$ mice contained an equivalent proportion of smooth muscle cells as the control mice, implying net smooth muscle cell migration and proliferation are unaffected by PAI-1. However, as described above, PAI-1 may have the potential to inhibit migration but increase proliferation of VSMCs. Repeating the current experiment in PAI-1/VN DKO mice elucidate the influence of VN on neointimal proliferation in the absence of the inhibitory role of PAI-1 on VN-mediated VSMC migration. In addition, as uPA has been implicated in

VSMC proliferation, it may be of interest to assay its activity. Despite PAI-1 being the endogenous inhibitor of uPA, there have been some reports that PAI-1 deficiency has no influence on uPA activity (Oda *et al.*, 2001; Wang *et al.*, 2005a) and another which confirms it increases uPA activity (Hertig *et al.*, 2003). Unfortunately, there were insufficient blood samples remaining to carry out this assay here.

In addition, using PAI-$1^{-/-}$ mice only allows insight into the impact of physiological levels of PAI-1 on neointimal proliferation. Basal circulating PAI-1 levels are relatively low, especially in mice (Carmeliet *et al.*, 1993b), and so perhaps removing PAI-1 from circulation is not a significant enough change to influence the complex process of vascular lesion development.

Because PAI-1 interacts with several molecules and cells types, global genetic deletion is perhaps not the most effective method of determining the role of PAI-1 on neointimal proliferation. An alternative approach is to inactivate specific functional domains of PAI-1, rather than the whole gene and corresponding protein (Fay, 2004). PAI-1 mutants lacking anti-proteolytic activity, while maintaining normal VN binding (and vice versa) have been generated (Stefansson *et al.*, 1996). In addition, targeted modulation of PAI-1 expression in specific cell types, for example VSMCs and macrophages, may provide useful clarification, as the source of PAI-1 that modulates neointimal proliferation is not precisely defined (Schafer *et al.*, 2006).

6.5.2. **Dexamethasone and neointimal proliferation**

6.5.2.1 Dexamethasone administration

Dex was administered to the mice at the same dose and by the same method as described and discussed in the previous chapter (section 4.5.2.1). Weight loss and reduction in size of glucocorticoid-sensitive organs again confirms the efficacy of dex in this investigation. Similarly, dex administration significantly increased systolic blood pressure, as we (section 4.5.2.1) and others (Goodwin *et al.*, 2008; Whitworth *et al.*, 2001; Zhang *et al.*, 2004) have previously described. Therefore, confidence can be drawn from the results of this investigation that dex is having a reproducible influence on the mice compared to the previous study.

In addition, it was confirmed that dex does indeed significantly increase total and active PAI-1 protein levels in the plasma of C57Bl/6 mice, with an associated reduction in tail-tip bleeding time. A key finding of this investigation was that tail-tip bleeding time was not influenced by dex administration in PAI-$1^{-/-}$ mice, implicating PAI-1 as the mediator of dex-induced effects on haemostasis. As discussed above (section 6.5.1.1), PAI-1 deficiency alone does not affect tail-tip bleeding time. This suggests that under normal physiological conditions, fibrinolysis plays a limited role in haemostasis. However, the results from this investigation indicate that inhibition of the pathway, by elevated PAI-1, does influence haemostasis. These results strongly support the hypothesis that dex administration is increasing the thrombogenicity of the mice through an increase in PAI-1.

6.5.2.2 Impact of dexamethasone administration on neointimal proliferation

The results from this investigation indicate that dex administration reduces neointimal lesion development following intra-luminal wire injury. This result confirms the many studies which have reported that glucocorticoid treatment reduces neointimal proliferation in animal models of vascular injury (Guzman *et al.*, 1996; Nagasaki *et al.*, 2004; Petrik *et al.*, 1998; Valero *et al.*, 1998; Van Put *et al.*, 1995; Villa *et al.*, 1994) and complements the work described in the previous chapter (section 4.5.2.2). In addition, the use of OPT to allow 3D quantification of lesion size has permitted, for the first time, verification that glucocorticoid administration reduces lesion volume.

The influence of dex appears to be more pronounced in the investigation described here compared with the investigation described in Chapter 4 (section 4.5.2.2). The most obvious difference between these two studies is that the animals in the previous study were adrenalectomised, while in this study the mice had intact adrenal glands. The negligible influence of bilateral adrenalectomy on neointimal proliferation is discussed in the previous chapter (section 4.5.1.2); however, it has not been determined whether removal of the adrenal glands influences dex-mediated effects on neointimal proliferation. A study involving the direct comparison between dex administration in adrenalectomised and intact mice would have to be carried out

before conclusions can be drawn. It is more likely that the more pronounced effect of dex in the current investigation is due to differences in practices between the two studies. Firstly, my surgical and histological skills have no doubt improved with the experiences of this PhD. Secondly, the animals in the current investigation were perfusion fixed, whereas in the previous study, the femoral arteries were dissected prior to fixation. Maintenance of vascular integrity by perfusion fixation is likely to have a significant effect on subsequent histological analysis. Therefore, due to a number of differences between the two studies, direct comparisons of the effect of dex administration on neointimal proliferation must be made with caution.

Glucocorticoids are thought to primarily inhibit neointimal proliferation through their anti-inflammatory properties (Liu *et al.*, 1999; Yamada *et al.*, 1993) and their potential to inhibit smooth muscle cell migration and proliferation (Goncharova *et al.*, 2003; Voisard *et al.*, 1994). The inflammatory status of the lesions was not evaluated in this study as this was not the primary focus. Although, there was an indication from the previous study (Figure 4.11) that this dose of dex reduces the macrophage content of lesions that develop following intra-luminal wire injury. Potential methods for more detailed analysis of the inflammatory status of the mice and specifically their neointimal lesions are described in Chapter 4 (section 4.5.2.2). Conversely, smooth muscle cell content was assessed in the lesions of this study as it is an important indicator of the nature of the lesions. Dex administration almost completely eliminated the smooth muscle cell content of the lesions, a similar, although perhaps more pronounced, result to that found in the previous investigation described in Chapter 4 (Figure 4.9). The anti-migratory (Cronstein *et al.*, 1992; Goncharova *et al.*, 2003; Pross *et al.*, 2002) and anti-proliferative (Bitzer *et al.*, 2004; Voisard *et al.*, 1994) effects of dex on VSMCs are relatively well established and are likely to play a crucial role in dex-mediated effects on neointimal proliferation. In addition, it has been suggested that inflammatory cells differentiate into smooth muscle cells in vascular lesions (Sahara *et al.*, 2007; Tanaka *et al.*, 2003), contributing to neointimal development. Therefore, the anti-inflammatory properties of dex may also directly contribute to reduced smooth muscle cell content of lesions.

The dramatic reduction in smooth muscle cell content, by dex administration, was associated with the development of an acellular lesion, appearing thrombotic in nature. This finding was consistent with the effects of dex reported in the previous investigation (section 4.5.2.2). As discussed in detail in Chapter 4, this thrombotic product may be attributable to a number of well-established glucocorticoid-mediated pathways, including stabilisation of the injury-induce thrombus, inhibition of inflammation-driven clearance of the clot and inhibition of smooth muscle cell recruitment, migration and proliferation. It was decided to focus this investigation on the influence of dex on the potential stabilisation of the thrombotic stage, specifically, the role of PAI-1, considering the dramatic increase in circulating levels of this protein with dex administration.

6.5.3. **Role of PAI-1 in dexamethasone-induced thrombotic response to injury.**

It was proposed that PAI-1 mediates the dex-induced thrombotic response to intra-vascular injury. Therefore, it was hypothesised that PAI-1 deficiency would prevent the thrombotic effect, but maintain the anti-restenotic effect of dex administration, in the wire-injury model of neointimal proliferation. However, PAI-1 deficiency appeared to have no influence on dex-mediated thrombus formation. The lesions that developed in the PAI-$1^{-/-}$ mice on dex treatment were indistinguishable from those that developed in the C57Bl/6 mice on dex treatment; acellular, smooth muscle-deficient and appearing thrombotic in nature.

One possible explanation as to why PAI-1 deficiency did not prevent the thrombotic effect of dex administration, following vascular injury, is that dex may also drive the up-regulation or activation of α_2-antiplasmin, thereby compensating for the lack of PAI-1-mediated inhibition of the fibrinolysis pathway. One study has suggested that dex administration increases plasma α_2-antiplasmin in a rat model of acute pancreatitis (Muller *et al.*, 2008). However, the dex-induced reduction in tail-tip bleeding time was abolished in the PAI-$1^{-/-}$ mice, implying there is no compensatory inhibition of the fibrinolytic pathway. The more likely explanation for the result is simply that PAI-1 is not the principle mediator of the local pro-thrombotic effect of

dex that results following vascular injury. As PAI-1 does appear to mediate the systemic pro-thrombotic effect of dex, the circulatory pathways involved (coagulation, fibrinolysis and platelet activation/aggregation) cannot significantly contribute to dex-induced thrombotic lesion development. This suggests that stabilisation of the thrombotic stage 1 of lesion development is not the principle mechanism by which dex causes thrombotic lesion development as was hypothesised. Rather, it implicates local pathways in the vessel wall as the mediators of the thrombotic side effect of dex administration following vascular injury.

As described in Chapter 4 (section 4.5.2.2) there are a number of cells that are thought to act within the vessel wall during neointimal proliferation that are sensitive to glucocorticoids and may contribute to a delayed healing process and a thrombotic product. One likely candidate is the macrophage. Monocytes/macrophages are likely to play important roles in the progression of the response to vascular injury, including lysis and phagocytosis of the thrombus (Shantsila *et al.*, 2009; Simon *et al.*, 1993) and mediating cellular recruitment (Clinton *et al.*, 1992). The potent anti-inflammatory properties of glucocorticoids can inhibit infiltration (Poon *et al.*, 2001) and proliferation (Asai *et al.*, 1993) of monocyte/macrophages at the site of injury, and reduce further recruitment of circulating monocytes and macrophages into the vessel wall (Prescott *et al.*, 1989; Yamada *et al.*, 1993), through inhibition of MCP-1 secretion (Dhawan *et al.*, 2007; Fasshauer *et al.*, 2004). Another potential glucocorticoid-sensitive candidate is the VSMC. It is well-established that glucocorticoid can directly inhibit VSMC migration (Goncharova *et al.*, 2003; Ribichini *et al.*, 2005) and proliferation (Berk *et al.*, 1988; Voisard *et al.*, 1994), which are both key processes in the pathogenesis of neointimal formation. Furthermore, glucocorticoids can inhibit PDGF release from VSMCs (Nakano *et al.*, 1993), a growth factor which has been implicated in both the induction of migration and the expression of inflammatory chemoattractant molecules by VSMCs following vascular injury (Marmur *et al.*, 1992).

6.5.4. **Summary**

In summary, physiological levels of PAI-1 appear to play a limited role in neointimal lesion development following intra-luminal wire injury. While PAI-1 does appear to mediate the systemic pro-thrombotic effect of dex, PAI-1 is not responsible for dex-mediated local thrombosis following vascular injury. Instead, it is proposed that the thrombotic effect of dex on neointimal proliferation may be mediated by alternative glucocorticoid-regulated pathways in the vessel wall.

Chapter 7

General discussion

CVD is the single biggest cause of death in developed countries. Central to its pathogenesis is the development of atherosclerotic lesions. In addition, the major advancement in CVD treatment with PCI has been limited by the complication of restenosis. It is therefore critical to study the processes involved in vascular lesion development, to allow further advancement in the prevention and treatment of CVD. Both atherogenesis and restenosis are reactions to vascular injury, involving inflammation and cellular proliferation. Glucocorticoid hormones have widely-recognised anti-inflammatory and anti-proliferative properties which appear to make them ideal candidates for inhibition of vascular lesion development. Indeed, administration of glucocorticoids to experimental animals does inhibit the growth of vascular lesions in some models. However, chronic glucocorticoid excess in patients, either as a result of Cushing's syndrome or chronic treatment, is associated with enhanced CVD risk (e.g. central obesity, insulin resistance, dyslipidemia and hypertension). Therefore, the overall effects of glucocorticoids on vascular lesion development remain imperfectly understood. Elucidating these effects will improve our understanding of the role of glucocorticoid activity in regulating atherogenesis and restenosis and the therapeutic potential of glucocorticoids as a treatment for, or as a target in, CVD.

Therefore, the overall objective of these studies was to determine the influence of endogenous and exogenous glucocorticoids on vascular lesion development using murine models of atherosclerosis and neointimal hyperplasia. The work described in this thesis addressed the hypothesis that glucocorticoids are pro-atherogenic, yet anti-restenotic, based on clinical evidence.

7.1 Animal models of vascular lesion development

An important pre-requisite for any such investigation is to select appropriate models of atherosclerosis and neointimal hyperplasia, which will allow quantification of the extent of lesion development and the opportunity to further investigate the mechanisms behind any effect found.

7.1.1. **Atherosclerosis**

Until 1992, the majority of *in vivo* atherosclerosis research used rabbits as their primary animal model. However, a major limitation of the rabbit model is that the lesions that develop tend to be fatty streaks rather than complex advanced lesions that are seen in humans. The use of mice became more popular following the development of the ApoE$^{-/-}$ mouse (Plump *et al.*, 1992; Zhang *et al.*, 1992). These genetically modified mice have diminished hepatic uptake of circulating cholesterol and so are hypercholesterolaemic and consistently develop advanced plaques at vascular branch points. Currently, the most commonly used murine model of atherosclerosis combines the ApoE$^{-/-}$ mouse with high cholesterol, "Western" diet to further accelerate plaque development. An alternative mouse model of atherosclerosis is the LDLR$^{-/-}$ mouse. No fundamental differences in pathogenesis have been reported between the two models, but the LDLR$^{-/-}$ mouse does have a milder phenotype than the ApoE$^{-/-}$ mice (Bentzon *et al.*, 2010a), and requires a high cholesterol diet to promote lesion development, whereas the ApoE$^{-/-}$ mice will develop lesions on a standard chow diet (Zhang *et al.*, 1992).

Although the ApoE$^{-/-}$ mouse is the most commonly used model of atherosclerosis, and has certain advantages over the rabbit model, there are a number of shortcomings of this murine atherosclerosis model (reviewed in (Bentzon *et al.*, 2010a)). The major limitations are the rarity of plaque rupture and thrombosis and the small size of the animals that prohibits interventional cardiology and diagnostic imaging. Several porcine models of advanced coronary atherosclerosis do exist which have the potential to overcome these limitations (Granada *et al.*, 2009). However, for the purpose of this investigation into the influence of glucocorticoids on atherogenesis, the "Western" diet-fed ApoE$^{-/-}$ mice remains the most appropriate model.

7.1.2. **Neointimal proliferation**

There are a number of commonly-used animal models of neointimal proliferation, including balloon angioplasty in rabbits and rats, stent implantation in the pig and dog, and various arterial injury models in the mouse. A mouse model was chosen for this investigation as use of this species allows study of the mechanisms of neointimal

proliferation at a molecular level, through the use of genetically-modified animals. The two most commonly used murine models of neointimal proliferation are intra-luminal wire injury (Lindner *et al.*, 1993; Sata *et al.*, 2000) and carotid artery ligation (Kumar *et al.*, 1997b). Both of these procedures produce large fibro-proliferative neointimal lesions after 2-3 weeks. While the ligation model has a less challenging operational procedure, the advantage of the wire injury model is it resembles the endothelial denudation seen with angioplasty and it maintains continuous blood flow. For this reason, a murine femoral artery wire-injury model, adapted from the method described by Sata *et al* (2000), was optimised in this department (Macdonald, 2007). The procedure involves the insertion of an angioplasty guidewire into the femoral artery via a small muscular side-branch. The wire stretches the vessel, causing endothelial denudation and extensive medial damage and results in the time-dependent development of a smooth muscle-rich neointimal lesion. Characteristics of the model, including thrombus formation, medial cell loss, and the vascular and inflammatory cell types involved in lesion development, were consistent with those described with the original method (Sata *et al.*, 2000). As this method affords reproducible, large neointimal lesions with relatively minimal detriment to the animals, it is now the preferred model of neointimal hyperplasia used in this department. Indeed, all previous and subsequent investigations into the role of glucocorticoids in neointimal proliferation in this department have used this model.

However, it must be acknowledged that using mice to model neointimal proliferation has the disadvantage of their small size, limiting interventional procedures such balloon angioplasty and stent implantation. Ideally, after using mice to elucidate the mechanisms involved in glucocorticoid-mediated effects on intimal hyperplasia, the investigation will be taken into larger animals (such as the porcine or canine coronary artery), which may provide more clinically-relevant models of restenosis.

7.2 Quantifying vascular lesion development

The most common methods for assessing atherosclerotic lesion development in mice are *en face* analysis and histological examination. For neointimal lesion development, only the latter is available due to limited, if any, lipid content of these

lesions. Although these techniques are the gold standard for vascular lesion quantification, they have a major, recognised limitation that they provide only a 2-dimensional (2D) measurement of a 3-dimensional lesion. In this investigation OPT has, for the first time, successfully been utilised to allow reproducible 3-dimensional quantification of atherosclerotic plaque and lumen volumes, as well as corresponding 2-dimensional cross-sectional areas. OPT has also been successfully applied to the visualisation and quantification of neointimal hyperplasia in the femoral artery of mice (induced by both intra-luminal wire injury and ligation injury), in this department (Kirkby *et al.*, 2011). The importance of lesion composition cannot be overlooked and although, at present, OPT cannot provide compositional description of lesions, it is non-destructive and so standard histological and immunohistochemical analysis of the arteries can be carried out to allow a valuable complement to OPT with the generation of further information regarding lesion composition.

Another potential development of the OPT technique in vascular analysis is the use of whole-mount immunofluorescence to allow visualisation and quantification of the distribution of particular cell types or proteins. This has already been successfully demonstrated in embryos and isolated organs (Alanentalo *et al.*, 2007; Sharpe *et al.*, 2002). However, preliminary investigations into staining injured arteries with a fluorescent macrophage marker yielded little success due to poor antibody penetration throughout the tissue and non-specific antibody binding as a result of the necessarily long incubation times. Further investigation will require careful optimisation of incubation and washing times, blocking solution compositions and perhaps trials with alternative primary antibodies.

7.3 Glucocorticoids and atherosclerosis

The influence of glucocorticoids on atherosclerosis is imperfectly understood and unpredictable. Clinically, glucocorticoid excess, whether as a result of chronic glucocorticoid treatment or in patients with Cushing's syndrome, is associated with enhanced cardiovascular disease. However, the majority of animal (rabbit) studies have suggested that systemic glucocorticoid treatment protects against

atherosclerosis. Interestingly, studies using mouse models have described a pro-atherosclerotic effect of glucocorticoids (Hermanowski-Vosatka *et al.*, 2005; Nuotio-Antar *et al.*, 2007; Tous *et al.*, 2006). Therefore, this investigation aimed to confirm whether these steroids are indeed pro-atherosclerotic and elucidate any difference between the influence of endogenous and exogenous glucocorticoids, using ApoE$^{-/-}$ mice on a high cholesterol "Western" diet.

The effects of endogenous and exogenous glucocorticoids on atherosclerosis were in fact quite different. Adrenalectomy had no effect on atherosclerotic plaque development, suggesting that physiological levels of endogenous glucocorticoids play a limited role in the regulation of atherogenesis in the mouse. The most likely explanation for the discrepancy between this result and the majority of the literature is that removal of the adrenal glands is too crude a method for manipulating the complicated and delicate homeostasis of endogenous glucocorticoid action. An important limitation of this study is that adrenalectomy did not completely abolish circulating corticosterone. Although this anomaly is widely-reported, there may have been insufficient corticosterone ablation to modulate atherogenesis. In addition, in order to explain the results, the influence of removing glucocorticoids would have to be isolated from the influence of removing mineralocorticoids and catecholamines. Perhaps a more selective approach to manipulating endogenous glucocorticoids would be more appropriate. Inhibition of 11βHSD1 (Hermanowski-Vosatka *et al.*, 2005; Nuotio-Antar *et al.*, 2007) and genetic deletion of 11βHSD2 (Deuchar *et al.*, 2011) have been shown to attenuate and augment atherosclerotic lesion development in mice, respectively. Alternative approaches could include ACTH administration, to mimic endogenous glucocorticoid excess, or pharmacological inhibition of GR.

In contrast, exogenous glucocorticoid treatment significantly augmented atherosclerotic plaque development. The mechanism behind this effect remains to be elucidated but appears to be independent of circulating lipid levels and macrophage numbers. This study supports the conclusion of Tous *et al*., who described an increase in aortic atherosclerosis in dex-treated ApoE$^{-/-}$ mice on a normal chow diet (Tous *et al.*, 2006), using the "Western" diet-fed ApoE$^{-/-}$ mouse model. In addition,

the results from this investigation support the proposal that the ApoE$^{-/-}$ mouse model is a more clinically-relevant model of atherosclerosis than the cholesterol-fed rabbit. Therefore, it would be of great interest to use this model to expand our understanding of the mechanism behind the pro-atherosclerotic effects of glucocorticoid treatment.

7.4 Glucocorticoids and neointimal proliferation

Previous animal studies have consistently shown that glucocorticoid administration inhibits neointimal proliferation, attributable to the potent anti-inflammatory and anti-proliferative properties of glucocorticoids. However, a previous study in this department observed that the anti-"restenotic" effect of glucocorticoids was associated with the formation of organised acellular lesions of a thrombotic nature, at the site of injury (Macdonald, 2007). Therefore, this investigation aimed to confirm the thrombotic effect of systemic glucocorticoid treatment and elucidate the mechanism behind the result. In addition, the influence of endogenous glucocorticoids was investigated as there do not appear to be any reports detailing the effects of these glucocorticoids on neointimal proliferation.

As with their effects on atherosclerotic lesions, the influences of endogenous and exogenous glucocorticoids were not comparable. Adrenalectomy had no influence on neointimal lesion development. This result supports a previous investigation in this department (Macdonald, 2007), which concluded that both genetic deletion and pharmacological inhibition of 11βHSD1 and pharmacological GR antagonism had no influence on neointimal proliferation in the same wire-injury model. Therefore, confidence can be drawn in the conclusion that physiological levels of endogenous glucocorticoids play a limited role in neointimal proliferation. However, as so little research has been done on this topic, further investigation into the more clinically-relevant issue of endogenous glucocorticoid excess on neointimal proliferation needs to be conducted before endogenous glucocorticoids are neglected as a potential therapeutic target in restenosis. A previous study in this department has concluded that genetic deletion of 11βHSD2 has no influence on neointimal proliferation following intra-luminal wire injury (Iqbal, 2010). An alternative approach could be to administer ACTH to wire-injured mice and assess neointima size.

In contrast to endogenous glucocorticoids, exogenous glucocorticoids had a striking inhibitory effect on neointimal proliferation, supplementing the widely-accepted anti-restenotic reports of glucocorticoid administration. However, this positive effect of glucocorticoids was accompanied by thrombotic lesion development at the site of injury. These results directly mimic the results of the previous study carried out in our department, which administered dex by a potentially more stressful method; daily intra-peritoneal injection (Macdonald, 2007). It is proposed that this thrombotic outcome results from glucocorticoid treatment impeding the progression of neointimal development past the initial thrombotic stage induced by vascular injury. As dex was found to significantly increase PAI-1, it was hypothesised that the glucocorticoid was preventing neointimal development by stabilising the initial thrombus. However, while elevated PAI-1 was found to mediate the systemic pro-thrombotic effect of dex, it was not responsible for the local thrombus formation following vascular injury. There are a number of alternative potential mechanisms, involving glucocorticoid-mediated pathways, which could be contributing to inhibition of lesion progression. For example, glucocorticoids have potent anti-inflammatory and anti-proliferative properties that may prevent key mechanisms involved in the progression of lesion formation beyond the thrombotic stage.

7.5 Endogenous vs exogenous glucocorticoids

Given the demonstrable ability of exogenous glucocorticoids to augment atherosclerosis and inhibit neointimal proliferation, it is surprising that manipulating endogenous glucocorticoids has no effect in these models. It is possible that, while high pharmacological concentrations of glucocorticoids exert potent anti-restenotic effects, changes in physiological levels of glucocorticoids are not sufficient to alter neointimal lesion development. Indeed, adrenalectomy did not influence glucocorticoid-sensitive systemic parameters, including body weight and spleen weight, or local effects, such as smooth muscle and inflammatory content of the lesion. In addition, a lower pharmacological dose of dex, which did influence the aforementioned systemic parameters, also did not influence neointima development.

An additional explanation may be in the type of glucocorticoid investigated. Adrenalectomy examines the influence of corticosterone, whereas the glucocorticoid administered was synthetic dex. The main difference in the action of these steroids is that dex is selective for GR (Cole *et al.*, 2007) whereas corticosterone activates both MR and GR (Kim *et al.*, 1998). The role of MR activation in atherosclerosis and intimal hyperplasia has been addressed previously (section 3.5.2.2 and 4.5.1.2, respectively), with evidence that it likely affects the influence of adrenalectomy on lesion development. For example, genetic deletion of 11βHSD2, thereby allowing activation of MR by glucocorticoids, exacerbates atherosclerosis in $ApoE^{-/-}$ mice (Deuchar *et al.*, 2011). In addition, elevated angiotensin II (due to low circulating aldosterone) may also confound the influence of adrenalectomy on vascular lesion development given the plethora of effects angiotensin II has on the cardiovascular system. Although saline replacement will prevent the pressor-mediated effects, there are a number of direct actions of angiotensin II on the vasculature, including vasoconstriction, VSMC proliferation and ECM production (Strawn *et al.*, 2002).

Consideration must also be given to the diurnal rhythm of endogenous glucocorticoid synthesis and, consequently, plasma levels (Oster *et al.*, 2006), which is not attained with the method of glucocorticoid administration used in this investigation. Therefore, there are important differences between the manipulation of endogenous and exogenous glucocorticoids, which may contribute to the differences described in their influences on vascular lesion development. However, it must be stressed that while removal of approx. 75% of endogenous glucocorticoids appears to have little effect on restenosis, endogenous glucocorticoid excess must also be considered.

7.6 Potential clinical significance of results

7.6.1. Endogenous glucocorticoids

Investigations into the influence of endogenous glucocorticoids on atherosclerosis and neointimal proliferation have important clinical implications for patients with Cushing's disease and the metabolic syndrome. Associated with increased circulating cortisol, these patients have a well-established, but incompletely understood increased risk of CVD and consequently are more likely to require PCI.

The finding that physiological levels of endogenous glucocorticoids appear to play a limited role in atherogenesis and neointimal proliferation questions the future clinical use of 11βHSD1 inhibitors for the prevention of cardiovascular lesion development. It is proposed that increased tissue 11βHSD1 activity, and so intracellular glucocorticoid levels, may contribute to the aetiology of metabolic syndrome and its underlying cardiovascular risk factors (which include central obesity, hypertension, insulin resistance, dyslipidemia and atherosclerosis). Therefore, inhibitors of 11βHSD1 have become an important novel therapeutic target for the treatment of the metabolic syndrome. There have been a number of more direct investigations into the impact of 11βHSD1 inhibition on atherosclerosis and restenosis, which suggest that it may have beneficial effects on atherosclerotic lesion development (Hermanowski-Vosatka *et al.*, 2005; Nuotio-Antar *et al.*, 2007), but a limited influence on restenosis (Macdonald, 2007). Further investigations into the potential clinical application of 11βHSD1 inhibitors are currently being carried out and should take into consideration the findings reported here on the effect of global removal of glucocorticoids on vascular lesion development.

7.6.2. **Exogenous glucocorticoids**

Investigations into the influence of exogenous glucocorticoids on atherosclerotic and neointimal lesion development have important clinical implications for patients on chronic steroid therapy for management of an inflammatory condition. These patients also have a well-established increased risk of CVD. In addition, glucocorticoids are currently being investigated for their anti-restenotic potential, but have been limited by their detrimental systemic effects and disappointing efficacy with local application. Alongside furthering our understanding of the impact of glucocorticoids on restenosis, it is imperative that the influence this treatment may have on the underlying atherosclerotic disease in patients undergoing PCI is understood.

Use of animal models to help understand the glucocorticoid-mediated mechanisms involved in atherosclerotic has been limited, so far, by their failure to mimic the pro-atherosclerotic effect of glucocorticoids seen in the clinic. However, the results from this study provide evidence that the Western diet-fed $ApoE^{-/-}$ mouse does mimic the potentiating influence of glucocorticoid on atherosclerosis. Use of this model has

also suggested that glucocorticoid-mediated augmentation of atherosclerosis is independent of circulating lipid levels and the macrophage content of the plaque. More detailed investigations are required to confirm these findings, but this model of atherosclerosis provides the opportunity to do so.

The finding that systemic pharmacological doses of glucocorticoid attenuate neointimal proliferation but induce thrombotic lesion development is important considering that: firstly, patients on chronic glucocorticoid treatment for inflammatory conditions an have increased risk of CVD and are more likely to require PCI; and secondly, glucocorticoids are currently being trialled clinically as anti-restenotic agents (Ribichini *et al.*, 2009). However, changes in composition such as this are unlikely to be visible by angiographic analysis of restenotic lesions, as used in the clinical trials. Instead, compositional analysis of restenotic lesions is limited to arterectomy or post-mortem samples. It would be of great benefit to confirm whether systemic steroid treatment has a similar thrombotic effect following PCI in humans. However, continued investigation using animal models of neointimal proliferation may provide crucial insight into the mechanism behind the thrombotic effect of exogenous glucocorticoids on neointimal proliferation, which later may be applied in the clinic. The results from this study have already allowed PAI-1 to be discounted as the primary mediator of this pro-thrombotic effect.

7.7 Future studies

The work described in this thesis has described the influence of exogenous glucocorticoids on atherosclerosis and neointimal proliferation. However, the mechanisms driving the contradictory effects on the different types of vascular lesion development remain to be clarified. In addition, the influence of endogenous glucocorticoids on atherosclerosis and neointimal proliferation was not fully elucidated. Therefore, there are several prospective studies that could extend the work described here.

7.7.1. Influence of endogenous glucocorticoid excess on vascular lesion development

Adrenalectomy allowed a broad insight into the role of endogenous glucocorticoids on atherosclerosis and neointimal proliferation. However, removal of the adrenal glands appeared to be too blunt a method for manipulating the complicated and delicate homeostasis of endogenous glucocorticoid action. Additionally, adrenalectomy does not completely remove circulating corticosterone. Perhaps a more appropriate, and clinically-relevant, method would be to investigate the influence of endogenous glucocorticoid excess, mimicking Cushing's syndrome, on vascular lesion development. There are a number of approaches which could be used to carry out such an investigation, the simplest of which would be administration of ACTH (Bailey *et al.*, 2009; Dunbar *et al.*, 2010) to Western diet-fed ApoE$^{-/-}$ mice or wire-injured C57Bl/6 mice. High levels of ACTH would stimulate excess corticosterone release from the adrenal glands. An alternative method would be to use GR over-expressing mice (Nguyen Dinh Cat *et al.*, 2009). However, potential compensational depression of the HPA axis would have to be considered. Taking the clinical observation of increased CVD risk in Cushing's patients into account, it is hypothesised that the aforementioned approaches would augment atherosclerosis and neointimal proliferation. If so, these "Cushing's" models would be an important platform to investigate the pro-atherosclerotic mechanisms of endogenous glucocorticoids excess and to trial potential agents against glucocorticoid-exacerbated vascular lesion development.

7.7.2. Mechanism of pro-atherosclerotic effects of glucocorticoids

The results from this investigation mimic the clinical observation that exogenous glucocorticoids exacerbate atherosclerosis, which was not observed in rabbit models (Asai *et al.*, 1993; Makheja *et al.*, 1989; Naito *et al.*, 1992). Therefore the Western diet-fed ApoE$^{-/-}$ provides model to investigate the mechanisms driving the pro-atherosclerotic effect of exogenous glucocorticoids. There are a number of glucocorticoid-mediated processes that are involved in atherogenesis which require exploration. Importantly, the local effects of glucocorticoids must be distinguished from the systemic influences. Previous *in vitro* studies suggest that the anti-

inflammatory and anti-proliferative effects glucocorticoids have locally on the vessel wall would in fact reduce atherosclerotic lesion development. This could be confirmed by the use of dex or cortisol pellets, implanted alongside the femoral artery branch point, an easily accessible predisposed area to lesion development. Morphometric analysis of the resulting lesions would allow a general conclusion of the role of local glucocorticoid-mediated effects on atherogenesis, while IHC and laser microdissection (Taatjes *et al.*, 2008) would allow influences at the cellular and genetic level, respectively, to be elucidated. The systemic glucocorticoid-sensitive parameters could be further investigated by again administering dex in the animals' drinking water. Detailed blood pressure measurements could be acquired with the use of implanted telemetry devices and a full lipid profile could be determined by fast protein liquid chromatography (FPLC). In addition, it would be important to identify any metabolic disturbances; insulin resistance could be monitored with a glucose-tolerance test, unfavourable fat distribution could be assessed with dual energy X-ray absorptiometry (DEXA) scanning (Leung *et al.*, 2008) and histological analysis of the liver would identify any liver steatosis. Elucidation of the influence of exogenous glucocorticoids on these parameters will likely indicate the primary mechanisms behind the pro-atherosclerotic effect of glucocorticoid excess, and further advance the quest to find a treatment for CVD.

7.7.3. Mechanism of glucocorticoid-induced thrombotic lesion development following intra-luminal injury

As described above (section 7.6.2), it is important that the mechanisms driving glucocorticoid-induced thrombotic lesion development are elucidated. It is proposed that administration of glucocorticoids impedes the progression of arterial healing past the initial thrombotic stage, instigated by denudation of the vessel. It has been shown that this effect is not mediated by stabilisation of the thrombus by elevated PAI-1. Alternatively, the inhibitory properties of glucocorticoids on macrophage function and smooth muscle cell migration and proliferation, may be responsible for preventing progression to a fibro-proliferative neointimal lesion. There are a number of methods by which the role of macrophages in glucocorticoid-mediated thrombotic lesion development could be further elucidated, by again using dex-treated,

wire-injured mice. Firstly, the adhesion of monocytes to the injured vessel wall at very early time points (immediately and 2 days following injury) could be investigated by assessing the expression of adhesion molecules using IHC or quantitative PCR. Complementary to that, macrophage accumulation and activation status could be assessed at the peak of macrophage infiltration (7 days following injury) with the use of IHC and flow cytometry. In addition, the impact of glucocorticoids on the release of inflammatory cytokines and chemokines could be assessed by measuring the level of these factors in an *in vitro* model of arterial injury.

The first step in determining the role of smooth muscle cells in glucocorticoid-mediated thrombotic lesion development is to verify the source of the intimal smooth muscle cells that accumulate during neointimal proliferation. There is evidence that these cells are derived from circulating bone-marrow-derived progenitors (Sahara *et al.*, 2007; Sata *et al.*, 2002; Tanaka *et al.*, 2003). This suggestion can be confirmed by carrying out wire-injury surgery in mice whose bone marrow has been replaced with that of ROSA26 mice, which express β-galactosidase (LacZ) ubiquitously (Zambrowicz *et al.*, 1997). Immunofluorescence double staining for LacZ and smooth muscle α-actin will reveal both whether any bone-marrow-derived cells are assuming a smooth muscle cell-like expression pattern, and the localisation of these cells. Administration of dex to this model would allow elucidation of the impact of glucocorticoids on the accumulation of these cells. Secondly, the influence of dex on the proliferation of smooth muscle cells could be assessed by injection of the thymidine analogue BrdU prior to sacrifice in vehicle-treated and dex-treated wire-injured mice. This would provide a nuclear marker for proliferating cells in subsequent histological analysis of the lesions. Ideally these would be assessed at 14 days post-injury, as most cellular proliferation occurs before this time-point (Macdonald, 2007). Determination of the role of macrophages and smooth muscle cells in dex-mediated thrombotic lesion development following arterial injury will provide invaluable information for optimising the use of glucocorticoids in interventional cardiology.

7.7.4. *In vivo imaging of vascular lesions*

While OPT has provided an important advancement in the *ex vivo* analysis of vascular lesions, representative *in vivo* quantification of lesion progression and of cellular and molecular changes is the ultimate goal. There are already a number of potential non-invasive imaging techniques which have been used for such quantification. Ultrasound biomicroscopy has previously been applied to assess plaque morphologies and flow velocities in the carotid artery of mice (Gan et al., 2007; Ni et al., 2008). Use of this technique could provide valuable information on the influence of glucocorticoids on neointimal and atherosclerotic lesion development, complementary to data derived from OPT and histology. In addition, use of this imaging modality can be further supplemented with use of microbubbles as tracers of specific cells types. For example, fluorescein-labelled lipid microbubbles, once phagocytosed, can be used to track monocytes/macrophages during atherogenesis (Lindner et al., 2000). Similarly, microbubbles targeted for p-selectin, may allow *in vivo* visualisation of the development of the thrombotic lesions induced by dex administration following intra-vascular injury.

MRI has also previously been utilised for non-invasive imaging of atherosclerotic plaque progression in mice (reviewed in (Weinreb et al., 2007)). In addition to plaque morphology, MRI has been described to allow determination of murine plaque composition, differentiating between lipid and fibrous material (Trogan *et al.*, 2004). This imaging technique could clearly be used to complement the findings of the investigations described in this thesis, with the added benefit of allowing lesion progression to be monitored with serial MRI scanning. Similar to ultrasound, contrast-enhanced MRI is permissible: superparamagnetic iron oxides can be used to track monocytes/macrophages, while other magnetofluorescent nanoparticles can be utilised to visualise specific proteins, for example VCAM-1 (Kelly *et al.*, 2005).

Employment of either/both of these imaging techniques would provide a valuable opportunity to improve both our understanding of the development of vascular lesions and the impact of endogenous and exogenous glucocorticoids on them.

7.8 Conclusions

In conclusion, these studies have provided valuable insights into the complex influence of glucocorticoids on vascular lesion development, facilitated by the novel use of optical projection tomography. Not only do glucocorticoids influence atherogenesis and neointimal proliferation differently, but crucially, endogenous and exogenous glucocorticoids appear to have distinct impacts on vascular lesion development. Physiological levels of endogenous glucocorticoids appear to play a limited role in atherogenesis and neointimal proliferation; however further exploration into the impact of endogenous glucocorticoid excess may be worthwhile, perhaps using a more clinically-relevant approach. Conversely, exogenous glucocorticoids augmented the development of atherosclerosis in $ApoE^{-/-}$ mice, mimicking the clinical influence of glucocorticoids on atherosclerosis. This model, therefore, provides an important tool for distinguishing the influence of the local and systemic mechanisms that may be responsible for the pro-atherosclerotic effect of glucocorticoid treatment. In contrast, exogenous glucocorticoids were found to induce thrombotic lesion development, negating their beneficial inhibition of fibro-proliferative lesion development. The primary mechanism behind this pro-thrombotic effect of glucocorticoid treatment is yet to be elucidated, but is known to not be mediated by reduced fibrinolysis. Further research is therefore required to improve the cardiovascular outcome of patients requiring glucocorticoids therapy and for the use of glucocorticoids as anti-restenotic agents.

References

Ahmad, SS, London, FS, Walsh, PN (2003) The assembly of the factor X-activating complex on activated human platelets. *J. Thromb. Haemost.* **1**(1)**:** 48-59.

Alanentalo, T, Asayesh, A, Morrison, H, Loren, CE, Holmberg, D, Sharpe, J, Ahlgren, U (2007) Tomographic molecular imaging and 3D quantification within adult mouse organs. *Nat Methods* **4**(1)**:** 31-33.

Alberts, P, Engblom, L, Edling, N, Forsgren, M, Klingstrom, G, Larsson, C, Ronquist-Nii, Y, Ohman, B, Abrahmsen, L (2002) Selective inhibition of 11beta-hydroxysteroid dehydrogenase type 1 decreases blood glucose concentrations in hyperglycaemic mice. *Diabetologia* **45**(11)**:** 1528-1532.

Alevizaki, M, Cimponeriu, A, Lekakis, J, Papamichael, C, Chrousos, GP (2007) High anticipatory stress plasma cortisol levels and sensitivity to glucocorticoids predict severity of coronary artery disease in subjects undergoing coronary angiography. *Metabolism.* **56**(2)**:** 222-226.

Amano, T, Matsubara, T, Izawa, H, Torigoe, M, Yoshida, T, Hamaguchi, Y, Ishii, H, Miura, M, Hayashi, Y, Ogawa, Y, Murohara, T (2006) Impact of plasma aldosterone levels for prediction of in-stent restenosis. *Am J Cardiol* **97**(6)**:** 785-788.

Ambrosi, B, Sartorio, A, Pizzocaro, A, Passini, E, Bottasso, B, Federici, A (2000) Evaluation of haemostatic and fibrinolytic markers in patients with Cushing's syndrome and in patients with adrenal incidentaloma. *Exp Clin Endocrinol Diabetes* **108**(4)**:** 294-298.

Amento, EP, Ehsani, N, Palmer, H, Libby, P (1991) Cytokines and growth factors positively and negatively regulate interstitial collagen gene expression in human vascular smooth muscle cells. *Arterioscler Thromb* **11**(5)**:** 1223-1230.

Anagnostis, P, Athyros, VG, Tziomalos, K, Karagiannis, A, Mikhailidis, DP (2009) Clinical review: The pathogenetic role of cortisol in the metabolic syndrome: a hypothesis. *J. Clin. Endocrinol. Metab.* **94**(8)**:** 2692-2701.

Anitua, E, Andia, I, Ardanza, B, Nurden, P, Nurden, AT (2004) Autologous platelets as a source of proteins for healing and tissue regeneration. *Thromb. Haemost.* **91**(1)**:** 4-15.

Antoni, FA (1993) Vasopressinergic control of pituitary adrenocorticotropin secretion comes of age. *Front. Neuroendocrinol.* **14**(2)**:** 76-122.

Aqel, NM, Ball, RY, Waldmann, H, Mitchinson, MJ (1985) Identification of macrophages and smooth muscle cells in human atherosclerosis using monoclonal antibodies. *J. Pathol.* **146**(3)**:** 197-204.

Aranoff, G, Rosler, A (1980) Urinary tetrahydrocortisone and tetrahydrocortisol glucosiduronates in normal newborns, children and adults. *Acta Endocrinol. (Copenh.)* **94**(3)**:** 371-375.

Asai, K, Funaki, C, Hayashi, T, Yamada, K, Naito, M, Kuzuya, M, Yoshida, F, Yoshimine, N, Kuzuya, F (1993) Dexamethasone-induced suppression of aortic atherosclerosis in cholesterol-fed rabbits. Possible mechanisms. *Arterioscler Thromb* **13**(6)**:** 892-899.

Axel, DI, Kunert, W, Goggelmann, C, Oberhoff, M, Herdeg, C, Kuttner, A, Wild, DH, Brehm, BR, Riessen, R, Koveker, G, Karsch, KR (1997) Paclitaxel inhibits arterial smooth muscle cell proliferation and migration in vitro and in vivo using local drug delivery. *Circulation* **96**(2)**:** 636-645.

Ayaori, M, Sawada, S, Yonemura, A, Iwamoto, N, Ogura, M, Tanaka, N, Nakaya, K, Kusuhara, M, Nakamura, H, Ohsuzu, F (2006) Glucocorticoid receptor regulates ATP-binding cassette transporter-A1 expression and apolipoprotein-mediated cholesterol efflux from macrophages. *Arterioscler. Thromb. Vasc. Biol.* **26**(1)**:** 163-168.

Backes, A, Seay, U, Sedding, DG, Tillmanns, HH, Braun-Dullaeus, RC (2010) Inhibition of matrix deposition: a new strategy for prevention of restenosis after balloon angioplasty. *J. Cardiovasc. Pharmacol.* **55**(2)**:** 213-218.

Bailey, JM, Butler, J (1973) Anti-inflammatory drugs in experimental atherosclerosis. I. Relative potencies for inhibiting plaque formation. *Atherosclerosis* **17**(3)**:** 515-522.

Bailey, MA, Mullins, JJ, Kenyon, CJ (2009) Mineralocorticoid and glucocorticoid receptors stimulate epithelial sodium channel activity in a mouse model of Cushing syndrome. *Hypertension* **54**(4)**:** 890-896.

Bar-Shavit, R, Kahn, AJ, Mann, KG, Wilner, GD (1986) Identification of a thrombin sequence with growth factor activity on macrophages. *Proc. Natl. Acad. Sci. U. S. A.* **83**(4)**:** 976-980.

Barnes, PJ (1998) Anti-inflammatory actions of glucocorticoids: molecular mechanisms. *Clin. Sci.* **94**(6)**:** 557-572.

Baugh, RJ, Broze, GJ, Jr., Krishnaswamy, S (1998) Regulation of extrinsic pathway factor Xa formation by tissue factor pathway inhibitor. *J. Biol. Chem.* **273**(8)**:** 4378-4386.

Becker, BF, Heindl, B, Kupatt, C, Zahler, S (2000) Endothelial function and hemostasis. *Z Kardiol* **89**(3)**:** 160-167.

Becker, DM, Chamberlain, B, Swank, R, Hegewald, MG, Girardet, R, Baughman, KL, Kwiterovich, PO, Pearson, TA, Ettinger, WH, Renlund, D (1988) Relationship between corticosteroid exposure and plasma lipid levels in heart transplant recipients. *Am. J. Med.* **85**(5)**:** 632-638.

Bellingham, DL, Sar, M, Cidlowski, JA (1992) Ligand-dependent down-regulation of stably transfected human glucocorticoid receptors is associated with the loss of functional glucocorticoid responsiveness. *Mol. Endocrinol.* **6**(12)**:** 2090-2102.

Bennett, MR, Macdonald, K, Chan, SW, Boyle, JJ, Weissberg, PL (1998) Cooperative interactions between RB and p53 regulate cell proliferation, cell senescence, and apoptosis in human vascular smooth muscle cells from atherosclerotic plaques. *Circ. Res.* **82**(6)**:** 704-712.

Bentzon, JF, Falk, E (2010a) Atherosclerotic lesions in mouse and man: is it the same disease? *Curr. Opin. Lipidol.* **21**(5)**:** 434-440.

Bentzon, JF, Falk, E (2010b) Circulating smooth muscle progenitor cells in atherosclerosis and plaque rupture: current perspective and methods of analysis. *Vascul Pharmacol* **52**(1-2)**:** 11-20.

Berardelli, R, Karamouzis, I, Marinazzo, E, Prats, E, Picu, A, Giordano, R, Ghigo, E, Arvat, E (2010) Effect of acute and prolonged mineralocorticoid receptor blockade on spontaneous and stimulated hypothalamic-pituitary-adrenal axis in humans. *Eur. J. Endocrinol.* **162**(6)**:** 1067-1074.

Berk, BC, Vallega, G, Griendling, KK, Gordon, JB, Cragoe, EJ, Jr., Canessa, M, Alexander, RW (1988) Effects of glucocorticoids on Na+/H+ exchange and growth in cultured vascular smooth muscle cells. *J. Cell. Physiol.* **137**(3)**:** 391-401.

Berk, BC, Vekshtein, V, Gordon, HM, Tsuda, T (1989) Angiotensin II-stimulated protein synthesis in cultured vascular smooth muscle cells. *Hypertension* **13**(4)**:** 305-314.

Bernberg, E, Andersson, IJ, Gan, LM, Naylor, AS, Johansson, ME, Bergstrom, G (2008) Effects of social isolation and environmental enrichment on atherosclerosis in ApoE-/- mice. *Stress* **11**(5)**:** 381-389.

Best, R, Nelson, SM, Walker, BR (1997) Dexamethasone and 11-dehydrodexamethasone as tools to investigate the isozymes of 11 beta-hydroxysteroid dehydrogenase in vitro and in vivo. *J. Endocrinol.* **153**(1)**:** 41-48.

Bhargava, B, Karthikeyan, G, Abizaid, AS, Mehran, R (2003) New approaches to preventing restenosis. *BMJ* **327**(7409)**:** 274-279.

Biemond, BJ, Levi, M, Ten Cate, H, Van der Poll, T, Buller, HR, Hack, CE, Ten Cate, JW (1995) Plasminogen activator and plasminogen activator inhibitor I release during experimental endotoxaemia in chimpanzees: effect of interventions in the cytokine and coagulation cascades. *Clin. Sci.* **88**(5)**:** 587-594.

Birch, CA (1965) The fine structure of the early atherosclerotic lesion. *Nutr. Rev.* **23:** 155-157.

Birukov, KG, Shirinsky, VP, Stepanova, OV, Tkachuk, VA, Hahn, AW, Resink, TJ, Smirnov, VN (1995) Stretch affects phenotype and proliferation of vascular smooth muscle cells. *Mol. Cell. Biochem.* **144**(2)**:** 131-139.

Bitzer, M, Wiskirchen, J, Schober, W, Schart, N, Kehlbach, R, Khorchidi, S, Claussen, CD, Duda, SH (2004) [Possibilities of the prophylaxis of arterial restenoses with dexamethasone -- an in-vitro study of human aortic smooth muscle cells]. *Rofo* **176**(10)**:** 1485-1492.

Black, PH, Garbutt, LD (2002) Stress, inflammation and cardiovascular disease. *J Psychosom Res* **52**(1)**:** 1-23.

Blasi, F, Carmeliet, P (2002) uPAR: a versatile signalling orchestrator. *Nat. Rev. Mol. Cell Biol.* **3**(12)**:** 932-943.

Blyth, DI, Pedrick, MS, Savage, TJ, Bright, H, Beesley, JE, Sanjar, S (1998) Induction, duration, and resolution of airway goblet cell hyperplasia in a murine model of atopic

asthma: effect of concurrent infection with respiratory syncytial virus and response to dexamethasone. *Am. J. Respir. Cell Mol. Biol.* **19**(1)**:** 38-54.

Bobik, A (2006) Transforming growth factor-betas and vascular disorders. *Arterioscler. Thromb. Vasc. Biol.* **26**(8)**:** 1712-1720.

Bohr, DF, Somlyo, AP, Sparks, HV (eds) (1980) *Handbook of Physiology. Section 2: The Cardiovascular System*.

Bornfeldt, KE, Arnqvist, HJ, Capron, L (1992) In vivo proliferation of rat vascular smooth muscle in relation to diabetes mellitus insulin-like growth factor I and insulin. *Diabetologia* **35**(2)**:** 104-108.

Boscaro, M, Sonino, N, Scarda, A, Barzon, L, Fallo, F, Sartori, MT, Patrassi, GM, Girolami, A (2002) Anticoagulant prophylaxis markedly reduces thromboembolic complications in Cushing's syndrome. *J. Clin. Endocrinol. Metab.* **87**(8)**:** 3662-3666.

Boyle, JJ, Bowyer, DE, Weissberg, PL, Bennett, MR (2001) Human blood-derived macrophages induce apoptosis in human plaque-derived vascular smooth muscle cells by Fas-ligand/Fas interactions. *Arterioscler. Thromb. Vasc. Biol.* **21**(9)**:** 1402-1407.

Brack, A, Rittner, HL, Younge, BR, Kaltschmidt, C, Weyand, CM, Goronzy, JJ (1997) Glucocorticoid-mediated repression of cytokine gene transcription in human arteritis-SCID chimeras. *J. Clin. Invest.* **99**(12)**:** 2842-2850.

Brasier, AR, Li, J (1996) Mechanisms for inducible control of angiotensinogen gene transcription. *Hypertension* **27**(3 Pt 2)**:** 465-475.

Braun, OO, Slotta, JE, Menger, MD, Erlinge, D, Thorlacius, H (2008) Primary and secondary capture of platelets onto inflamed femoral artery endothelium is dependent on P-selectin and PSGL-1. *Eur. J. Pharmacol.* **592**(1-3)**:** 128-132.

Brem, AS, Bina, RB, King, TC, Morris, DJ (1998) Localization of 2 11beta-OH steroid dehydrogenase isoforms in aortic endothelial cells. *Hypertension* **31**(1 Pt 2)**:** 459-462.

Brisson, C, Azorsa, DO, Jennings, LK, Moog, S, Cazenave, JP, Lanza, F (1997) Co-localization of CD9 and GPIIb-IIIa (alpha IIb beta 3 integrin) on activated platelet pseudopods and alpha-granule membranes. *Histochem. J.* **29**(2)**:** 153-165.

Brotman, DJ, Girod, JP, Garcia, MJ, Patel, JV, Gupta, M, Posch, A, Saunders, S, Lip, GY, Worley, S, Reddy, S (2005) Effects of short-term glucocorticoids on cardiovascular biomarkers. *J. Clin. Endocrinol. Metab.* **90**(6)**:** 3202-3208.

Brotman, DJ, Girod, JP, Posch, A, Jani, JT, Patel, JV, Gupta, M, Lip, GY, Reddy, S, Kickler, TS (2006) Effects of short-term glucocorticoids on hemostatic factors in healthy volunteers. *Thromb. Res.* **118**(2)**:** 247-252.

Brown, RW, Diaz, R, Robson, AC, Kotelevtsev, YV, Mullins, JJ, Kaufman, MH, Seckl, JR (1996) The ontogeny of 11 beta-hydroxysteroid dehydrogenase type 2 and mineralocorticoid receptor gene expression reveal intricate control of glucocorticoid action in development. *Endocrinology* **137**(2)**:** 794-797.

Buchwald, AB, Hammerschmidt, S, Stevens, J, Goring, J, Nebendahl, K, Unterberg, C (1996) Inhibition of neointimal proliferation after coronary angioplasty by low-molecular-weight heparin (clivarine) and polyethyleneglycol-hirudin. *J. Cardiovasc. Pharmacol.* **28**(4)**:** 481-487.

Bujalska, IJ, Kumar, S, Hewison, M, Stewart, PM (1999) Differentiation of adipose stromal cells: the roles of glucocorticoids and 11beta-hydroxysteroid dehydrogenase. *Endocrinology* **140**(7)**:** 3188-3196.

Burke, AP, Farb, A, Kolodgie, FD, Narula, J, Virmani, R (2002) Atherosclerotic plaque morphology and coronary thrombi. *J. Nucl. Cardiol.* **9**(1)**:** 95-103.

Burke, SE, Lubbers, NL, Chen, YW, Hsieh, GC, Mollison, KW, Luly, JR, Wegner, CD (1999) Neointimal formation after balloon-induced vascular injury in Yucatan minipigs is reduced by oral rapamycin. *J. Cardiovasc. Pharmacol.* **33**(6)**:** 829-835.

Burleigh, MC, Briggs, AD, Lendon, CL, Davies, MJ, Born, GV, Richardson, PD (1992) Collagen types I and III, collagen content, GAGs and mechanical strength of human atherosclerotic plaque caps: span-wise variations. *Atherosclerosis* **96**(1)**:** 71-81.

Busse, R, Edwards, G, Feletou, M, Fleming, I, Vanhoutte, PM, Weston, AH (2002) EDHF: bringing the concepts together. *Trends Pharmacol Sci* **23**(8)**:** 374-380.

Carlsson, J, von Wagenheim, B, Linder, R, Anwari, TM, Qvist, J, Petersson, I, Magounakis, T, Lagerqvist, B (2007) Is late stent thrombosis in drug-eluting stents a real clinical issue? A single-center experience and review of the literature. *Clin Res Cardiol* **96**(2)**:** 86-93.

Carmeliet, P (2003) Angiogenesis in health and disease. *Nat. Med.* **9**(6)**:** 653-660.

Carmeliet, P, Kieckens, L, Schoonjans, L, Ream, B, van Nuffelen, A, Prendergast, G, Cole, M, Bronson, R, Collen, D, Mulligan, RC (1993a) Plasminogen activator inhibitor-1 gene-deficient mice. I. Generation by homologous recombination and characterization. *J. Clin. Invest.* **92**(6)**:** 2746-2755.

Carmeliet, P, Mackman, N, Moons, L, Luther, T, Gressens, P, Van Vlaenderen, I, Demunck, H, Kasper, M, Breier, G, Evrard, P, Muller, M, Risau, W, Edgington, T, Collen, D (1996) Role of tissue factor in embryonic blood vessel development. *Nature* **383**(6595)**:** 73-75.

Carmeliet, P, Moons, L, Herbert, JM, Crawley, J, Lupu, F, Lijnen, R, Collen, D (1997a) Urokinase but not tissue plasminogen activator mediates arterial neointima formation in mice. *Circ. Res.* **81**(5)**:** 829-839.

Carmeliet, P, Moons, L, Lijnen, R, Janssens, S, Lupu, F, Collen, D, Gerard, RD (1997b) Inhibitory role of plasminogen activator inhibitor-1 in arterial wound healing and neointima formation: a gene targeting and gene transfer study in mice. *Circulation* **96**(9)**:** 3180-3191.

Carmeliet, P, Moons, L, Stassen, JM, De Mol, M, Bouche, A, van den Oord, JJ, Kockx, M, Collen, D (1997c) Vascular wound healing and neointima formation induced by perivascular electric injury in mice. *Am. J. Pathol.* **150**(2)**:** 761-776.

Carmeliet, P, Stassen, JM, Schoonjans, L, Ream, B, van den Oord, JJ, De Mol, M, Mulligan, RC, Collen, D (1993b) Plasminogen activator inhibitor-1 gene-deficient mice. II. Effects on hemostasis, thrombosis, and thrombolysis. *J. Clin. Invest.* **92**(6)**:** 2756-2760.

Carver, A, Rafelt, S, Gershlick, AH, Fairbrother, KL, Hughes, S, Wilcox, R (2009) Longer-term follow-up of patients recruited to the REACT (Rescue Angioplasty Versus Conservative Treatment or Repeat Thrombolysis) trial. *J. Am. Coll. Cardiol.* **54**(2)**:** 118-126.

Castonguay, TW (1991) Glucocorticoids as modulators in the control of feeding. *Brain Res. Bull.* **27**(3-4)**:** 423-428.

Cervenka, L, Vaneckova, I, Maly, J, Horacek, V, El-Dahr, SS (2003) Genetic inactivation of the B2 receptor in mice worsens two-kidney, one-clip hypertension: role of NO and the AT2 receptor. *J Hypertens* **21**(8)**:** 1531-1538.

Cesarman-Maus, G, Hajjar, KA (2005) Molecular mechanisms of fibrinolysis. *Br. J. Haematol.* **129**(3)**:** 307-321.

Chamberlain, J, Evans, D, King, A, Dewberry, R, Dower, S, Crossman, D, Francis, S (2006) Interleukin-1beta and signaling of interleukin-1 in vascular wall and circulating cells modulates the extent of neointima formation in mice. *Am. J. Pathol.* **168**(4)**:** 1396-1403.

Chamley-Campbell, J, Campbell, GR, Ross, R (1979) The smooth muscle cell in culture. *Physiol Rev* **59**(1)**:** 1-61.

Chandrasekar, B, Tanguay, JF (2000) Platelets and restenosis. *J. Am. Coll. Cardiol.* **35**(3)**:** 555-562.

Chavez, M, Seeley, RJ, Green, PK, Wilkinson, CW, Schwartz, MW, Woods, SC (1997) Adrenalectomy increases sensitivity to central insulin. *Physiol. Behav.* **62**(3)**:** 631-634.

Chen, G, Suzuki, H, Weston, AH (1988) Acetylcholine releases endothelium-derived hyperpolarizing factor and EDRF from rat blood vessels. *Br J Pharmacol* **95**(4)**:** 1165-1174.

Chen, Y, Budd, RC, Kelm, RJ, Jr., Sobel, BE, Schneider, DJ (2006) Augmentation of proliferation of vascular smooth muscle cells by plasminogen activator inhibitor type 1. *Arterioscler. Thromb. Vasc. Biol.* **26**(8)**:** 1777-1783.

Chen, YW, Smith, ML, Sheets, M, Ballaron, S, Trevillyan, JM, Burke, SE, Rosenberg, T, Henry, C, Wagner, R, Bauch, J, Marsh, K, Fey, TA, Hsieh, G, Gauvin, D, Mollison, KW, Carter, GW, Djuric, SW (2007) Zotarolimus, a novel sirolimus analogue with potent anti-proliferative activity on coronary smooth muscle cells and reduced potential for systemic immunosuppression. *J. Cardiovasc. Pharmacol.* **49**(4)**:** 228-235.

Cheng, W, Kvilekval, KV, Abumrad, NA (1995) Dexamethasone enhances accumulation of cholesteryl esters by human macrophages. *Am J Physiol* **269**(4 Pt 1)**:** E642-648.

Cho, A, Reidy, MA (2002) Matrix metalloproteinase-9 is necessary for the regulation of smooth muscle cell replication and migration after arterial injury. *Circ. Res.* **91**(9)**:** 845-851.

Chono, S, Morimoto, K (2006) Uptake of dexamethasone incorporated into liposomes by macrophages and foam cells and its inhibitory effect on cellular cholesterol ester accumulation. *J. Pharm. Pharmacol.* **58**(9)**:** 1219-1225.

Choritz, L, Grub, J, Wegner, M, Pfeiffer, N, Thieme, H (2010) Paclitaxel inhibits growth, migration and collagen production of human Tenon's fibroblasts--potential use in drug-eluting glaucoma drainage devices. *Graefes Arch. Clin. Exp. Ophthalmol.* **248**(2)**:** 197-206.

Cilingiroglu, M, Oh, JH, Sugunan, B, Kemp, NJ, Kim, J, Lee, S, Zaatari, HN, Escobedo, D, Thomsen, S, Milner, TE, Feldman, MD (2006) Detection of vulnerable plaque in a murine model of atherosclerosis with optical coherence tomography. *Catheter Cardiovasc Interv* **67**(6)**:** 915-923.

Claahsen-van der Grinten, HL, Hermus, AR, Otten, BJ (2009) Testicular adrenal rest tumours in congenital adrenal hyperplasia. *Int J Pediatr Endocrinol* **2009:** 624823.

Cleasby, ME, Livingstone, DE, Nyirenda, MJ, Seckl, JR, Walker, BR (2003) Is programming of glucocorticoid receptor expression by prenatal dexamethasone in the rat secondary to metabolic derangement in adulthood? *Eur. J. Endocrinol.* **148**(1)**:** 129-138.

Clinton, SK, Libby, P (1992) Cytokines and growth factors in atherogenesis. *Arch Pathol Lab Med* **116**(12)**:** 1292-1300.

Clopath, P (1980) The effect of acetylsalicylic acid (ASA) on the development of atherosclerotic lesions in miniature swine. *Br J Exp Pathol* **61**(4)**:** 440-443.

Clowes, AW, Clowes, MM, Fingerle, J, Reidy, MA (1989) Kinetics of cellular proliferation after arterial injury. V. Role of acute distension in the induction of smooth muscle proliferation. *Lab. Invest.* **60**(3)**:** 360-364.

Clowes, AW, Clowes, MM, Reidy, MA (1986) Kinetics of cellular proliferation after arterial injury. III. Endothelial and smooth muscle growth in chronically denuded vessels. *Lab. Invest.* **54**(3)**:** 295-303.

Clowes, AW, Reidy, MA, Clowes, MM (1983) Mechanisms of stenosis after arterial injury. *Lab. Invest.* **49**(2)**:** 208-215.

Clozel, JP, Muller, RK, Roux, S, Fischli, W, Baumgartner, HR (1993) Influence of the status of the renin-angiotensin system on the effect of cilazapril on neointima formation after vascular injury in rats. *Circulation* **88**(3)**:** 1222-1227.

Coghlan, MJ, Jacobson, PB, Lane, B, Nakane, M, Lin, CW, Elmore, SW, Kym, PR, Luly, JR, Carter, GW, Turner, R, Tyree, CM, Hu, J, Elgort, M, Rosen, J, Miner, JN (2003) A novel antiinflammatory maintains glucocorticoid efficacy with reduced side effects. *Mol. Endocrinol.* **17**(5)**:** 860-869.

Colao, A, Pivonello, R, Spiezia, S, Faggiano, A, Ferone, D, Filippella, M, Marzullo, P, Cerbone, G, Siciliani, M, Lombardi, G (1999) Persistence of increased cardiovascular risk in patients with Cushing's disease after five years of successful cure. *J. Clin. Endocrinol. Metab.* **84**(8)**:** 2664-2672.

Cole, CW, Hagen, PO, Lucas, JF, Mikat, EM, O'Malley, MK, Radic, ZS, Makhoul, RG, McCann, RL (1987) Association of polymorphonuclear leukocytes with sites of aortic catheter-induced injury in rabbits. *Atherosclerosis* **67**(2-3)**:** 229-236.

Cole, MA, Kim, PJ, Kalman, BA, Spencer, RL (2000) Dexamethasone suppression of corticosteroid secretion: evaluation of the site of action by receptor measures and functional studies. *Psychoneuroendocrinology* **25**(2)**:** 151-167.

Cole, TG, Wilcox, HG, Heimberg, M (1982) Effects of adrenalectomy and dexamethasone on hepatic lipid metabolism. *J Lipid Res* **23**(1)**:** 81-91.

Cole, TJ (2006) Glucocorticoid action and the development of selective glucocorticoid receptor ligands. *Biotechnol Annu Rev* **12:** 269-300.

Cole, TJ, Blendy, JA, Monaghan, AP, Schmid, W, Aguzzi, A, Schutz, G (1995) Molecular genetic analysis of glucocorticoid signaling during mouse development. *Steroids* **60**(1)**:** 93-96.

Cole, TJ, Mollard, R (2007) Selective glucocorticoid receptor ligands. *Med. Chem.* **3**(5)**:** 494-506.

Colles, SM, Maxson, JM, Carlson, SG, Chisolm, GM (2001) Oxidized LDL-induced injury and apoptosis in atherosclerosis. Potential roles for oxysterols. *Trends Cardiovasc Med* **11**(3-4)**:** 131-138.

Collins, RG, Velji, R, Guevara, NV, Hicks, MJ, Chan, L, Beaudet, AL (2000) P-Selectin or intercellular adhesion molecule (ICAM)-1 deficiency substantially protects against atherosclerosis in apolipoprotein E-deficient mice. *J. Exp. Med.* **191**(1)**:** 189-194.

Colotta, F, Re, F, Muzio, M, Bertini, R, Polentarutti, N, Sironi, M, Giri, JG, Dower, SK, Sims, JE, Mantovani, A (1993) Interleukin-1 type II receptor: a decoy target for IL-1 that is regulated by IL-4. *Science* **261**(5120)**:** 472-475.

Cornelissen, I, Palmer, D, David, T, Wilsbacher, L, Concengco, C, Conley, P, Pandey, A, Coughlin, SR (2010) Roles and interactions among protease-activated receptors and P2ry12 in hemostasis and thrombosis. *Proc Natl Acad Sci U S A* **107**(43)**:** 18605-18610.

Cronstein, BN, Kimmel, SC, Levin, RI, Martiniuk, F, Weissmann, G (1992) A mechanism for the antiinflammatory effects of corticosteroids: the glucocorticoid receptor regulates leukocyte adhesion to endothelial cells and expression of endothelial-leukocyte adhesion molecule 1 and intercellular adhesion molecule 1. *Proc Natl Acad Sci U S A* **89**(21)**:** 9991-9995.

Crum, R, Szabo, S, Folkman, J (1985) A new class of steroids inhibits angiogenesis in the presence of heparin or a heparin fragment. *Science* **230**(4732)**:** 1375-1378.

Curtis, JJ, Galla, JH, Woodford, SY, Lucas, BA, Luke, RG (1982) Effect of alternate-day prednisone on plasma lipids in renal transplant recipients. *Kidney Int.* **22**(1)**:** 42-47.

Czekay, RP, Aertgeerts, K, Curriden, SA, Loskutoff, DJ (2003) Plasminogen activator inhibitor-1 detaches cells from extracellular matrices by inactivating integrins. *J Cell Biol* **160**(5)**:** 781-791.

D'Elia, R, Else, KJ (2009) In vitro antigen presenting cell-derived IL-10 and IL-6 correlate with Trichuris muris isolate-specific survival. *Parasite Immunol* **31**(3)**:** 123-131.

Dal Bo Zanon, R, Fornasiero, L, Boscaro, M, Ruffato, G, Luzzato, G, Fabris, F, Girolami, A (1983) Clotting changes in Cushing's syndrome: elevated factor VIII activity. *Folia Haematol. Int. Mag. Klin. Morphol. Blutforsch.* **110**(2)**:** 268-277.

Dangas, GD, Claessen, BE, Caixeta, A, Sanidas, EA, Mintz, GS, Mehran, R (2010) In-stent restenosis in the drug-eluting stent era. *J. Am. Coll. Cardiol.* **56**(23)**:** 1897-1907.

Dave-Sharma, S, Wilson, RC, Harbison, MD, Newfield, R, Azar, MR, Krozowski, ZS, Funder, JW, Shackleton, CH, Bradlow, HL, Wei, JQ, Hertecant, J, Moran, A, Neiberger, RE, Balfe, JW, Fattah, A, Daneman, D, Akkurt, HI, De Santis, C, New, MI (1998) Examination of genotype and phenotype relationships in 14 patients with apparent mineralocorticoid excess. *J. Clin. Endocrinol. Metab.* **83**(7)**:** 2244-2254.

Davies, MJ, Richardson, PD, Woolf, N, Katz, DR, Mann, J (1993) Risk of thrombosis in human atherosclerotic plaques: role of extracellular lipid, macrophage, and smooth muscle cell content. *Br Heart J* **69**(5)**:** 377-381.

Davies, MJ, Thomas, A (1984) Thrombosis and acute coronary-artery lesions in sudden cardiac ischemic death. *N. Engl. J. Med.* **310**(18)**:** 1137-1140.

Davis, JM, 3rd, Maradit Kremers, H, Crowson, CS, Nicola, PJ, Ballman, KV, Therneau, TM, Roger, VL, Gabriel, SE (2007) Glucocorticoids and cardiovascular events in rheumatoid arthritis: a population-based cohort study. *Arthritis Rheum.* **56**(3)**:** 820-830.

de Jong, IE, Oitzl, MS, de Kloet, ER (2007) Adrenalectomy prevents behavioural sensitisation of mice to cocaine in a genotype-dependent manner. *Behav Brain Res* **177**(2)**:** 329-339.

de Kloet, ER (1991) Brain corticosteroid receptor balance and homeostatic control. *Front. Neuroendocrinol.* **12:** 95–164.

de Kloet, ER, Reul, JM, Sutanto, W (1990) Corticosteroids and the brain. *J. Steroid Biochem. Mol. Biol.* **37**(3)**:** 387-394.

de Kloet, ER, Vreugdenhil, E, Oitzl, MS, Joels, M (1998) Brain corticosteroid receptor balance in health and disease. *Endocr. Rev.* **19**(3)**:** 269-301.

de Kruif, MD, Lemaire, LC, Giebelen, IA, van Zoelen, MA, Pater, JM, van den Pangaart, PS, Groot, AP, de Vos, AF, Elliott, PJ, Meijers, JC, Levi, M, van der Poll, T (2007) Prednisolone dose-dependently influences inflammation and coagulation during human endotoxemia. *J. Immunol.* **178**(3)**:** 1845-1851.

De Servi, S, Mazzone, A, Ricevuti, G, Fioravanti, A, Bramucci, E, Angoli, L, Stefano, G, Specchia, G (1990) Granulocyte activation after coronary angioplasty in humans. *Circulation* **82**(1)**:** 140-146.

de Waard, V, Arkenbout, EK, Carmeliet, P, Lindner, V, Pannekoek, H (2002) Plasminogen activator inhibitor 1 and vitronectin protect against stenosis in a murine carotid artery ligation model. *Arterioscler. Thromb. Vasc. Biol.* **22**(12)**:** 1978-1983.

del Rincon, I, O'Leary, DH, Haas, RW, Escalante, A (2004) Effect of glucocorticoids on the arteries in rheumatoid arthritis. *Arthritis Rheum.* **50**(12)**:** 3813-3822.

Delaunay, F, Khan, A, Cintra, A, Davani, B, Ling, ZC, Andersson, A, Ostenson, CG, Gustafsson, J, Efendic, S, Okret, S (1997) Pancreatic beta cells are important targets for the diabetogenic effects of glucocorticoids. *J. Clin. Invest.* **100**(8)**:** 2094-2098.

Dempfle, CE (2007) The TAFI system. The new role of fibrinolysis. *Hamostaseologie* **27**(4)**:** 278-281.

Deng, G, Curriden, SA, Hu, G, Czekay, RP, Loskutoff, DJ (2001) Plasminogen activator inhibitor-1 regulates cell adhesion by binding to the somatomedin B domain of vitronectin. *J Cell Physiol* **189**(1)**:** 23-33.

Deng, G, Curriden, SA, Wang, S, Rosenberg, S, Loskutoff, DJ (1996) Is plasminogen activator inhibitor-1 the molecular switch that governs urokinase receptor-mediated cell adhesion and release? *J Cell Biol* **134**(6)**:** 1563-1571.

Deuchar, GA, McLean, D, Hadoke, PW, Brownstein, DG, Webb, DJ, Mullins, JJ, Chapman, K, Seckl, JR, Kotelevtsev, YV (2011) 11beta-hydroxysteroid dehydrogenase type 2 deficiency accelerates atherogenesis and causes proinflammatory changes in the endothelium in apoe-/- mice. *Endocrinology* **152**(1)**:** 236-246.

Dhawan, L, Liu, B, Blaxall, BC, Taubman, MB (2007) A novel role for the glucocorticoid receptor in the regulation of monocyte chemoattractant protein-1 mRNA stability. *J Biol Chem* **282**(14)**:** 10146-10152.

Di Rosa, M, Radomski, M, Carnuccio, R, Moncada, S (1990) Glucocorticoids inhibit the induction of nitric oxide synthase in macrophages. *Biochem. Biophys. Res. Commun.* **172**(3)**:** 1246-1252.

Diederich, S, Eigendorff, E, Burkhardt, P, Quinkler, M, Bumke-Vogt, C, Rochel, M, Seidelmann, D, Esperling, P, Oelkers, W, Bahr, V (2002) 11beta-hydroxysteroid dehydrogenase types 1 and 2: an important pharmacokinetic determinant for the activity of synthetic mineralo- and glucocorticoids. *J. Clin. Endocrinol. Metab.* **87**(12)**:** 5695-5701.

Dieval, J, Nguyen, G, Gross, S, Delobel, J, Kruithof, EK (1991) A lifelong bleeding disorder associated with a deficiency of plasminogen activator inhibitor type 1. *Blood* **77**(3)**:** 528-532.

Dong, ZM, Chapman, SM, Brown, AA, Frenette, PS, Hynes, RO, Wagner, DD (1998) The combined role of P- and E-selectins in atherosclerosis. *J. Clin. Invest.* **102**(1)**:** 145-152.

Douglas, JS, Jr., Holmes, DR, Jr., Kereiakes, DJ, Grines, CL, Block, E, Ghazzal, ZM, Morris, DC, Liberman, H, Parker, K, Jurkovitz, C, Murrah, N, Foster, J, Hyde, P, Mancini, GB, Weintraub, WS (2005) Coronary stent restenosis in patients treated with cilostazol. *Circulation* **112**(18)**:** 2826-2832.

Dover, AR, Hadoke, PW, Walker, BR, Newby, DE (2007) Acute effects of glucocorticoids on endothelial fibrinolytic and vasodilator function in humans. *J. Cardiovasc. Pharmacol.* **50**(3)**:** 321-326.

Dubuc, PU, Wilden, NJ (1986) Adrenalectomy reduces but does not reverse obesity in ob/ob mice. *Int J Obes* **10**(2)**:** 91-98.

Dunbar, DR, Khaled, H, Evans, LC, Al-Dujaili, EA, Mullins, LJ, Mullins, JJ, Kenyon, CJ, Bailey, MA (2010) Transcriptional and physiological responses to chronic ACTH treatment by the mouse kidney. *Physiol Genomics* **40**(3)**:** 158-166.

Dzau, VJ, Braun-Dullaeus, RC, Sedding, DG (2002) Vascular proliferation and atherosclerosis: new perspectives and therapeutic strategies. *Nat. Med.* **8**(11)**:** 1249-1256.

Edwards, CR, Benediktsson, R, Lindsay, RS, Seckl, JR (1993) Dysfunction of placental glucocorticoid barrier: link between fetal environment and adult hypertension? *Lancet* **341**(8841)**:** 355-357.

Egashira, K, Nakano, K, Ohtani, K, Funakoshi, K, Zhao, G, Ihara, Y, Koga, J, Kimura, S, Tominaga, R, Sunagawa, K (2007) Local delivery of anti-monocyte chemoattractant protein-1 by gene-eluting stents attenuates in-stent stenosis in rabbits and monkeys. *Arterioscler. Thromb. Vasc. Biol.* **27**(12)**:** 2563-2568.

Elokdah, H, Abou-Gharbia, M, Hennan, JK, McFarlane, G, Mugford, CP, Krishnamurthy, G, Crandall, DL (2004) Tiplaxtinin, a novel, orally efficacious inhibitor of plasminogen activator inhibitor-1: design, synthesis, and preclinical characterization. *J Med Chem* **47**(14)**:** 3491-3494.

Enkhbaatar, P, Okajima, K, Murakami, K, Uchiba, M, Okabe, H, Okabe, K, Yamaguchi, Y (2000) Recombinant tissue factor pathway inhibitor reduces lipopolysaccharide-induced pulmonary vascular injury by inhibiting leukocyte activation. *Am. J. Respir. Crit. Care Med.* **162**(5)**:** 1752-1759.

Epel, ES, McEwen, B, Seeman, T, Matthews, K, Castellazzo, G, Brownell, KD, Bell, J, Ickovics, JR (2000) Stress and body shape: stress-induced cortisol secretion is consistently greater among women with central fat. *Psychosom. Med.* **62**(5)**:** 623-632.

Erami, C, Zhang, H, Ho, JG, French, DM, Faber, JE (2002) Alpha(1)-adrenoceptor stimulation directly induces growth of vascular wall in vivo. *Am. J. Physiol. Heart Circ. Physiol.* **283**(4)**:** H1577-1587.

Esmon, CT (2004) The impact of the inflammatory response on coagulation. *Thromb. Res.* **114**(5-6)**:** 321-327.

Esmon, CT (2003) Inflammation and thrombosis. *J. Thromb. Haemost.* **1**(7)**:** 1343-1348.

Esmon, CT (2000) Introduction: are natural anticoagulants candidates for modulating the inflammatory response to endotoxin? *Blood* **95**(4)**:** 1113-1116.

Etxabe, J, Vazquez, JA (1994) Morbidity and mortality in Cushing's disease: an epidemiological approach. *Clinical endocrinology* **40**(4)**:** 479-484.

Faggiano, A, Pivonello, R, Spiezia, S, De Martino, MC, Filippella, M, Di Somma, C, Lombardi, G, Colao, A (2003) Cardiovascular risk factors and common carotid artery caliber and stiffness in patients with Cushing's disease during active disease and 1 year after disease remission. *J. Clin. Endocrinol. Metab.* **88**(6)**:** 2527-2533.

Falati, S, Liu, Q, Gross, P, Merrill-Skoloff, G, Chou, J, Vandendries, E, Celi, A, Croce, K, Furie, BC, Furie, B (2003) Accumulation of tissue factor into developing thrombi in vivo is

dependent upon microparticle P-selectin glycoprotein ligand 1 and platelet P-selectin. *J. Exp. Med.* **197**(11)**:** 1585-1598.

Falk, E, Shah, PK, Fuster, V (1995) Coronary plaque disruption. *Circulation* **92**(3)**:** 657-671.

Fantidis, P (2010) The role of the stress-related anti-inflammatory hormones ACTH and cortisol in atherosclerosis. *Curr. Vasc. Pharmacol.* **8**(4)**:** 517-525.

Farb, A, Weber, DK, Kolodgie, FD, Burke, AP, Virmani, R (2002) Morphological predictors of restenosis after coronary stenting in humans. *Circulation* **105**(25)**:** 2974-2980.

Farrell, GC (2002) Drugs and steatohepatitis. *Semin Liver Dis* **22**(2)**:** 185-194.

Fasshauer, M, Klein, J, Kralisch, S, Klier, M, Lossner, U, Bluher, M, Paschke, R (2004) Monocyte chemoattractant protein 1 expression is stimulated by growth hormone and interleukin-6 in 3T3-L1 adipocytes. *Biochem Biophys Res Commun* **317**(2)**:** 598-604.

Fatti, LM, Bottasso, B, Invitti, C, Coppola, R, Cavagnini, F, Mannucci, PM (2000) Markers of activation of coagulation and fibrinolysis in patients with Cushing's syndrome. *J. Endocrinol. Invest.* **23**(3)**:** 145-150.

Fay, WP (2004) Plasminogen activator inhibitor 1, fibrin, and the vascular response to injury. *Trends Cardiovasc Med* **14**(5)**:** 196-202.

Fay, WP, Shapiro, AD, Shih, JL, Schleef, RR, Ginsburg, D (1992) Brief report: complete deficiency of plasminogen-activator inhibitor type 1 due to a frame-shift mutation. *N. Engl. J. Med.* **327**(24)**:** 1729-1733.

Fenton, JW, 2nd, Ofosu, FA, Brezniak, DV, Hassouna, HI (1998) Thrombin and antithrombotics. *Semin. Thromb. Hemost.* **24**(2)**:** 87-91.

Fenton, JW, 2nd, Ofosu, FA, Moon, DG, Maraganore, JM (1991) Thrombin structure and function: why thrombin is the primary target for antithrombotics. *Blood Coagul. Fibrinolysis* **2**(1)**:** 69-75.

Ferns, GA, Raines, EW, Sprugel, KH, Motani, AS, Reidy, MA, Ross, R (1991) Inhibition of neointimal smooth muscle accumulation after angioplasty by an antibody to PDGF. *Science (New York, N.Y* **253**(5024)**:** 1129-1132.

Ferrari, P (2010) The role of 11beta-hydroxysteroid dehydrogenase type 2 in human hypertension. *Biochim. Biophys. Acta* **1802**(12)**:** 1178-1187.

Ferrero, V, Tomai, F, Versaci, F, Feola, M, Proietti, I, Rognoni, A, Ghini, AS, Gaspardone, A, Vacca, G, De Luca, L, Vassanelli, C, Ribichini, F (2009) Long-term results of immunosuppressive oral prednisone after coronary angioplasty in non-diabetic patients with elevated C-reactive protein levels. *EuroIntervention* **5**(2)**:** 250-254.

Filippov, S, Koenig, GC, Chun, TH, Hotary, KB, Ota, I, Bugge, TH, Roberts, JD, Fay, WP, Birkedal-Hansen, H, Holmbeck, K, Sabeh, F, Allen, ED, Weiss, SJ (2005) MT1-matrix metalloproteinase directs arterial wall invasion and neointima formation by vascular smooth muscle cells. *J. Exp. Med.* **202**(5)**:** 663-671.

Filipsson, H, Monson, JP, Koltowska-Haggstrom, M, Mattsson, A, Johannsson, G (2006) The impact of glucocorticoid replacement regimens on metabolic outcome and comorbidity in hypopituitary patients. *J. Clin. Endocrinol. Metab.* **91**(10)**:** 3954-3961.

Fingerle, J, Johnson, R, Clowes, AW, Majesky, MW, Reidy, MA (1989) Role of platelets in smooth muscle cell proliferation and migration after vascular injury in rat carotid artery. *Proc. Natl. Acad. Sci. U. S. A.* **86**(21)**:** 8412-8416.

Fingerle, J, Sanders, KH, Fotev, Z (1991) Alpha 1-receptor antagonists urapidil and prazosin inhibit neointima formation in rat carotid artery induced by balloon catheter injury. *Basic Res Cardiol* **86 Suppl 1:** 75-81.

Fischman, DL, Leon, MB, Baim, DS, Schatz, RA, Savage, MP, Penn, I, Detre, K, Veltri, L, Ricci, D, Nobuyoshi, M, et al. (1994) A randomized comparison of coronary-stent placement and balloon angioplasty in the treatment of coronary artery disease. Stent Restenosis Study Investigators. *The New England journal of medicine* **331**(8)**:** 496-501.

Fishel, RS, Eisenberg, S, Shai, SY, Redden, RA, Bernstein, KE, Berk, BC (1995) Glucocorticoids induce angiotensin-converting enzyme expression in vascular smooth muscle. *Hypertension* **25**(3)**:** 343-349.

Folkman, J, Langer, R, Linhardt, RJ, Haudenschild, C, Taylor, S (1983) Angiogenesis inhibition and tumor regression caused by heparin or a heparin fragment in the presence of cortisone. *Science* **221**(4612)**:** 719-725.

Fornitz, GG, Nielsen, P, Amtorp, O, Kassis, E, Abildgard, U, Sloth, C, Winther, K, Orskov, H, Dalsgard, J, Husted, S (2001) Impaired fibrinolysis determines the outcome of percutaneus transluminal coronary angioplasty (PTCA). *Eur. J. Clin. Invest.* **31**(7)**:** 586-592.

Fridlender, ZG, Sun, J, Kim, S, Kapoor, V, Cheng, G, Ling, L, Worthen, GS, Albelda, SM (2009) Polarization of tumor-associated neutrophil phenotype by TGF-beta: "N1" versus "N2" TAN. *Cancer Cell* **16**(3)**:** 183-194.

Friedman, M, Byers, S, Stgeorge, S (1964) Cortisone and experimental atherosclerosis; effects upon administration. *Arch. Pathol.* **77:** 142-158.

Frijters, R, Fleuren, W, Toonen, EJ, Tuckermann, JP, Reichardt, HM, van der Maaden, H, van Elsas, A, van Lierop, MJ, Dokter, W, de Vlieg, J, Alkema, W (2010) Prednisolone-induced differential gene expression in mouse liver carrying wild type or a dimerization-defective glucocorticoid receptor. *BMC Genomics* **11:** 359.

Fukuda, D, Enomoto, S, Nagai, R, Sata, M (2009) Inhibition of renin-angiotensin system attenuates periadventitial inflammation and reduces atherosclerotic lesion formation. *Biomed Pharmacother* **63**(10)**:** 754-761.

Fukumoto, S, Allan, EH, Zeheb, R, Gelehrter, TD, Martin, TJ (1992) Glucocorticoid regulation of plasminogen activator inhibitor-1 messenger ribonucleic acid and protein in normal and malignant rat osteoblasts. *Endocrinology* **130**(2)**:** 797-804.

Fukumoto, Y, Shimokawa, H, Ito, A, Kadokami, T, Yonemitsu, Y, Aikawa, M, Owada, MK, Egashira, K, Sueishi, K, Nagai, R, Yazaki, Y, Takeshita, A (1997) Inflammatory cytokines cause coronary arteriosclerosis-like changes and alterations in the smooth-muscle phenotypes in pigs. *J. Cardiovasc. Pharmacol.* **29**(2)**:** 222-231.

Funder, JW (2007) Why are mineralocorticoid receptors so nonselective? *Curr. Hypertens. Rep.* **9**(2)**:** 112-116.

Furchgott, RF, Zawadzki, JV (1980) The obligatory role of endothelial cells in the relaxation of arterial smooth muscle by acetylcholine. *Nature* **288**(5789)**:** 373-376.

Furie, B, Furie, BC (2005) Thrombus formation in vivo. *J. Clin. Invest.* **115**(12)**:** 3355-3362.

Furman, C, Luo, Z, Walsh, K, Duverger, N, Copin, C, Fruchart, JC, Rouis, M (2002) Systemic tissue inhibitor of metalloproteinase-1 gene delivery reduces neointimal hyperplasia in balloon-injured rat carotid artery. *FEBS Lett* **531**(2)**:** 122-126.

Fyfe, AI, Rosenthal, A, Gotlieb, AI (1995) Immunosuppressive agents and endothelial repair. Prednisolone delays migration and cytoskeletal rearrangement in wounded porcine aortic monolayers. *Arterioscler. Thromb. Vasc. Biol.* **15**(8)**:** 1166-1171.

Gahring, LC, Osborne, AV, Reed, M, Rogers, SW (2010) Neuronal nicotinic alpha7 receptors modulate early neutrophil infiltration to sites of skin inflammation. *J Neuroinflammation* **7**(1)**:** 38.

Gailani, D, Renne, T (2007) The intrinsic pathway of coagulation: a target for treating thromboembolic disease? *J. Thromb. Haemost.* **5**(6)**:** 1106-1112.

Galis, ZS, Johnson, C, Godin, D, Magid, R, Shipley, JM, Senior, RM, Ivan, E (2002) Targeted disruption of the matrix metalloproteinase-9 gene impairs smooth muscle cell migration and geometrical arterial remodeling. *Circ. Res.* **91**(9)**:** 852-859.

Gametchu, B, Chen, F, Sackey, F, Powell, C, Watson, CS (1999) Plasma membrane-resident glucocorticoid receptors in rodent lymphoma and human leukemia models. *Steroids* **64**(1-2)**:** 107-119.

Gan, LM, Gronros, J, Hagg, U, Wikstrom, J, Theodoropoulos, C, Friberg, P, Fritsche-Danielson, R (2007) Non-invasive real-time imaging of atherosclerosis in mice using ultrasound biomicroscopy. *Atherosclerosis* **190**(2)**:** 313-320.

Gaspardone, A, Versaci, F, Tomai, F, Citone, C, Proietti, I, Gioffre, G, Skossyreva, O (2006) C-Reactive protein, clinical outcome, and restenosis rates after implantation of different drug-eluting stents. *Am J Cardiol* **97**(9)**:** 1311-1316.

Geng, YJ, Wu, Q, Muszynski, M, Hansson, GK, Libby, P (1996) Apoptosis of vascular smooth muscle cells induced by in vitro stimulation with interferon-gamma, tumor necrosis factor-alpha, and interleukin-1 beta. *Arterioscler. Thromb. Vasc. Biol.* **16**(1)**:** 19-27.

Giachelli, CM, Lombardi, D, Johnson, RJ, Murry, CE, Almeida, M (1998) Evidence for a role of osteopontin in macrophage infiltration in response to pathological stimuli in vivo. *Am. J. Pathol.* **152**(2)**:** 353-358.

Giesen, PL, Rauch, U, Bohrmann, B, Kling, D, Roque, M, Fallon, JT, Badimon, JJ, Himber, J, Riederer, MA, Nemerson, Y (1999) Blood-borne tissue factor: another view of thrombosis. *Proc. Natl. Acad. Sci. U. S. A.* **96**(5)**:** 2311-2315.

Giles, KM, Ross, K, Rossi, AG, Hotchin, NA, Haslett, C, Dransfield, I (2001) Glucocorticoid augmentation of macrophage capacity for phagocytosis of apoptotic cells is associated with reduced p130Cas expression, loss of paxillin/pyk2 phosphorylation, and high levels of active Rac. *J Immunol* **167**(2)**:** 976-986.

Gils, A, Declerck, PJ (2004) Plasminogen activator inhibitor-1. *Curr. Med. Chem.* **11**(17)**:** 2323-2334.

Glagov, S, Weisenberg, E, Zarins, CK, Stankunavicius, R, Kolettis, GJ (1987) Compensatory enlargement of human atherosclerotic coronary arteries. *N. Engl. J. Med.* **316**(22)**:** 1371-1375.

Glorioso, N, Filigheddu, F, Parpaglia, PP, Soro, A, Troffa, C, Argiolas, G, Mulatero, P (2005) 11beta-Hydroxysteroid dehydrogenase type 2 activity is associated with left ventricular mass in essential hypertension. *Eur. Heart J.* **26**(5)**:** 498-504.

Golino, P, Ambrosio, G, Ragni, M, Cirillo, P, Esposito, N, Willerson, JT, Rothlein, R, Petrucci, L, Condorelli, M, Chiariello, M, Buja, LM (1997) Inhibition of leucocyte and platelet adhesion reduces neointimal hyperplasia after arterial injury. *Thromb. Haemost.* **77**(4)**:** 783-788.

Goncharova, EA, Billington, CK, Irani, C, Vorotnikov, AV, Tkachuk, VA, Penn, RB, Krymskaya, VP, Panettieri, RA, Jr. (2003) Cyclic AMP-mobilizing agents and glucocorticoids modulate human smooth muscle cell migration. *Am. J. Respir. Cell Mol. Biol.* **29**(1)**:** 19-27.

Goodwin, JE, Zhang, J, Geller, DS (2008) A critical role for vascular smooth muscle in acute glucocorticoid-induced hypertension. *J. Am. Soc. Nephrol.* **19**(7)**:** 1291-1299.

Goodwin, JE, Zhang, J, Velazquez, H, Geller, DS (2010) The glucocorticoid receptor in the distal nephron is not necessary for the development or maintenance of dexamethasone-induced hypertension. *Biochem Biophys Res Commun* **394**(2)**:** 266-271.

Gounarides, JS, Korach-Andre, M, Killary, K, Argentieri, G, Turner, O, Laurent, D (2008) Effect of dexamethasone on glucose tolerance and fat metabolism in a diet-induced obesity mouse model. *Endocrinology* **149**(2)**:** 758-766.

Graf, R, Gossrau, R, Frank, HG (1990) Enhancement of immunoreactivity of von Willebrand factor in vascular endothelial cells of rat organs after glucocorticoid administration. *Acta histochemica* **38:** 219-226.

Granada, JF, Kaluza, GL, Wilensky, RL, Biedermann, BC, Schwartz, RS, Falk, E (2009) Porcine models of coronary atherosclerosis and vulnerable plaque for imaging and interventional research. *EuroIntervention* **5**(1)**:** 140-148.

Grassia, G, Maddaluno, M, Guglielmotti, A, Mangano, G, Biondi, G, Maffia, P, Ialenti, A (2009) The anti-inflammatory agent bindarit inhibits neointima formation in both rats and hyperlipidaemic mice. *Cardiovasc. Res.* **84**(3)**:** 485-493.

Gravanis, MB, Roubin, GS (1989) Histopathologic phenomena at the site of percutaneous transluminal coronary angioplasty: the problem of restenosis. *Hum. Pathol.* **20**(5)**:** 477-485.

Green, D (2006) Coagulation cascade. *Hemodial. Int.* **10 Suppl 2:** S2-4.

Griesshammer, M, Beneke, H, Nussbaumer, B, Grunewald, M, Bangerter, M, Bergmann, L (1999) Increased platelet surface expression of P-selectin and thrombospondin as markers of platelet activation in essential thrombocythaemia. *Thromb. Res.* **96**(3)**:** 191-196.

Griffin, SA, Brown, WC, MacPherson, F, McGrath, JC, Wilson, VG, Korsgaard, N, Mulvany, MJ, Lever, AF (1991) Angiotensin II causes vascular hypertrophy in part by a non-pressor mechanism. *Hypertension* **17**(5)**:** 626-635.

Grunfeld, JP, Eloy, L, Araujo, A, Russo-Marie, F (1986) Effects of gluco- and antiglucocorticoids on renal and aortic prostaglandin synthesis. *Am. J. Physiol.* **251**(5 Pt 2)**:** F810-816.

Gruntzig, AR, Senning, A, Siegenthaler, WE (1979) Nonoperative dilatation of coronary-artery stenosis: percutaneous transluminal coronary angioplasty. *N. Engl. J. Med.* **301**(2)**:** 61-68.

Gu, L, Okada, Y, Clinton, SK, Gerard, C, Sukhova, GK, Libby, P, Rollins, BJ (1998) Absence of monocyte chemoattractant protein-1 reduces atherosclerosis in low density lipoprotein receptor-deficient mice. *Mol. Cell* **2**(2)**:** 275-281.

Gunin, AG, Emelianov, VU, Tolmachev, AS (2003) Expression of estrogen receptor-alpha, glucocorticoid receptor, beta-catenin and glycogen synthase kinase-3beta in the uterus of mice following long-term treatment with estrogen and glucocorticoid hormones. *Eur. J. Obstet. Gynecol. Reprod. Biol.* **107**(1)**:** 62-67.

Guzman, LA, Labhasetwar, V, Song, C, Jang, Y, Lincoff, AM, Levy, R, Topol, EJ (1996) Local intraluminal infusion of biodegradable polymeric nanoparticles. A novel approach for prolonged drug delivery after balloon angioplasty. *Circulation* **94**(6)**:** 1441-1448.

Hadoke, P, Wainwright, CL, Wadsworth, RM, Butler, K, Giddings, MJ (1995) Characterization of the morphological and functional alterations in rabbit subclavian artery subjected to balloon angioplasty. *Coron. Artery Dis.* **6**(5)**:** 403-415.

Hadoke, PW, Macdonald, L, Logie, JJ, Small, GR, Dover, AR, Walker, BR (2006) Intra-vascular glucocorticoid metabolism as a modulator of vascular structure and function. *Cell. Mol. Life Sci.* **63**(5)**:** 565-578.

Hafezi-Moghadam, A, Simoncini, T, Yang, Z, Limbourg, FP, Plumier, JC, Rebsamen, MC, Hsieh, CM, Chui, DS, Thomas, KL, Prorock, AJ, Laubach, VE, Moskowitz, MA, French, BA, Ley, K, Liao, JK (2002) Acute cardiovascular protective effects of corticosteroids are mediated by non-transcriptional activation of endothelial nitric oxide synthase. *Nat. Med.* **8**(5)**:** 473-479.

Hagihara, H, Nomoto, A, Mutoh, S, Yamaguchi, I, Ono, T (1991) Role of inflammatory responses in initiation of atherosclerosis: effects of anti-inflammatory drugs on cuff-induced leukocyte accumulation and intimal thickening of rabbit carotid artery. *Atherosclerosis* **91**(1-2)**:** 107-116.

Halleux, CM, Declerck, PJ, Tran, SL, Detry, R, Brichard, SM (1999) Hormonal control of plasminogen activator inhibitor-1 gene expression and production in human adipose tissue: stimulation by glucocorticoids and inhibition by catecholamines. *J. Clin. Endocrinol. Metab.* **84**(11)**:** 4097-4105.

Haluzik, M, Dietz, KR, Kim, JK, Marcus-Samuels, B, Shulman, GI, Gavrilova, O, Reitman, ML (2002) Adrenalectomy improves diabetes in A-ZIP/F-1 lipoatrophic mice by increasing both liver and muscle insulin sensitivity. *Diabetes* **51**(7)**:** 2113-2118.

Han, SH, Ahn, TH, Kang, WC, Oh, KJ, Chung, WJ, Shin, MS, Koh, KK, Choi, IS, Shin, EK (2006) The favorable clinical and angiographic outcomes of a high-dose dexamethasone-eluting stent: randomized controlled prospective study. *Am Heart J* **152**(5)**:** 887 e881-887.

Handa, M, Kondo, K, Suzuki, H, Saruta, T (1984) Dexamethasone hypertension in rats: role of prostaglandins and pressor sensitivity to norepinephrine. *Hypertension* **6**(2 Pt 1)**:** 236-241.

Hanna, EB, Hennebry, TA, Abu-Fadel, MS (2010) Combined reperfusion strategies in ST-segment elevation MI: Rationale and current role. *Cleve. Clin. J. Med.* **77**(9)**:** 629-638.

Harada, N, Okajima, K, Kushimoto, S, Isobe, H, Tanaka, K (1999) Antithrombin reduces ischemia/reperfusion injury of rat liver by increasing the hepatic level of prostacyclin. *Blood* **93**(1)**:** 157-164.

Harris, A, Seckl, J (2010) Glucocorticoids, prenatal stress and the programming of disease. *Horm. Behav.*

Hatakeyama, H, Inaba, S, Miyamori, I (1999) 11beta-hydroxysteroid dehydrogenase in cultured human vascular cells. Possible role in the development of hypertension. *Hypertension* **33**(5)**:** 1179-1184.

Hausleiter, J, Kastrati, A, Mehilli, J, Vogeser, M, Zohlnhofer, D, Schuhlen, H, Goos, C, Pache, J, Dotzer, F, Pogatsa-Murray, G, Dirschinger, J, Heemann, U, Schomig, A (2004) Randomized, double-blind, placebo-controlled trial of oral sirolimus for restenosis prevention in patients with in-stent restenosis: the Oral Sirolimus to Inhibit Recurrent In-stent Stenosis (OSIRIS) trial. *Circulation* **110**(7)**:** 790-795.

Hayashi, S, Watanabe, N, Nakazawa, K, Suzuki, J, Tsushima, K, Tamatani, T, Sakamoto, S, Isobe, M (2000) Roles of P-selectin in inflammation, neointimal formation, and vascular remodeling in balloon-injured rat carotid arteries. *Circulation* **102**(14)**:** 1710-1717.

Heasman, SJ, Giles, KM, Ward, C, Rossi, AG, Haslett, C, Dransfield, I (2003) Glucocorticoid-mediated regulation of granulocyte apoptosis and macrophage phagocytosis of apoptotic cells: implications for the resolution of inflammation. *J. Endocrinol.* **178**(1)**:** 29-36.

Hermanowski-Vosatka, A, Balkovec, JM, Cheng, K, Chen, HY, Hernandez, M, Koo, GC, Le Grand, CB, Li, Z, Metzger, JM, Mundt, SS, Noonan, H, Nunes, CN, Olson, SH, Pikounis, B, Ren, N, Robertson, N, Schaeffer, JM, Shah, K, Springer, MS, Strack, AM, Strowski, M, Wu, K, Wu, T, Xiao, J, Zhang, BB, Wright, SD, Thieringer, R (2005) 11beta-HSD1 inhibition ameliorates metabolic syndrome and prevents progression of atherosclerosis in mice. *The Journal of experimental medicine* **202**(4)**:** 517-527.

Hertig, A, Berrou, J, Allory, Y, Breton, L, Commo, F, Costa De Beauregard, MA, Carmeliet, P, Rondeau, E (2003) Type 1 plasminogen activator inhibitor deficiency aggravates the course of experimental glomerulonephritis through overactivation of transforming growth factor beta. *FASEB J* **17**(13)**:** 1904-1906.

Hoffmann, R, Langenberg, R, Radke, P, Franke, A, Blindt, R, Ortlepp, J, Popma, JJ, Weber, C, Hanrath, P (2004a) Evaluation of a high-dose dexamethasone-eluting stent. *Am J Cardiol* **94**(2)**:** 193-195.

Hoffmann, R, Mintz, GS, Dussaillant, GR, Popma, JJ, Pichard, AD, Satler, LF, Kent, KM, Griffin, J, Leon, MB (1996) Patterns and mechanisms of in-stent restenosis. A serial intravascular ultrasound study. *Circulation* **94**(6)**:** 1247-1254.

Hoffmann, R, Radke, PW, Ortlepp, JR, Haager, PK, Blindt, R, Iofina, E, Franke, A, Langenberg, R, Weber, C, Hanrath, P (2004b) Intravascular ultrasonic comparative analysis of degree of intimal hyperplasia produced by four different stents in the coronary arteries. *Am J Cardiol* **94**(12)**:** 1548-1550.

Hojo, Y, Ikeda, U, Katsuki, T, Mizuno, O, Fukazawa, H, Fujikawa, H, Shimada, K (2001) Chemokine expression in coronary circulation after coronary angioplasty as a prognostic factor for restenosis. *Atherosclerosis* **156**(1)**:** 165-170.

Holmes, MC, French, KL, Seckl, JR (1997) Dysregulation of diurnal rhythms of serotonin 5-HT2C and corticosteroid receptor gene expression in the hippocampus with food restriction and glucocorticoids. *J Neurosci* **17**(11)**:** 4056-4065.

Hoogerbrugge, N, de Groot, E, de Heide, LH, de Ridder, MA, Birkenhageri, JC, Stijnen, T, Jansen, H (2002) Doxazosin and hydrochlorothiazide equally affect arterial wall thickness in hypertensive males with hypercholesterolaemia (the DAPHNE study). Doxazosin Atherosclerosis Progression Study in Hypertensives in the Netherlands. *Neth J Med* **60**(9)**:** 354-361.

Horie, S, Ishii, H, Kazama, M (1990) Heparin-like glycosaminoglycan is a receptor for antithrombin III-dependent but not for thrombin-dependent prostacyclin production in human endothelial cells. *Thromb. Res.* **59**(6)**:** 895-904.

Howlett, TA (1997) An assessment of optimal hydrocortisone replacement therapy. *Clin. Endocrinol. (Oxf.)* **46**(3)**:** 263-268.

Hsu, BR, Kuhn, RW (1988) The role of the adrenal in generating the diurnal variation in circulating levels of corticosteroid-binding globulin in the rat. *Endocrinology* **122**(2)**:** 421-426.

Huang, LQ, Whitworth, JA, Chesterman, CN (1995) Effects of cyclosporin A and dexamethasone on haemostatic and vasoactive functions of vascular endothelial cells. *Blood Coagul Fibrinolysis* **6**(5)**:** 438-445.

Huber, K, Jorg, M, Probst, P, Schuster, E, Lang, I, Kaindl, F, Binder, BR (1992) A decrease in plasminogen activator inhibitor-1 activity after successful percutaneous transluminal coronary angioplasty is associated with a significantly reduced risk for coronary restenosis. *Thromb. Haemost.* **67**(2)**:** 209-213.

Hui, DY (2008) Intimal hyperplasia in murine models. *Curr Drug Targets* **9**(3)**:** 251-260.

Humphries, J, McGuinness, CL, Smith, A, Waltham, M, Poston, R, Burnand, KG (1999) Monocyte chemotactic protein-1 (MCP-1) accelerates the organization and resolution of venous thrombi. *J. Vasc. Surg.* **30**(5)**:** 894-899.

Iams, SG, Wexler, BC (1977) Inhibition of spontaneously developing arteriosclerosis in female breeder rats by adrenalectomy. *Atherosclerosis* **27**(3)**:** 311-323.

Ignarro, LJ, Buga, GM, Wood, KS, Byrns, RE, Chaudhuri, G (1987) Endothelium-derived relaxing factor produced and released from artery and vein is nitric oxide. *Proc Natl Acad Sci U S A* **84**(24)**:** 9265-9269.

Ikeda, U, Ikeda, M, Oohara, T, Kano, S, Yaginuma, T (1990) Mitogenic action of interleukin-1 alpha on vascular smooth muscle cells mediated by PDGF. *Atherosclerosis* **84**(2-3)**:** 183-188.

Ikeda, U, Ikeda, M, Oohara, T, Oguchi, A, Kamitani, T, Tsuruya, Y, Kano, S (1991) Interleukin 6 stimulates growth of vascular smooth muscle cells in a PDGF-dependent manner. *Am J Physiol* **260**(5 Pt 2)**:** H1713-1717.

Indolfi, C, Pavia, M, Angelillo, IF (2005) Drug-eluting stents versus bare metal stents in percutaneous coronary interventions (a meta-analysis). *Am J Cardiol* **95**(10)**:** 1146-1152.

Ingerman-Wojenski, C, Silver, MJ, Smith, JB, Macarak, E (1981) Bovine endothelial cells in culture produce thromboxane as well as prostacyclin. *J. Clin. Invest.* **67**(5)**:** 1292-1296.

Ingram, N, Martin, S, Wang, JH, van der Laan, S, Loiacono, R, van den Buuse, M (2005) Interaction of corticosterone and nicotine in regulation of prepulse inhibition in mice. *Neuropharmacology* **48**(1)**:** 80-92.

Inoue, T, Yaguchi, I, Mizoguchi, K, Uchida, T, Takayanagi, K, Hayashi, T, Morooka, S, Eguchi, Y (2003) Accelerated plasminogen activator inhibitor may prevent late restenosis after coronary stenting in acute myocardial infarction. *Clin. Cardiol.* **26**(3)**:** 153-157.

Iqbal, J Role of intra-cellular glucocorticoid regulation in vascular lesion development. PhD, University of Edinburgh, Edinburgh, 2010.

Iuchi, T, Akaike, M, Mitsui, T, Ohshima, Y, Shintani, Y, Azuma, H, Matsumoto, T (2003) Glucocorticoid excess induces superoxide production in vascular endothelial cells and elicits vascular endothelial dysfunction. *Circ. Res.* **92**(1)**:** 81-87.

Jacobson, L (1999) Glucocorticoid replacement, but not corticotropin-releasing hormone deficiency, prevents adrenalectomy-induced anorexia in mice. *Endocrinology* **140**(1)**:** 310-317.

Jennings, LK (2009) Role of platelets in atherothrombosis. *Am. J. Cardiol.* **103**(3 Suppl)**:** 4A-10A.

Jeong, YH, Lee, SW, Choi, BR, Kim, IS, Seo, MK, Kwak, CH, Hwang, JY, Park, SW (2009) Randomized comparison of adjunctive cilostazol versus high maintenance dose clopidogrel in patients with high post-treatment platelet reactivity: results of the ACCEL-RESISTANCE (Adjunctive Cilostazol Versus High Maintenance Dose Clopidogrel in Patients With Clopidogrel Resistance) randomized study. *J Am Coll Cardiol* **53**(13)**:** 1101-1109.

Jilma, B, Blann, AD, Stohlawetz, P, Eichler, HG, Kautzky-Willer, A, Wagner, OF (2000) Dexamethasone lowers circulating E-selectin and ICAM-1 in healthy men. *J. Lab. Clin. Med.* **135**(3)**:** 270-274.

Jilma, B, Cvitko, T, Winter-Fabry, A, Petroczi, K, Quehenberger, P, Blann, AD (2005) High dose dexamethasone increases circulating P-selectin and von Willebrand factor levels in healthy men. *Thromb. Haemost.* **94**(4)**:** 797-801.

Jimenez-Valero, S, Santos, B, Pajin, F, Canton, T, Lazaro, E, Moreu, J, Hernandez, G, Padial, LR (2007) Clinical outcomes of dexamethasone-eluting stent implantation in ST-elevation acute myocardial infarction. *Catheter Cardiovasc Interv* **70**(4)**:** 492-497.

Johnson, C, Galis, ZS (2004) Matrix metalloproteinase-2 and -9 differentially regulate smooth muscle cell migration and cell-mediated collagen organization. *Arterioscler. Thromb. Vasc. Biol.* **24**(1)**:** 54-60.

Jonasson, L, Holm, J, Skalli, O, Bondjers, G, Hansson, GK (1986) Regional accumulations of T cells, macrophages, and smooth muscle cells in the human atherosclerotic plaque. *Arteriosclerosis (Dallas, Tex* **6**(2)**:** 131-138.

Joyce, DE, Gelbert, L, Ciaccia, A, DeHoff, B, Grinnell, BW (2001) Gene expression profile of antithrombotic protein c defines new mechanisms modulating inflammation and apoptosis. *J. Biol. Chem.* **276**(14)**:** 11199-11203.

Kageyama, K, Suda, T (2009) Regulatory mechanisms underlying corticotropin-releasing factor gene expression in the hypothalamus. *Endocr J* **56**(3)**:** 335-344.

Kaikita, K, Fogo, AB, Ma, L, Schoenhard, JA, Brown, NJ, Vaughan, DE (2001) Plasminogen activator inhibitor-1 deficiency prevents hypertension and vascular fibrosis in response to long-term nitric oxide synthase inhibition. *Circulation* **104**(7)**:** 839-844.

Kanthou, C, Benzakour, O, Patel, G, Deadman, J, Kakkar, VV, Lupu, F (1995) Thrombin receptor activating peptide (TRAP) stimulates mitogenesis, c-fos and PDGF-A gene expression in human vascular smooth muscle cells. *Thromb. Haemost.* **74**(5)**:** 1340-1347.

Karim, MA, Frizzell, S, Inman, L, Shinn, M, Miller, DD (1997) In vivo role of glucocorticoids in barotrauma vascular repair and fibrosis. *J. Mol. Cell. Cardiol.* **29**(4)**:** 1111-1122.

Kastrati, A, Schuhlen, H, Hausleiter, J, Walter, H, Zitzmann-Roth, E, Hadamitzky, M, Elezi, S, Ulm, K, Dirschinger, J, Neumann, FJ, Schomig, A (1997) Restenosis after coronary stent placement and randomization to a 4-week combined antiplatelet or anticoagulant therapy: six-month angiographic follow-up of the Intracoronary Stenting and Antithrombotic Regimen (ISAR) Trial. *Circulation* **96**(2)**:** 462-467.

Katz, SS, Shipley, GG, Small, DM (1976) Physical chemistry of the lipids of human atherosclerotic lesions. Demonstration of a lesion intermediate between fatty streaks and advanced plaques. *J. Clin. Invest.* **58**(1)**:** 200-211.

Kawasaki, T, Dewerchin, M, Lijnen, HR, Vreys, I, Vermylen, J, Hoylaerts, MF (2001) Mouse carotid artery ligation induces platelet-leukocyte-dependent luminal fibrin, required for neointima development. *Circulation research* **88**(2)**:** 159-166.

Kawiak, J, Hoser, G, Malendowicz, LK, Miks, B, Skurzak, H (1996) Thymocyte and splenocyte subpopulations in normal and leukemia-bearing mice after adrenalectomy. *Folia Histochem Cytobiol* **34**(2)**:** 75-78.

Kedhi, E, Stone, GW (2010) Everolimus-eluting stents: insights from the SPIRIT IV and COMPARE trials. *Expert Rev Cardiovasc Ther* **8**(9)**:** 1207-1210.

Keeley, EC, Boura, JA, Grines, CL (2003) Primary angioplasty versus intravenous thrombolytic therapy for acute myocardial infarction: a quantitative review of 23 randomised trials. *Lancet* **361**(9351)**:** 13-20.

Keidar, S, Kaplan, M, Pavlotzky, E, Coleman, R, Hayek, T, Hamoud, S, Aviram, M (2004) Aldosterone administration to mice stimulates macrophage NADPH oxidase and increases atherosclerosis development: a possible role for angiotensin-converting enzyme and the receptors for angiotensin II and aldosterone. *Circulation* **109**(18)**:** 2213-2220.

Kelly, JJ, Martin, A, Whitworth, JA (2000) Role of erythropoietin in cortisol-induced hypertension. *J. Hum. Hypertens.* **14**(3)**:** 195-198.

Kelly, KA, Allport, JR, Tsourkas, A, Shinde-Patil, VR, Josephson, L, Weissleder, R (2005) Detection of vascular adhesion molecule-1 expression using a novel multimodal nanoparticle. *Circ. Res.* **96**(3)**:** 327-336.

Kenagy, RD, Vesti, BR, Clowes, AW (2002) The urokinase receptor mediates basic fibroblast growth factor-dependent smooth muscle cell migration through baboon aortic explants. *Atherosclerosis* **162**(1)**:** 63-67.

Kerlin, B, Cooley, BC, Isermann, BH, Hernandez, I, Sood, R, Zogg, M, Hendrickson, SB, Mosesson, MW, Lord, S, Weiler, H (2004) Cause-effect relation between hyperfibrinogenemia and vascular disease. *Blood* **103**(5)**:** 1728-1734.

Kibos, A, Campeanu, A, Tintoiu, I (2007) Pathophysiology of coronary artery in-stent restenosis. *Acute Card Care* **9**(2)**:** 111-119.

Kim, PJ, Cole, MA, Kalman, BA, Spencer, RL (1998) Evaluation of RU28318 and RU40555 as selective mineralocorticoid receptor and glucocorticoid receptor antagonists, respectively: receptor measures and functional studies. *J Steroid Biochem Mol Biol* **67**(3)**:** 213-222.

Kirkby, NS, Low, L, Seckl, JR, Walker, BR, Webb, DJ, Hadoke, PW (2011) Quantitative 3-dimensional imaging of murine neointimal and atherosclerotic lesions by optical projection tomography. *PLoS ONE* **6**(2)**:** e16906.

Ko, KW, Corry, DB, Brayton, CF, Paul, A, Chan, L (2009) Extravascular inflammation does not increase atherosclerosis in apoE-deficient mice. *Biochem. Biophys. Res. Commun.* **384**(1)**:** 93-99.

Kochiadakis, GE, Marketou, ME, Arfanakis, DA, Sfiridaki, K, Skalidis, EI, Igoumenidis, NE, Hamilos, MI, Kolyvaki, S, Chlouverakis, G, Kantidaki, E, Castanas, E, Vardas, PE (2007) Reduced systemic inflammatory response to implantation of sirolimus-eluting stents in patients with stable coronary artery disease. *Atherosclerosis* **194**(2)**:** 433-438.

Konishi, A, Tazawa, C, Miki, Y, Darnel, AD, Suzuki, T, Ohta, Y, Tabayashi, K, Sasano, H (2003) The possible roles of mineralocorticoid receptor and 11beta-hydroxysteroid dehydrogenase type 2 in cardiac fibrosis in the spontaneously hypertensive rat. *J. Steroid Biochem. Mol. Biol.* **85**(2-5)**:** 439-442.

Kotelevtsev, Y, Brown, RW, Fleming, S, Kenyon, C, Edwards, CR, Seckl, JR, Mullins, JJ (1999) Hypertension in mice lacking 11beta-hydroxysteroid dehydrogenase type 2. *J. Clin. Invest.* **103**(5)**:** 683-689.

Kotelevtsev, Y, Holmes, MC, Burchell, A, Houston, PM, Schmoll, D, Jamieson, P, Best, R, Brown, R, Edwards, CR, Seckl, JR, Mullins, JJ (1997) 11beta-hydroxysteroid dehydrogenase type 1 knockout mice show attenuated glucocorticoid-inducible responses and resist hyperglycemia on obesity or stress. *Proc. Natl. Acad. Sci. U. S. A.* **94**(26)**:** 14924-14929.

Krug, AW, Allenhofer, L, Monticone, R, Spinetti, G, Gekle, M, Wang, M, Lakatta, EG (2010) Elevated mineralocorticoid receptor activity in aged rat vascular smooth muscle cells promotes a proinflammatory phenotype via extracellular signal-regulated kinase 1/2 mitogen-activated protein kinase and epidermal growth factor receptor-dependent pathways. *Hypertension* **55**(6)**:** 1476-1483.

Kumar, A, Hoover, JL, Simmons, CA, Lindner, V, Shebuski, RJ (1997a) Remodeling and neointimal formation in the carotid artery of normal and P-selectin-deficient mice. *Circulation* **96**(12)**:** 4333-4342.

Kumar, A, Lindner, V (1997b) Remodeling with neointima formation in the mouse carotid artery after cessation of blood flow. *Arterioscler. Thromb. Vasc. Biol.* **17**(10)**:** 2238-2244.

Kung, SK, Lau, HK (1993) Modulation of the plasminogen activation system in murine macrophages. *Biochim Biophys Acta* **1176**(1-2)**:** 113-122.

La Brocca, A, Terzolo, M, Pia, A, Paccotti, P, De Giuli, P, Angeli, A (1997) Recurrent thromboembolism as a hallmark of Cushing's syndrome. *J. Endocrinol. Invest.* **20**(4)**:** 211-214.

Lambert, CM, Roy, M, Meloche, J, Robitaille, GA, Agharazii, M, Richard, DE, Bonnet, S (2010) Tumor necrosis factor inhibitors as novel therapeutic tools for vascular remodeling diseases. *Am J Physiol Heart Circ Physiol* **299**(4)**:** H995-1001.

Lambillotte, C, Gilon, P, Henquin, JC (1997) Direct glucocorticoid inhibition of insulin secretion. An in vitro study of dexamethasone effects in mouse islets. *J. Clin. Invest.* **99**(3)**:** 414-423.

Langheinrich, AC, Bohle, RM, Greschus, S, Hackstein, N, Walker, G, von Gerlach, S, Rau, WS, Holschermann, H (2004) Atherosclerotic lesions at micro CT: feasibility for analysis of coronary artery wall in autopsy specimens. *Radiology* **231**(3)**:** 675-681.

Latouche, C, Sainte-Marie, Y, Steenman, M, Castro Chaves, P, Naray-Fejes-Toth, A, Fejes-Toth, G, Farman, N, Jaisser, F (2010) Molecular signature of mineralocorticoid receptor signaling in cardiomyocytes: from cultured cells to mouse heart. *Endocrinology* **151**(9)**:** 4467-4476.

Lauer, P, Metzner, HJ, Zettlmeissl, G, Li, M, Smith, AG, Lathe, R, Dickneite, G (2002) Targeted inactivation of the mouse locus encoding coagulation factor XIII-A: hemostatic abnormalities in mutant mice and characterization of the coagulation deficit. *Thromb. Haemost.* **88**(6)**:** 967-974.

Lavelle, SM, MacIomhair, M (1998) Bleeding times and the antithrombotic effects of high-dose aspirin, hirudin and heparins in the rat. *Ir J Med Sci* **167**(4)**:** 216-220.

Lee, KN, Jackson, KW, Christiansen, VJ, Chung, KH, McKee, PA (2004) Alpha2-antiplasmin: potential therapeutic roles in fibrin survival and removal. *Curr Med Chem Cardiovasc Hematol Agents* **2**(4)**:** 303-310.

Lee, MH, Vosburgh, E, Anderson, K, McDonagh, J (1993) Deficiency of plasma plasminogen activator inhibitor 1 results in hyperfibrinolytic bleeding. *Blood* **81**(9)**:** 2357-2362.

Letteron, P, Brahimi-Bourouina, N, Robin, MA, Moreau, A, Feldmann, G, Pessayre, D (1997) Glucocorticoids inhibit mitochondrial matrix acyl-CoA dehydrogenases and fatty acid beta-oxidation. *Am J Physiol* **272**(5 Pt 1)**:** G1141-1150.

Leung, FW, Murray, S, Murray, E, Go, VL (2008) Determination of body fat distribution by dual-energy X-ray absorptiometry and attenuation of visceral fat vasoconstriction by enalapril. *Dig Dis Sci* **53**(4)**:** 1084-1087.

Levi, M, van der Poll, T (2010) Inflammation and coagulation. *Crit. Care Med.* **38**(2 Suppl)**:** S26-34.

Levi, M, van der Poll, T (2008) The role of natural anticoagulants in the pathogenesis and management of systemic activation of coagulation and inflammation in critically ill patients. *Semin. Thromb. Hemost.* **34**(5)**:** 459-468.

Levick, JR (2003) *An introduction to cardiovascular physiology*. Arnold: London.

Levine, SJ, Benfield, T, Shelhamer, JH (1996) Corticosteroids induce intracellular interleukin-1 receptor antagonist type I expression by a human airway epithelial cell line. *Am. J. Respir. Cell Mol. Biol.* **15**(2)**:** 245-251.

Lewis, JG, Bagley, CJ, Elder, PA, Bachmann, AW, Torpy, DJ (2005) Plasma free cortisol fraction reflects levels of functioning corticosteroid-binding globulin. *Clin. Chim. Acta* **359**(1-2)**:** 189-194.

Lewis, JG, Mopert, B, Shand, BI, Doogue, MP, Soule, SG, Frampton, CM, Elder, PA (2006) Plasma variation of corticosteroid-binding globulin and sex hormone-binding globulin. *Horm. Metab. Res.* **38**(4)**:** 241-245.

Leys, D (2001) Atherothrombosis: a major health burden. *Cerebrovasc. Dis.* **11 Suppl 2:** 1-4.

Libby, P (2000) Changing concepts of atherogenesis. *Journal of internal medicine* **247**(3)**:** 349-358.

Libby, P (2002) Inflammation in atherosclerosis. *Nature* **420**(6917)**:** 868-874.

Libby, P (1995) Molecular bases of the acute coronary syndromes. *Circulation* **91**(11)**:** 2844-2850.

Libby, P, Aikawa, M (2002) Stabilization of atherosclerotic plaques: new mechanisms and clinical targets. *Nat. Med.* **8**(11)**:** 1257-1262.

Libby, P, Schwartz, D, Brogi, E, Tanaka, H, Clinton, SK (1992) A cascade model for restenosis. A special case of atherosclerosis progression. *Circulation* **86**(6 Suppl)**:** III47-52.

Liehn, EA, Piccinini, AM, Koenen, RR, Soehnlein, O, Adage, T, Fatu, R, Curaj, A, Popescu, A, Zernecke, A, Kungl, AJ, Weber, C (2010) A new monocyte chemotactic protein-1/chemokine CC motif ligand-2 competitor limiting neointima formation and myocardial ischemia/reperfusion injury in mice. *J. Am. Coll. Cardiol.* **56**(22)**:** 1847-1857.

Lijnen, HR, Van Hoef, B, Lupu, F, Moons, L, Carmeliet, P, Collen, D (1998) Function of the plasminogen/plasmin and matrix metalloproteinase systems after vascular injury in mice with targeted inactivation of fibrinolytic system genes. *Arterioscler. Thromb. Vasc. Biol.* **18**(7)**:** 1035-1045.

Lijnen, HR, Van Hoef, B, Umans, K, Collen, D (2004) Neointima formation and thrombosis after vascular injury in transgenic mice overexpressing plasminogen activator inhibitor-1 (PAI-1). *J. Thromb. Haemost.* **2**(1)**:** 16-22.

Lim, HY, Muller, N, Herold, MJ, van den Brandt, J, Reichardt, HM (2007) Glucocorticoids exert opposing effects on macrophage function dependent on their concentration. *Immunology* **122**(1)**:** 47-53.

Linder, B, Hong, Y, Jarrett, T (2009) Intra-renal adrenal adenoma: a compelling addition to the differential diagnosis of renal mass. *Int J Urol* **16**(11)**:** 912-914.

Lindner, JR, Dayton, PA, Coggins, MP, Ley, K, Song, J, Ferrara, K, Kaul, S (2000) Noninvasive imaging of inflammation by ultrasound detection of phagocytosed microbubbles. *Circulation* **102**(5)**:** 531-538.

Lindner, V (1995) Role of basic fibroblast growth factor and platelet-derived growth factor (B-chain) in neointima formation after arterial injury. *Z Kardiol* **84 Suppl 4:** 137-144.

Lindner, V, Fingerle, J, Reidy, MA (1993) Mouse model of arterial injury. *Circulation research* **73**(5)**:** 792-796.

Lindner, V, Lappi, DA, Baird, A, Majack, RA, Reidy, MA (1991) Role of basic fibroblast growth factor in vascular lesion formation. *Circ. Res.* **68**(1)**:** 106-113.

Ling, ZC, Khan, A, Delauny, F, Davani, B, Ostenson, CG, Gustafsson, JA, Okret, S, Landau, BR, Efendic, S (1998) Increased glucocorticoid sensitivity in islet beta-cells: effects on glucose 6-phosphatase, glucose cycling and insulin release. *Diabetologia* **41**(6)**:** 634-639.

Liu, X, Huang, Y, Hanet, C, Vandormael, M, Legrand, V, Dens, J, Vandenbossche, JL, Missault, L, Vrints, C, De Scheerder, I (2003) Study of antirestenosis with the BiodivYsio dexamethasone-eluting stent (STRIDE): a first-in-human multicenter pilot trial. *Catheter Cardiovasc Interv* **60**(2)**:** 172-178; discussion 179.

Liu, Y, Cousin, JM, Hughes, J, Van Damme, J, Seckl, JR, Haslett, C, Dransfield, I, Savill, J, Rossi, AG (1999) Glucocorticoids promote nonphlogistic phagocytosis of apoptotic leukocytes. *J Immunol* **162**(6)**:** 3639-3646.

Llau, JV, Ferrandis, R, Sierra, P, Gomez-Luque, A (2010) Prevention of the renarrowing of coronary arteries using drug-eluting stents in the perioperative period: an update. *Vasc Health Risk Manag* **6:** 855-867.

Logie, JJ, Ali, S, Marshall, KM, Heck, MM, Walker, BR, Hadoke, PW (2010) Glucocorticoid-mediated inhibition of angiogenic changes in human endothelial cells is not caused by reductions in cell proliferation or migration. *PLoS ONE* **5**(12)**:** e14476.

Loppnow, H, Bil, R, Hirt, S, Schonbeck, U, Herzberg, M, Werdan, K, Rietschel, ET, Brandt, E, Flad, HD (1998) Platelet-derived interleukin-1 induces cytokine production, but not proliferation of human vascular smooth muscle cells. *Blood* **91**(1)**:** 134-141.

Loscalzo, J, Pasche, B, Ouimet, H, Freedman, JE (1995) Platelets and plasminogen activation. *Thromb. Haemost.* **74**(1)**:** 291-293.

Lu, G, Broze, GJ, Jr., Krishnaswamy, S (2004) Formation of factors IXa and Xa by the extrinsic pathway: differential regulation by tissue factor pathway inhibitor and antithrombin III. *J. Biol. Chem.* **279**(17)**:** 17241-17249.

Ma, J, Weisberg, A, Griffin, JP, Vaughan, DE, Fogo, AB, Brown, NJ (2006) Plasminogen activator inhibitor-1 deficiency protects against aldosterone-induced glomerular injury. *Kidney Int* **69**(6)**:** 1064-1072.

Ma, Y, Ryu, JS, Dulay, A, Segal, M, Guller, S (2002) Regulation of plasminogen activator inhibitor (PAI)-1 expression in a human trophoblast cell line by glucocorticoid (GC) and transforming growth factor (TGF)-beta. *Placenta* **23**(10)**:** 727-734.

Macaya, C, Serruys, PW, Ruygrok, P, Suryapranata, H, Mast, G, Klugmann, S, Urban, P, den Heijer, P, Koch, K, Simon, R, Morice, MC, Crean, P, Bonnier, H, Wijns, W, Danchin, N, Bourdonnec, C, Morel, MA (1996) Continued benefit of coronary stenting versus balloon angioplasty: one-year clinical follow-up of Benestent trial. Benestent Study Group. *J. Am. Coll. Cardiol.* **27**(2)**:** 255-261.

Macdonald, LJ Glucocorticoid metabolism and the vascular response to injury. PhD, University of Edinburgh, Edinburgh, 2007.

Mackman, N, Tilley, RE, Key, NS (2007) Role of the extrinsic pathway of blood coagulation in hemostasis and thrombosis. *Arterioscler. Thromb. Vasc. Biol.* **27**(8)**:** 1687-1693.

Makheja, AN, Bloom, S, Muesing, R, Simon, T, Bailey, JM (1989) Anti-inflammatory drugs in experimental atherosclerosis. 7. Spontaneous atherosclerosis in WHHL rabbits and inhibition by cortisone acetate. *Atherosclerosis* **76**(2-3)**:** 155-161.

Makimura, H, Mizuno, TM, Beasley, J, Silverstein, JH, Mobbs, CV (2003) Adrenalectomy stimulates hypothalamic proopiomelanocortin expression but does not correct diet-induced obesity. *BMC Physiol* **3:** 4.

Makimura, H, Mizuno, TM, Roberts, J, Silverstein, J, Beasley, J, Mobbs, CV (2000) Adrenalectomy reverses obese phenotype and restores hypothalamic melanocortin tone in leptin-deficient ob/ob mice. *Diabetes* **49**(11)**:** 1917-1923.

Mangos, GJ, Walker, BR, Kelly, JJ, Lawson, JA, Webb, DJ, Whitworth, JA (2000) Cortisol inhibits cholinergic vasodilation in the human forearm. *Am. J. Hypertens.* **13**(11)**:** 1155-1160.

Mangos, GJ, Whitworth, JA, Williamson, PM, Kelly, JJ (2003) Glucocorticoids and the kidney. *Nephrology (Carlton)* **8**(6)**:** 267-273.

Mann, J, Davies, MJ (1999) Mechanisms of progression in native coronary artery disease: role of healed plaque disruption. *Heart* **82**(3)**:** 265-268.

Mann, KG, Jenny, RJ, Krishnaswamy, S (1988) Cofactor proteins in the assembly and expression of blood clotting enzyme complexes. *Annu. Rev. Biochem.* **57:** 915-956.

Marmur, JD, Poon, M, Rossikhina, M, Taubman, MB (1992) Induction of PDGF-responsive genes in vascular smooth muscle. Implications for the early response to vessel injury. *Circulation* **86**(6 Suppl)**:** III53-60.

Martinet, W, Verheye, S, De Meyer, GR (2007) Everolimus-induced mTOR inhibition selectively depletes macrophages in atherosclerotic plaques by autophagy. *Autophagy* **3**(3)**:** 241-244.

Mason, DP, Kenagy, RD, Hasenstab, D, Bowen-Pope, DF, Seifert, RA, Coats, S, Hawkins, SM, Clowes, AW (1999) Matrix metalloproteinase-9 overexpression enhances vascular smooth muscle cell migration and alters remodeling in the injured rat carotid artery. *Circ. Res.* **85**(12)**:** 1179-1185.

Matsuno, H, Kozawa, O, Niwa, M, Tanabe, K, Ichimaru, K, Takiguchi, Y, Yokota, M, Hayashi, H, Uematsu, T (1998) Multiple inhibition of platelet activation by aurintricarboxylic acid prevents vascular stenosis after endothelial injury in hamster carotid artery. *Thromb. Haemost.* **79**(4)**:** 865-871.

Maxwell, SR, Moots, RJ, Kendall, MJ (1994) Corticosteroids: do they damage the cardiovascular system? *Postgrad. Med. J.* **70**(830)**:** 863-870.

McAteer, MA, Schneider, JE, Clarke, K, Neubauer, S, Channon, KM, Choudhury, RP (2004) Quantification and 3D reconstruction of atherosclerotic plaque components in apolipoprotein E knockout mice using ex vivo high-resolution MRI. *Arteriosclerosis, thrombosis, and vascular biology* **24**(12)**:** 2384-2390.

Meaney, MJ, Szyf, M, Seckl, JR (2007) Epigenetic mechanisms of perinatal programming of hypothalamic-pituitary-adrenal function and health. *Trends Mol. Med.* **13**(7)**:** 269-277.

Mendel, CM (1989) The free hormone hypothesis: a physiologically based mathematical model. *Endocr. Rev.* **10**(3)**:** 232-274.

Mendelsohn, FA, Lloyd, CJ, Kachel, C, Funder, JW (1982) Induction by glucocorticoids of angiotensin converting enzyme production from bovine endothelial cells in culture and rat lung in vivo. *J. Clin. Invest.* **70**(3)**:** 684-692.

Miller, AM, McPhaden, AR, Wadsworth, RM, Wainwright, CL (2001) Inhibition by leukocyte depletion of neointima formation after balloon angioplasty in a rabbit model of restenosis. *Cardiovasc. Res.* **49**(4)**:** 838-850.

Miller, DD, Karim, MA, Edwards, WD, Schwartz, RS (1996) Relationship of vascular thrombosis and inflammatory leukocyte infiltration to neointimal growth following porcine coronary artery stent placement. *Atherosclerosis* **124**(2)**:** 145-155.

Moghadam-Kia, S, Werth, VP (2010) Prevention and treatment of systemic glucocorticoid side effects. *Int. J. Dermatol.* **49**(3)**:** 239-248.

Moncada, S, Gryglewski, R, Bunting, S, Vane, JR (1976) An enzyme isolated from arteries transforms prostaglandin endoperoxides to an unstable substance that inhibits platelet aggregation. *Nature* **263**(5579)**:** 663-665.

Moore, S, Friedman, RJ, Singal, DP, Gauldie, J, Blajchman, MA, Roberts, RS (1976) Inhibition of injury induced thromboatherosclerotic lesions by anti-platelet serum in rabbits. *Thromb. Haemost.* **35**(1)**:** 70-81.

Mora, R, Lupu, F, Simionescu, N (1987) Prelesional events in atherogenesis. Colocalization of apolipoprotein B, unesterified cholesterol and extracellular phospholipid liposomes in the aorta of hyperlipidemic rabbit. *Atherosclerosis* **67**(2-3)**:** 143-154.

Moraes-Fontes, MF, Rebelo, M, Caramalho, I, Zelenay, S, Bergman, ML, Coutinho, A, Demengeot, J (2009) Steroid treatments in mice do not alter the number and function of regulatory T cells, but amplify cyclophosphamide-induced autoimmune disease. *J Autoimmun* **33**(2)**:** 109-120.

Moraes, LA, Paul-Clark, MJ, Rickman, A, Flower, RJ, Goulding, NJ, Perretti, M (2005) Ligand-specific glucocorticoid receptor activation in human platelets. *Blood* **106**(13)**:** 4167-4175.

Moreno, PR, Bernardi, VH, Lopez-Cuellar, J, Newell, JB, McMellon, C, Gold, HK, Palacios, IF, Fuster, V, Fallon, JT (1996) Macrophage infiltration predicts restenosis after coronary intervention in patients with unstable angina. *Circulation* **94**(12)**:** 3098-3102.

Morin, C, Asselin, C, Boudreau, F, Provencher, PH (1998) Transcriptional regulation of pre-pro-endothelin-1 gene by glucocorticoids in vascular smooth muscle cells. *Biochem. Biophys. Res. Commun.* **244**(2)**:** 583-587.

Morton, AC, Arnold, ND, Gunn, J, Varcoe, R, Francis, SE, Dower, SK, Crossman, DC (2005) Interleukin-1 receptor antagonist alters the response to vessel wall injury in a porcine coronary artery model. *Cardiovasc. Res.* **68**(3)**:** 493-501.

Morton, NM, Holmes, MC, Fievet, C, Staels, B, Tailleux, A, Mullins, JJ, Seckl, JR (2001) Improved lipid and lipoprotein profile, hepatic insulin sensitivity, and glucose tolerance in 11beta-hydroxysteroid dehydrogenase type 1 null mice. *J. Biol. Chem.* **276**(44)**:** 41293-41300.

Muller, B, Kleschyov, AL, Gyorgy, K, Stoclet, JC (2000) Inducible NO synthase activity in blood vessels and heart: new insight into cell origin and consequences. *Physiol Res* **49**(1)**:** 19-26.

Muller, CA, Belyaev, O, Appelros, S, Buchler, M, Uhl, W, Borgstrom, A (2008) Dexamethasone affects inflammation but not trypsinogen activation in experimental acute pancreatitis. *Eur Surg Res* **40**(4)**:** 317-324.

Mulvihill, EE, Assini, JM, Sutherland, BG, DiMattia, AS, Khami, M, Koppes, JB, Sawyez, CG, Whitman, SC, Huff, MW (2010) Naringenin decreases progression of atherosclerosis by improving dyslipidemia in high-fat-fed low-density lipoprotein receptor-null mice. *Arterioscler. Thromb. Vasc. Biol.* **30**(4)**:** 742-748.

Munro, JM, Cotran, RS (1988) The pathogenesis of atherosclerosis: atherogenesis and inflammation. *Lab. Invest.* **58**(3)**:** 249-261.

Munro, JM, van der Walt, JD, Munro, CS, Chalmers, JA, Cox, EL (1987) An immunohistochemical analysis of human aortic fatty streaks. *Human pathology* **18**(4)**:** 375-380.

Murata, K, Motayama, T, Kotake, C (1986) Collagen types in various layers of the human aorta and their changes with the atherosclerotic process. *Atherosclerosis* **60**(3)**:** 251-262.

Nabel, EG, Shum, L, Pompili, VJ, Yang, ZY, San, H, Shu, HB, Liptay, S, Gold, L, Gordon, D, Derynck, R, et al. (1993) Direct transfer of transforming growth factor beta 1 gene into arteries stimulates fibrocellular hyperplasia. *Proc Natl Acad Sci U S A* **90**(22)**:** 10759-10763.

Nagasaki, K, Matsumoto, K, Kaneda, M, Shintani, T, Shibutani, S, Murayama, T, Wakabayashi, G, Shimazu, M, Mukai, M, Kitajima, M (2004) Effects of preinjury administration of corticosteroids on pseudointimal hyperplasia and cytokine response in a rat model of balloon aortic injury. *World J. Surg.* **28**(9)**:** 910-916.

Naghavi, M, Wyde, P, Litovsky, S, Madjid, M, Akhtar, A, Naguib, S, Siadaty, MS, Sanati, S, Casscells, W (2003) Influenza infection exerts prominent inflammatory and thrombotic effects on the atherosclerotic plaques of apolipoprotein E-deficient mice. *Circulation* **107**(5)**:** 762-768.

Naito, M, Yasue, M, Asai, K, Yamada, K, Hayashi, T, Kuzuya, M, Funaki, C, Yoshimine, N, Kuzuya, F (1992) Effects of dexamethasone on experimental atherosclerosis in cholesterol-fed rabbits. *J. Nutr. Sci. Vitaminol. (Tokyo)* **38**(3)**:** 255-264.

Nakano, T, Raines, EW, Abraham, JA, Wenzel, FGt, Higashiyama, S, Klagsbrun, M, Ross, R (1993) Glucocorticoid inhibits thrombin-induced expression of platelet-derived growth factor A-chain and heparin-binding epidermal growth factor-like growth factor in human aortic smooth muscle cells. *J. Biol. Chem.* **268**(30)**:** 22941-22947.

Napoli, C, D'Armiento, FP, Mancini, FP, Postiglione, A, Witztum, JL, Palumbo, G, Palinski, W (1997) Fatty streak formation occurs in human fetal aortas and is greatly enhanced by maternal hypercholesterolemia. Intimal accumulation of low density lipoprotein and its oxidation precede monocyte recruitment into early atherosclerotic lesions. *J. Clin. Invest.* **100**(11)**:** 2680-2690.

Naski, MC, Lawrence, DA, Mosher, DF, Podor, TJ, Ginsburg, D (1993) Kinetics of inactivation of alpha-thrombin by plasminogen activator inhibitor-1. Comparison of the effects of native and urea-treated forms of vitronectin. *J Biol Chem* **268**(17)**:** 12367-12372.

Newby, AC (2000) An overview of the vascular response to injury: a tribute to the late Russell Ross. *Toxicol. Lett.* **112-113:** 519-529.

Newby, AC, Zaltsman, AB (2000) Molecular mechanisms in intimal hyperplasia. *J. Pathol.* **190**(3)**:** 300-309.

Newell-Price, J, Bertagna, X, Grossman, AB, Nieman, LK (2006) Cushing's syndrome. *Lancet* **367**(9522)**:** 1605-1617.

Newsome, LT, Kutcher, MA, Royster, RL (2008) Coronary artery stents: Part I. Evolution of percutaneous coronary intervention. *Anesth. Analg.* **107**(2)**:** 552-569.

Nguyen Dinh Cat, A, Griol-Charhbili, V, Loufrani, L, Labat, C, Benjamin, L, Farman, N, Lacolley, P, Henrion, D, Jaisser, F (2010) The endothelial mineralocorticoid receptor regulates vasoconstrictor tone and blood pressure. *FASEB J.* **24**(7)**:** 2454-2463.

Nguyen Dinh Cat, A, Ouvrard-Pascaud, A, Tronche, F, Clemessy, M, Gonzalez-Nunez, D, Farman, N, Jaisser, F (2009) Conditional transgenic mice for studying the role of the glucocorticoid receptor in the renal collecting duct. *Endocrinology* **150**(5)**:** 2202-2210.

Ni, M, Zhang, M, Ding, SF, Chen, WQ, Zhang, Y (2008) Micro-ultrasound imaging assessment of carotid plaque characteristics in apolipoprotein-E knockout mice. *Atherosclerosis* **197**(1)**:** 64-71.

Nicholson, AC, Frieda, S, Pearce, A, Silverstein, RL (1995) Oxidized LDL binds to CD36 on human monocyte-derived macrophages and transfected cell lines. Evidence implicating the lipid moiety of the lipoprotein as the binding site. *Arterioscler. Thromb. Vasc. Biol.* **15**(2)**:** 269-275.

Nuotio-Antar, AM, Hachey, D, Hasty, AH (2007) Carbenoxolone treatment attenuates symptoms of metabolic syndrome and atherogenesis in obese, hyperlipidemic mice. *Am. J. Physiol. Endocrinol. Metab.*

Nussey, S, Whitehead, S (2001) *Endocrinology: An Integrated Approach.* BIOS Scientific Publishers: Oxford.

O'Malley, MK, McDermott, EW, Mehigan, D, O'Higgins, NJ (1989) Role for prazosin in reducing the development of rabbit intimal hyperplasia after endothelial denudation. *Br J Surg* **76**(9)**:** 936-938.

Oakley, RH, Cidlowski, JA (1993) Homologous down regulation of the glucocorticoid receptor: the molecular machinery. *Crit. Rev. Eukaryot. Gene Expr.* **3**(2)**:** 63-88.

Oda, T, Jung, YO, Kim, HS, Cai, X, Lopez-Guisa, JM, Ikeda, Y, Eddy, AA (2001) PAI-1 deficiency attenuates the fibrogenic response to ureteral obstruction. *Kidney Int* **60**(2)**:** 587-596.

Oguchi, S, Dimayuga, P, Zhu, J, Chyu, KY, Yano, J, Shah, PK, Nilsson, J, Cercek, B (2000) Monoclonal antibody against vascular cell adhesion molecule-1 inhibits neointimal formation after periadventitial carotid artery injury in genetically hypercholesterolemic mice. *Arterioscler. Thromb. Vasc. Biol.* **20**(7)**:** 1729-1736.

Oishi, A, Takahashi, K, Ohmichi, M, Mochizuki, Y, Inaba, N, Kurachi, H (2011) Role of glucocorticoid receptor in the inhibitory effect of medroxyprogesterone acetate on the estrogen-induced endothelial nitric oxide synthase phosphorylation in human umbilical vein endothelial cells. *Fertil. Steril.* **95**(3)**:** 1168-1170.

Okada, SS, Tomaszewski, JE, Barnathan, ES (1995) Migrating vascular smooth muscle cells polarize cell surface urokinase receptors after injury in vitro. *Exp Cell Res* **217**(1)**:** 180-187.

Okwusidi, JI, Wong, HY, Cheng, KS, Loo, G (1991) Effects of diazepam, psychosocial stress and dietary cholesterol on pituitary-adrenocortical hormone levels and experimental atherosclerosis. *Artery* **18**(2)**:** 71-86.

Oster, H, Damerow, S, Kiessling, S, Jakubcakova, V, Abraham, D, Tian, J, Hoffmann, MW, Eichele, G (2006) The circadian rhythm of glucocorticoids is regulated by a gating mechanism residing in the adrenal cortical clock. *Cell Metab* **4**(2)**:** 163-173.

Osterrieder, W, Muller, RK, Powell, JS, Clozel, JP, Hefti, F, Baumgartner, HR (1991) Role of angiotensin II in injury-induced neointima formation in rats. *Hypertension* **18**(4 Suppl)**:** II60-64.

Palmer, RM, Ferrige, AG, Moncada, S (1987) Nitric oxide release accounts for the biological activity of endothelium-derived relaxing factor. *Nature* **327**(6122)**:** 524-526.

Parker, MG (1993) Steroid and related receptors. *Curr. Opin. Cell Biol.* **5**(3)**:** 499-504.

Patrassi, GM, Dal Bo Zanon, R, Boscaro, M, Martinelli, S, Girolami, A (1985) Further studies on the hypercoagulable state of patients with Cushing's syndrome. *Thromb. Haemost.* **54**(2)**:** 518-520.

Patrassi, GM, Sartori, MT, Livi, U, Casonato, A, Danesin, C, Vettore, S, Girolami, A (1997) Impairment of fibrinolytic potential in long-term steroid treatment after heart transplantation. *Transplantation* **64**(11)**:** 1610-1614.

Patrassi, GM, Sartori, MT, Rigotti, P, Di Landro, D, Theodoridis, P, Fioretti, M, Capalbo, M, Saggiorato, G, Boeri, G, Girolami, A (1995) Reduced fibrinolytic potential one year after kidney transplantation. Relationship to long-term steroid treatment. *Transplantation* **59**(10)**:** 1416-1420.

Patrassi, GM, Sartori, MT, Viero, ML, Scarano, L, Boscaro, M, Girolami, A (1992) The fibrinolytic potential in patients with Cushing's disease: a clue to their hypercoagulable state. *Blood Coagul Fibrinolysis* **3**(6)**:** 789-793.

Patti, G, Pasceri, V, Carminati, P, D'Ambrosio, A, Carcagni, A, Di Sciascio, G (2005) Effect of dexamethasone-eluting stents on systemic inflammatory response in patients with unstable angina pectoris or recent myocardial infarction undergoing percutaneous coronary intervention. *Am J Cardiol* **95**(4)**:** 502-505.

Peng, L, Bhatia, N, Parker, AC, Zhu, Y, Fay, WP (2002) Endogenous vitronectin and plasminogen activator inhibitor-1 promote neointima formation in murine carotid arteries. *Arterioscler. Thromb. Vasc. Biol.* **22**(6)**:** 934-939.

Pesarini, G, Ferrero, V, Tomai, F, Paloscia, L, De Cesare, N, Tamburino, C, Piscione, F, Vassanelli, F, Ribichini, F (2009) Steroid-eluting stents in patients with acute coronary syndromes. Angiographic results of DESIRE: Dexamethasone-Eluting Stent Italian REgistry. *J Invasive Cardiol* **21**(3)**:** 86-91.

Petrichenko, IE, Daret, D, Kolpakova, GV, Shakhov, YA, Larrue, J (1997) Glucocorticoids stimulate cholesteryl ester formation in human smooth muscle cells. *Arterioscler. Thromb. Vasc. Biol.* **17**(6)**:** 1143-1151.

Petrik, PV, Law, MM, Moore, WS, Colburn, MD, Quinones-Baldrich, W, Gelabert, HA (1998) Dexamethasone and enalapril suppress intimal hyperplasia individually but have no synergistic effect. *Annals of vascular surgery* **12**(3)**:** 216-220.

Pietersma, A, Kofflard, M, de Wit, LE, Stijnen, T, Koster, JF, Serruys, PW, Sluiter, W (1995) Late lumen loss after coronary angioplasty is associated with the activation status of circulating phagocytes before treatment. *Circulation* **91**(5)**:** 1320-1325.

Pinheiro, CH, de Sousa Filho, WM, de Oliveira Neto, J, Marinho Mde, J, Motta Neto, R, Smith, MM, Silva, CA (2009) Exercise prevents cardiometabolic alterations induced by chronic use of glucocorticoids. *Arq Bras Cardiol* **93**(4)**:** 400-408, 392-400.

Pinto, A, Carnuccio, R, Sorrentino, R, Di Rosa, M (1993) The inhibition of platelet aggregation by activated macrophages is blocked by dexamethasone. *Pharmacol Res* **27**(2)**:** 165-172.

Pires, NM, Schepers, A, van der Hoeven, BL, de Vries, MR, Boesten, LS, Jukema, JW, Quax, PH (2005) Histopathologic alterations following local delivery of dexamethasone to inhibit restenosis in murine arteries. *Cardiovasc. Res.* **68**(3)**:** 415-424.

Pirpiris, M, Yeung, S, Dewar, E, Jennings, GL, Whitworth, JA (1993) Hydrocortisone-induced hypertension in men. The role of cardiac output. *Am. J. Hypertens.* **6**(4)**:** 287-294.

Pitzalis, C, Pipitone, N, Perretti, M (2002) Regulation of leukocyte-endothelial interactions by glucocorticoids. *Ann N Y Acad Sci* **966:** 108-118.

Pivonello, R, De Martino, MC, De Leo, M, Lombardi, G, Colao, A (2008) Cushing's Syndrome. *Endocrinol. Metab. Clin. North Am.* **37**(1)**:** 135-149, ix.

Plekhanova, O, Parfyonova, Y, Bibilashvily, R, Domogatskii, S, Stepanova, V, Gulba, DC, Agrotis, A, Bobik, A, Tkachuk, V (2001) Urokinase plasminogen activator augments cell proliferation and neointima formation in injured arteries via proteolytic mechanisms. *Atherosclerosis* **159**(2)**:** 297-306.

Ploplis, VA, Castellino, FJ (2001) Attenuation of neointima formation following arterial injury in PAI-1 deficient mice. *Ann. N. Y. Acad. Sci.* **936:** 466-468.

Plump, AS, Smith, JD, Hayek, T, Aalto-Setala, K, Walsh, A, Verstuyft, JG, Rubin, EM, Breslow, JL (1992) Severe hypercholesterolemia and atherosclerosis in apolipoprotein E-deficient mice created by homologous recombination in ES cells. *Cell* **71**(2)**:** 343-353.

Pluta, RM (2006) Dysfunction of nitric oxide synthases as a cause and therapeutic target in delayed cerebral vasospasm after SAH. *Neurol Res* **28**(7)**:** 730-737.

Pollock, DM, Polakowski, JS, Divish, BJ, Opgenorth, TJ (1993) Angiotensin blockade reverses hypertension during long-term nitric oxide synthase inhibition. *Hypertension* **21**(5)**:** 660-666.

Poole, JC (1966) Phagocytosis of platelets by monocytes in organizing arterial thrombi. An electron microscopical study. *Q. J. Exp. Physiol. Cogn. Med. Sci.* **51**(1)**:** 54-59.

Poon, M, Gertz, SD, Fallon, JT, Wiegman, P, Berman, JW, Sarembock, IJ, Taubman, MB (2001) Dexamethasone inhibits macrophage accumulation after balloon arterial injury in cholesterol fed rabbits. *Atherosclerosis* **155**(2)**:** 371-380.

Powell, JS, Clozel, JP, Muller, RK, Kuhn, H, Hefti, F, Hosang, M, Baumgartner, HR (1989) Inhibitors of angiotensin-converting enzyme prevent myointimal proliferation after vascular injury. *Science (New York, N.Y* **245**(4914)**:** 186-188.

Preiss, DJ, Sattar, N (2007) Vascular cell adhesion molecule-1: a viable therapeutic target for atherosclerosis? *Int J Clin Pract* **61**(4)**:** 697-701.

Prescott, MF, McBride, CK, Court, M (1989) Development of intimal lesions after leukocyte migration into the vascular wall. *Am. J. Pathol.* **135**(5)**:** 835-846.

Preusch, MR, Rattazzi, M, Albrecht, C, Merle, U, Tuckermann, J, Schutz, G, Blessing, E, Zoppellaro, G, Pauletto, P, Krempien, R, Rosenfeld, ME, Katus, HA, Bea, F (2008) Critical role of macrophages in glucocorticoid driven vascular calcification in a mouse-model of atherosclerosis. *Arterioscler. Thromb. Vasc. Biol.* **28**(12)**:** 2158-2164.

Prisco, D, Fedi, S, Antonucci, E, Capanni, M, Chiarugi, L, Chioccioli, M, Falai, M, Giglioli, C, Abbate, R, Gensini, GF (2001) Postprocedural PAI-1 activity is a risk marker of subsequent clinical restenosis in patients both with and without stent implantation after elective balloon PTCA. *Thromb. Res.* **104**(3)**:** 181-186.

Pross, C, Farooq, MM, Angle, N, Lane, JS, Cerveira, JJ, Xavier, AE, Freischlag, JA, Law, RE, Gelabert, HA (2002) Dexamethasone inhibits vascular smooth muscle cell migration via modulation of matrix metalloproteinase activity. *J. Surg. Res.* **102**(2)**:** 57-62.

Pruett, SB, Padgett, EL (2004) Thymus-derived glucocorticoids are insufficient for normal thymus homeostasis in the adult mouse. *BMC Immunol* **5:** 24.

Puchtler, H, Waldrop, FS, Valentine, LS (1973) Polarization microscopic studies of connective tissue stained with picro-sirius red FBA. *Beitr Pathol* **150**(2)**:** 174-187.

Quax, PH, Lamfers, ML, Lardenoye, JH, Grimbergen, JM, de Vries, MR, Slomp, J, de Ruiter, MC, Kockx, MM, Verheijen, JH, van Hinsbergh, VW (2001) Adenoviral expression of a urokinase receptor-targeted protease inhibitor inhibits neointima formation in murine and human blood vessels. *Circulation* **103**(4)**:** 562-569.

Qureshi, AI, Suri, MF (2008) Acute reversal of clopidogrel-related platelet inhibition using methyl prednisolone in a patient with intracranial hemorrhage. *AJNR Am J Neuroradiol* **29**(10)**:** e97.

Rader, DJ, Pure, E (2005) Lipoproteins, macrophage function, and atherosclerosis: beyond the foam cell? *Cell Metab* **1**(4)**:** 223-230.

Raff, H (1987) Glucocorticoid inhibition of neurohypophysial vasopressin secretion. *Am. J. Physiol.* **252**(4 Pt 2)**:** R635-644.

Rao, DA, Eid, RE, Qin, L, Yi, T, Kirkiles-Smith, NC, Tellides, G, Pober, JS (2008) Interleukin (IL)-1 promotes allogeneic T cell intimal infiltration and IL-17 production in a model of human artery rejection. *J. Exp. Med.* **205**(13)**:** 3145-3158.

Reber, SO, Birkeneder, L, Veenema, AH, Obermeier, F, Falk, W, Straub, RH, Neumann, ID (2007) Adrenal insufficiency and colonic inflammation after a novel chronic psycho-social stress paradigm in mice: implications and mechanisms. *Endocrinology* **148**(2)**:** 670-682.

Reynolds, RM (2010) Corticosteroid-mediated programming and the pathogenesis of obesity and diabetes. *J. Steroid Biochem. Mol. Biol.* **122**(1-3)**:** 3-9.

Ribichini, F, Ferrero, V, Feola, M, Rognoni, A, Brunelleschi, S, Vacca, G, Vassanelli, C (2007a) Neutropenia in patients treated with thienopyridines and high-dose oral prednisone after percutaneous coronary interventions. *J Interv Cardiol* **20**(3)**:** 209-213.

Ribichini, F, Ferrero, V, Rognoni, A, Marino, P, Brunelleschi, S, Vassanelli, C (2007b) Percutaneous treatment of coronary bifurcations: lesion preparation before provisional bare metal stenting and subsequent immunosuppression with oral prednisone. The IMPRESS-Y study. *J. Interv. Cardiol.* **20**(2)**:** 114-121.

Ribichini, F, Joner, M, Ferrero, V, Finn, AV, Crimins, J, Nakazawa, G, Acampado, E, Kolodgie, FD, Vassanelli, C, Virmani, R (2007c) Effects of oral prednisone after stenting in a rabbit model of established atherosclerosis. *J. Am. Coll. Cardiol.* **50**(2)**:** 176-185.

Ribichini, F, Tomai, F, De Luca, G, Boccuzzi, G, Presbitero, P, Pesarini, G, Ferrero, V, Ghini, AS, Pastori, F, De Luca, L, Zavalloni, D, Soregaroli, D, Garbo, R, Franchi, E, Marino, P, Minelli, M, Vassanelli, C (2009) A multicenter, randomized study to test immunosuppressive therapy with oral prednisone for the prevention of restenosis after percutaneous coronary interventions: cortisone plus BMS or DES versus BMS alone to eliminate restenosis (CEREA-DES) - study design and rationale. *J Cardiovasc Med (Hagerstown)* **10**(2)**:** 192-199.

Ribichini, F, Tomai, F, Ferrero, V, Versaci, F, Boccuzzi, G, Proietti, I, Prati, F, Crea, F, Vassanelli, C (2005) Immunosuppressive oral prednisone after percutaneous interventions in patients with multi-vessel coronary artery disease. The IMPRESS-2/MVD study. *EuroIntervention* **1**(2)**:** 173-180.

Richardson, PD, Davies, MJ, Born, GV (1989) Influence of plaque configuration and stress distribution on fissuring of coronary atherosclerotic plaques. *Lancet* **2**(8669)**:** 941-944.

Rickard, AJ, Young, MJ (2009) Corticosteroid receptors, macrophages and cardiovascular disease. *J Mol Endocrinol* **42**(6)**:** 449-459.

Rodriguez, AE (2009) Emerging drugs for coronary restenosis: the role of systemic oral agents the in stent era. *Expert Opin Emerg Drugs* **14**(4)**:** 561-576.

Rodriguez, AE, Granada, JF, Rodriguez-Alemparte, M, Vigo, CF, Delgado, J, Fernandez-Pereira, C, Pocovi, A, Rodriguez-Granillo, AM, Schulz, D, Raizner, AE, Palacios, I, O'Neill, W, Kaluza, GL, Stone, G (2006) Oral rapamycin after coronary bare-metal stent implantation to prevent restenosis: the Prospective, Randomized Oral Rapamycin in Argentina (ORAR II) Study. *J. Am. Coll. Cardiol.* **47**(8)**:** 1522-1529.

Rodriguez, AE, Maree, A, Tarragona, S, Fernandez-Pereira, C, Santaera, O, Granillo, AM, Rodriguez-Granillo, GA, Russo-Felssen, M, Kukreja, N, Antoniucci, D, Palacios, IF, Serruys, PW (2009) Percutaneous coronary intervention with oral sirolimus and bare metal stents has comparable safety and efficacy to treatment with drug eluting stents, but with

significant cost saving: long-term follow-up results from the randomised, controlled ORAR III (Oral Rapamycin in ARgentina) study. *EuroIntervention* **5**(2)**:** 255-264.

Rogers, C, Edelman, ER, Simon, DI (1998) A mAb to the beta2-leukocyte integrin Mac-1 (CD11b/CD18) reduces intimal thickening after angioplasty or stent implantation in rabbits. *Proc. Natl. Acad. Sci. U. S. A.* **95**(17)**:** 10134-10139.

Rosenfeld, S, Marmorston, J, Sobel, H, White, AE (1960) Enhancement of experimental atherosclerosis by ACTH in the dog. *Proc. Soc. Exp. Biol. Med.* **103:** 83-86.

Rosenstock, J, Banarer, S, Fonseca, VA, Inzucchi, SE, Sun, W, Yao, W, Hollis, G, Flores, R, Levy, R, Williams, WV, Seckl, JR, Huber, R (2010) The 11-beta-hydroxysteroid dehydrogenase type 1 inhibitor INCB13739 improves hyperglycemia in patients with type 2 diabetes inadequately controlled by metformin monotherapy. *Diabetes Care* **33**(7)**:** 1516-1522.

Ross, EJ, Linch, DC (1982) Cushing's syndrome--killing disease: discriminatory value of signs and symptoms aiding early diagnosis. *Lancet* **2**(8299)**:** 646-649.

Ross, R (1999) Atherosclerosis--an inflammatory disease. *N. Engl. J. Med.* **340**(2)**:** 115-126.

Ross, R (1993) The pathogenesis of atherosclerosis: a perspective for the 1990s. *Nature* **362**(6423)**:** 801-809.

Ross, R, Glomset, J, Harker, L (1977) Response to injury and atherogenesis. *Am. J. Pathol.* **86**(3)**:** 675-684.

Ross, R, Glomset, JA (1976a) The pathogenesis of atherosclerosis (first of two parts). *N. Engl. J. Med.* **295**(7)**:** 369-377.

Ross, R, Glomset, JA (1976b) The pathogenesis of atherosclerosis (second of two parts). *N. Engl. J. Med.* **295**(8)**:** 420-425.

Roy, P, Okabe, T, Pinto Slottow, TL, Steinberg, DH, Smith, K, Torguson, R, Xue, Z, Gevorkian, N, Satler, LF, Kent, KM, Suddath, WO, Pichard, AD, Waksman, R (2007) Correlates of clinical restenosis following intracoronary implantation of drug-eluting stents. *Am. J. Cardiol.* **100**(6)**:** 965-969.

Ruetten, H, Thiemermann, C (1997) Endothelin-1 stimulates the biosynthesis of tumour necrosis factor in macrophages: ET-receptors, signal transduction and inhibition by dexamethasone. *J Physiol Pharmacol* **48**(4)**:** 675-688.

Sahara, M, Sata, M, Morita, T, Nakamura, K, Hirata, Y, Nagai, R (2007) Diverse contribution of bone marrow-derived cells to vascular remodeling associated with pulmonary arterial hypertension and arterial neointimal formation. *Circulation* **115**(4)**:** 509-517.

Sakai, M, Biwa, T, Matsumura, T, Takemura, T, Matsuda, H, Anami, Y, Sasahara, T, Kobori, S, Shichiri, M (1999) Glucocorticoid inhibits oxidized LDL-induced macrophage growth by suppressing the expression of granulocyte/macrophage colony-stimulating factor. *Arterioscler. Thromb. Vasc. Biol.* **19**(7)**:** 1726-1733.

Sakata, K, Miura, F, Sugino, H, Shinobe, M, Shirotani, M, Yoshida, H, Mori, N, Hoshino, T, Takada, A (1996) Impaired fibrinolysis early after percutaneous transluminal coronary angioplasty is associated with restenosis. *Am. Heart J.* **131**(1)**:** 1-6.

Saladin, R, Vu-Dac, N, Fruchart, JC, Auwerx, J, Staels, B (1996) Transcriptional induction of rat liver apolipoprotein A-I gene expression by glucocorticoids requires the glucocorticoid receptor and a labile cell-specific protein. *Eur. J. Biochem.* **239**(2)**:** 451-459.

Salvayre, R, Auge, N, Benoist, H, Negre-Salvayre, A (2002) Oxidized low-density lipoprotein-induced apoptosis. *Biochim Biophys Acta* **1585**(2-3)**:** 213-221.

San Feliciano, L, Remesal, A, Isidoro-Garcia, M, Ludena, D (2011) Dexamethasone and betamethasone for prenatal lung maturation: differences in vascular endothelial growth factor expression and alveolarization in rats. *Neonatology* **100**(1)**:** 105-110.

Sartori, TM, Maurizio, PG, Sara, P, Ugolino, L, Annalisa, A, Panagiotis, T, Massimo, F, Antonio, G (1999) Relation between long-term steroid treatment after heart transplantation, hypofibrinolysis and myocardial microthrombi generation. *J Heart Lung Transplant* **18**(7)**:** 693-700.

Sata, M, Maejima, Y, Adachi, F, Fukino, K, Saiura, A, Sugiura, S, Aoyagi, T, Imai, Y, Kurihara, H, Kimura, K, Omata, M, Makuuchi, M, Hirata, Y, Nagai, R (2000) A mouse model of vascular injury that induces rapid onset of medial cell apoptosis followed by reproducible neointimal hyperplasia. *J. Mol. Cell. Cardiol.* **32**(11)**:** 2097-2104.

Sata, M, Saiura, A, Kunisato, A, Tojo, A, Okada, S, Tokuhisa, T, Hirai, H, Makuuchi, M, Hirata, Y, Nagai, R (2002) Hematopoietic stem cells differentiate into vascular cells that participate in the pathogenesis of atherosclerosis. *Nat. Med.* **8**(4)**:** 403-409.

Sato, A, Suzuki, H, Murakami, M, Nakazato, Y, Iwaita, Y, Saruta, T (1994) Glucocorticoid increases angiotensin II type 1 receptor and its gene expression. *Hypertension* **23**(1)**:** 25-30.

Scarpati, EM, Sadler, JE (1989) Regulation of endothelial cell coagulant properties. Modulation of tissue factor, plasminogen activator inhibitors, and thrombomodulin by phorbol 12-myristate 13-acetate and tumor necrosis factor. *J. Biol. Chem.* **264**(34)**:** 20705-20713.

Schafer, K, Konstantinides, S, Riedel, C, Thinnes, T, Muller, K, Dellas, C, Hasenfuss, G, Loskutoff, DJ (2002) Different mechanisms of increased luminal stenosis after arterial injury in mice deficient for urokinase- or tissue-type plasminogen activator. *Circulation* **106**(14)**:** 1847-1852.

Schafer, K, Schroeter, MR, Dellas, C, Puls, M, Nitsche, M, Weiss, E, Hasenfuss, G, Konstantinides, SV (2006) Plasminogen activator inhibitor-1 from bone marrow-derived cells suppresses neointimal formation after vascular injury in mice. *Arterioscler. Thromb. Vasc. Biol.* **26**(6)**:** 1254-1259.

Schepers, A, Eefting, D, Bonta, PI, Grimbergen, JM, de Vries, MR, van Weel, V, de Vries, CJ, Egashira, K, van Bockel, JH, Quax, PH (2006) Anti-MCP-1 gene therapy inhibits vascular smooth muscle cells proliferation and attenuates vein graft thickening both in vitro and in vivo. *Arterioscler. Thromb. Vasc. Biol.* **26**(9)**:** 2063-2069.

Schwartz, L, Bourassa, MG, Lesperance, J, Aldridge, HE, Kazim, F, Salvatori, VA, Henderson, M, Bonan, R, David, PR (1988) Aspirin and dipyridamole in the prevention of restenosis after percutaneous transluminal coronary angioplasty. *N. Engl. J. Med.* **318**(26)**:** 1714-1719.

Schwartz, RS, Henry, TD (2002) Pathophysiology of coronary artery restenosis. *Rev. Cardiovasc. Med.* **3 Suppl 5:** S4-9.

Schwartz, RS, Holmes, DR, Jr., Topol, EJ (1992a) The restenosis paradigm revisited: an alternative proposal for cellular mechanisms. *J. Am. Coll. Cardiol.* **20**(5)**:** 1284-1293.

Schwartz, RS, Huber, KC, Murphy, JG, Edwards, WD, Camrud, AR, Vlietstra, RE, Holmes, DR (1992b) Restenosis and the proportional neointimal response to coronary artery injury: results in a porcine model. *J. Am. Coll. Cardiol.* **19**(2)**:** 267-274.

Schwartz, SM, Campbell, GR, Campbell, JH (1986) Replication of smooth muscle cells in vascular disease. *Circ. Res.* **58**(4)**:** 427-444.

Schwartz, SM, Stemerman, MB, Benditt, EP (1975) The aortic intima. II. Repair of the aortic lining after mechanical denudation. *Am. J. Pathol.* **81**(1)**:** 15-42.

Schwer, HD, Lecine, P, Tiwari, S, Italiano, JE, Jr., Hartwig, JH, Shivdasani, RA (2001) A lineage-restricted and divergent beta-tubulin isoform is essential for the biogenesis, structure and function of blood platelets. *Curr Biol* **11**(8)**:** 579-586.

Seckl, JR (2004) Prenatal glucocorticoids and long-term programming. *Eur. J. Endocrinol.* **151 Suppl 3:** U49-62.

Seckl, JR, Walker, BR (2001) Minireview: 11beta-hydroxysteroid dehydrogenase type 1- a tissue-specific amplifier of glucocorticoid action. *Endocrinology* **142**(4)**:** 1371-1376.

Selzman, CH, Shames, BD, Reznikov, LL, Miller, SA, Meng, X, Barton, HA, Werman, A, Harken, AH, Dinarello, CA, Banerjee, A (1999) Liposomal delivery of purified inhibitory-kappaBalpha inhibits tumor necrosis factor-alpha-induced human vascular smooth muscle proliferation. *Circ. Res.* **84**(8)**:** 867-875.

Severino, C, Brizzi, P, Solinas, A, Secchi, G, Maioli, M, Tonolo, G (2002) Low-dose dexamethasone in the rat: a model to study insulin resistance. *Am J Physiol Endocrinol Metab* **283**(2)**:** E367-373.

Shah, PK, Amin, J (1992) Low high density lipoprotein level is associated with increased restenosis rate after coronary angioplasty. *Circulation* **85**(4)**:** 1279-1285.

Shanahan, CM, Weissberg, PL (1998) Smooth muscle cell heterogeneity: patterns of gene expression in vascular smooth muscle cells in vitro and in vivo. *Arterioscler. Thromb. Vasc. Biol.* **18**(3)**:** 333-338.

Shantsila, E, Lip, GY (2009) The role of monocytes in thrombotic disorders. Insights from tissue factor, monocyte-platelet aggregates and novel mechanisms. *Thromb. Haemost.* **102**(5)**:** 916-924.

Sharpe, J, Ahlgren, U, Perry, P, Hill, B, Ross, A, Hecksher-Sorensen, J, Baldock, R, Davidson, D (2002) Optical projection tomography as a tool for 3D microscopy and gene expression studies. *Science (New York, N.Y* **296**(5567)**:** 541-545.

Shiba, Y, Takahashi, M, Yoshioka, T, Yajima, N, Morimoto, H, Izawa, A, Ise, H, Hatake, K, Motoyoshi, K, Ikeda, U (2007) M-CSF accelerates neointimal formation in the early phase after vascular injury in mice: the critical role of the SDF-1-CXCR4 system. *Arteriosclerosis, thrombosis, and vascular biology* **27**(2)**:** 283-289.

Shields, PP, Dixon, JE, Glembotski, CC (1988) The secretion of atrial natriuretic factor-(99-126) by cultured cardiac myocytes is regulated by glucocorticoids. *J. Biol. Chem.* **263**(25)**:** 12619-12628.

Shiomi, M, Yamada, S, Amano, Y, Nishimoto, T, Ito, T (2008) Lapaquistat acetate, a squalene synthase inhibitor, changes macrophage/lipid-rich coronary plaques of hypercholesterolaemic rabbits into fibrous lesions. *Br. J. Pharmacol.* **154**(5)**:** 949-957.

Shirasawa, K, Chandler, AB (1971) Phagocytosis of platelets by leukocytes in artificial thrombi and in platelet aggregates induced by adenosine diphosphate. *Am. J. Pathol.* **63**(2)**:** 215-230.

Shively, CA, Register, TC, Clarkson, TB (2009) Social stress, visceral obesity, and coronary artery atherosclerosis: product of a primate adaptation. *Am. J. Primatol.* **71**(9)**:** 742-751.

Shofuda, K, Nagashima, Y, Kawahara, K, Yasumitsu, H, Miki, K, Miyazaki, K (1998) Elevated expression of membrane-type 1 and 3 matrix metalloproteinases in rat vascular smooth muscle cells activated by arterial injury. *Lab. Invest.* **78**(8)**:** 915-923.

Siebe, H, Baude, G, Lichtenstein, I, Wang, D, Buhler, H, Hoyer, GA, Hierholzer, K (1993) Metabolism of dexamethasone: sites and activity in mammalian tissues. *Ren. Physiol. Biochem.* **16**(1-2)**:** 79-88.

Simon, DI, Ezratty, AM, Francis, SA, Rennke, H, Loscalzo, J (1993) Fibrin(ogen) is internalized and degraded by activated human monocytoid cells via Mac-1 (CD11b/CD18): a nonplasmin fibrinolytic pathway. *Blood* **82**(8)**:** 2414-2422.

Sims, PJ, Wiedmer, T, Esmon, CT, Weiss, HJ, Shattil, SJ (1989) Assembly of the platelet prothrombinase complex is linked to vesiculation of the platelet plasma membrane. Studies in Scott syndrome: an isolated defect in platelet procoagulant activity. *J. Biol. Chem.* **264**(29)**:** 17049-17057.

Sintnicolaas, K, de Vries, W, van der Linden, R, Gratama, JW, Bolhuis, RL (1991) Simultaneous flow cytometric detection of antibodies against platelets, granulocytes and lymphocytes. *J Immunol Methods* **142**(2)**:** 215-222.

Sjoberg, HE, Blomback, M, Granberg, PO (1976) Thromboembolic complications, heparin treatment in increase in coagulation factors in Cushing's syndrome. *Acta Med. Scand.* **199**(1-2)**:** 95-98.

Small, DM (1988) George Lyman Duff memorial lecture. Progression and regression of atherosclerotic lesions. Insights from lipid physical biochemistry. *Arteriosclerosis* **8**(2)**:** 103-129.

Small, GR, Hadoke, PW, Sharif, I, Dover, AR, Armour, D, Kenyon, CJ, Gray, GA, Walker, BR (2005) Preventing local regeneration of glucocorticoids by 11beta-hydroxysteroid dehydrogenase type 1 enhances angiogenesis. *Proc. Natl. Acad. Sci. U. S. A.* **102**(34)**:** 12165-12170.

Smets, P, Meyer, E, Maddens, B, Daminet, S (2010) Cushing's syndrome, glucocorticoids and the kidney. *Gen. Comp. Endocrinol.* **169**(1)**:** 1-10.

Smith, ID, Shearman, RP (1974) Fetal plasma steroids in relation to parturition. I. The effect of gestational age upon umbilical plasma corticosteroid levels following vaginal delivery. *J. Obstet. Gynaecol. Br. Commonw.* **81**(1)**:** 11-15.

Smith, L, Smith, JB (1994) Regulation of sodium-calcium exchanger by glucocorticoids and growth factors in vascular smooth muscle. *J. Biol. Chem.* **269**(44)**:** 27527-27531.

Solomon, DH, Avorn, J, Katz, JN, Weinblatt, ME, Setoguchi, S, Levin, R, Schneeweiss, S (2006) Immunosuppressive medications and hospitalization for cardiovascular events in patients with rheumatoid arthritis. *Arthritis Rheum.* **54**(12)**:** 3790-3798.

Soo, KS, Northeast, AD, Happerfield, LC, Burnand, KG, Bobrow, LG (1996) Tissue plasminogen activator production by monocytes in venous thrombolysis. *J. Pathol.* **178**(2)**:** 190-194.

Souverein, PC, Berard, A, Van Staa, TP, Cooper, C, Egberts, AC, Leufkens, HG, Walker, BR (2004) Use of oral glucocorticoids and risk of cardiovascular and cerebrovascular disease in a population based case-control study. *Heart (British Cardiac Society)* **90**(8)**:** 859-865.

Sower, LE, Froelich, CJ, Carney, DH, Fenton, JW, 2nd, Klimpel, GR (1995) Thrombin induces IL-6 production in fibroblasts and epithelial cells. Evidence for the involvement of the seven-transmembrane domain (STD) receptor for alpha-thrombin. *J. Immunol.* **155**(2)**:** 895-901.

Stary, HC (1992) Composition and classification of human atherosclerotic lesions. *Virchows Arch. A Pathol. Anat. Histopathol.* **421**(4)**:** 277-290.

Stary, HC (1990) The sequence of cell and matrix changes in atherosclerotic lesions of coronary arteries in the first forty years of life. *Eur. Heart J.* **11 Suppl E:** 3-19.

Stary, HC, Chandler, AB, Dinsmore, RE, Fuster, V, Glagov, S, Insull, W, Jr., Rosenfeld, ME, Schwartz, CJ, Wagner, WD, Wissler, RW (1995) A definition of advanced types of atherosclerotic lesions and a histological classification of atherosclerosis. A report from the Committee on Vascular Lesions of the Council on Arteriosclerosis, American Heart Association. *Circulation* **92**(5)**:** 1355-1374.

Stary, HC, Chandler, AB, Glagov, S, Guyton, JR, Insull, W, Jr., Rosenfeld, ME, Schaffer, SA, Schwartz, CJ, Wagner, WD, Wissler, RW (1994) A definition of initial, fatty streak, and intermediate lesions of atherosclerosis. A report from the Committee on Vascular Lesions of the Council on Arteriosclerosis, American Heart Association. *Circulation* **89**(5)**:** 2462-2478.

Stefansson, S, Lawrence, DA (1996) The serpin PAI-1 inhibits cell migration by blocking integrin alpha V beta 3 binding to vitronectin. *Nature* **383**(6599)**:** 441-443.

Steg, PG, Pasquier, C, Huu, TP, Chollet-Martin, S, Juliard, JM, Himbert, D, Pocidalo, MA, Gourgon, R, Hakim, J (1993) Evidence for priming and activation of neutrophils early after coronary angioplasty. *Eur J Med* **2**(1)**:** 6-10.

Stellato, C (2004) Post-transcriptional and nongenomic effects of glucocorticoids. *Proc. Am. Thorac. Soc.* **1**(3)**:** 255-263.

Stone, GW, Moses, JW, Ellis, SG, Schofer, J, Dawkins, KD, Morice, MC, Colombo, A, Schampaert, E, Grube, E, Kirtane, AJ, Cutlip, DE, Fahy, M, Pocock, SJ, Mehran, R, Leon, MB (2007) Safety and efficacy of sirolimus- and paclitaxel-eluting coronary stents. *N. Engl. J. Med.* **356**(10)**:** 998-1008.

Stratakis, CA, Boikos, SA (2007) Genetics of adrenal tumors associated with Cushing's syndrome: a new classification for bilateral adrenocortical hyperplasias. *Nat. Clin. Pract. Endocrinol. Metab.* **3**(11)**:** 748-757.

Strauss, BH, Lau, HK, Bowman, KA, Sparkes, J, Chisholm, RJ, Garvey, MB, Fenkell, LL, Natarajan, MK, Singh, I, Teitel, JM (1999) Plasma urokinase antigen and plasminogen activator inhibitor-1 antigen levels predict angiographic coronary restenosis. *Circulation* **100**(15)**:** 1616-1622.

Stravitz, RT, Sanyal, AJ (2003) Drug-induced steatohepatitis. *Clin Liver Dis* **7**(2)**:** 435-451.

Strawn, WB, Ferrario, CM (2002) Mechanisms linking angiotensin II and atherogenesis. *Curr. Opin. Lipidol.* **13**(5)**:** 505-512.

Strecker, EP, Gabelmann, A, Boos, I, Lucas, C, Xu, Z, Haberstroh, J, Freudenberg, N, Stricker, H, Langer, M, Betz, E (1998) Effect on intimal hyperplasia of dexamethasone released from coated metal stents compared with non-coated stents in canine femoral arteries. *Cardiovasc. Intervent. Radiol.* **21**(6)**:** 487-496.

Sun, H, Sheveleva, E, Chen, QM (2008) Corticosteroids induce cyclooxygenase 1 expression in cardiomyocytes: role of glucocorticoid receptor and Sp3 transcription factor. *Mol. Endocrinol.* **22**(9)**:** 2076-2084.

Sun, HW, Miao, CY, Liu, L, Zhou, J, Su, DF, Wang, YX, Jiang, CL (2006) Rapid inhibitory effect of glucocorticoids on airway smooth muscle contractions in guinea pigs. *Steroids* **71**(2)**:** 154-159.

Suzuki, J, Iwai, M, Mogi, M, Oshita, A, Yoshii, T, Higaki, J, Horiuchi, M (2006) Eplerenone with valsartan effectively reduces atherosclerotic lesion by attenuation of oxidative stress and inflammation. *Arterioscler. Thromb. Vasc. Biol.* **26**(4)**:** 917-921.

Suzuki, J, Ogawa, M, Muto, S, Yamaguchi, Y, Itai, A, Isobe, M (2008) The effects of pharmacological PAI-1 inhibition on thrombus formation and neointima formation after arterial injury. *Expert Opin. Ther. Targets* **12**(7)**:** 783-794.

Suzuki, T, Ishiwata, S, Hasegawa, K, Yamamoto, K, Yamazaki, T (2000) Raised interleukin 6 concentrations as a predictor of postangioplasty restenosis. *Heart (British Cardiac Society)* **83**(5)**:** 578.

Swindell, AC, Krupp, MN, Twomey, TM, Reynolds, JA, Chichester, CO (1993) Effects of doxazosin on atherosclerosis in cholesterol-fed rabbits. *Atherosclerosis* **99**(2)**:** 195-206.

Szaba, FM, Smiley, ST (2002) Roles for thrombin and fibrin(ogen) in cytokine/chemokine production and macrophage adhesion in vivo. *Blood* **99**(3)**:** 1053-1059.

Taatjes, DJ, Wadsworth, MP, Quinn, AS, Rand, JH, Bovill, EG, Sobel, BE (2008) Imaging aspects of cardiovascular disease at the cell and molecular level. *Histochem Cell Biol* **130**(2)**:** 235-245.

Takai, S, Jin, D, Muramatsu, M, Kirimura, K, Sakonjo, H, Miyazaki, M (2005) Eplerenone inhibits atherosclerosis in nonhuman primates. *Hypertension* **46**(5)**:** 1135-1139.

Take, S, Matsutani, M, Ueda, H, Hamaguchi, H, Konishi, H, Baba, Y, Kawaratani, H, Sugiura, T, Iwasaka, T, Inada, M (1997) Effect of cilostazol in preventing restenosis after percutaneous transluminal coronary angioplasty. *Am J Cardiol* **79**(8)**:** 1097-1099.

Tanaka, H, Sukhova, GK, Swanson, SJ, Clinton, SK, Ganz, P, Cybulsky, MI, Libby, P (1993) Sustained activation of vascular cells and leukocytes in the rabbit aorta after balloon injury. *Circulation* **88**(4 Pt 1)**:** 1788-1803.

Tanaka, K, Sata, M, Hirata, Y, Nagai, R (2003) Diverse contribution of bone marrow cells to neointimal hyperplasia after mechanical vascular injuries. *Circulation research* **93**(8)**:** 783-790.

Tasker, JG, Di, S, Malcher-Lopes, R (2006) Minireview: rapid glucocorticoid signaling via membrane-associated receptors. *Endocrinology* **147**(12)**:** 5549-5556.

Tauchi, Y, Zushida, L, Chono, S, Sato, J, Ito, K, Morimoto, K (2001) Effect of dexamethasone palmitate-low density lipoprotein complex on cholesterol ester accumulation in aorta of atherogenic model mice. *Biol. Pharm. Bull.* **24**(8)**:** 925-929.

Tauchi, Y, Zushida, L, Yokota, M, Chono, S, Sato, J, Ito, K, Morimoto, K (2000) Inhibitory effect of dexamethasone palmitate-low density lipoprotein complex on low density lipoprotein-induced macrophage foam cell formation. *Biol Pharm Bull* **23**(4)**:** 466-471.

Tauchmanova, L, Rossi, R, Biondi, B, Pulcrano, M, Nuzzo, V, Palmieri, EA, Fazio, S, Lombardi, G (2002) Patients with subclinical Cushing's syndrome due to adrenal adenoma have increased cardiovascular risk. *J. Clin. Endocrinol. Metab.* **87**(11)**:** 4872-4878.

Temel, RE, Rudel, LL (2007) Diet effects on atherosclerosis in mice. *Curr Drug Targets* **8**(11)**:** 1150-1160.

Ten, S, New, M, Maclaren, N (2001) Clinical review 130: Addison's disease 2001. *J. Clin. Endocrinol. Metab.* **86**(7)**:** 2909-2922.

Thieringer, R, Le Grand, CB, Carbin, L, Cai, TQ, Wong, B, Wright, SD, Hermanowski-Vosatka, A (2001) 11 Beta-hydroxysteroid dehydrogenase type 1 is induced in human monocytes upon differentiation to macrophages. *J. Immunol.* **167**(1)**:** 30-35.

Thomson, SP, Stump, CS, Kurukulasuriya, LR, Sowers, JR (2007) Adrenal steroids and the metabolic syndrome. *Curr. Hypertens. Rep.* **9**(6)**:** 512-519.

Thuesen, L, Holm, NR (2010) Late coronary stent thrombosis. *Minerva Med* **101**(1)**:** 25-33.

Thyberg, J (1998) Phenotypic modulation of smooth muscle cells during formation of neointimal thickenings following vascular injury. *Histol Histopathol* **13**(3)**:** 871-891.

Tomlinson, JW, Walker, EA, Bujalska, IJ, Draper, N, Lavery, GG, Cooper, MS, Hewison, M, Stewart, PM (2004) 11beta-hydroxysteroid dehydrogenase type 1: a tissue-specific regulator of glucocorticoid response. *Endocr. Rev.* **25**(5)**:** 831-866.

Toomey, JR, Kratzer, KE, Lasky, NM, Stanton, JJ, Broze, GJ, Jr. (1996) Targeted disruption of the murine tissue factor gene results in embryonic lethality. *Blood* **88**(5)**:** 1583-1587.

Tordoff, MG (1996) Adrenalectomy decreases NaCl intake of rats fed low-calcium diets. *Am J Physiol* **270**(1 Pt 2)**:** R11-21.

Tortora, GJ, Grabowski, SR (2003) *Principles of anatomy and physiology*. John Wiley & Sons, Inc.

Tounian, P, Schneiter, P, Henry, S, Delarue, J, Tappy, L (1997) Effects of dexamethasone on hepatic glucose production and fructose metabolism in healthy humans. *Am. J. Physiol.* **273**(2 Pt 1)**:** E315-320.

Tous, M, Ribas, V, Escola-Gil, JC, Blanco-Vaca, F, Calpe-Berdiel, L, Coll, B, Ferre, N, Alonso-Villaverde, C, Rull, A, Camps, J, Joven, J (2006) Manipulation of inflammation modulates hyperlipidemia in apolipoprotein E-deficient mice: a possible role for interleukin-6. *Cytokine* **34**(3-4)**:** 224-232.

Trogan, E, Fayad, ZA, Itskovich, VV, Aguinaldo, JG, Mani, V, Fallon, JT, Chereshnev, I, Fisher, EA (2004) Serial studies of mouse atherosclerosis by in vivo magnetic resonance imaging detect lesion regression after correction of dyslipidemia. *Arterioscler. Thromb. Vasc. Biol.* **24**(9)**:** 1714-1719.

Tsantarliotou, M, Taitzoglou, I, Kokolis, N (1999) The effect of dexamethasone on tissue fibrinolytic system in male and female rats. *In Vivo* **13**(2)**:** 119-124.

Tsuchikane, E, Fukuhara, A, Kobayashi, T, Kirino, M, Yamasaki, K, Izumi, M, Otsuji, S, Tateyama, H, Sakurai, M, Awata, N (1999) Impact of cilostazol on restenosis after percutaneous coronary balloon angioplasty. *Circulation* **100**(1)**:** 21-26.

Uchiba, M, Okajima, K, Murakami, K (1998) Effects of various doses of antithrombin III on endotoxin-induced endothelial cell injury and coagulation abnormalities in rats. *Thromb. Res.* **89**(5)**:** 233-241.

Uchida, K, Sasahara, M, Morigami, N, Hazama, F, Kinoshita, M (1996) Expression of platelet-derived growth factor B-chain in neointimal smooth muscle cells of balloon injured rabbit femoral arteries. *Atherosclerosis* **124**(1)**:** 9-23.

Ueda, M, Becker, AE, Tsukada, T, Numano, F, Fujimoto, T (1991) Fibrocellular tissue response after percutaneous transluminal coronary angioplasty. An immunocytochemical analysis of the cellular composition. *Circulation* **83**(4)**:** 1327-1332.

Ullian, ME (1999) The role of corticosteriods in the regulation of vascular tone. *Cardiovasc. Res.* **41**(1)**:** 55-64.

Val, P, Jeays-Ward, K, Swain, A (2006) Identification of a novel population of adrenal-like cells in the mammalian testis. *Dev Biol* **299**(1)**:** 250-256.

Valero, F, Hamon, M, Fournier, C, Meurice, T, Flautre, B, Van Belle, E, Lablanche, JM, Gosselin, B, Bauters, C, Bertrand, M (1998) Intramural injection of biodegradable microspheres as a local drug-delivery system to inhibit neointimal thickening in a rabbit model of balloon angioplasty. *Journal of cardiovascular pharmacology* **31**(4)**:** 513-519.

van der Hoeven, BL, Pires, NM, Warda, HM, Putter, H, Quax, PH, Schalij, MJ, Jukema, JW (2008) Dexamethasone-eluting stents for the prevention of in-stent restenosis: evidence for a differential effect in insulin-dependent and non-insulin-dependent diabetic patients. *Int J Cardiol* **124**(2)**:** 166-171.

van der Poll, T, de Jonge, E, Levi, M (2001) Regulatory role of cytokines in disseminated intravascular coagulation. *Semin. Thromb. Hemost.* **27**(6)**:** 639-651.

van der Poll, T, Levi, M, Buller, HR, van Deventer, SJ, de Boer, JP, Hack, CE, ten Cate, JW (1991) Fibrinolytic response to tumor necrosis factor in healthy subjects. *J. Exp. Med.* **174**(3)**:** 729-732.

van Deventer, SJ, Buller, HR, ten Cate, JW, Aarden, LA, Hack, CE, Sturk, A (1990) Experimental endotoxemia in humans: analysis of cytokine release and coagulation, fibrinolytic, and complement pathways. *Blood* **76**(12)**:** 2520-2526.

van Giezen, JJ, Brakkee, JG, Dreteler, GH, Bouma, BN, Jansen, JW (1994) Dexamethasone affects platelet aggregation and fibrinolytic activity in rats at different doses which is reflected by their effect on arterial thrombosis. *Blood Coagul. Fibrinolysis* **5**(2)**:** 249-255.

van Giezen, JJ, Jansen, JW (1992) Inhibition of fibrinolytic activity in-vivo by dexamethasone is counterbalanced by an inhibition of platelet aggregation. *Thromb. Haemost.* **68**(1)**:** 69-73.

Van Herck, JL, De Meyer, GR, Martinet, W, Van Hove, CE, Foubert, K, Theunis, MH, Apers, S, Bult, H, Vrints, CJ, Herman, AG (2009) Impaired fibrillin-1 function promotes features of plaque instability in apolipoprotein E-deficient mice. *Circulation* **120**(24)**:** 2478-2487.

Van Put, DJ, Van Hove, CE, De Meyer, GR, Wuyts, F, Herman, AG, Bult, H (1995) Dexamethasone influences intimal thickening and vascular reactivity in the rabbit collared carotid artery. *European journal of pharmacology* **294**(2-3)**:** 753-761.

van Raalte, DH, Ouwens, DM, Diamant, M (2009) Novel insights into glucocorticoid-mediated diabetogenic effects: towards expansion of therapeutic options? *Eur. J. Clin. Invest.* **39**(2)**:** 81-93.

Vashisht, R, Sian, M, Franks, PJ, O'Malley, MK (1992) Long-term reduction of intimal hyperplasia by the selective alpha-1 adrenergic antagonist doxazosin. *Br J Surg* **79**(12)**:** 1285-1288.

Vedeler, CA, Nyland, H, Matre, R (1984) In situ characterization of the foam cells in early human atherosclerotic lesions. *Acta Pathol. Microbiol. Immunol. Scand. [C]* **92**(2)**:** 133-137.

Versaci, F, Gaspardone, A, Tomai, F, Ribichini, F, Russo, P, Proietti, I, Ghini, AS, Ferrero, V, Chiariello, L, Gioffre, PA, Romeo, F, Crea, F (2002) Immunosuppressive Therapy for the Prevention of Restenosis after Coronary Artery Stent Implantation (IMPRESS Study). *J. Am. Coll. Cardiol.* **40**(11)**:** 1935-1942.

Villa, AE, Guzman, LA, Chen, W, Golomb, G, Levy, RJ, Topol, EJ (1994) Local delivery of dexamethasone for prevention of neointimal proliferation in a rat model of balloon angioplasty. *J. Clin. Invest.* **93**(3)**:** 1243-1249.

Virchow, R (1856) Phlogose und Thrombose im Gefasssystem. *Gesammelte Abhandlungen zur Wissenschaftlichen Medicin.***:** 458.

Voisard, R, Seitzer, U, Baur, R, Dartsch, PC, Osterhues, H, Hoher, M, Hombach, V (1994) Corticosteroid agents inhibit proliferation of smooth muscle cells from human atherosclerotic arteries in vitro. *Int. J. Cardiol.* **43**(3)**:** 257-267.

Vrang, N, Kristensen, P, Tang-Christensen, M, Larsen, PJ (2002) Effects of leptin on arcuate pro-opiomelanocortin and cocaine-amphetamine-regulated transcript expression are independent of circulating levels of corticosterone. *J Neuroendocrinol* **14**(11)**:** 880-886.

Wainwright, CL, Miller, AM, Wadsworth, RM (2001) Inflammation as a key event in the development of neointima following vascular balloon injury. *Clin. Exp. Pharmacol. Physiol.* **28**(11)**:** 891-895.

Wakefield, TW, Myers, DD, Henke, PK (2008) Mechanisms of venous thrombosis and resolution. *Arterioscler. Thromb. Vasc. Biol.* **28**(3)**:** 387-391.

Waksman, R, Ajani, AE, Pichard, AD, Torguson, R, Pinnow, E, Canos, D, Satler, LF, Kent, KM, Kuchulakanti, P, Pappas, C, Gambone, L, Weissman, N, Abbott, MC, Lindsay, J (2004) Oral rapamycin to inhibit restenosis after stenting of de novo coronary lesions: the Oral Rapamune to Inhibit Restenosis (ORBIT) study. *J. Am. Coll. Cardiol.* **44**(7)**:** 1386-1392.

Walker, BR (2007) Glucocorticoids and cardiovascular disease. *Eur J Endocrinol* **157**(5)**:** 545-559.

Walker, BR, Connacher, AA, Lindsay, RM, Webb, DJ, Edwards, CR (1995) Carbenoxolone increases hepatic insulin sensitivity in man: a novel role for 11-oxosteroid reductase in enhancing glucocorticoid receptor activation. *J. Clin. Endocrinol. Metab.* **80**(11)**:** 3155-3159.

Walker, EA, Stewart, PM (2003) 11beta-hydroxysteroid dehydrogenase: unexpected connections. *Trends Endocrinol Metab* **14**(7)**:** 334-339.

Wallace, AD, Cidlowski, JA (2001) Proteasome-mediated glucocorticoid receptor degradation restricts transcriptional signaling by glucocorticoids. *J. Biol. Chem.* **276**(46)**:** 42714-42721.

Wang, D, Liu, Z, Li, Q, Karpurapu, M, Kundumani-Sridharan, V, Cao, H, Dronadula, N, Rizvi, F, Bajpai, AK, Zhang, C, Muller-Newen, G, Harris, KW, Rao, GN (2007a) An essential role for gp130 in neointima formation following arterial injury. *Circ. Res.* **100**(6)**:** 807-816.

Wang, H, Vohra, BP, Zhang, Y, Heuckeroth, RO (2005a) Transcriptional profiling after bile duct ligation identifies PAI-1 as a contributor to cholestatic injury in mice. *Hepatology* **42**(5)**:** 1099-1108.

Wang, H, Zhang, Y, Heuckeroth, RO (2007b) PAI-1 deficiency reduces liver fibrosis after bile duct ligation in mice through activation of tPA. *FEBS Lett* **581**(16)**:** 3098-3104.

Wang, K, Zhou, X, Zhou, Z, Mal, N, Fan, L, Zhang, M, Lincoff, AM, Plow, EF, Topol, EJ, Penn, MS (2005b) Platelet, not endothelial, P-selectin is required for neointimal formation after vascular injury. *Arterioscler. Thromb. Vasc. Biol.* **25**(8)**:** 1584-1589.

Wang, L, Salu, K, Verbeken, E, Bosmans, J, Van de Werf, F, De Scheerder, I, Huang, Y (2005c) Stent-mediated methylprednisolone delivery reduces macrophage contents and in-stent neointimal formation. *Coron. Artery Dis.* **16**(4)**:** 237-243.

Wang, P, Wu, P, Siegel, MI, Egan, RW, Billah, MM (1995) Interleukin (IL)-10 inhibits nuclear factor kappa B (NF kappa B) activation in human monocytes. IL-10 and IL-4 suppress cytokine synthesis by different mechanisms. *J. Biol. Chem.* **270**(16)**:** 9558-9563.

Wang, Z, Newman, WH (2003) Smooth muscle cell migration stimulated by interleukin 6 is associated with cytoskeletal reorganization. *J Surg Res* **111**(2)**:** 261-266.

Wanscher, O, Clemmesen, J, Nielsen, A (1951) Negative correlation between atherosclerosis and carcinoma. *Br J Cancer* **5**(2)**:** 172-174.

Ward, MR, Agrotis, A, Kanellakis, P, Dilley, R, Jennings, G, Bobik, A (1997) Inhibition of protein tyrosine kinases attenuates increases in expression of transforming growth factor-beta isoforms and their receptors following arterial injury. *Arterioscler. Thromb. Vasc. Biol.* **17**(11)**:** 2461-2470.

Ward, MR, Kanellakis, P, Ramsey, D, Funder, J, Bobik, A (2001) Eplerenone suppresses constrictive remodeling and collagen accumulation after angioplasty in porcine coronary arteries. *Circulation* **104**(4)**:** 467-472.

Wei, L, MacDonald, TM, Walker, BR (2004) Taking glucocorticoids by prescription is associated with subsequent cardiovascular disease. *Ann Intern Med* **141**(10)**:** 764-770.

Weinreb, DB, Aguinaldo, JG, Feig, JE, Fisher, EA, Fayad, ZA (2007) Non-invasive MRI of mouse models of atherosclerosis. *NMR Biomed* **20**(3)**:** 256-264.

Weintraub, WS (2007) The pathophysiology and burden of restenosis. *Am J Cardiol* **100**(5A)**:** 3K-9K.

Weiss, D, Kools, JJ, Taylor, WR (2001) Angiotensin II-induced hypertension accelerates the development of atherosclerosis in apoE-deficient mice. *Circulation* **103**(3)**:** 448-454.

Weiss, D, Taylor, WR (2008) Deoxycorticosterone acetate salt hypertension in apolipoprotein E-/- mice results in accelerated atherosclerosis: the role of angiotensin II. *Hypertension* **51**(2)**:** 218-224.

Weissberg, PL (2000) Atherogenesis: current understanding of the causes of atheroma. *Heart (British Cardiac Society)* **83**(2)**:** 247-252.

Weksler, BB, Marcus, AJ, Jaffe, EA (1977) Synthesis of prostaglandin I2 (prostacyclin) by cultured human and bovine endothelial cells. *Proc Natl Acad Sci U S A* **74**(9)**:** 3922-3926.

Welt, FG, Edelman, ER, Simon, DI, Rogers, C (2000) Neutrophil, not macrophage, infiltration precedes neointimal thickening in balloon-injured arteries. *Arterioscler. Thromb. Vasc. Biol.* **20**(12)**:** 2553-2558.

Welt, FG, Rogers, C (2002) Inflammation and restenosis in the stent era. *Arterioscler. Thromb. Vasc. Biol.* **22**(11)**:** 1769-1776.

Wexler, BC, Brown, TE, Miller, BF (1960) Atherosclerosis in rats induced by repeated breedings, ACTH and unilateral nephrectomy. Acid mucopolysaccharides, fibroplasia, elastosis and other changes in early lesions. *Circ. Res.* **8:** 278-286.

White, B, Schmidt, M, Murphy, C, Livingstone, W, O'Toole, D, Lawler, M, O'Neill, L, Kelleher, D, Schwarz, HP, Smith, OP (2000) Activated protein C inhibits lipopolysaccharide-induced nuclear translocation of nuclear factor kappaB (NF-kappaB) and tumour necrosis factor alpha (TNF-alpha) production in the THP-1 monocytic cell line. *Br. J. Haematol.* **110**(1)**:** 130-134.

Whitworth, JA, Schyvens, CG, Zhang, Y, Andrews, MC, Mangos, GJ, Kelly, JJ (2002) The nitric oxide system in glucocorticoid-induced hypertension. *J. Hypertens.* **20**(6)**:** 1035-1043.

Whitworth, JA, Schyvens, CG, Zhang, Y, Mangos, GJ, Kelly, JJ (2001) Glucocorticoid-induced hypertension: from mouse to man. *Clin. Exp. Pharmacol. Physiol.* **28**(12)**:** 993-996.

Wissing, ER, Millay, DP, Vuagniaux, G, Molkentin, JD (2010) Debio-025 is more effective than prednisone in reducing muscular pathology in mdx mice. *Neuromuscul. Disord.*

Witztum, JL (1994) The oxidation hypothesis of atherosclerosis. *Lancet* **344**(8925)**:** 793-795.

Wolbink, GJ, Bossink, AW, Groeneveld, AB, de Groot, MC, Thijs, LG, Hack, CE (1998) Complement activation in patients with sepsis is in part mediated by C-reactive protein. *J. Infect. Dis.* **177**(1)**:** 81-87.

Wolff, RA, Tomas, JJ, Hullett, DA, Stark, VE, van Rooijen, N, Hoch, JR (2004) Macrophage depletion reduces monocyte chemotactic protein-1 and transforming growth factor-beta1 in healing rat vein grafts. *J. Vasc. Surg.* **39**(4)**:** 878-888.

Xu, F, Ji, J, Li, L, Chen, R, Hu, W (2007) Activation of adventitial fibroblasts contributes to the early development of atherosclerosis: a novel hypothesis that complements the "Response-to-Injury Hypothesis" and the "Inflammation Hypothesis". *Med Hypotheses* **69**(4)**:** 908-912.

Yamada, K, Naito, M, Hayashi, T, Asai, K, Yoshimine, N, Iguchi, A (1993) Effects of dexamethasone on migration of human monocytes in response to oxidized beta-very low density lipoprotein. *Artery* **20**(5)**:** 253-267.

Yamamoto, K, Morishita, R, Tomita, N, Shimozato, T, Nakagami, H, Kikuchi, A, Aoki, M, Higaki, J, Kaneda, Y, Ogihara, T (2000) Ribozyme oligonucleotides against transforming growth factor-beta inhibited neointimal formation after vascular injury in rat model: potential application of ribozyme strategy to treat cardiovascular disease. *Circulation* **102**(11)**:** 1308-1314.

Yamamoto, Y, Ishizu, A, Ikeda, H, Otsuka, N, Yoshiki, T (2004) Dexamethasone increased plasminogen activator inhibitor-1 expression on human umbilical vein endothelial cells: an additive effect to tumor necrosis factor-alpha. *Pathobiology* **71**(6)**:** 295-301.

Yamamoto, Y, Yamashita, T, Kitagawa, F, Sakamoto, K, Giddings, JC, Yamamoto, J (2009) The effect of the long term aspirin administration on the progress of atherosclerosis in apoE(-/-) LDLR(-/-) double knockout mouse. *Thromb. Res.*

Yanagisawa, M, Kurihara, H, Kimura, S, Tomobe, Y, Kobayashi, M, Mitsui, Y, Yazaki, Y, Goto, K, Masaki, T (1988) A novel potent vasoconstrictor peptide produced by vascular endothelial cells. *Nature* **332**(6163)**:** 411-415.

Yang, L, Yang, JB, Chen, J, Yu, GY, Zhou, P, Lei, L, Wang, ZZ, Cy Chang, C, Yang, XY, Chang, TY, Li, BL (2004a) Enhancement of human ACAT1 gene expression to promote the macrophage-derived foam cell formation by dexamethasone. *Cell Res* **14**(4)**:** 315-323.

Yang, S, Zhang, L (2004b) Glucocorticoids and vascular reactivity. *Curr. Vasc. Pharmacol.* **2**(1)**:** 1-12.

Yasukawa, H, Imaizumi, T, Matsuoka, H, Nakashima, A, Morimatsu, M (1997) Inhibition of intimal hyperplasia after balloon injury by antibodies to intercellular adhesion molecule-1 and lymphocyte function-associated antigen-1. *Circulation* **95**(6)**:** 1515-1522.

Yau, JL, Noble, J, Kenyon, CJ, Hibberd, C, Kotelevtsev, Y, Mullins, JJ, Seckl, JR (2001) Lack of tissue glucocorticoid reactivation in 11beta -hydroxysteroid dehydrogenase type 1 knockout mice ameliorates age-related learning impairments. *Proc. Natl. Acad. Sci. U. S. A.* **98**(8)**:** 4716-4721.

Yeager, MP, Guyre, PM, Munck, AU (2004) Glucocorticoid regulation of the inflammatory response to injury. *Acta Anaesthesiol. Scand.* **48**(7)**:** 799-813.

Yla-Herttuala, S, Sumuvuori, H, Karkola, K, Mottonen, M, Nikkari, T (1986) Glycosaminoglycans in normal and atherosclerotic human coronary arteries. *Lab. Invest.* **54**(4)**:** 402-407.

Yudkin, JS, Eringa, E, Stehouwer, CD (2005) "Vasocrine" signalling from perivascular fat: a mechanism linking insulin resistance to vascular disease. *Lancet* **365**(9473)**:** 1817-1820.

Zambrowicz, BP, Imamoto, A, Fiering, S, Herzenberg, LA, Kerr, WG, Soriano, P (1997) Disruption of overlapping transcripts in the ROSA beta geo 26 gene trap strain leads to widespread expression of beta-galactosidase in mouse embryos and hematopoietic cells. *Proc Natl Acad Sci U S A* **94**(8)**:** 3789-3794.

Zempo, N, Kenagy, RD, Au, YP, Bendeck, M, Clowes, MM, Reidy, MA, Clowes, AW (1994) Matrix metalloproteinases of vascular wall cells are increased in balloon-injured rat carotid artery. *J. Vasc. Surg.* **20**(2)**:** 209-217.

Zhang, H, Faber, JE (2001) Trophic effect of norepinephrine on arterial intima-media and adventitia is augmented by injury and mediated by different alpha1-adrenoceptor subtypes. *Circ. Res.* **89**(9)**:** 815-822.

Zhang, SH, Reddick, RL, Piedrahita, JA, Maeda, N (1992) Spontaneous hypercholesterolemia and arterial lesions in mice lacking apolipoprotein E. *Science (New York, N.Y* **258**(5081)**:** 468-471.

Zhang, TY, Ding, X, Daynes, RA (2005a) The expression of 11 beta-hydroxysteroid dehydrogenase type I by lymphocytes provides a novel means for intracrine regulation of glucocorticoid activities. *J. Immunol.* **174**(2)**:** 879-889.

Zhang, Y, Croft, KD, Mori, TA, Schyvens, CG, McKenzie, KU, Whitworth, JA (2004) The antioxidant tempol prevents and partially reverses dexamethasone-induced hypertension in the rat. *Am. J. Hypertens.* **17**(3)**:** 260-265.

Zhang, Y, Janssen, L, Chu, FV (2005b) Atherosclerosis of radial arterial graft may increase the potential of vessel spasm in coronary bypass surgery. *J. Thorac. Cardiovasc. Surg.* **130**(5)**:** 1477-1478.

Zhu, LJ, Altmann, SW (2005) mRNA and 18S-RNA coapplication-reverse transcription for quantitative gene expression analysis. *Anal Biochem* **345**(1)**:** 102-109.

Zhu, Y, Farrehi, PM, Fay, WP (2001) Plasminogen activator inhibitor type 1 enhances neointima formation after oxidative vascular injury in atherosclerosis-prone mice. *Circulation* **103**(25)**:** 3105-3110.

Zou, Y, Hu, Y, Mayr, M, Dietrich, H, Wick, G, Xu, Q (2000) Reduced neointima hyperplasia of vein bypass grafts in intercellular adhesion molecule-1-deficient mice. *Circ. Res.* **86**(4)**:** 434-440.

Appendix

Publications

OPEN ACCESS Freely available online

PLoS one

Quantitative 3-Dimensional Imaging of Murine Neointimal and Atherosclerotic Lesions by Optical Projection Tomography

Nicholas S. Kirkby, Lucinda Low, Jonathan R. Seckl, Brian R. Walker, David J. Webb, Patrick W. F. Hadoke*

Centre for Cardiovascular Science, University of Edinburgh, Edinburgh, United Kingdom

Abstract

Objective: Traditional methods for the analysis of vascular lesion formation are labour intensive to perform - restricting study to 'snapshots' within each vessel. This study was undertaken to determine the suitability of optical projection tomographic (OPT) imaging for the 3-dimensional representation and quantification of intimal lesions in mouse arteries.

Methods and Results: Vascular injury was induced by wire-insertion or ligation of the mouse femoral artery or administration of an atherogenic diet to apoE-deficient mice. Lesion formation was examined by OPT imaging of autofluorescent emission. Lesions could be clearly identified and distinguished from the underlying vascular wall. Planimetric measurements of lesion area correlated well with those made from histological sections subsequently produced from the same vessels (wire-injury: $R^2 = 0.92$; ligation-injury: $R^2 = 0.89$; atherosclerosis: $R^2 = 0.85$), confirming both the accuracy of this methodology and its non-destructive nature. It was also possible to record volumetric measurements of lesion and lumen and these were highly reproducible between scans (coefficient of variation = 5.36%, 11.39% and 4.79% for wire- and ligation-injury and atherosclerosis, respectively).

Conclusions: These data demonstrate the eminent suitability of OPT for imaging of atherosclerotic and neointimal lesion formation, providing a much needed means for the routine 3-dimensional analysis of vascular morphology in studies of this type.

Citation: Kirkby NS, Low L, Seckl JR, Walker BR, Webb DJ, et al. (2011) Quantitative 3-Dimensional Imaging of Murine Neointimal and Atherosclerotic Lesions by Optical Projection Tomography. PLoS ONE 6(2): e16906. doi:10.1371/journal.pone.0016906

Editor: Alma Zernecke, Universität Würzburg, Germany

Received October 6, 2010; **Accepted** January 17, 2011; **Published** February 17, 2011

Funding: This work was supported by studentships from the University of Edinburgh (NSK) and Carnegie Trust (LL; Henri Dryerre scheme) and funding from the British Heart Foundation (PWFH, BRW, DJW; RG/05/008; PG/05/007) and Wellcome Trust (JRS, BRW, DJW; 08314/Z/07/Z). The Centre for Cardiovascular Science is a BHF-funded Centre of Excellence. The funders had no role in study design, data collection and analysis, decision to publish, or preparation of the manuscript.

Competing Interests: The authors have declared that no competing interests exist.

* E-mail: phadoke@staffmail.ed.ac.uk

Introduction

The formation of vascular lesions in response to acute or chronic injury to the arterial wall defines atherosclerosis and post-interventional restenosis, conditions that contribute greatly to cardiovascular morbidity and mortality[1]. Understanding of the processes that lead to such lesion formation has been advanced considerably by exploiting murine models of acute vascular injury and atherosclerosis that are amenable to genetic manipulation[2]. Despite these advances, *ex vivo* identification and quantification of vascular lesions typically relies on 2-dimensional histological analysis. This is time consuming and provides only limited information on lesion volume. In particular, lesion burden in an artery is commonly assessed by measurement of cross-sectional lesion area, either at randomly selected sites along its profile or at the site of maximum occlusion, providing an imperfect analysis of overall lesion burden.

Whole-mount 3-dimensional imaging technology should provide a solution to this problem, yet surprisingly few suitable approaches have been described. This reflects the scale of the murine vasculature – too large for microscopic techniques such as single-photon confocal microscopy but too small for techniques derived from the clinic, including magnetic resonance imaging (MRI)[3] and computed tomography (CT)[4]. Indeed, whilst both *ex vivo* MRI and micro CT have been applied to the study of murine atherosclerosis, they offer limited resolution, even in relatively large arteries and require long acquisition times limiting throughput [3,5]. Several newer optical imaging modalities have been described in attempt to span this region of scale poorly served by traditional systems. For example, optical coherence tomography [6] and photo-acoustic tomography [7] offer tissue penetration depths of 1–3 mm and imaging of optical scattering and absorbance, and do so at relatively high resolution.

Another such technique is optical projection tomography (OPT). Originally conceived for the study of mouse embryos, OPT is able to image biological specimens approximately ~0.3 to 10 mm in diameter, using two image modes [8]. Transmission imaging records the opacity of a semi-translucent sample to polychromatic visible light and therefore primarily describes its pattern of absorbance. This may reflect the presence of pigments such as hemoglobin or of particles resistant to optical clearing, and can often be used to distinguish anatomical structures. Emission

imaging records the ability of endogenous (e.g. collagen, elastin, NADPH, certain amino acids) and exogenous fluorophores contained within that sample to emit light upon excitation at specific wavelengths. This imaging mode may also describe anatomical structure because the individual tissue components making up a sample can differ in the type and density of autofluorescent species present. Further, through the use of fluorescent reporters the distribution of immunoreactivity or gene expression may be determined [9]. For both imaging modes, light (transmitted or emitted) is focused to a charge coupled device by conventional microscope optics, and images captured at multiple increments of rotation (typically 400 images at 0.9° increments). From these, the 3-dimensional volume can be calculated by standard tomographic reconstruction methods such as filtered back-projection or iterative reconstruction. A full description of the method can be found elsewhere [8,9].

Since its introduction, the application of OPT has been broadened considerably, for example, having being adapted to the study of β-cells in the diabetic mouse pancreas, and the development of neuronal structures in human tissue samples[10]. Surprisingly given the need for such methodology, the suitability of OPT imaging for the 3-dimensional assessment of morphology in vascular tissues from adult animals has not been determined.

We addressed the proposal that OPT could be used as a rapid and cost-effective method to produce quantifiable 3-dimensional images of intimal lesions within murine arteries. The suitability of this technique was assessed using three commonly used models of murine vascular injury: femoral artery wire-injury and ligation models of neointimal hyperplasia and the apolipoprotein E-deficient ($apoE^{-/-}$) mouse model of atherosclerosis.

Methods

Induction of neointima formation

All animal experiments were performed in accordance with the Animals (Scientific Procedures) Act (UK), 1986 and approved by the University of Edinburgh ethical review committee (PPL 60/3867). Surgical procedures were carried out under isoflurane anaesthesia and with buprenorphine post-operative analgesia. Acute vascular injury was performed in male, 12 week old C57Bl6/J mice (Harlan, UK). Wire-injury to the femoral artery was performed by insertion of a 0.014" diameter wire into the left femoral artery, previously described[11]. Ligation-injury was performed by occlusion of the right femoral artery of the same mice with a 5-0 silk ligature across the femoropopliteal bifurcation, analogous to the carotid artery ligation-injury model[12]. Animals were allowed to recover for 28 days before sacrifice by transcardiac perfusion fixation.

Induction of atherosclerosis

Atherosclerotic lesion formation was induced in male, 6 week old ApoE-null mice (bred in house) by feeding a Western diet (0.2% cholesterol; Research Diets, USA) for 12 weeks. At the end of this period, animals were killed by perfusion fixation.

OPT scanning and quantification

For OPT imaging, isolated vessels were embedded in 1.5% low melting point agarose (Invitrogen, UK), dehydrated in methanol (100%; 24 hours) and optically cleared in benzyl alcohol:benzyl benzoate (1:2 v/v; 24 hours). Vessels were imaged using a Bioptonics 3001 OPT tomograph. All studies on injured arteries were performed using emission imaging, after UV illumination (425 nm excitation filter with 40 nm band pass; 475 nm long pass emission filter; 1.048Mpixel scanning resolution). For each vessel type, a magnification was chosen to provide the smallest voxel size whilst allowing the entire region of interest to be covered. This resulted in voxel sizes of 216, 64 and 166 μm^3 respectively for wire- and ligation-injured femoral arteries and atherosclerotic aortic arches. For each vessel, exposure time was adjusted to maximise the dynamic range of the resulting image and was approximately 400, 800 and 1000ms per projection for wire- and ligation-injured femoral arteries and atherosclerotic aortic arches, respectively. Raw data (400 projections per scan at 0.9° increments) was subject to Hamming-filtered back-projection using NRecon software (Skyscan, Belgium). Quantification was performed using CTan software (Skyscan, Belgium). Briefly, lesion and lumen volumes were segmented by semi-automated tracing of the internal elastic lamina and subsequent grey-level thresholding to distinguish neointima from lumen. (See **Methods S1** for a step-by-step protocol).

Histology

After tomographic scanning, vessels were immersed in methanol for 24 hours, trimmed of excess agarose and processed to paraffin wax. Histological sections (3–4 μm thick) underwent 'United States Trichrome' (UST) staining to highlight morphology[13] or picro-sirius red to highlight collagen. Measurements of lesion area (defined as the area between the luminal border and internal elastic lamina) were recorded from photomicrographs of UST-stained sections using Photoshop CS4 Extended software (Adobe Inc, USA).

Immunohistochemistry

Immunohistochemistry was performed for α-smooth muscle actin (αSMA) and Mac2. Briefly, rehydrated sections were incubated with mouse anti-αSMA (Sigma, UK; 1/400 dilution; 30 mins) or rat anti-Mac2 primary antibodies (Cederlane Inc, USA; 1/6000 dilution; overnight) before treatment with goat anti-mouse IgG (Vector Labs, UK; 1/400 dilution; 30 mins) or goat anti-rat IgG secondary antibodies (Vector Labs, UK; 1/200 dilution; 30 mins), respectively. Sections were then treated with streptavidin-conjugated peroxidase (Extravidin-Peroxidase; Sigma, UK; 1/400 dilution; 30 mins) and the stain developed by application of 3,3-diaminobenzidine.

Statistics and data analysis

OPT slices corresponding to histological sections were identified based on the distance of each from a fixed reference point within the sample (the femoropopliteal bifurcation, the ligation and the root of the brachiocephalic artery, respectively, for wire- and ligation-injured femoral arteries and atherosclerotic aortic arches). As z-axis distances can only be approximated from serial sections, visual cues, such as the position of arterial branches and vessel conformation were, in some cases, used to aid selection of appropriate image pairs. Measurements of lesion areas from OPT and histological sections were then compared by linear regression. The deviation of the slope from 1.0 was determined by F-test. Precision was assessed by calculation of the coefficient of variation between lesion volume measurements made from four independent scans/reconstructions of the same vessels.

Additional methodological detail is provided in **Methods S2.**

Results

Transmission and emission imaging of isolated arteries

To determine the suitability of OPT for the study of isolated murine blood vessels, healthy femoral arteries (n = 5) were each scanned twice - for visible light transmittance, and for fluorescent

emission. In the transmission channel, the opacity of these tissues was so low as to preclude the capture and reconstruction of useful data. In emission channels, however, femoral arteries were seen to autofluoresce strongly, with the greatest signal following excitation at 405–445 nm, corresponding to a 410 nm excitation peak for elastin[14]. In reconstructed 2-dimensional slices of arteries imaged in this way, the medial layer was clearly distinguished from the adventitia and lumen by its greater fluorescent signal (not shown). Fluorescent emission imaging was thus adopted for all further investigations.

Imaging Intimal Lesions

To establish whether OPT imaging could characterise neointimal lesion formation, mouse femoral arteries were subject to wire- (n = 6) or ligation- (n = 5) injury. Following either insult, neointimal thickening could be seen clearly in non-tomographic emission projections (**Figure 1a**). In reconstructed 2-dimensional slices, concentric neointimal lesions were obvious and could be distinguished from the media by their weaker emission (**Figure 1b, Figure S1**).

To extend the possible application of this technique to atherosclerotic lesions in large conduit arteries, the aortic arch from apoE$^{-/-}$ mice was also examined (n = 8). In OPT emission images of atherosclerotic aortic arches, lesion formation was again clearly evident with the expected anatomical distribution comprising lesions in the lesser curvature of the arch, in the brachiocephalic artery and at the origins of the left carotid and left subclavian arteries (**Figure 2a**). In cross-section, these lesions typically possessed an eccentric morphology and could be distinguished from media and lumen (**Figure 2b,c, Figure S2**).

2-dimensional validation and quantification

To validate the interpretation of OPT reconstructions following tomographic imaging, the same arteries were processed for histological examination. For both neointimal (**Figure 1c**) and atherosclerotic lesions (**Figure 2c**), histological sections and corresponding OPT reconstructions were strikingly similar. We compared planimetric measurements of lesion area obtained by each method. For wire- and ligation-induced neointimal lesions and atherosclerotic plaques, these correlated strongly by linear regression

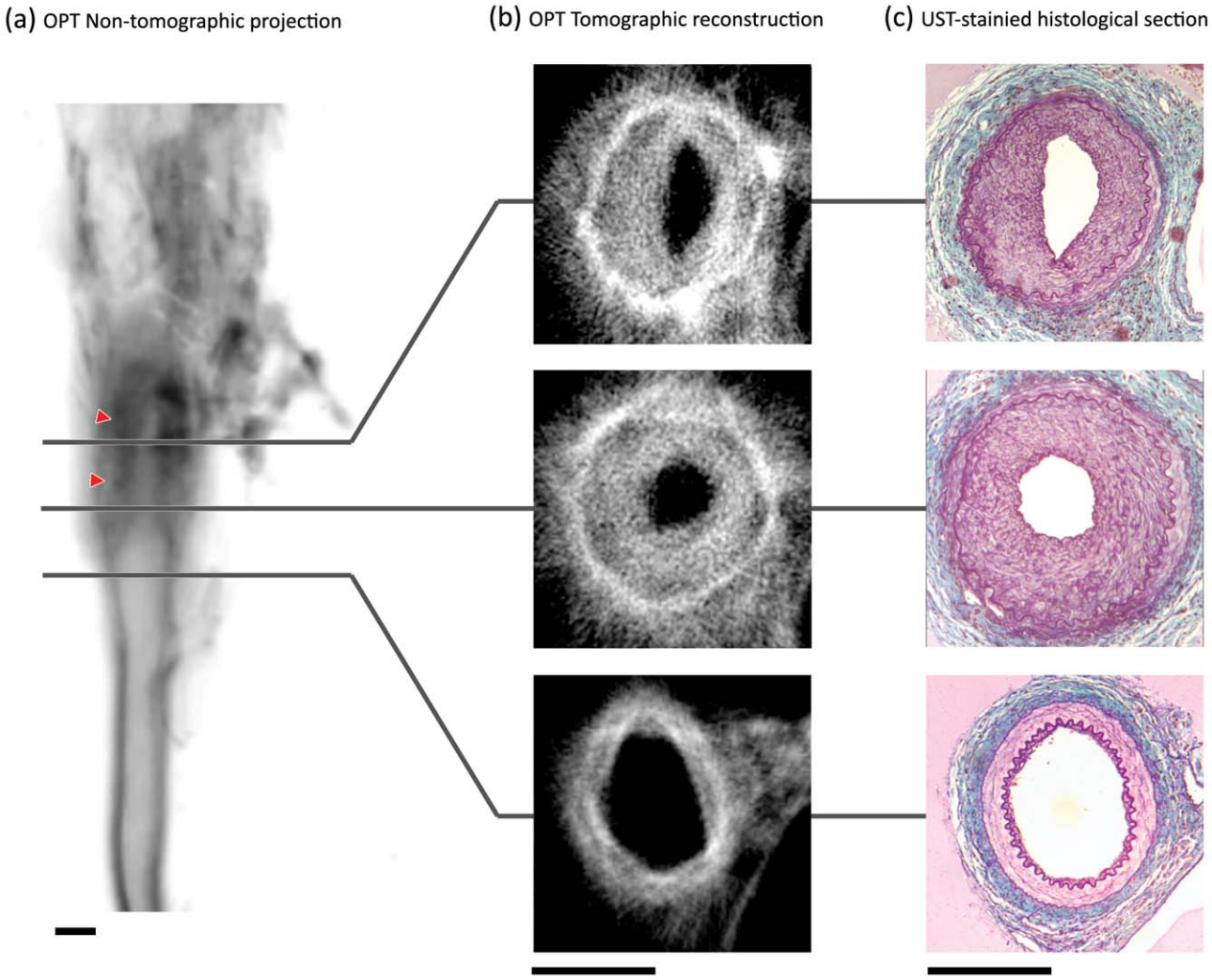

Figure 1. Identification of neointimal lesions in the ligation-injured mouse femoral artery. In non-tomographic fluorescent emission images of a ligation-injured femoral artery (a) neointimal thickening is clearly visible (red arrowheads). Image has been inverted for clarity (darker regions reflect stronger emission). In tomographic reconstructions (b), all layers of the vessel wall can be identified. Reconstructions strongly resemble US trichrome-stained histological sections of the same vessels (c). Scale bars in (a–c) are 200 μm.
doi:10.1371/journal.pone.0016906.g001

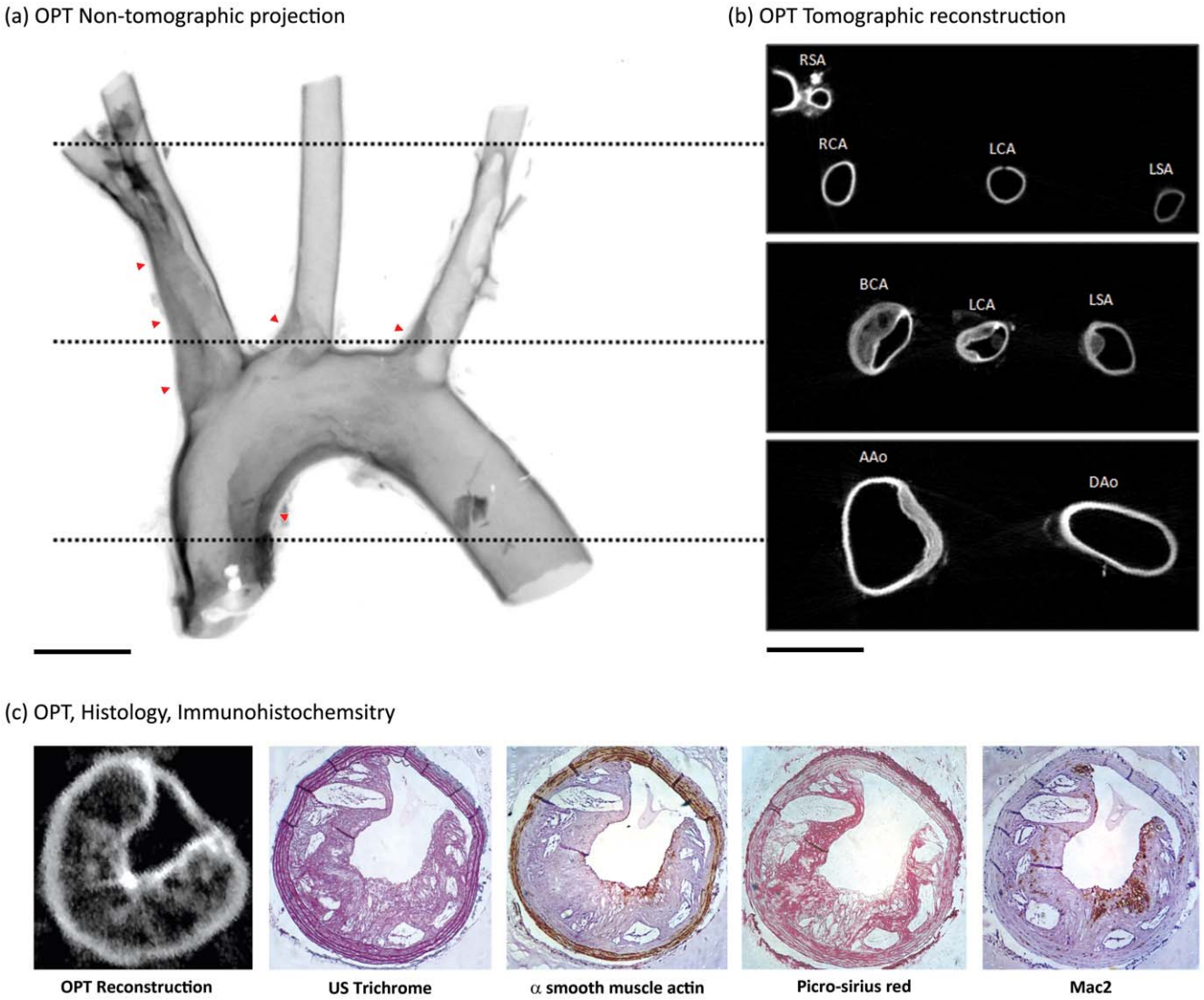

Figure 2. Identification of atherosclerotic lesion formation in the aortic arch of apoE$^{-/-}$ mice. In non-tomographic fluorescent emission images of the aortic arch of atherosclerotic mice (a), lesion formation (red arrowheads) is apparent with the expected distribution. Image has been inverted for clarity (darker regions reflect stronger emission). In cross-sectional reconstructions, lesions are visible with the same distribution (b) and possess strong resemblance to histological sections of the same vessels (c). Successful analysis of the brachiocephalic artery by standard (immuno)-histochemical procedures further emphasises the non-destructive nature of this technique (c). Scale bars in (a–b) are 1 mm. RSA, right subclavian artery; RCA, right carotid artery; LCA, left carotid artery; LSA, left subclavian artery; BCA, brachiocephalic artery; AAo, ascending aorta; DAo, descending aorta.
doi:10.1371/journal.pone.0016906.g002

($R^2 = 0.92$, $R^2 = 0.89$ and $R^2 = 0.85$, respectively) and the slope of these relationships did not differ from 1 ($p = 0.49$, $p = 0.58$ and $p = 0.88$, respectively). Bland-Altman analysis indicated no obvious bias in measurements of neointimal lesions induced by either injury (**Figure 3a,b**) but a small positive bias in OPT-derived measurements of lesion size in the brachiocephalic artery (**Figure 3c**), possibly reflecting shrinkage of these larger vessels during histological processing. Importantly, however, this bias was independent of lesion size indicating that measurements made in this way are comparable within and between vessels. We also confirmed that the OPT imaging procedure did not compromise subsequent analysis of lesion composition. In vessels previously subjected to OPT scanning, (immuno)staining for markers of smooth muscle (α-smooth muscle actin), macrophages (Mac2) and collagen (picro-sirius red) all occurred with the expected intensity and distribution (**Figures 2c**).

3-dimensional quantification and reproducibility

Whilst 2-dimensional comparisons of OPT and histology provide crucial validation, the greater potential of OPT is in the consideration of 3-dimensional parameters. We established protocols for the volumetric quantification of lesions by OPT. Using these methods, we were able to record lesion volumes in wire- (0.1100 ± 0.0091 mm^3; $n = 6$) and ligation-injured femoral arteries (0.0200 ± 0.0089 mm^3; $n = 5$) and in atherosclerotic brachiocephalic arteries (0.18 ± 0.018 mm^3; $n = 8$). As would be expected from the degree of injury, lesions in wire-injured vessels were significantly greater ($p < 0.0001$ by unpaired t-test) than those in ligation-injured vessels. Coefficients of variation (5.36%, 11.39% and 4.79%, respectively, $n = 4$) indicated that for all lesion types, measurements were highly reproducible. These data were also expressed as profiles of lesion burden along the length of the vessel (**Figure 4**) and

(a) Wire-injury (femoral artery)

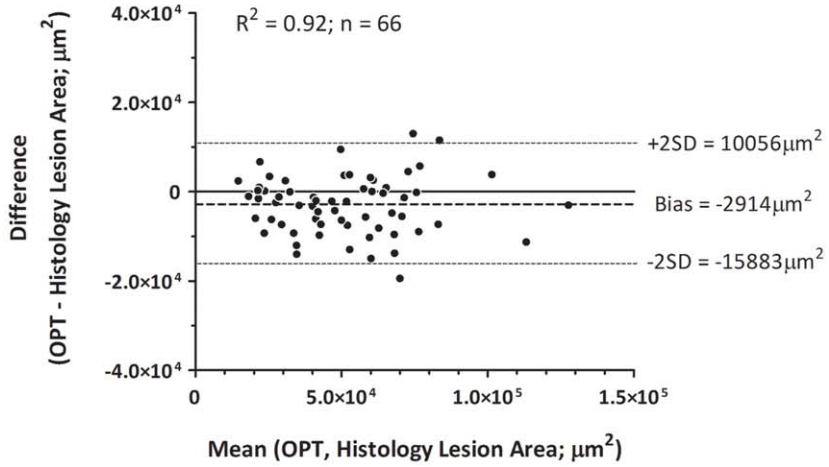

(b) Ligation-injury (femoral artery)

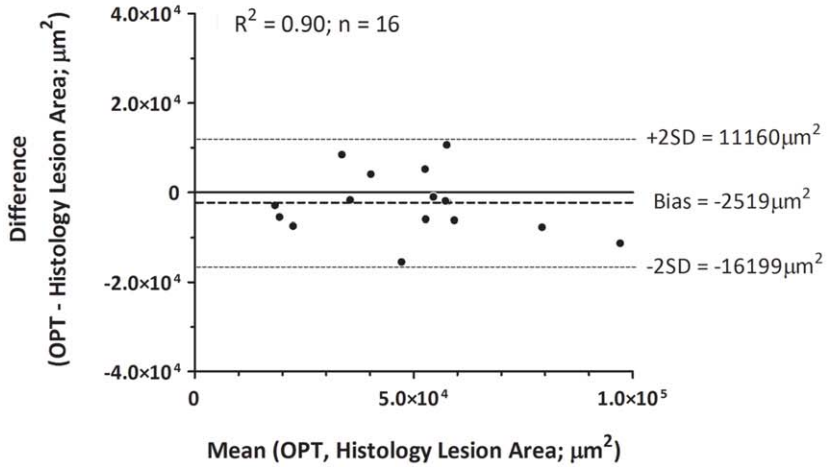

(c) ApoE$^{-/-}$ + western diet (brachiocephalic artery)

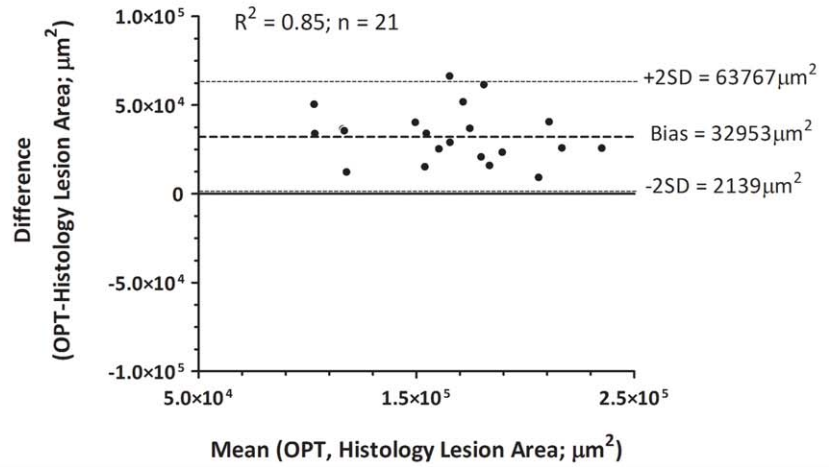

Figure 3. Comparison of planimetric measurements of lesion size between OPT reconstructions and histological sections. Planimetric measurements of lesion size recorded from OPT and histology image sets correlate strongly for all lesion types; Bland-Altman analysis indicates that this is unbiased for wire- (a) and ligation-injured femoral arteries (b) and that OPT measurements have a consistent positive bias in atherosclerotic brachiocephalic arteries (c).
doi:10.1371/journal.pone.0016906.g003

rendered for dynamic, qualitative evaluation (see **Figures S1–S3**), in both cases, highlighting the uneven distribution of lesion formation occurring in injured vessels.

Discussion

We have demonstrated, for the first time, the eminent suitability of OPT for the assessment of vascular structure in isolated arteries. Using this technique, 3-dimensional images describing the autofluorescent emission of the specimen were used to provide anatomical information on lesion size and distribution, as well as reproducible quantification of both the lesion and the residual lumen. This was achieved in vessels spanning the commonly studied size range in mice, and should be equally suitable for analysis of vascular lesions from other species, including small-to-medium sized human vessels. This methodology represents a

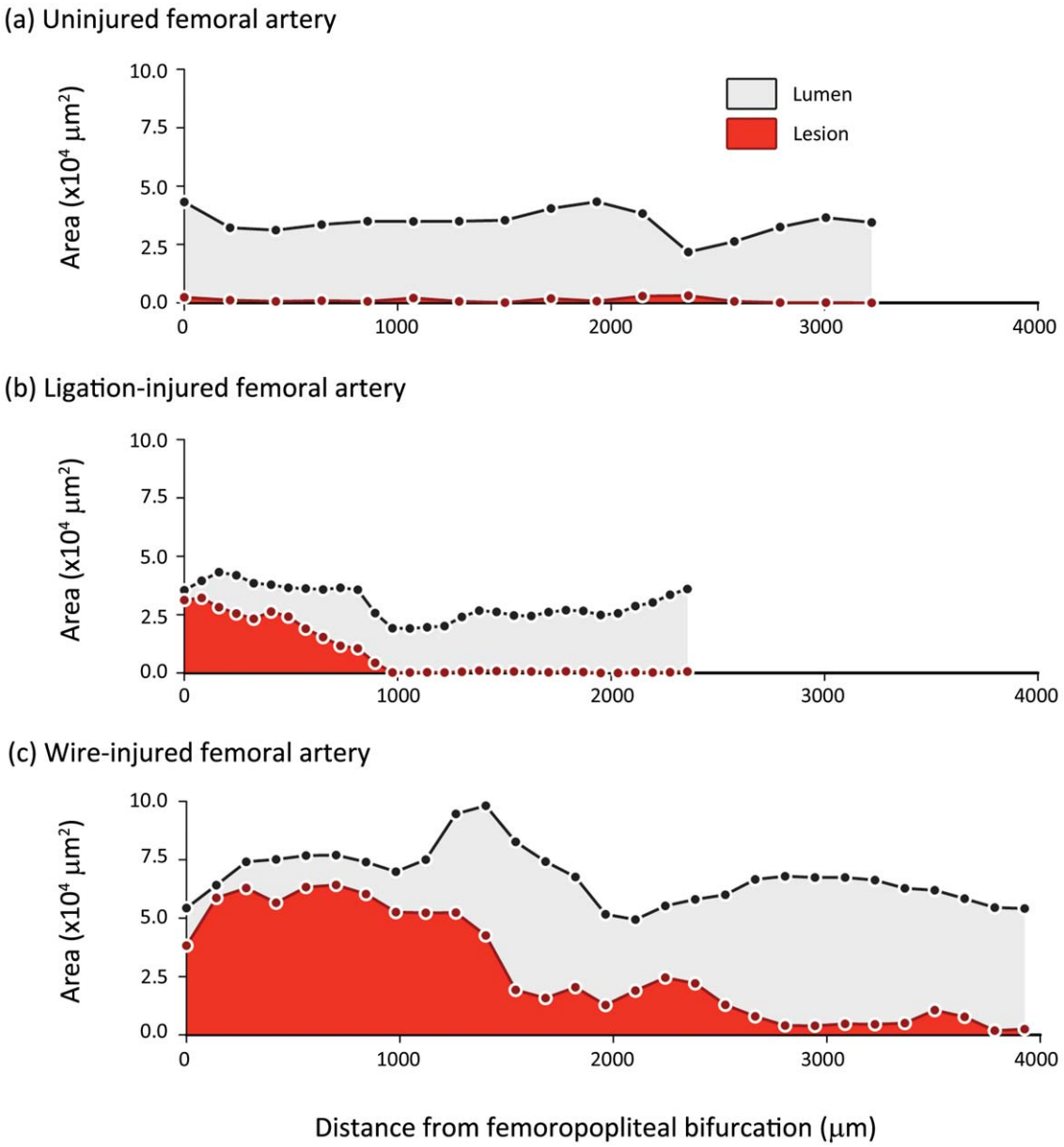

Figure 4. Longitudinal profiles of lesion and lumen cross-sectional area in un-injured, ligation- and wire-injured femoral arteries. When cross-sectional area of lesion (red) and lumen (grey) are plotted against distance along the axial length of the femoral artery, the difference in extent of lesion formation between ligation- (b) and wire-injury models (c) is apparent. In both cases, the variability in lesion size that occurs along the length of each vessel is also highlighted.
doi:10.1371/journal.pone.0016906.g004

considerable advance over traditional histological and, alternative 3-dimensional imaging techniques for the analysis of intimal lesion formation in small arteries.

Application of OPT to three widely-used models of arterial lesion development in the mouse, was designed to assess its potential for imaging atherosclerotic and proliferative lesions in large (aorta) and small (femoral) arteries. Importantly, these vessels define the required resolution for studies of this type - the aorta being the largest artery, and the femoral artery, which has a lumen diameter of ~200–250 μm[15], being amongst the smallest vessels in which studies of vascular lesion formation are commonly performed. The striking similarities of OPT-generated images and those obtained from subsequent histological analysis of the same samples confirmed the suitability of the technique in both vessels. Moreover, we were able to quantitatively validate this similarity. The consistency of cross-sectional area measurements obtained from OPT with those obtained by planimetric analysis of the corresponding histologically-stained sections (the current gold standard) confirmed the accuracy of the former. Further, because each OPT data set is composed of many hundreds of cross-sectional scan lines, using OPT it was simple to generate profiles of lesion area along the injured vessel. The advantage of this was exemplified by the comparison of lesions induced by wire-injury[11] with those caused by arterial ligation[12]. This demonstrated that whilst cross-sectional narrowing caused by wire-injury and ligation were broadly similar close to the origin of the injury, the lesions resulting from insertion of a wire extended a far greater distance along the arterial wall. Generating comparable data from histological sections would have been expensive and extremely labour intensive.

Whilst these advantages alone might be sufficient to warrant adoption of OPT as the analytical method of choice; the real strength of the technique is conferred by the ability to quantify lesion volume. Measurements of lesion volume provide a more representative of the total lesion burden in an artery[3], and are therefore not subject to the bias and error introduced by selection of particular portions of the vessel for analysis. This is again emphasised in the current investigation by longitudinal profiles of lesion formation produced from OPT images, which indicate just how much lesion size can vary over short lengths of injured vessel. Whilst these advantages may be shared with other 3D imaging modalities, in comparison to previously reported MRI and micro-CT *ex vivo* examinations of small arteries, OPT appears to produce images of comparable or superior quality, yet with much shorter imaging times and less expense. Indeed, despite preparation of samples for OPT imaging taking several days, little labour is required on each occasion. As such, many vessels can be prepared in parallel and data acquired in one session, thereby providing a relatively high throughput method of imaging arterial lesions and not requiring prolonged use of the imaging device.

In addition to direct 2- and 3-dimensional quantification of vessel morphology from OPT images, because this technique is non-destructive, it can be considered complementary to traditional analysis. Rather than laboriously sectioning, staining and analysing long lengths of lesions to find sites of interest for immunohistochemical examination, OPT images can be used to quickly identify such regions for selective sectioning and subsequent, in-depth analysis using standard histology and immunohistochemistry. Thus, OPT imaging of vascular lesions can be easily adopted into existing workflows to accelerate traditional methods of analysis and provide volumetric information from the same tissues.

There are inevitably limitations of OPT-based analysis of arterial lesions that must be considered. First, although image quality is comparable or superior to that of other tomographic imaging systems, it is noticeably inferior to microscopic imaging techniques (which can, of course, only be performed on smaller segments). Several refinements to the back-projection algorithms used to reconstruct OPT data sets have been proposed which may in future, further improve the quality of images produced by this method[16,17]. Second, the reagents used to prepare samples for OPT imaging might potentially alter certain aspects of the specimen. Perhaps the biggest potential source of artefacts resulting from the OPT procedure described here is the choice of a lipophilic agent (benzyl alcohol/benzyl benzoate) for optical clearing, which is likely to, for example, remove lipid pools from atherosclerotic plaques, and requires prior dehydration, which may cause shrinkage of tissue. In contrast to hydrophilic clearing agents such as glycerol, however, benzyl alcohol/benzyl benzoate is reported to cause minimal deformation of tissue morphology [18]. It is also important to consider that similar dehydration and lipid removal steps are otherwise required in the preparation of paraffin-embedded tissue sections. Further, although we have not directly compared tissues subject to both OPT imaging and histological analysis, with those only subject to the latter, we feel that the appearance and immunoreactivity of lesions in these models are subjectively similar to those we have previously observed in directly prepared histological sections. Beyond these rather general limitations, those more specific to the methodology presented here appear relatively minor. Ironically, perhaps the most obvious of these derives from the strong autofluorescence of arterial tissue, which enables such clear anatomical imaging. We have found this to be resistant to bleaching by previously set out methods[19], and as such, it may restrict the use of fluorescent probes to assess RNA and protein distribution patterns.

Much potential for further development of this technique exists, particularly with regard to tracking the 3-dimensional arrangement of key cells and signalling factors involved in arterial remodelling. Despite the above-described limitations, this may be achievable by several means. For example, the low opacity of optically-cleared arteries might suggest that colorimetric reporters, such as β-galactosidase, that can be visualised by transmission imaging, might be more suitable than fluorescent probes for this purpose. Alternatively, we have generated preliminary data (Bezuidenhout *et al.*, unpublished) to suggest that OPT can be used to identify nanoparticulate within arterial lesions, perhaps providing the means to track phagocytic cells. Finally, whilst the data presented here describe only studies of the mouse vasculature, preliminary studies suggest that is also suitable for imaging morphology and atherosclerotic lesion formation in larger vessels including rat and rabbit aortas (Bezuidenhout *et al.*, unpublished). OPT, should, therefore, be equally suited to the study of comparably sized human vessels.

In summary, OPT imaging is a valuable tool for the 3-dimensional evaluation of neointimal and atherosclerotic lesion burden and distribution in mouse arteries; a considerable advance because traditional 2-dimensional methods for the analysis of these lesions are labour intensive and do not effectively represent total lesion volume. Imaging by OPT is relatively fast and high throughput, convenient and non-destructive. Further, in contrast to previously published studies of OPT in adult mouse tissues[19], these methods are achievable using commercially-available equipment and software. This technique should provide the much-needed means to allow 3-dimensional evaluation of morphology to become a routine component of vascular remodelling studies.

Supporting Information

Figure S1 Tomographic cross-sections of an OPT-imaged, ligation-injured mouse femoral artery. After tomographic reconstruction, cross-sectional OPT images (excitation 425 nm with 40 nm band-pass; emission 475 nm long pass) can be animated for qualitative evaluation of vascular structure (in addition to quantitative measurement). In ligation-injured femoral arteries, presented in this way, morphologically-normal vessel can be seen proximal to the site of ligation and the media and lumen can be distinguished. Closer to the ligation, neointima formation is apparent, and this can also be distinguished from the media and lumen. The size of this lesion increases with proximity to the ligation, and eventually completely occludes the vessel. The position of each cross-section within the artery is indicated on the non-tomographic image inset left.
(MOV)

Figure S2 Tomographic cross-sections of an OPT-imaged, atherosclerotic aortic arch. After tomographic reconstruction, cross-sectional OPT images (excitation 425 nm with 40 nm band-pass; emission 475 nm long pass) can be animated for qualitative evaluation of vascular structure (in addition to quantitative measurement). In atherosclerotic aortic arches, presented in this way, the media and lumen of the ascending and descending aorta can be seen clearly and some lesion formation is apparent on the lesser curvature of the arch. This can be clearly distinguished from the vessel media and lumen. More severe lesion formation is present at the roots of right carotid and subclavian arteries, and throughout the length of the brachiocephalic artery. The position of each cross-section within the artery is indicated on the non-tomographic image inset left.
(MOV)

Figure S3 Volume rendering of a tomographically reconstructed, OPT-imaged, atherosclerotic aortic arch. After tomographic reconstruction, cross-sectional OPT images (excitation 425 nm with 40 nm band-pass; emission 475 nm long pass) can be volume rendered to visualise vascular structure and lesion formation in 3-dimensions. In atherosclerotic aortic arches, presented in this way (a), lesion formation can be observed with the predicated anatomical distribution (brachiocephalic artery, roots of the right carotid and subclavian arteries and lesser curvature of the arch). Regions within cross-sections corresponding to lesion can be segmented, separately rendered, and superimposed on original data to further highlight distribution and extent of lesion formation (b; lesion displayed in red). This process is analogous to that required to quantify lesion volume.
(MOV)

Methods S1 Protocol for OPT imaging and quantification of murine intimal and atherosclerotic lesions. Step-by-step protocol detailing procedures for OPT-based examination of intimal and atherosclerotic lesions in mouse arteries.
(DOC)

Methods S2 Additional methodological detail. Comprehensive description of the methodology used for all the techniques utilised in these studies.
(DOC)

Acknowledgments

The authors wish to acknowledge Prof. Rudolph A. Riemersma (University of Edinburgh) for his technical assistance and valuable comments.

Author Contributions

Conceived and designed the experiments: NSK LL JRS BRW DJW PWFH. Performed the experiments: NSK LL. Analyzed the data: NSK LL. Contributed reagents/materials/analysis tools: JRS BRW DJW PWFH. Wrote the paper: NSK.

References

1. Ross R (1999) Atherosclerosis–an inflammatory disease. N Engl J Med 340: 115–126.
2. Lusis AJ (2000) Atherosclerosis. Nature 407: 233–241.
3. McAteer MA, Schneider JE, Clarke K, Neubauer S, Channon KM, et al. (2004) Quantification and 3D reconstruction of atherosclerotic plaque components in apolipoprotein E knockout mice using ex vivo high-resolution MRI. Arterioscler Thromb Vasc Biol 24: 2384–2390.
4. Martinez HG, Prajapati SI, Estrada CA, Jimenez F, Quinones MP, et al. (2009) Microscopic Computed Tomography-Based Virtual Histology for Visualization and Morphometry of Atherosclerosis in Diabetic Apolipoprotein E Mutant Mice. Circulation 120: 821–822.
5. Langheinrich AC, Bohle RM, Greschus S, Hackstein N, Walker G, et al. (2004) Atherosclerotic Lesions at Micro CT: Feasibility for Analysis of Coronary Artery Wall in Autopsy Specimens1. Radiology 231: 675–681.
6. Ambrosi CM, Moazami N, Rollins AM, Efimov IR (2009) Virtual histology of the human heart using optical coherence tomography. J Biomed Opt 14: 054002.
7. Ku G, Maslov K, Li L, Wang LV (2010) Photoacoustic microscopy with 2-microm transverse resolution. J Biomed Opt 15: 021302.
8. Sharpe J, Ahlgren U, Perry P, Hill B, Ross A, et al. (2002) Optical projection tomography as a tool for 3D microscopy and gene expression studies. Science 296: 541–545.
9. Sharpe J (2004) Optical projection tomography. Annu Rev Biomed Eng 6: 209–228.
10. Kerwin J, Scott M, Sharpe J, Puelles L, Robson SC, et al. (2004) 3 dimensional modelling of early human brain development using optical projection tomography. BMC Neurosci 5: 27.
11. Sata M, Maejima Y, Adachi F, Fukino K, Saiura A, et al. (2000) A mouse model of vascular injury that induces rapid onset of medial cell apoptosis followed by reproducible neointimal hyperplasia. J Mol Cell Cardiol 32: 2097–2104.
12. Kumar A, Lindner V (1997) Remodeling with neointima formation in the mouse carotid artery after cessation of blood flow. Arterioscler Thromb Vasc Biol 17: 2238–2244.
13. Hadoke P, Wainwright CL, Wadsworth RM, Butler K, Giddings MJ (1995) Characterization of the morphological and functional alterations in rabbit subclavian artery subjected to balloon angioplasty. Coron Artery Dis 6: 403–415.
14. Richards-Kortum R, Sevick-Muraca E (1996) Quantitative optical spectroscopy for tissue diagnosis. Annu Rev Phys Chem 47: 555–606.
15. You D, Waeckel L, Ebrahimian TG, Blanc-Brude O, Foubert P, et al. (2006) Increase in vascular permeability and vasodilation are critical for proangiogenic effects of stem cell therapy. Circulation 114: 328–338.
16. Walls JR, Sled JG, Sharpe J, Henkelman RM (2005) Correction of artefacts in optical projection tomography. Phys Med Biol 50: 4645–4665.
17. Walls JR, Sled JG, Sharpe J, Henkelman RM (2007) Resolution improvement in emission optical projection tomography. Phys Med Biol 52: 2775–2790.
18. Bucher D, Scholz M, Stetter M, Obermayer K, Pflger HJ (2000) Correction methods for three-dimensional reconstructions from confocal images: I. tissue shrinking and axial scaling. Journal of Neuroscience Methods 100: 135–143.
19. Alanentalo T, Asayesh A, Morrison H, Loren CE, Holmberg D, et al. (2007) Tomographic molecular imaging and 3D quantification within adult mouse organs. Nat Methods 4: 31–33.